Joana Catarina Lima Marinho

Molecular and Cellular Analysis of the Function of *viriato* gene during *Drosophila* Development

Joana Catarina Lima Marinho

Molecular and Cellular analysis of the function of *viriato* gene during *Drosophila* development

Joana Catarina Lima Marinho

Universidade de Coimbra | 2011

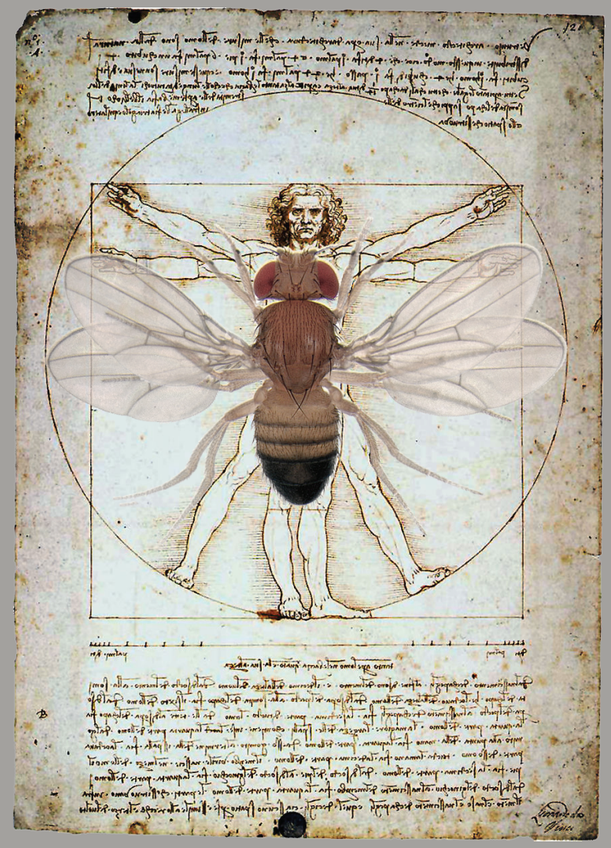

• U C •

FCTUC FACULDADE DE CIÊNCIAS
E TECNOLOGIA
UNIVERSIDADE DE COIMBRA

Coimbra 2011

Joana Catarina Lima Marinho

Molecular and Cellular Analysis of the Function of *viriato* Gene During *Drosophila* Development

FCTUC FACULDADE DE CIÊNCIAS
E TECNOLOGIA
UNIVERSIDADE DE COIMBRA

Coimbra - 2011

Dissertation submitted to the Faculty of Sciences and Technology, University of Coimbra for the Degree of Doctor of Philosophy in Biochemistry, specialization in Molecular Biology

Dissertação apresentada à Faculdade de Ciências e Tecnologia da Universidade de Coimbra para cumprimento dos requisitos necessários à obtenção do Grau de Doutor em Bioquímica, especialização em Biologia Molecular

Supervisor:
Paulo S. Pereira - Instituto de Biologia Molecular e Celular, Universidade do Porto, Porto, Portugal

Co-supervisor:
Paula Verissímo - Centro de Neurociências e Biologia Celular, Universidade de Coimbra, Coimbra, Portugal
and
Auxiliar Professor, Departamento de Ciências da Vida, FCTUC, Universidade de Coimbra, Coimbra, Portugal

The work present in this dissertation was carried out in the scope of the Doctoral Programme in Experimental Biology and Biomedicine (PDBEB), Center for Neuroscience and Cell Biology (CNC), University of Coimbra, Portugal.

The research described in the present thesis was performed at the Instituto de Biologia Molecular e Celular, Universidade do Porto, Porto, Portugal.

Joana Marinho was funded by Fundação Para a Ciência e Tecnologia, Portugal (fellowship SFRH/BD/33182/2007; co-funded by Fundo Social Europeu (FSE) in the scope of Programa Operacional Potencial Humano (POPH) do QREN.

FCT Fundação para a Ciência e a Tecnologia
MINISTÉRIO DA CIÊNCIA, TECNOLOGIA E ENSINO SUPERIOR Portugal

De acordo com o disposto no nº 2 do Artº 8º do Decreto-Lei nº 388/70, nesta dissertação foram utilizados resultados das publicações abaixo indicadas. No cumprimento do disposto no referido Decreto-Lei, o autor desta dissertação declara que interveio na concepção e na execução do trabalho experimental, na interpretação dos resultados e na redacção dos manuscritos publicados ou em preparação, sob o nome de **Marinho J**:

Marinho, J., Casares, F. and Pereira, P. S. (2011). The Drosophila Nol12 homologue viriato is a dMyc target that regulates nucleolar architecture and is required for dMyc-stimulated cell growth. Development 138(2): 349-357.

Marinho, J., Martins, T., Neto, M. G., Casares, F and Pereira, P. S. (2011) A targeted RNAi screen identifies a genetic interaction between TGF-β signaling pathway and the nucleolar regulator Viriato during eye development. **In preparation.**

AGRADECIMENTOS

Finalmente chegou a hora de deixar o lado mais racional do meu cérebro de lado e pôr as emoções a funcionar. Tenho uma sensação muito boa ao ver mais uma jornada da minha vida completa, mais um desafio ao qual eu me propus à 4 anos atrás superado. Estes 4 anos voaram, ainda ontem estava a entrar naquela sala do PDBEB para ter aulas, e hoje estou aqui a escrever as poucas palavras que restam da minha tese. Não gosto muito de olhar para o passado, gosto sim de olhar em frente, pensar e avançar para o futuro, mas este é um pequeno momento de reflexão e vou por isso tentar aqui deixar umas palavras de agradecimento àqueles que fizeram destes 4 anos, anos de alegria, diversão, amor e também de conhecimento.

Vou regressar a 2007 e começar por agradecer aos meus colegas do programa doutoral, que passaram também por tudo o que eu passei naqueles 6 meses, onde fomos testados ao máximo e superamos todas as nossas expectativas (lembram-se do maravilhoso trabalho de transcrição, do dia de Carnaval passado em aulas, dos nomes dos prémios Nobel que tínhamos de supostamente saber..).Tudo isto serviu para que criássemos um elo forte. Sara, Sofia A., Sueli, Nélio, Lígia, Tó, Filipe, Sofia C., Susana, Noutel e Gil (que nos abandonou pelo caminho), desejo-vos a maior sorte do mundo na vossa vida quer ela passe pela Ciência ou não. Um beijinho muito especial ao Filipe porque foi o nosso herói contra o ladrão de computadores, à Lígia por me acolher na sua casa depois deste episódio traumático, e à Sofia Cabral que já minha amiga de longa data partilhou comigo a casa (acho que deves ter ficado traumatizada) e juntas partilhamos as amarguras e alegrias. Queria também deixar aqui um beijinho muito grande a ti Tó, que nesta nossa jornada tiveste a "coragem" de avançar na vida e completá-la com uma das coisas mais preciosas que existe no mundo: a Mafalda. A tua tarefa foi tão ou mais árdua que um PhD e por isso admiro-te e admiro a pessoa que és. Obrigada também pelos momentos de desabafo ao longo destes anos. Espero que consigas aquilo que desejas. Gostava ainda de agradecer em especial ao João Ramalho e ao Luis Almeida por tomarem conta de nós e se preocuparem sempre com o nosso sucesso, e agradecer também à Paula Veríssimo por me ter aceite como orientanda.

Ao longo do meu PhD tantas pessoas passaram e foram importantes e por isso vou fazer uma breve referência a quem cá está e a quem já saiu..

Um beijinho muito grande para o pessoal que me acolheu no IBMC já antes desta minha aventura: Raquel a tua sabedoria e garra são um exemplo; André, nunca percas a tua alegria, o teu conhecimento e força de vontade e Ritinha admiro os teus valores, integridade como a que tens já não se vê por aí. Tália obrigada pelas ajudas técnicas e pelos desabafos, é sempre bom ter um ouvido na porta ao lado. Filipa e Sara, esperava neste momento que estivéssemos juntas para esta nova jornada que se inicia, mas apesar de não ter acontecido, os nosso caminhos acabarão por se cruzar algures no futuro, muita sorte Sara para esta nova etapa, e Filipa não desistas. Obrigada também pelo apoio ao longo destes últimos meses. Quero agradecer também às minhas companheiras de almoço que na sua maioria foram companheiras das aulas de canto: o enorme grupo CAGE e à Rita Seabra. Vocês são tantas que corro o risco deste capítulo ficar maior que a introdução da tese. Vânia e Catarina continuem com a vossa alegria, muita sorte para o resto do vosso PhD; Mafalda Santos és inspiradora, os teus valores e princípios são admiráveis, nunca os percas, e graças a ti agora já não parto os vidros de casa quando canto; Mafalda Pinto, realista e prática, uma excelente mãe, boa sorte para o teu futuro; Carine e Patrícia muita sorte também nesta nova etapa pessoal e obrigada

pela vossa companhia; Mafalda Araújo, uma mulher de coragem que já enfrentou na vida grandes obstáculos, continua assim forte e sempre com espírito positivo e obrigada por seres boa ouvinte; Rita Seabra, companheira de teatro, a tua alegria e boa disposição são contagiantes, nunca percas isso.

Um agradecimento especial aos meus amigos de sempre pelos muitos momentos que temos passado ao longo deste anos, em especial à Iva, Lígia, Susana, Vanessa e Mokas. Obrigada por serem boas ouvintes. Não posso deixar de dar um beijinho a uma pessoa muito especial: Mokas, podes não te aperceber mas és uma mulher muito forte, com garra e determinação, quando pensares que isto falta procura bem. Eu vou estar sempre aqui e sei que tu vais estar sempre aí também. Obrigada também por sempre me apoiares.

Agora chegou a altura do meu Lab, a minha segunda ou muitas vezes primeira casa. Queria deixar um beijinho muito grande à Joana Santos, uma mulher prática e que gosta de viver a vida, obrigada pela companhia. Um beijinho muito grande e especial à Martinha, juntas partilhamos muitos e muitos momentos, muitas risadas, muitos desabafos, ajudas e importantes discussões científicas. Sei que vais chegar longe Martinha, acredita no teu potencial eu sei que ele está aí. O Torcato converteu-se ao desenvolvimento e foi a mais recente "aquisição" do lab. Torcato foste o meu companheiro neste último ano, mas antes disso foste sempre um bom ouvinte, admiro o teu conhecimento, o teu raciocínio e acima de tudo a tua paixão pela genética que é contagiante. Desejo-te toda a sorte do mundo. Durante alguns meses o lab resumiu-se à minha pessoa e ao Paulo. O Paulo foi alguém que contribuiu muito para a minha evolução como pessoa e cientista ao longo deste anos. Admiro-te! O teu conhecimento é imenso, a tua capacidade de assimilação, de raciocínio e discussão são únicas. Obrigada pela pequena parte de conhecimento que me transmitiste, pelo raciocínio científico que me ensinaste, por seres um orientador "raro". Ainda tinha tanto para aprender contigo. Desejo muito sinceramente que o teu mérito seja reconhecido, pois seria um desperdício perder um cientista do teu calibre. Muita sorte e um sincero obrigada por tudo. Agradeço também ao Fernando pelas discussões e todo o input científico, acreditem que ao lado do Paulo e do Fernando nos sentimos tão pequeninos, os dois são pessoas excecionais. Um beijinho muito grande aos companheiros da sala das moscas, a conversa e a música ajudavam a passar o dia a dia. Especial beijinho à Sofia Guimarães, à Sara Silva e à Sofia Pinho.

Por último, mas sem dúvida mais importantes que ninguém a minha família. Eles são o pilar da minha vida, estão sempre presentes no bom e no mau. Um agradecimento especial ao Toli. Amor obrigada pelo apoio incondicional em tudo. Obrigada por todas as esperas intermináveis à porta do instituto, por seres compreensivo em todas as noites e fins de semana de trabalho, e em todos os momentos que tivemos de abdicar. Mais importante do que tudo: Obrigada pelo amor que partilhamos. Mãe e Pai, obrigada a vocês também por terem feito de mim a mulher que sou, por me terem ensinado bons princípios, e serem um exemplo de força e trabalho. É por vocês que vou batalhar sempre pelo que quero na vida. Amo-vos muito. Um beijinho também ao meu irmão, por ser uma inspiração e um exemplo sempre ao longo da minha vida.

Um Obrigada a todos!

Joana

TABLE OF CONTENTS

Chapter 3 - A targeted RNAi screen identifies a genetic interaction between TGF-β signaling pathway and the nucleolar regulator Viriato during eye development

Chapter 4 - General Discussion

Appendixes

LIST OF FIGURES

CHAPTER 1

CHAPTER 2

CHAPTER 3

CHAPTER 4

LIST OF TABLES

CHAPTER 3

APPENDIX 1

ABBREVIATIONS LIST

AP	anterior/posterior
Babo	Baboon
bHLHZ	basic helix-loop-helix leucine zipper
BMP	Bone morphogenetic protein
BrdU	Bromodeoxyuridine
Dac	Dachshund
dAct	*Drosophila* Activin
DamID	DNA adenine methyltransferase identification
Dark	*Drosophila* Apaf-1 related killer
Daw	Dawdle
DC	Dyskeratosis Congenita
Dcp-1	Death caspase-1
Diap1	*Drosophila* inhibitor of apoptosis1
Dl	Delta
dm	diminutive
dMyc	*Drosophila* Myc
Dpp	Decapentaplegic
DrICE	*Drosophila* interleukin-1-converting enzyme
DV	dorsal/ventral
ETS	external transcribed spacer
Ey	Eyeless
Eya	Eyes absent
Eyg	Eyegone
Fng	Fringe
Gbb	Glass Bottom Boat
GO	Gene Ontology
Hh	Hedgehog
Hid	Head involution defective
hpRNA	hairpin RNA
Hth	Homothorax
i.e.	*Id Est*
ITS	internal transcribed spacer
JAK/STAT	Janus kinase/signal transducers and activators of transcription
JNK	c-Jun N-terminal Kinase
Mad	Mothers against dpp
Mav	Maverick
Med	Medea
MF	Morphogenetic furrow
miRNA	microRNA
Myg	Myoglianin
Opt	Optix
Otd	Orthodenticle
p-Mad	phosphorylated Mad
PI3K	Phosphoinositide 3-kinase
Pol I	RNA polymerase I

Pol II	RNA polymerase II
Pol III	RNA polymerase III
pre-rRNA	precursor ribosomal RNA
Put	Punt
qPCR	quantitative Real-Time PCR
RD	Retinal Determination
rDNA	ribosomal DNA
RNAi	RNA interference
Rp	Ribosomal protein
RpL	Ribosomal protein (Large subunit)
Rpr	Reaper
RpS	Ribosomal protein (Small subunit)
rRNA	ribosomal RNA
Sax	Saxophone
Scw	Screw
SEM	Scanning electron microscopy
Ser	Serrate
Smo	Smoothened
snoRNP	small nucleolar ribonucleoproteins
So	Sine oculis
Stg	String
TEM	Transmission electron microscopy
TGF-β	Transforming growth factor beta
Tkv	Thickveins
Toe	Twin of eyegone
TOR	Target of rapamycin
Toy	Twin of eyeless
Tsh	Teashirt
Upd	Unpaired
Vito	Viriato
Wg	Wingless
Wit	Wishful thinking
Yki	Yorkie

ABSTRACT

A precise coordination between cell growth, proliferation, differentiation and apoptosis is required in the development of multicellular organisms. In recent years several key signaling pathways regulating cell and tissue growth have been identified, in particular using genetic studies in *Drosophila melanogaster*. The mechanisms by which cells integrate positional and identity information to control core growth events during development remain poorly understood, but some of these basic functions are carried out by the nucleolus. The nucleolus is a subnuclear factory whose activity is required beyond ribosome biogenesis for the regulation of cell growth, death and proliferation. In both *Drosophila* and mammalian cells, the activity of the nucleolus is regulated by the basic helix-loop-helix leucine zipper (bHLHZ) transcription factor Myc. Myc is a crucial regulator of cell growth and proliferation, and is frequently deregulated in cancer.

In an ongoing screen to identify novel genes required for proper growth and patterning of the *Drosophila* eye, we have identified *viriato* (*vito*), the sole fruitfly homologue of the vertebrate Nol12 proteins. In this thesis we report the characterization of *vito* function during *Drosophila* development.

In Chapter 2 we report that *vito*/Nol12 plays a crucial role in tissue growth independently of its role in cell survival in the early *Drosophila* eye primordium. During development a decrease in Vito levels induces caspase-dependent apoptosis that is mediated by the three apoptotic genes reaper/grim/hid. We showed that the Vito protein localizes to the nucleolus, regulating the structure and main molecular events of this subnuclear compartment in a dynamic manner. We have further shown that dMyc controls *vito* mRNA levels to regulate nucleolar architecture and that *vito* is required for dMyc to reach its full potential as a potent cell growth inducer.

In Chapter 3 we describe a targeted double RNAi screen performed in order to get a deep knowledge about the pathways working with *vito* during eye development. Further investigation culminated with the identification of a strong genetic interaction between *vito* and TGF-β signaling pathway, in particular with the Dpp signaling pathway. We showed that *vito* plays a dual role during eye development and collaborates with Dpp signaling pathway both in the promotion of tissue growth during early eye development, and in photoreceptor differentiation at a later stage. We have further shown that *vito* regulates Dpp signaling activity in the eye imaginal disc being particularly important for the maintenance of a uniform Dpp signaling in the morphogenetic furrow possibly by the regulation of Tkv levels and *dpp* transcription. Finally, the results of this thesis disclose a novel function for the TGF-β signaling pathway by showing an unpredicted role of this pathway in the regulation of the nucleolar structure and function, which might contribute to a better understanding of the broader roles of the TGF-β signaling pathway during *Drosophila* and mammalian development.

RESUMO

Para um correto desenvolvimento dos organismos multicelulares é necessário que ocorra uma perfeita coordenação entre o crescimento celular, proliferação, diferenciação e apoptose. Nos últimos anos foram identificadas várias vias de sinalização que regulam o crescimento celular e dos tecidos, fundamentalmente recorrendo a estudos genéticos na *Drosophila melanogaster*. Os mecanismos pelo qual as células integram a sua identidade e informação posicional de forma a controlarem os principais eventos de crescimento durante o desenvolvimento continuam a ser pouco conhecidos, no entanto algumas destas funções básicas são asseguradas pelo nucléolo. O nucléolo é uma estrutura presente no núcleo cuja atividade é importante não só para a biogénese dos ribossomas, mas também para a regulação do crescimento celular, proliferação e morte celular. Na *Drosophila* e em células de mamífero a atividade do nucléolo é regulada pelo factor de transcrição bHLHZ Myc. Myc é um importante regulador do crescimento e proliferação celulares e apresenta-se frequentemente desregulado em cancro.

Um *screen* genético com o objetivo de identificar novos genes importantes para um crescimento e arranjo adequados do olho de *Drosophila* levou à identificação do gene *viriato* (*vito*), o único homologo em *Drosophila* das proteínas Nol12 dos vertebrados. Na presente tese encontra-se descrita a caracterização da função de *vito* durante o desenvolvimento da *Drosophila.*

No Capítulo 2 é mostrado que *vito*/*Nol12* tem um papel crucial no crescimento dos tecidos, e que este é independente da sua função na sobrevivência das células no primórdio do olho de *Drosophila*. Durante o desenvolvimento é importante que os níveis de Vito sejam regulados, uma vez que a diminuição da sua expressão induz apoptose que é dependente de caspases e mediada pelos genes reaper/grim/hid. Mostra-se que a proteína Vito localiza-se no nucléolo, regulando a sua estrutura e os principais eventos moleculares deste compartimento nuclear de uma forma dinâmica. É ainda mostrado que dMyc controla os níveis de RNA mensageiro de *vito* de forma a regular a estrutura nucleolar, e que *vito* é requerido para que dMyc alcance todo o seu potencial como um potente indutor de crescimento celular.

No Capítulo 3 é descrito um *screen* genético dirigido de duplo RNAi, que foi realizado com o objetivo de melhor conhecer as vias que cooperam com *vito* durante o desenvolvimento do olho de *Drosophila.* Várias experiências culminaram com a identificação de uma forte interação genética entre *vito* e membros da via de sinalização TGF-β, em particular com a via de Dpp. Mostra-se que *vito* apresenta um duplo papel quando a via de Dpp está comprometida, colaborando com a via no crescimento de tecidos cedo no desenvolvimento do olho, e também mais tarde durante a diferenciação dos fotorecetores. Mostra-se ainda que *vito* regula a atividade da via de sinalização de Dpp no disco imaginal do olho, sendo particularmente importante para a manutenção de uma sinalização de dpp uniforme no *furrow*, possivelmente pela regulação dos níveis de Tkv e da transcrição de *dpp*.

Por último, os resultados desta tese apresentam e sugerem uma nova função para a via de sinalização TGF-β, pois mostram que esta via tem um papel importante na regulação da estrutura e função do nucléolo, o que pode contribuir para uma melhor compreensão das variadas funções desta via durante o desenvolvimento da *Drosophila* e também de mamíferos.

CHAPTER 1

GENERAL INTRODUCTION

CONTENTS

1. A ANIMAL GROWTH/SIZE CONTROL DURING DEVELOPMENT

Why are flies smaller than men? Why are our arms the same size? These and other questions trying to understand animal growth and size control have fascinated Biologists over the years and are still one of the major unsolved problems in Biology. When Darwin was studying the birds collected in the voyage of the Beagle he noticed that bird species varied mainly in beak size and shape. In fact, shape and size differences account for most of the animal diversity seen in Nature. Animal and organ size depends on total cell mass (cell size and cell number) as well as on the amount of extracellular materials (proteins, bones, shells, etc). Increase in cell numbers are what most matters for growth and this depends on cell division and cell death that also contributes to the final size of an organ.

The observation that mature tetraploid Salamanders were similar in size to diploid ones but had half the number of cells, being the volume of tetraploids cells about twice the volume of diploid cells (Fankhauser, 1945), was the first evidence that animals can monitor their final size. Similarly, in *Drosophila*, Santamaria showed that in mosaics of haploid/diploid cells, the haploid cells form a normal sized compartment with more but smaller cells (Santamaria, 1983; Edgar and Orr-Weaver, 2001). Accordingly, manipulating cell proliferation and cell size either by changes in DNA content, altering expression of cell cycle-genes and consequently division rates, or overexpressing genes that regulate growth (as for example the Myc transcription factor) can result in normal sized organs and organisms, pointing to a size regulation mechanism that counts dimensions rather than counting cell divisions (Neufeld et al., 1998; Johnston et al., 1999).

There are two kinds of processes that control the size of an organ: those that operate intrinsically in the organ and the systemic control, as for example hormones and growth factors. Metcalf experiments in the 60's were crucial to differentiate these two processes. In an experiment where multiple fetal spleens were transplanted to a new born mouse he observed that the total mass of all those spleens equals the mass of a normal spleen, suggesting that the control was outside the spleen, therefore their growth was extrinsically controlled (Metcalf, 1964). When the same experiments were done with the thymus he got the opposite result, each transplanted thymus grew to its normal adult size no matter how many thymuses were in the animal, indicating that this organ is subjected to intrinsic size control (Metcalf, 1963). Other experiments also add support to the view that organ size can be determined intrinsically. From early transplantation experiments in Salamanders by Twitty and Schwind, it was observed from the switching

of limbs and eyes transplanted between small and large Salamander species that the transplants grew to the normal size of the donor species (Twitty and Schwind, 1931). They seem to know what size to attain. Similarly, in *Drosophila*, growth control was shown to be largely intrinsic to the organ as when wing imaginal discs (precursor cells of the adult wing) were transplanted to female fly abdomens they grew until reach a normal size (Bryant and Simpson, 1984).

2. *DROSOPHILA MELANOGASTER* AS A MODEL SYSTEM TO STUDY GROWTH

Drosophila melanogaster has been widely used as a model organism to study several problems in Biology, being the primary reason due to the genetic tractability of the fly, and the existence of multiple techniques allowing for a precise modulation of gene activity during development. In *Drosophila* it is possible to generate clones of cells of a given genotype within a normal tissue environment, by mitotic recombination, either lacking a particular gene of interest, or harboring mutations (Xu and Rubin, 1993). Another important genetic tool is the GAL4/UAS system for targeted gene expression in a tissue- and cell-specific manner (Brand and Perrimon, 1993), and more recently combining the latter with the conditional gene inactivation by RNA interference (RNAi) (Fig. 1.1) (Dietzl et al., 2007). The combination of the GAL4 system with the Flp-FRT technology allows the generation of clonal cell populations that efficiently and specifically target the gene of interest, therefore one can determine if a particular gene has a function within that specific cell population. Importantly, studies in *Drosophila* have contributed to clarify several similar mechanisms in higher species due to extensive DNA sequence homology.

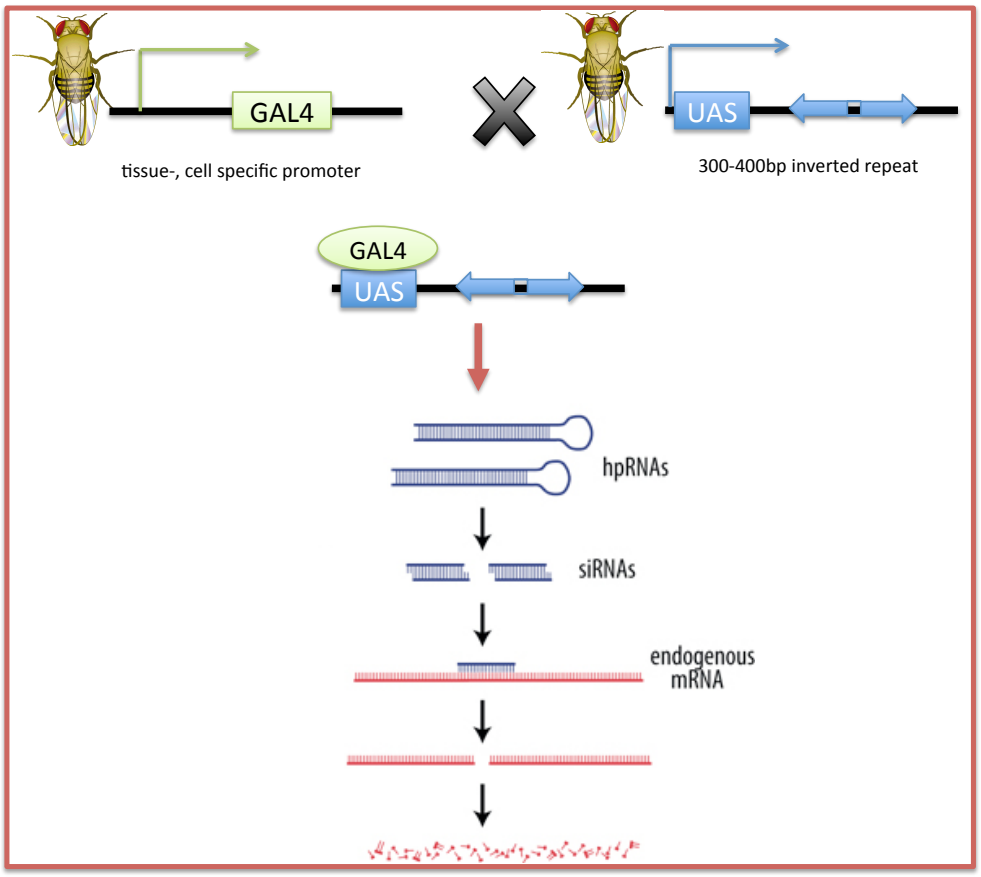

Figure 1.1 – Transgenic RNAi in *Drosophila* using the GAL4/UAS system. The yeast adapted GAL4/UAS system is a two-part system in which a regulatory region that induces GAL4 expression in a temporal and/or spatial pattern comprises one transgenic line, the driver. The GAL4 will bind to the upstream activating sequence (UAS) carried by a second transgenic line, activating the expression of the downstream transgene. In *Drosophila* this system can be used to silence genes by RNAi. Using a tissue- or cell-specific promoter one can drive the expression of a hairpin RNA (hpRNA) in a targeted manner. Once in the cytoplasm the long double stranded RNA is processed by the RNase III enzyme Dicer into several distinct siRNAs that will direct sequence specific degradation of the target mRNA by inducing the RNA-induced silencing complex (RISC) (partially adapted from http://stockcenter.vdrc.at/control/rnailibrary).

Much of the recent work on growth has been carried out using *Drosophila* as model system. *Drosophila* develops from an embryo to an adult in 10 days at 25°C. The most interesting developmental phase for those who study growth is the larval phase. The three larval phases or instars are characterized by a massive increase in weight (about 200-fold increase) where little differentiation occurs. Cells in the imaginal discs, epithelial bilayer structures present in the larvae that will give rise to the adult body structures, proliferate almost exponentially during larval stages undergoing a dramatic increase in mass (Fig. 1.2). On average an imaginal disc grows approximately from 40 to 50000 cells during that period. The eye-antennal imaginal disc is specified during embryogenesis by a group of nearly 20 cells (Garcia-Bellido and Merriam, 1969). During the first two larval stages or instars, the eye-imaginal disc grows almost exponentially to generate a sufficient pool of progenitors necessary for the formation of the adult

structures. Differentiation starts later in development during the third larval instar, when a differentiation wave, the morphogenetic furrow (MF), crosses the eye disc from the posterior to the anterior leading to retina formation (Fig. 1.2) (Ready et al., 1976; Wolff and Ready, 1991a).

Insects do not grow as adults, in contrast to fish for example, that still grows during adulthood, so their final size is a reflection of the duration of the growth period as well as the growth rate during larval phases (reviewed in Edgar, 2006).

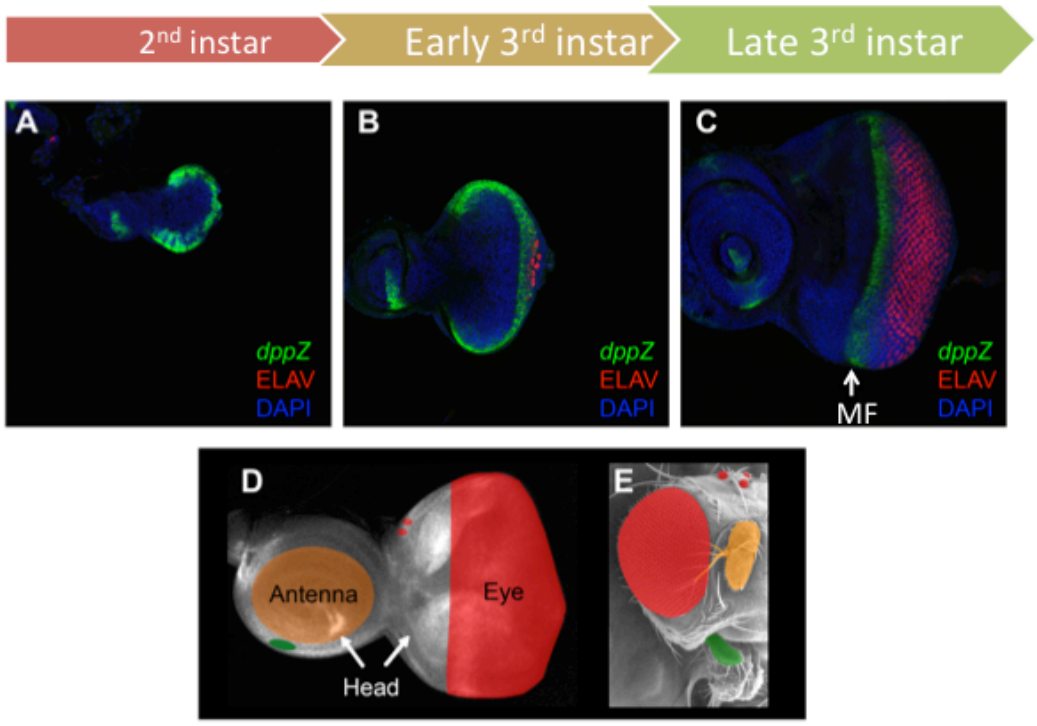

Figure 1.2 – Eye-antennal imaginal disc development. The precursors of the eye imaginal disc are specified during the first 24 hours of development in the embryo. During the first larval instar cell growth and division begins in the disc. In the second instar cell proliferation continues in the disc and dorsal-ventral patterning starts to be established. Decapentaplegic (Dpp), a member of the TGF-β superfamily, is important for eye disc growth and retina differentiation and is expressed at the lateral margins of the disc (*dpp-lacZ*, green) until the MF has passed **(A)**. At 72 hours of larval development the MF initiates at the posterior margin, moves anteriorly, and differentiation begins, as can be seen with the neuronal marker ELAV in red **(B)**. At 120 hours of development the MF has crossed most of the eye field, *dpp* is expressed in the MF (green), and cells anterior to it divide asynchronously **(C)**. The adult *Drosophila* head (E) derives from an epithelial structure the eye-antennal imaginal disc (D). **(D,E)** Fate map of the eye-antennal imaginal disc and the corresponding color-coded structures in the adult head. Orange represents the antenna, photoreceptors and ocellus are represented in red, in green the maxillary palps and in grey the rest of the head cuticle.

3. BASIC GROWTH CONTROL MECHANISMS

3.1 Organ extrinsic size regulation

Environmental stress, temperature and limited nutrient availability have a huge impact on *Drosophila* larval development (Kohane, 1988). It is well known that poorly fed

larvae develop slowly and pupate at an abnormal small size generating a small but normal adult animal, with the pattern unaffected (Robertson and Cohen, 1972; Bryant and Simpson, 1984; Britton and Edgar, 1998).

The insulin receptor/target of rapamycin (InR/TOR) pathway is a conserved signaling cascade that has emerged in the recent years as the major regulator of growth (Oldham and Hafen, 2003; Grewal, 2009). *Drosophila* mutants of the components of the insulin/TOR pathway show a similar pattern to the ones induced by starvation: delayed development, small body size due to fewer and smaller cells but the patterning is normal (Chen et al., 1996a; Leevers et al., 1996; Böhni et al., 1999; Verdu et al., 1999; Weinkove et al., 1999). The central mediator of cellular nutrient sensing is the protein kinase TOR (Oldham et al., 2000; Zhang, 2000), controlling growth mainly by regulation of protein synthesis (translation machinery activity and ribosome production) (Grewal et al., 2007; Hall et al., 2007). TOR kinase is important for each cell to sense its nutrient status, however each organ needs to receive information about the nutritional status of the whole animal in order to coordinate growth between tissues. This role is done by the highly conserved insulin/IGF signaling which acts through the key effector PI3K/AKT pathway that in turn also regulates nutrient sensing by controlling the activity of TOR (reviewed in Hietakangas and Cohen, 2009). Thus the InR/TOR signaling coordinates growth with the animal nutrient status, thereby regulating body size and organism homeostasis.

3.2 Organ intrinsic growth regulation: Focus on the eye disc

Although hormones, nutrients and growth factors have a profound impact on growth as discussed above, several lines of evidence support the idea that intrinsic size regulatory mechanisms are at work in the developing organ. In the case of *Drosophila*, animals with lesions caused by cell-lethal mutations that are undergoing regeneration, pupariation was found to be delayed by the length of time needed for completion of the extra growth in the imaginal discs, and more interestingly the non-regenerating discs stopped growing when they reached the normal size (Simpson et al., 1980). Furthermore, the imaginal disc size control was shown to be mainly disc-autonomous in transplantation experiments from Bryant and Simpson (Bryant and Simpson, 1984). This local autonomy extends at the compartment level since growth of a particular compartment is not affected by significant changes in growth rates of cells of the adjacent compartment (Simpson, 1976; Weigmann et al., 1997; Neufeld et al., 1998) and ultimately give rise to adult structures of normal size and proportion.

3.2.1 Pattern regulators control growth

An important role on the control of growth and patterning in the imaginal discs has been attributed to the gene networks involved in establishing the anterior/posterior (AP) and dorsal/ventral (DV) compartment boundaries (Diaz-Benjumea and Cohen, 1993; Basler and Struhl, 1994; Williams et al., 1994). Some of the organizing activities of the compartment boundaries are mediated by localized expression of Wingless (Wg) or Decapentaplegic (Dpp), Wnt and TGF-β family members respectively, secreted signaling proteins that act as morphogens, i.e., molecules that spread from a localized source, activating target gene expression in a concentration-dependent manner, therefore influencing cell fate and tissue patterning.

Generally, in metazoans, the Transforming growth factor-β (TGF-β) family members include TGF-β, activins, and bone morphogenetic proteins (BMPs). TGF-β signaling is initiated by ligand binding to a multimeric complex of specific type I and type II transmembrane receptors at the cell surface. Then, type I receptors are phosphorylated at a cytoplasmic domain by type II receptors, and the activated type I receptor initiates a signaling cascade by phosphorylation of receptor-regulated Smads (R-Smads). R-Smad binds to the Co-Smad and translocate into the nucleus to activate the transcription of target genes (reviewed in Moustakas and Heldin, 2009).

Several TGF-β molecules have been identified in *Drosophila* belonging to either the BMP or the Activin/TGF-β subfamilies (Parker et al., 2004). At the ligand level, Dpp, Glass Bottom Boat (Gbb) and Screw (Scw) belong to the BMP group and dActivin (dAct), Dawdle (Daw), Myoglianin (Myg) and Maverick (Mav) belong to the Activin/TGF-β group. The type II receptors Punt (Put) and Wishful thinking (Wit) are common to both branches of the pathway, whereas the type I receptors mediate pathway specificity: Thickveins (Tkv) and Saxophone (Sax) for BMP signaling, and Baboon (Babo), the single type I receptor of the Activin pathway. The receptor complexes can phosphorylate the Smads, Mothers against dpp (Mad; BMP branch), and dSmad2 (also known as Smox; Activin branch) that associate with the common co-Smad Medea (Med) to regulate target gene expression (Fig. 1.3).

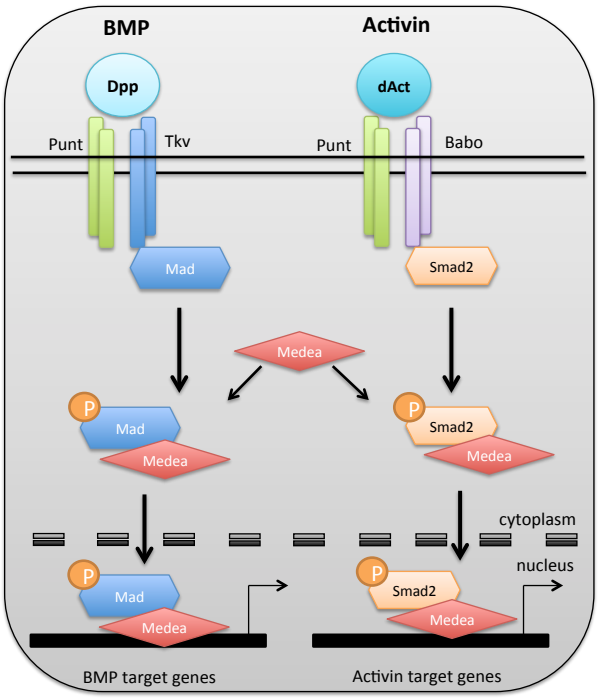

Figure 1.3 – A schematic representation of the *Drosophila* TGF-β signaling pathways. See text for details.

Among the TGF-β family members, the Dpp signaling pathway has been extensively studied and it is the best characterized due to its involvement in a variety of developmental processes in *Drosophila*. Dpp was one of the first molecules showed to be a morphogen defining the spatial pattern of cell fates within a tissue in a concentration-dependent manner. Besides defining patterns, as diffusible, concentration-dependent regulators of gene expression, these molecules can also influence organ size (Zecca et al., 1995; Lecuit et al., 1996; Nellen et al., 1996). Several analyses suggest that both pathways, BMP and Activin, are required for imaginal disc growth.

Mutants of the dAct type I receptor Babo die at a late larval phase, and the one-third population that reach early pupa exhibit small body size. Additionally, the eye imaginal discs of these mutants are 30% smaller whereas overexpression of an activated form of Babo results in larger wings (Brummel et al., 1999). These experiments demonstrate a primary role of the Activin pathway in regulating growth and proliferation in imaginal discs. Recently, it was shown that the Activin pathway might control patterning in the wing by opposing Dpp/Mad signaling (Sander et al., 2010).

Dpp signaling has been considered to play a double task in the imaginal disc development: growth regulation in addition to patterning. This was demonstrated by several experiments in the wing and eye imaginal discs. A lower production of Dpp in the wing discs leads to a severe reduction in wing size (Spencer et al., 1982; Zecca et al., 1995). Similarly, mutations that decrease Dpp expression in the eye primordia resulted in reduced eyes (Masucci et al., 1990; Blackman et al., 1991; Heberlein et al., 1993; Chanut

and Heberlein, 1997a). Furthermore, clones of cells mutant for the Dpp receptors, Tkv or Put, or for the downstream component Mad fail to proliferate and are ultimately eliminated (Burke and Basler, 1996). Conversely, ectopic expression of Dpp or an activated form of Tkv in clones can provide additional growth and redesign the wing (Capdevila and Guerrero, 1994; Zecca et al., 1995; Burke and Basler, 1996; Lecuit et al., 1996; Nellen et al., 1996). In the wing, Dpp is produced along the AP boundary and its overexpression has a huge effect on growth in the anterior and posterior compartments of the wing that do not generally receive high levels of Dpp, leading to the formation of ectopic winglets (Capdevila and Guerrero, 1994; Zecca et al., 1995). This effect is more pronounced when Dpp is overexpressed near the DV boundary, where Wg is also expressed (Zecca et al., 1995).

Importantly, there is increasing evidence that Activin and Dpp pathways might collaborate in the control of cell proliferation during tissue growth. Both pathways seem to regulate proliferation in *Drosophila* brain as, similarly to *babo* mutants, *dpp* loss-of-function mutations show a reduction in the size of the optic lobes due to a reduced rate of proliferation (Kaphingst and Kunes, 1994; Yoshida et al., 2005; Zhu et al., 2008). Additionally, eye imaginal discs of *babo* mutants show ectopic proliferation near the MF, which is also observed in *tkv* mutants, suggesting that Activin pathway could also be required for G1 arrest within the MF (Horsfield et al., 1998; Zhu et al., 2008).

Similarly to Dpp, Wg appears to regulate growth: less Wg signaling either by mutations in the *wg* gene or in Wg receptors induces a reduction in the wing or in the clone size (Sharma and Chopra, 1976; Couso et al., 1994; Chen and Struhl, 1999), whereas ectopic Wg can induce supernumerary wings (Ng et al., 1996) or clone overgrowths (Diaz-Benjumea and Cohen, 1995). In the eye disc, excess of Wg signaling was shown to promote overgrowths and its loss induces a reduction in the disc size (Ma and Moses, 1995; Treisman and Rubin, 1995; Lee and Treisman, 2001).

The fact that proliferation in the imaginal discs seems to occur uniformly particularly during periods of rapid growth in the first and second larval instars, and the lack of any obvious proliferation pattern (as BrdU incorporation or phospho-Histone3 expression) in the wing imaginal disc, supports the view that these patterning morphogens do not act directly to promote growth (Fig. 1.4) (Adler and MacQueen, 1984). Additionally, the proliferation patterns do not directly reflect the regions where Wg and Dpp are expressed (Fig. 1.4). How morphogens influence organ growth has been the subject of intense study, but a detailed understanding has yet to be achieved (reviewed in Schwank and Basler, 2010; Wartlick et al., 2011a).

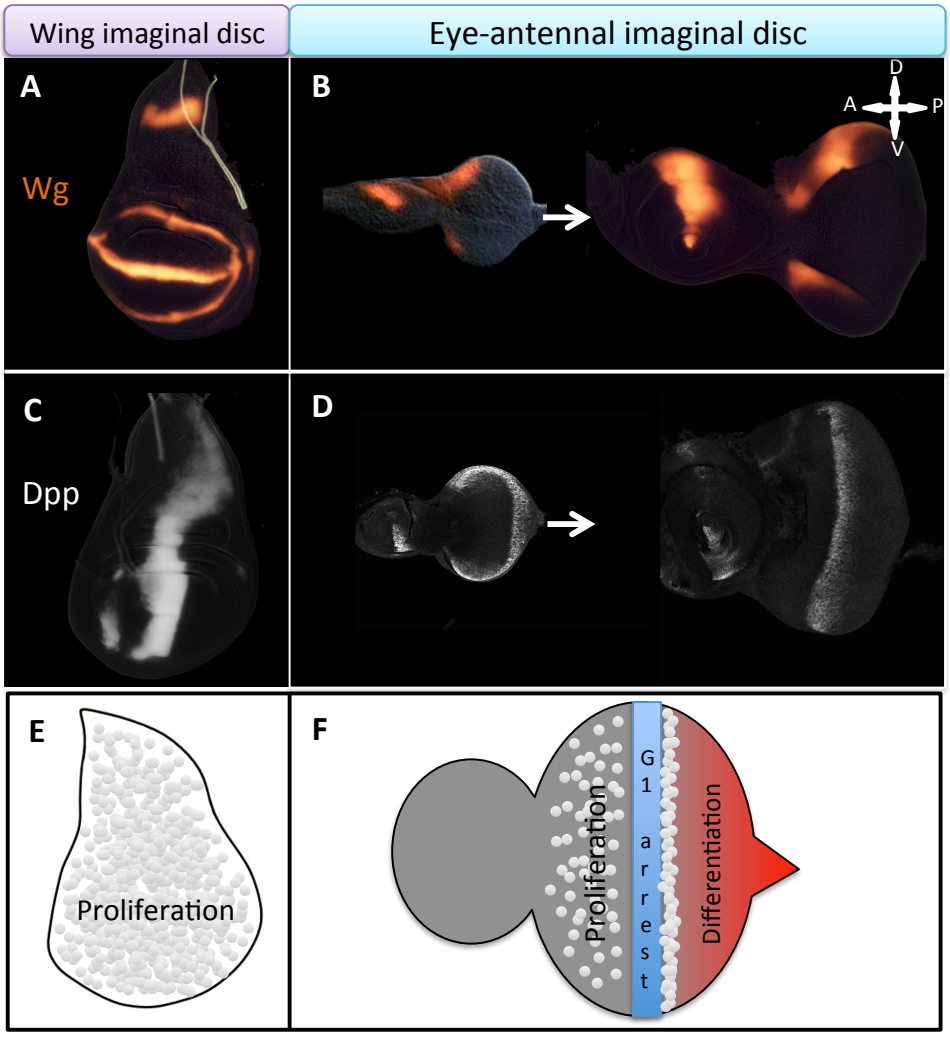

Figure 1.4 – Developmental signaling pathways in the wing and eye imaginal discs control cell proliferation and tissue growth. Wing (left) and eye (right) imaginal discs express Wg (A,B) and Dpp (C,D) in restricted patterns. In the third instar wing imaginal disc Wg is expressed along the DV boundary and in two concentric rings around the wing pouch **(A)**, whereas in the eye imaginal disc Wg is expressed along the anterior dorsal and ventral margins at the beginning of the third instar (image adapted from Niwa et al., 2004) and later in this stage the dorsal domain becomes larger **(B)**. Dpp is expressed in a stripe of anterior cells adjacent to the AP border in wing imaginal discs of third instar larva **(C)**, and in the eye, in early third instar discs, it is expressed at the margins and after initiation of differentiation becomes restricted to a stripe of cells within the MF **(D)**. The proliferation patterns in the wing **(E)** and eye **(F)** imaginal discs are schematically represented in the lower panel. Scattered grey dots represent random BrdU incorporation. In the eye imaginal disc the band of grey dots marks the synchronous incorporation of BrdU along the second mitotic wave.

There are several models trying to address the question on how a gradient can drive uniform growth. For example, it has been suggested that the slope of the morphogen gradient regulates growth during development, therefore growth would be controlled by the differences in Dpp signaling between neighboring cells (Day and Lawrence, 2000; Rogulja and Irvine, 2005). Theoretical models on the role of mechanical forces on growth control were also developed, leading to the idea that Dpp would drive uniform proliferation once its levels are above a certain threshold and that mechanical

stress, as cell compression, would be the restraining factor by limiting growth (Shraiman, 2005; Aegerter-Wilmsen et al., 2007; Hufnagel et al., 2007). However the idea that the Dpp gradient is required for driving growth was rebutted when a study showed that the wing can grow without a Dpp gradient (Schwank et al., 2008). In this study, when the Dpp gradient was replaced by a spatially uniform Dpp signaling, the lateral regions of the wing disc proliferated more than medial regions (Schwank et al., 2008). As these regions were facing the same levels of Dpp signaling, it was hypothesized that an additional gradient of a growth repressor might also exist. In 2011 two novel studies attempted to address this issue. According to Schwank *et al.* Dpp and Fat (a growth suppressor and upstream regulator of the Hippo/Warts pathway) regulate growth in a complementary manner, Fat opposing the growth promoting effect of Dpp in the medial region of the wing where the morphogen signaling is highest (Schwank et al., 2011). Wartlick *et al.* claim that cells control growth by considering the relative temporal variation in Dpp activity. The study shows that the Dpp gradient scales with tissue size so that, on average, a cell divides when Dpp concentration and activity have increased by 50% since the beginning of the cell cycle (Wartlick et al., 2011b). Wartlick's study establishes Dpp as a genuine growth factor, but whether the effect of Dpp in regulating uniform growth is mediated by Fat-Hippo signaling was not addressed in the study. However it is possible that adjacent cells measure the spatial differences in Dpp using the Fat-Hippo signaling, as Dachs (a myosin-related protein, member of the Fat-Hippo pathway) localizes between adjacent cells where differences in Dpp signaling are maximal (Rogulja et al., 2008).

3.2.1.1 Regulation of growth and patterning in the eye imaginal disc

In the eye imaginal disc the early stages of development, first and second larval instars, are crucial to study growth because most cells in the disc are actively proliferating. In the eye disc, the Notch signaling pathway plays an important role in promoting growth. During the second instar, when DV patterning is being established in the disc by the asymmetric expression of the *Iro-C* complex genes (Fig. 1.5A), localized Notch activation along the DV boundary together with its downstream target *eyegone* (*eyg*) was shown to drive global eye disc growth (Cho and Choi, 1998; Domínguez and de Celis, 1998; Papayannopoulos et al., 1998; Chao et al., 2004; Dominguez et al., 2004). Loss of Notch signaling blocks growth and results in a complete failure in eye development, while in contrast, constitutive activation leads to tissue overgrowth causing hyperplastic eye-antennal discs (Cho and Choi, 1998; Domínguez and de Celis, 1998; Papayannopoulos et al., 1998; Reynolds-Kenneally and Mlodzik, 2005). Similarly *eyg* loss-of-function mutants

show a reduction or absence of the adult eye, with the eye-imaginal discs being very small already in the early third instar, before photoreceptor differentiation. Moreover gain of *eyg* was shown to fully revert growth defects in Notch mutants (Jang et al., 2003).

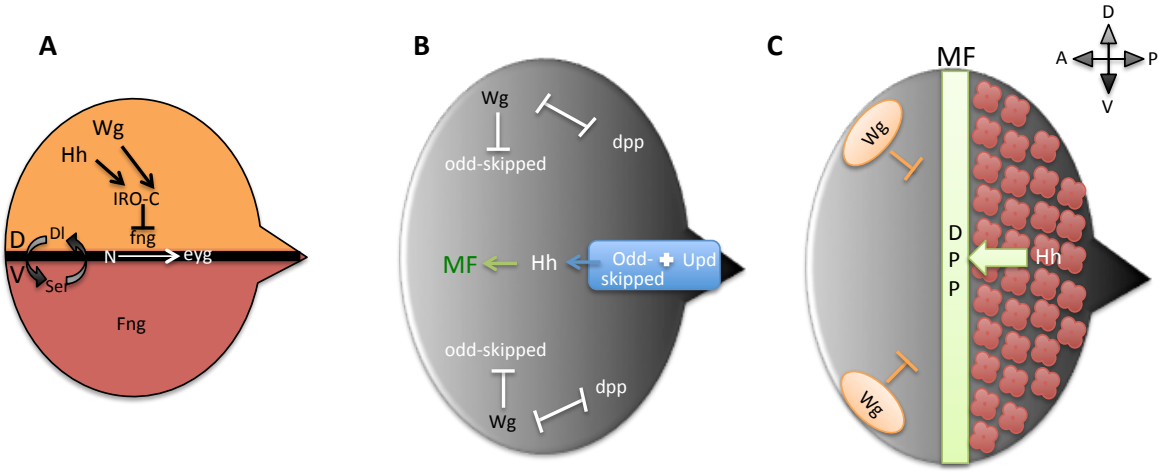

Figure 1.5 – Initiation and propagation of the morphogenetic furrow. (A) Schematic representation of a second instar eye imaginal disc illustrating DV patterning. Before MF initiation *wg* expression on the dorsal side of the eye disc together with Hh leads to the activation of *Iro-C* genes in the dorsal compartment. The *Iro-C* genes repress *fringe* (*fng*) and the boundary of *fng* expression together with the restriction of Notch ligands Delta (Dl) to the dorsal compartment and Serrate (Ser) to the ventral one, leads to Notch activation in the midline. Dl signals to activate Ser expression via Notch, and in turn Ser expression in the ventral compartment signals to induce Notch-dependent activation of *Dl* transcription. **(B)** The initiation point of the MF is restricted to the intersection of the posterior margin and the midline by Dpp, Hh, JAK/STAT and Wg. At this point of intersection the odd-skipped family genes induce Hh expression, this way driving retina differentiation. **(C)** Later in development progression of the MF is driven by the cooperation between Hh and Dpp signaling pathways. Hh present in differentiating photoreceptors behind the furrow signals to cells at the anterior edge of the furrow to express *dpp* and Wg expression in the dorsal and ventral anterior regions of the disc prevent differentiation in that region, leading to head cuticle formation. MF, morphogenetic furrow.

Activation of the Janus kinase/signal transducers and activators of transcription (JAK/STAT) signaling pathway is also important to drive global tissue growth. Mutants for the ligand *unpaired* (*upd*) have small eyes, while overexpression leads to eye overgrowth (Bach et al., 2003; Tsai and Sun, 2004). This pathway seems to act in conjunction with Notch and *eyg* in the midline to promote eye disc growth, however whether *upd* is upstream or downstream of Notch remains under debate (Chao et al., 2004; Reynolds-Kenneally and Mlodzik, 2005; Gutierrez-Aviño et al., 2009).

In the eye disc Wg promotes head capsule fate and restrict eye specification, maintaining proliferation of the undifferentiated eye disc cells that continue to express anterior markers (Lee and Treisman, 2001). However, Dpp has a distinct role: early in eye imaginal disc development it also promotes growth and cell survival, but later on it switches its function to induce a developmentally regulated cell cycle arrest in the G1 phase, and neuronal photoreceptor differentiation. During the first instar larvae, *wg* and *dpp* are already expressed in the eye-antennal imaginal disc, as well as the Retinal

Determination (RD) genes, however Wg signal keeps the retinal determination pathway repressed, which in turn is promoted by Dpp (Kenyon et al., 2003). Consequently eye specification only starts when the disc reaches a certain size, being the increase in disc size very important for eye specification (Kenyon et al., 2003). The disc growth is promoted essentially by Notch-Eyg-Upd and is crucial to place Wg and Dpp expression domains away from each other, in order to start early retinal gene expression and therefore eye specification.

Later in development, Notch, Dpp and Hedgehog (Hh) promote the initiation of the furrow and consequently differentiation, whereas Wg acts as an inhibitor (Treisman and Rubin, 1995; Chanut and Heberlein, 1997b; Domínguez and Hafen, 1997; Borod and Heberlein, 1998; Curtiss and Mlodzik, 2000). During the first two instars *wg* is expressed in a dorsal domain and prior to MF initiation it becomes restricted to the anterior dorsal and ventral margins. *dpp* is expressed along the posterior margin of the eye disc together with *hh* and following retina differentiation it becomes restricted to a stripe of cells within the furrow (Fig. 1.4) (Masucci et al., 1990; Blackman et al., 1991). Hh regulates *dpp* expression and moreover, *dpp* positively regulates its own expression at the eye disc margin (Heberlein et al., 1993; Heberlein et al., 1995; Chanut and Heberlein, 1997b). An important role for Wg is to prevent ectopic MF initiation from the lateral margins by inhibiting Dpp activity, and also by blocking the transcriptional activation of the odd-skipped family genes, and consequently *hh* expression (Ma and Moses, 1995; Treisman and Rubin, 1995; Baonza and Freeman, 2002; Bras-Pereira et al., 2006). Loss of Wg induces *dpp* expression and a MF initiates at the dorsal margin, conversely ectopic Wg can block initiation and progression of the MF (Ma and Moses, 1995; Treisman and Rubin, 1995).

Ectopic Dpp signal leads to an ectopic MF initiation and retina development from the anterior margin and blocks *wg* expression (Chanut and Heberlein, 1997b; Pignoni and Zipursky, 1997). By contrast, large clones mutant for *dpp* or for its downstream components fail to differentiate when they contact with the posterior margin, suggesting that Dpp signaling is indeed required for furrow initiation (Burke and Basler, 1996; Wiersdorff et al., 1996). Pointing to a joint role in furrow progression, clones double mutant for *Mad* or *tkv* and the Hh receptor encoded by *smoothened* (*smo)* do not show photoreceptor differentiation (Greenwood and Struhl, 1999; Curtiss and Mlodzik, 2000). Thus it seems that Wg and Dpp function antagonistically during eye development, Wg acting to prevent MF initiation prematurely and anterior in the eye disc (Fig. 1.5B,C).

3.2.1.2 Growth control by the Retinal Determination Genes

A genetic network of evolutionary conserved transcription factors provides the basis for eye development in flies and vertebrates. The specification of the eye is controlled by the core RD genes: the Pax6 genes *eyeless* (*ey*) and *twin of eyeless* (*toy*); the SIX family member *sine oculis* (*so*), a tyrosine phosphatase *eyes absent* (*eya*) and a distant relative of the Ski/Sno family of proto-oncogenes, *dachshund* (dac), all of them encoding nuclear factors. Other members of this RD gene network are also important for eye specification: the Pax genes, *eyg* and *twin of eyegone* (*toe*); the Six family gene, *optix* (*opt*); a homeobox containing transcriptional co-activator *homothorax* (*hth*) and the transcription factor with multiple zinc-finger DNA binding domains *teashirt* (*tsh*) (reviewed in Kumar, 2010). They were initially grouped together because of their ability to induce the program of retina development when ectopically activated in non-retinal tissues (Halder et al., 1995; Bonini et al., 1997; Chen et al., 1997; Shen and Mardon, 1997; Weasner et al., 2007). However the expression of the RD genes within imaginal discs is not capable of transforming an entire tissue, and only a small number of cells can acquire an eye fate (Salzer and Kumar, 2010). Conversely its loss-of-function results in a strongly reduced or absent eye due to a strong reduction in eye disc size (Bonini et al., 1993; Cheyette et al., 1994; Mardon et al., 1994; Quiring et al., 1994; Serikaku and O'Tousa, 1994). These genes regulate eye development in a complex regulatory network (Fig. 1.6).

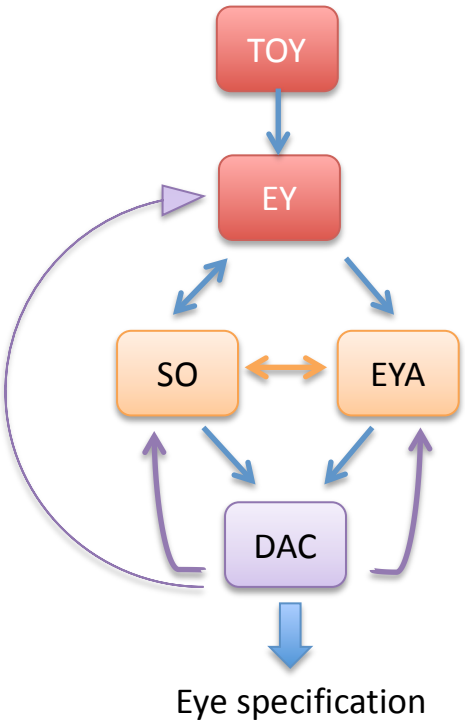

Figure 1.6 – Diagram representing the core retinal determination gene network known to establish eye fate. *toy* is genetically upstream of *ey*. Transcription of *so*, *eya* and *dac* is responsive to *ey* expression. The So-Eya complex is able to induce *dac* expression as well as feeding back to regulate *ey* expression. Although genetically downstream, *dac* is able to induce *ey* when ectopically expressed in the antenna, and loss of *dac* in the eye margin leads to loss of both *so* and *eya* expression.

Some of these RD genes were also shown to regulate growth in addition to their role on eye specification. Clones of *so* or *eya* mutant cells overproliferate if induced at an early stage of development, suggesting a role of these genes in controlling proliferation in the eye primordium (Pignoni et al., 1997), which was additionally confirmed by the positive regulation, at the transcriptional level, of the cell cycle regulatory gene *string* (*stg*) by Eya and So (Jemc and Rebay, 2007). The highly proliferative state of the anterior cells in the disc is maintained by *hth* and *tsh* which cooperate with *ey*, to prevent the expression of the retinal determination genes *eya*, *so* and *dac* (Baonza and Freeman, 2002; Bessa et al., 2002; Singh et al., 2002). Tsh and Hth, which are expressed in the anterior undifferentiated cells of the eye disc, were also shown to promote growth in the developing eye by stimulating cell proliferation and protecting eye progenitor cells from apoptosis (Pichaud and Casares, 2000; Bessa et al., 2002; Singh et al., 2002; Peng et al., 2009). Cells mutant for *hth* do not survive in the anterior region of the eye disc, while cells overexpressing *tsh* overgrowth (Pichaud and Casares, 2000; Bessa et al., 2002; Singh et al., 2002). Moreover, clones overexpressing *hth* repress the cell cycle regulator *stg* (Lopes and Casares, 2009), and in addition it was shown that Tsh and Hth promote tissue growth by directly interacting with Yorkie (Yki) (Peng et al., 2009), the transcriptional co-

activator downstream of the Hippo tumor suppressor pathway, an important cell proliferation control pathway in *Drosophila* and mammals (Dong et al., 2007). Indeed, Hth physically interacts with Yki and together bind to an enhancer within the microRNA (miRNA) *bantam* activating its expression in eye imaginal disc cells (Peng et al., 2009). *bantam* was previously shown to both promote proliferation and prevent apoptosis by inhibiting expression of the pro-apoptotic gene *hid* (Brennecke et al., 2003). This Hth-Yki regulation of *bantam* uncovers a mechanism used by some of the RD genes to promote growth in the developing eye.

During the last years the Hippo pathway has emerged as an important growth control pathway, regulating transcription through its mediator Yki (reviewed in Halder and Johnson, 2011). Several Yki targets have been identified, including genes that promote growth, as the miRNA *bantam*, the cell cycle progression genes Cyclins B and E, and the inhibitor of apoptosis *diap1*. Recently, two independent studies identified the proto-oncogene Myc as a novel transcriptional target of Yki (Neto-Silva et al., 2010; Ziosi et al., 2010). Neto-Silva and co-workers showed that Yki requires Myc function to drive growth, as the growth capacity of Yki-overexpressing cells was abolished in a *dmyc* mutant background (Neto-Silva et al., 2010). Moreover, it was also shown that Myc negatively regulates Yki expression and this negative feedback regulation is proposed to balance growth, limiting the overall growth of the tissue (Neto-Silva et al., 2010). Overall, these results show that tissue-specific determination genes regulate growth in combination with the Hippo pathway, and identify Myc as a critical downstream target of the pathway, which drives basic cell growth and metabolism events as ribosome biogenesis.

3.3 Growth effectors: Focus on Myc

Tissue and organ growth ultimately occurs at the cellular level. A large effort has been placed in the detailed characterization of the genes and pathways that control growth at the cellular level. For the focus of this thesis I will discuss one of the most extensively studied genes and major growth regulator, the proto-oncogene Myc. The transforming principle of avian retroviruses, which were shown to promote a spectrum of tumors in chickens, was identified as the oncogene *v-myc* (viral avian myelocytomatosis). The human homologue c-MYC was later identified and shown to be frequently deregulated in various human tumors. Extensive research in vertebrates lead to the identification of a complex network that includes the transcriptional activators (c-, N-, L-MYC) and functional antagonists (Mxi/Mnt/Mad) all of them heterodimerize with the

partner protein Max through the bHLHZ domains to bind canonical (CACGTG) or non-canonical (CACATG) E-box sequences in DNA (reviewed in Meyer and Penn, 2008).

The Myc proto-oncogene is one of the most commonly activated oncogenes and is estimated to be involved in 20% of all human cancers (Dang et al., 2006). Despite its activity as an oncogene it also regulates a variety of other cellular process as cell cycle, cell growth, apoptosis, among others (Fig. 1.7), and this is mainly due to its role as a transcription factor, which is likely to control 15% of genes in genomes from flies to humans (Orian et al., 2003; de la Cova and Johnston, 2006; Meyer and Penn, 2008). Genome-wide approaches, like microarrays, DamID chromatin profiling and chromatin immunoprecipitation have contributed much to the increased knowledge about novel Myc targets. The major fraction of Myc targets include genes involved in ribosome biogenesis, translation and metabolism, and more recently it was shown that Myc also regulates genes encoding miRNAs and non-coding RNAs involved in those processes (Orian et al., 2003; Schlosser et al., 2003; Grewal et al., 2005; O'Donnell et al., 2005; Dang et al., 2006; Pierce et al., 2008; Bui and Mendell, 2010).

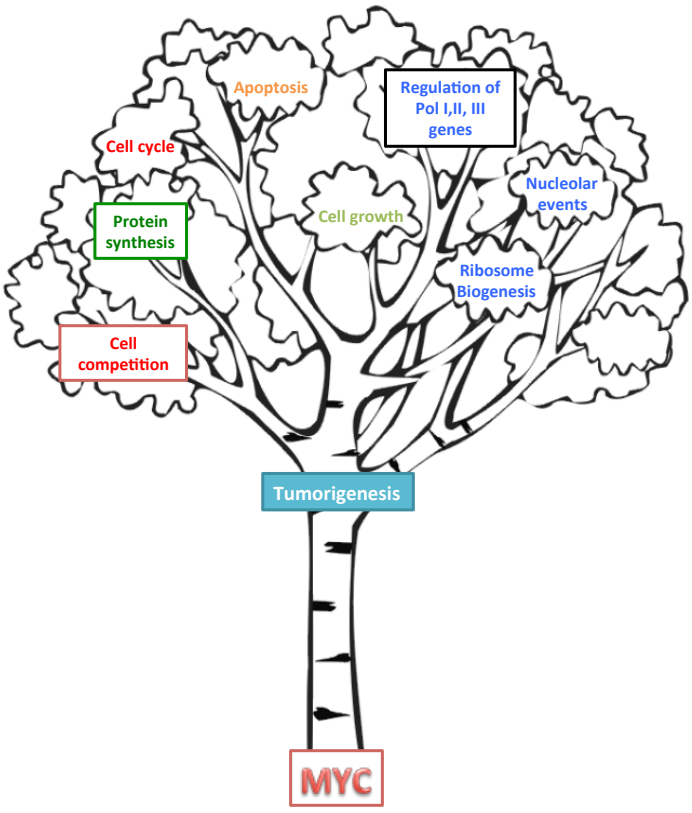

Figure 1.7 – Myc's different biological activities (partially adapted from Meyer and Penn, 2008).

Studies in *Drosophila* have made an enormous contribution to the understanding of Myc function. The first *Drosophila* Myc mutant was identified as a spontaneous

mutation that resulted in smaller body size and because of that feature was called *diminutive* (Bridges, 1935). *Drosophila* is a great model to study Myc because, in contrast to the multiple Myc vertebrate genes, it contains only one gene coding for Myc (called dMyc or *diminutive*, in short *dm*), a single repressor (called Mnt), and their common partner Max (Gallant et al., 1996; Schreiber-Agus et al., 1997), offering less redundancy. Moreover, vertebrate and *Drosophila* Myc proteins can partially substitute each other. dMyc was shown to transform primary mammalian cells and rescue proliferation defects in *c-myc-null* fibroblasts (Schreiber-Agus et al., 1997). Conversely, the human c-MYC protein can rescue lethal mutations of *dmyc* (Trumpp et al., 2001; Benassayag et al., 2005).

3.3.1 Biological activities of Myc: Growth Control

Myc plays a crucial role in the control of growth and animal size. As mentioned above, *Drosophila* Myc weak hypomorphic mutants identified by Bridges had a characteristic small body size. Years later additional Myc mutations were identified and confirmed Bridges observations: it was shown that flies carrying the dMyc dm^4 null mutant allele died very early in development, at the beginning of the second instar (Pierce et al., 2004). Additionally, flies carrying hypomorphic Myc alleles exhibited delayed development, but they eventually reached adulthood as small (due to smaller and in some cases fewer cells) but yet proportioned flies, with short and thin bristles (Gallant et al., 1996; Johnston et al., 1999). Conversely, overexpression of dMyc in clones of the diploid imaginal disc cells resulted in larger clones due to larger cells, without changes in clone cell numbers (Johnston et al., 1999), and ubiquitous expression of dMyc yields a 30% increase in weight of the adult flies (de la Cova et al., 2004). A very dramatic effect is observed in the endoreplicating tissues of the *Drosophila* larva. These tissues are essential for larval development and are composed of cells that grow without dividing, reaching polyploidy and dramatically increasing in size (reviewed in Edgar and Orr-Weaver, 2001). Myc mutants affect cell growth and endoreplication of these cells producing smaller larvae, whereas overexpression of Myc results in a dramatic increase on the cell and nucleolar size (Maines et al., 2004; Pierce et al., 2004; Demontis and Perrimon, 2009).

Similarly in vertebrates Myc is also involved in growth regulation: *c-myc* null mice die between 9.5 and 10.5 days of gestation as generally smaller and retarded in development with a variety of developmental defects and pathologic abnormalities (Davis et al., 1993). However, initially the mechanism appeared to be different from flies.

Despite the fact that, like *Drosophila*, mice carrying strong hypomorphic alleles of *c-myc* also show a smaller body and organ size, this seems to be the result of fewer cells (cell death) rather than a reduction in cell size, as several tissues exhibit a normal cell size even in the strongest hypomorphic *c-myc* mouse (Trumpp et al., 2001). *Drosophila* dMyc hypomorphic mutants also show fewer cells, however these cells are smaller (Johnston et al., 1999). As a consequence Trumpp *et al.* suggested there might be central differences in the mechanisms by which mammals and insects control body size. However, other studies reported that tissue specific inactivation of Myc (null mutations) in mice could result in a reduction of keratinocyte cell size (Zanet et al., 2005), as well as hepatocyte cell size (Baena et al., 2005). These differences could be explained by the intrinsic nature of the system used (hypomorphic vs. null *c-myc* alleles) or different tissue-regulatory mechanisms. In flies, overexpression of Myc induces tissue growth by promoting enlargement of the cells. These cells proceed quickly through G1, but compensate with a longer G2 phase dividing at normal rates. Thus the differences observed between mice and flies could reflect a difference in the coupling of cell growth and cell proliferation rather than a fundamental difference in the function of the fly and mice Myc proteins.

From these series of experiments it is clear that Myc is crucial to regulate growth, and in the next section we will address the molecular mechanisms underlying this function.

3.3.2 Myc as a regulator of ribosome biogenesis and nucleolar events

Cell growth requires an impressive number of the factories that carry out protein synthesis, the ribosomes. Thus, ribosome biogenesis reflects the cell capacity to grow. In eukaryotes, this process occurs sequentially in the nucleolus, the nucleoplasm and the cytoplasm. To synthesize all the components required for ribosome biogenesis the activity of all three RNA polymerases (I, II and III) are needed. Ribosome biogenesis requires the initial transcription of rDNA genes by RNA polymerase I (Pol I) in the nucleolus. The initial 47S rRNA precursor transcript (pre-rRNA) is subjected to endonucleolytic and exonucleolytic cleavages into 18S, 5.8S and 28S rRNAs, the structural RNA components of the ribosome. Another structural RNA component 5S is transcribed independently by RNA polymerase III (Pol III) outside the nucleolus. During the co-transcriptional phase, the rRNA undergoes extensive chemical modifications, mainly 2-O'-methylations and pseudouridylations carried out by the small nucleolar ribonucleoproteins (snoRNP). Ribosomal proteins and accessory factors, whose transcription is dependent on the RNA polymerase II (Pol II), are synthesized in the

cytoplasm and are then imported into the nucleus to be assembled into the small and large ribosomal subunits. These assembly steps generate the pre-ribosomal particles. The small pre-40S ribosomal subunit contains 18S rRNA and several ribosomal proteins called RpSs, and the pre-60S large ribosomal subunit is composed of 28S, 5.8S and 5SrRNA and numerous RpLs. These pre-ribosomes are then exported to the cytoplasm for protein translation (Fig. 1.8).

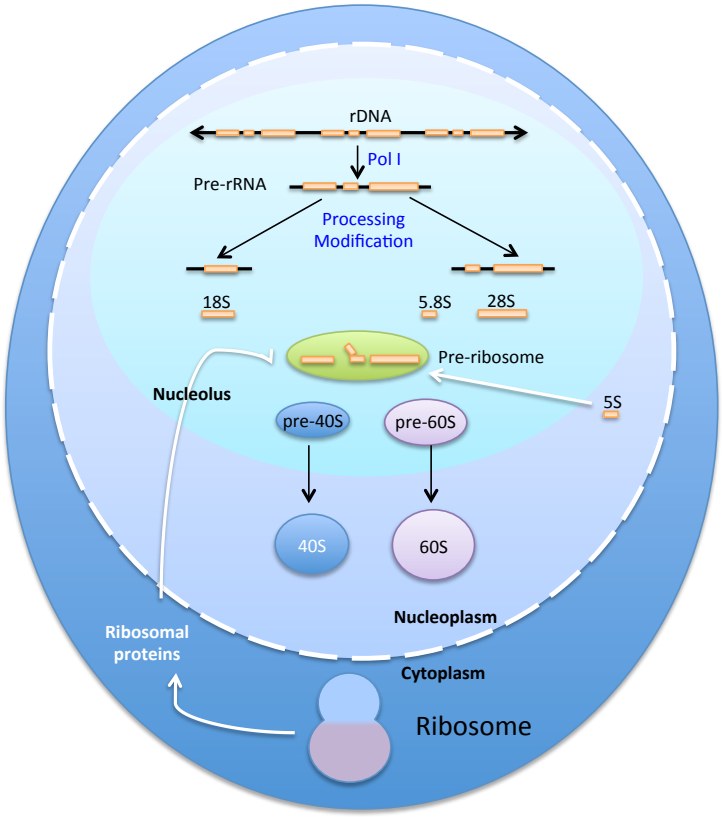

Figure 1.8 – Model of ribosome biogenesis. The biogenesis of ribosomes occurs mostly in the nucleolus, however 5S rRNA synthesis occurs in the nucleoplasm and the synthesis of ribosomal proteins takes place in the cytoplasm. The biogenesis of ribosomes comprises the synthesis of rRNA by Pol I and further processing, synthesis and import of ribosomal proteins into the nucleus, assembly of ribosomal proteins with rRNA and accessory factors and subsequent transport of the mature subunits into the cytoplasm.

The rate of ribosome production correlates with the cell capacity to growth and proliferate. During G1 phase of the cell cycle, an augmented rRNA synthesis and ribosome assembly is a requirement for an increased protein synthesis to allow the cell to double its DNA content (Pardee, 1989). A class of dominant mutants called *Minutes* in *Drosophila* harbor mutations in genes encoding ribosomal proteins. These *Minutes* display similar phenotypes that are characterized by prolonged development, short and thin bristles,

and poor fertility and viability, resulting from reduced number of ribosomes and protein synthesis (Lambertsson, 1998; Marygold et al., 2007).

Thus, interfering with ribosome biogenesis can affect growth, proliferation and consequently animal development. Recently, there has been a significant increase in the number of studies correlating the deregulation of ribosome biogenesis with cellular transformation, either by over-production or haploinsufficiency of ribosomal biogenesis (reviewed in Montanaro et al., 2008; Silvera et al., 2010).

Several lines of evidence point to a role of Myc in ribosome biogenesis, which could explain its role in promoting cell growth. The overexpression of dMyc in *Drosophila* was shown to promote cellular and nuclear growth, and an even more accentuated growth of the nucleolus, suggestive of an increased ribosome activity (Pierce et al., 2004; Grewal et al., 2005). In fact the cytoplasm of these cells was shown to be packed with ribosomes (Grewal et al., 2005). In mammalian cells, Myc was shown to enhance the synthesis of rRNA by Pol I, a rate-limiting step for cellular growth, by binding to rDNA promoters (Arabi et al., 2005; Grandori et al., 2005). In contrast, *Drosophila* rDNA promoters do not contain E-boxes and no dMyc binding to the promoter could be detected. However, in *Drosophila*, dMyc overexpression induces an increase in rRNA transcriptional machinery, such as the basal Pol I transcription factor *Tif-IA*, which was shown to be required for rRNA synthesis, and the Pol I subunit *RPI135* (Grewal et al., 2005; Grewal et al., 2007). dMyc was also shown to be necessary and sufficient to induce a large number of Pol II-dependent ribosomal genes and pre-rRNA processing and modifying enzymes such as *Nop60* and *Fibrillarin*, and to stimulate Pol III transcription (Grewal et al., 2005; Pierce et al., 2008; Steiger et al., 2008; Li et al., 2010). Moreover, the ability of dMyc to induce a coordinated nucleolar hypertrophy, and to stimulate pre-rRNA transcription and ribosome biogenesis in general, was found to be required for dMyc-stimulated growth since when overexpressing Myc in a background mutant for the largest Pol I subunit *RPI135*, the cell size effects of dMyc were significantly reduced (Grewal et al., 2005).

Additionally, in vertebrates, c-MYC increases Pol II-dependent transcription of ribosomal proteins as well as factors involved in the translation machinery (Coller et al., 2000; Guo et al., 2000; Boon et al., 2001; Menssen and Hermeking, 2002). c-MYC was also shown to bind to TFIIIB, a Pol III-specific general transcription factor, directly activating Pol III-mediated transfer RNA and 5S rRNA transcription (Gomez-Roman et al., 2003) and to regulate the efficiency of rRNA processing (Schlosser et al., 2003).

3.3.3 Myc, ribosomes and tumorigenesis

More than a century ago an hypertrophic and irregularly shaped nucleoli was noticed as characteristic of highly transformed cells (Pianese, 1896), providing a diagnostic tool to determine the clinical outcome for cancer malignancy (Derenzini, 2000; Derenzini, 2009). While the hypothesis at that time was that the larger nucleoli could just reflect the higher proliferation rates of these cells, in recent years new data has suggested an active role of ribosome biogenesis in tumorigenesis (Montanaro et al., 2008). An increased protein synthesis capacity of non-transformed cells was correlated with an augmented risk of tumorigenic transformation, as it was shown for the overexpression of the eukaryotic initiation factor subunit 4E (eIF-4E) in rat fibroblasts which induces their malignant transformation (Lazaris-Karatzas et al., 1990; Lazaris-Karatzas et al., 1992) and more recently for the overexpression of the Pol III-specific transcription factor Brf1, which drives tumor formation in mice (Marshall et al., 2008). Importantly, a defect in genes encoding factors involved in ribosome biogenesis cause severe inherited diseases such as Dyskeratosis Congenita (DC) or Diamond–Blackfan anemia characterized by the production of abnormal ribosomes, and the individuals affected by these diseases have an increased risk of developing certain cancers (Heiss et al., 1998; Draptchinskaia et al., 1999). In the case of DC, dyskerin, a component of the snoRNP is affected, which mutations will lead to defects of ribosome biogenesis, resulting from a reduction of rRNA pseudouridylation and decelerating rRNA processing rate (Ruggero et al., 2003). These disorders, commonly named Ribosomopathies, are characterized by defects in ribosome biogenesis or function and can cause anemia and other hematologic phenotypes, defects in growth and development, and congenital abnormalities (reviewed in Narla and Ebert, 2010). Additionally, the acquisition of an aggressive tumor phenotype in human breast cancer cells was shown to be associated with profound alterations in ribosome biogenesis from alterations of the rate of ribosome synthesis to alterations of rRNA processing pathways and translation fidelity, indicating that changes on the process of making ribosomes can also occur later in tumor development (Belin et al., 2009).

The cases described above show examples of alterations to the normal biogenesis of ribosomes as being the cause of neoplastic transformation. In fact, ribosome biogenesis alterations play a central role in tumorigenesis. Several tumor related proteins, such as Myc (described in the previous section) and p53 can play direct roles in ribosome biogenesis (Zhai and Comai, 2000; Hölzel et al., 2010). The capacity of Myc to induce tumorigenesis could be related to its ability to regulate ribosome biogenesis. Recently, in

an elegant study, Barna *et al.* addressed this issue by taking advantage of *Minute* mice, haploinsufficient for the ribosomal proteins RpL24 or RpL38, to genetically restore normal protein synthesis rates in Eμ-Myc transgenic mice (mice model of Myc-induced lymphomagenesis). They were able to demonstrate that, in Eμ-Myc;RpL24$^{+/-}$ and Eμ-Myc;RpL38$^{+/-}$ mice, Myc-overexpression was not sufficient to promote cell growth. In a more striking manner, Myc oncogenic activity, which drives lymphomagenesis in the Eμ-Myc mice model, was suppressed when the protein synthesis was restored to normal (Barna et al., 2008).

p53 is the major mediator of the cellular stress responses in mammalian cells and is frequently impaired in human cancers (Vousden and Lane, 2007). It is usually called the 'guardian of the genome' because of its protective role in cells, since in response to cellular stress p53 is activated to induce cell cycle arrest or apoptosis (reviewed in Levine and Oren, 2009; Vousden and Prives, 2009). Under normal conditions, p53 levels are kept low by the binding to MDM2 and other E3-ubiquitin ligases that control p53 protein activity, stability and subcellular localization. (Haupt et al., 1997; Kubbutat et al., 1997). Besides directly influencing ribosome biogenesis by controlling rRNA synthesis, a role in sensing nucleolar stress has also been suggested for p53 (reviewed in Zhang and Lu, 2009; Deisenroth and Zhang, 2010). A nucleolar stress is defined as an event or condition that can impair nucleolar function and ribosome biogenesis. It was shown that p53 is stabilized and activated after a stress induced in the nucleolus (Pestov et al., 2001; Rubbi and Milner, 2003; Yuan et al., 2005; Donati et al., 2011), and the nucleolus was shown to be a major stress sensor and the pivot in coordinating stress responses with the p53 system (reviewed in Boulon et al., 2010). One explanation is that under nucleolar stress, ribosome biogenesis is inhibited and the free ribosomal proteins enter the nucleoplasm sequestering the MDM2 with subsequent p53 stabilization and activation (Zhang and Lu, 2009). Together with other RPs, the large subunit ribosomal protein RpL11 participates in the p53 nucleolar stress response pathway by binding to MDM2 and sequestering it (Lohrum et al., 2003; Zhang et al., 2003). RpL11 also inhibits c-Myc-mediated activation of target genes limiting Myc-driven proliferation (Dai et al., 2007a; Dai et al., 2007b).

In conclusion, even though alterations in factors involved in the biogenesis of ribosomes have been found in several tumors, in some cases these changes can have a protective role and suppress tumorigenesis, as is the case for RpL11.

3.4 Apoptosis as a mechanism of tissue homeostasis or in response to injuries

During development, cell growth, cell proliferation and cell death mechanisms must be tightly regulated to maintain tissue homeostasis. Apoptosis, or programmed cell death is a genetically controlled process essential for normal development and homeostasis being one of the best examples the sculpting of digits in vertebrate limb bud (Zuzarte-Luís and Hurlé, 2002). During normal development in *Drosophila*, apoptosis plays a central role in tissue homeostasis. In the eye imaginal disc, after pupal formation, it is required for the death of the interommatidial cells for a normal retina to be formed (Wolff and Ready, 1991b), and also during pupal phase it is required for the death of the larval structures (salivary glands, larval midgut) that are no longer needed in the adulthood (Jiang et al., 1997). Apoptosis also has a central role in removing cells in response to injuries. The apoptotic machinery is widely conserved from flies to humans. Most of the apoptosis that occurs in *Drosophila* can be explained by the induction of the three crucial pro-apoptotic genes *reaper* (*rpr), head involution defective* (*hid*, also known as *Wrinkle*) and *grim* (White et al., 1994; Grether et al., 1995; Chen et al., 1996b). Apoptosis is virtually absent in embryos when these three genes are removed, conversely its overexpression induces cell death (White et al., 1994). These genes initiate apoptosis by binding to Diap1 (*Drosophila* inhibitor of apoptosis1) triggering its degradation by ubiquitination, releasing caspases for the execution of apoptosis (Fig. 1.9).

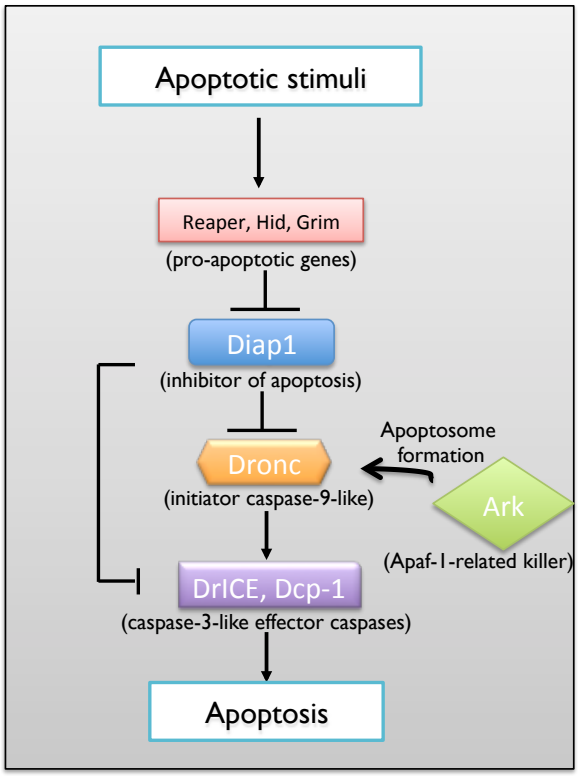

Figure 1.9 – The apoptotic pathway in *Drosophila*. Apoptotic stimuli activate the pro-apoptotic genes Rpr, Hid, and Grim, which promote ubiquitin-mediated degradation of Diap1. Diap1 degradation releases Dronc that then associate with Ark, creating an apoptosome-like structure that activates the downstream effector caspases DrICE and Dcp-1.

Diaps functions as a E3-ubiquitin ligase targeting caspases for degradation. The *Drosophila* genome encodes seven caspase genes, being Dronc (caspase-9-like) the essential initiator caspase (Dorstyn et al., 1999; Xu et al., 2005) that cleaves the two major effector caspases DrICE (*Drosophila* interleukin-1-converting enzyme) and Dcp-1 (Death caspase-1) (Fraser and Evan, 1997; Fraser et al., 1997; Song et al., 1997; Xu et al., 2006). The activation of Dronc requires the adaptor protein Dark (*Drosophila* Apaf-1 related killer), the fly homologue of mammalian Apaf-1, and both can interact to form a multimeric complex that resembles the mammalian apoptosome (Rodriguez et al., 1999; Yu et al., 2006). Despite being the core components of the cell death machinery in *Drosophila*, not all apoptosis can be explained by the function of Dronc, Dark, DrICE and Dcp-1, and it is likely that other caspases or regulatory proteins might play a role in apoptosis as well as in other forms of cell death important during metamorphosis and starvation.

Drosophila imaginal discs can compensate for the massive loss of cells in response to injuries and even form a normal sized organ after 40-60% of the cells have been eliminated (Haynie and Bryant, 1977). This process is termed apoptosis-induced compensatory proliferation (reviewed in Fan and Bergmann, 2008). The *Drosophila* eye has been widely used for apoptotic studies in genetic screens due to the ease of scoring

adult phenotypes and because the retina is very sensitive to perturbations. In terms of the signals that can trigger apoptosis in the *Drosophila* eye, overexpression of p53 induces massive cell death in the developing eye (Jin et al., 2000). p53 is also a key regulator of apoptosis in response to DNA damage (Brodsky et al., 2000; Ollmann et al., 2000). Recently it was shown that *hid* is the main effector of p53-induced apoptosis in the *Drosophila* eye, and *rpr* despite being induced, plays a minor role (Fan et al., 2009).

In *Drosophila*, as well as in mammals, the c-Jun N-terminal Kinase (JNK) pathway plays a crucial role in apoptosis in response to a diversity of cellular and developmental contexts (reviewed in Igaki, 2009). It was shown that discontinuities in Dpp and Wg morphogen gradients can induce JNK-mediated apoptosis (Adachi-Yamada et al., 1999; Adachi-Yamada and O'Connor, 2002). Moreover, the JNK pathway has been implicated in a process named cell competition (reviewed in Johnston, 2009); a process triggered by differences in the growth rates of neighboring cells. However JNK's role in cell competition is not clear: JNK was shown to be essential for the suicide of the slow-proliferating cells (also called 'weaker' cells) (Moreno et al., 2002a), although different studies report that death of the weaker cells can occur in its absence (de la Cova et al., 2004; Tyler et al., 2007). These two processes place JNK with a key role in the regulation of tissue homeostasis. In imaginal discs, *rpr*-induced cell death can be partially rescued by reducing a component of the JNK pathway (Kuranaga et al., 2002). Besides its role downstream of *rpr*, JNK can also function upstream since gamma radiation-induced activation of JNK trigger upregulation of *rpr* (McEwen and Peifer, 2005). By blocking caspases, JNK-mediated cell death was not completely abolished, which pointed to an existence of a caspase-independent pathway (Igaki et al., 2002). This turned out to be true after the identification of the *Drosophila* homolog of the tumor necrosis factor (TNF), Eiger and the characterization of an Eiger-JNK pathway (Igaki et al., 2002; Moreno et al., 2002b). Overexpression of Eiger in the eye imaginal disc activates a Diap-sensitive cell death pathway that does not require caspase activity. Instead, death was mediated by the JNK signaling cascade followed by a transcriptional up-regulation of *hid* (Igaki et al., 2002; Moreno et al., 2002b). This pathway was recently shown to be particularly important for the elimination of oncogenically transformed cells (Ohsawa et al., 2011).

In conclusion, it is clear that for a tissue or organ to reach its final size a tight regulation of cell proliferation, cell growth and division processes are crucial, being cell death also key to the regulation of tissue homeostasis. Nevertheless, in the context of animal development several important questions remain largely open, and in this thesis I aimed to contribute for a deeper knowledge into some of these mechanisms.

4. AIM OF THE THESIS

The goal of this thesis is the study of the uncharacterized *CG32418 Drosophila* gene, named by us as *viriato* (*vito*). This gene was identified in a screen performed in the lab to identify novel gene functions required for proper tissue growth in the developing *Drosophila* eye. My main aim was to progress in the characterization of *vito* molecular and cellular functions during *Drosophila* development, particularly during eye development. I will show that Vito is a nucleolar protein, and consequently I will try to characterize if *vito* regulates the nucleolar structure and/or events that take place in the nucleolus as pre-rRNA transcription and processing.

I will go further and try to understand how a novel nucleolar protein, Vito, functions to regulate cell growth and survival in a context-dependent manner during *Drosophila* development. I will also analyze in molecular and cellular terms why is the function of Vito required downstream of Myc in growth stimulation.

Finally, I will try to characterize *vito* partners in the promotion of growth during eye development by performing an in vivo double RNAi screen. I will further study the identified genetic interaction between *vito* and members of the TGF-β signaling pathway during eye development.

The fact that the processes I will study in this thesis are general during organ development, and taking into account the sequence conservation in Vito/Nol12 protein family members from insects to mammals, the results of this thesis are of general relevance.

5. REFERENCES

Adachi-Yamada, T., Fujimura-Kamada, K., Nishida, Y. and Matsumoto, K. (1999). Distortion of proximodistal information causes JNK-dependent apoptosis in Drosophila wing. *Nature* 400(6740): 166-9.

Adachi-Yamada, T. and O'Connor, M. B. (2002). Morphogenetic apoptosis: a mechanism for correcting discontinuities in morphogen gradients. *Dev Biol* 251(1): 74-90.

Adler, P. N. and MacQueen, M. (1984). Cell proliferation and DNA replication in the imaginal wing disc of Drosophila melanogaster. *Dev Biol* 103(1): 28-37.

Aegerter-Wilmsen, T., Aegerter, C. M., Hafen, E. and Basler, K. (2007). Model for the regulation of size in the wing imaginal disc of Drosophila. *Mech Dev* 124(4): 318-26.

Arabi, A., Wu, S., Ridderstråle, K., Bierhoff, H., Shiue, C., Fatyol, K., Fahlén, S., Hydbring, P., Söderberg, O., Grummt, I. et al. (2005). c-Myc associates with ribosomal DNA and activates RNA polymerase I transcription. *Nat Cell Biol* 7(3): 303-310.

Bach, E. A., Vincent, S., Zeidler, M. P. and Perrimon, N. (2003). A sensitized genetic screen to identify novel regulators and components of the Drosophila janus kinase/signal transducer and activator of transcription pathway. *Genetics* 165(3): 1149-66.

Baena, E., Gandarillas, A., Vallespinós, M., Zanet, J., Bachs, O., Redondo, C., Fabregat, I., Martinez-A, C. and de Alborán, I. M. (2005). c-Myc regulates cell size and ploidy but is not essential for postnatal proliferation in liver. *Proc Natl Acad Sci USA* 102(20): 7286-91.

Baonza, A. and Freeman, M. (2002). Control of Drosophila eye specification by Wingless signalling. *Development* 129(23): 5313-22.

Barna, M., Pusic, A., Zollo, O., Costa, M., Kondrashov, N., Rego, E., Rao, P. H. and Ruggero, D. (2008). Suppression of Myc oncogenic activity by ribosomal protein haploinsufficiency. *Nature* 456(7224): 971-5.

Basler, K. and Struhl, G. (1994). Compartment boundaries and the control of Drosophila limb pattern by hedgehog protein. *Nature* 368(6468): 208-14.

Belin, S., Beghin, A., Solano-Gonzàlez, E., Bezin, L., Brunet-Manquat, S., Textoris, J., Prats, A.-C., Mertani, H. C., Dumontet, C. and Diaz, J.-J. (2009). Dysregulation of ribosome biogenesis and translational capacity is associated with tumor progression of human breast cancer cells. *PLoS ONE* 4(9): e7147.

Benassayag, C., Montero, L., Colombié, N., Gallant, P., Cribbs, D. and Morello, D. (2005). Human c-Myc isoforms differentially regulate cell growth and apoptosis in Drosophila melanogaster. *Mol Cell Biol* 25(22): 9897-909.

Bessa, J., Gebelein, B., Pichaud, F., Casares, F. and Mann, R. S. (2002). Combinatorial control of Drosophila eye development by eyeless, homothorax, and teashirt. *Genes & Development* 16(18): 2415-27.

Blackman, R. K., Sanicola, M., Raftery, L. A., Gillevet, T. and Gelbart, W. M. (1991). An extensive 3' cis-regulatory region directs the imaginal disk expression of decapentaplegic, a member of the TGF-beta family in Drosophila. *Development* 111(3): 657-66.

Böhni, R., Riesgo-Escovar, J., Oldham, S., Brogiolo, W., Stocker, H., Andruss, B. F., Beckingham, K. and Hafen, E. (1999). Autonomous control of cell and organ size by CHICO, a Drosophila homolog of vertebrate IRS1-4. *Cell* 97(7): 865-75.

Bonini, N. M., Bui, Q. T., Gray-Board, G. L. and Warrick, J. M. (1997). The Drosophila eyes absent gene directs ectopic eye formation in a pathway conserved between flies and vertebrates. *Development* 124(23): 4819-26.

Bonini, N. M., Leiserson, W. M. and Benzer, S. (1993). The eyes absent gene: genetic control of cell survival and differentiation in the developing Drosophila eye. *Cell* 72(3): 379-95.

Boon, K., Caron, H. N., van Asperen, R., Valentijn, L., Hermus, M. C., van Sluis, P., Roobeek, I., Weis, I., Voûte, P. A., Schwab, M. et al. (2001). N-myc enhances the expression of a large set of genes functioning in ribosome biogenesis and protein synthesis. *EMBO J* 20(6): 1383-93.

Borod, E. R. and Heberlein, U. (1998). Mutual regulation of decapentaplegic and hedgehog during the initiation of differentiation in the Drosophila retina. *Dev Biol* 197(2): 187-97.

Boulon, S., Westman, B. J., Hutten, S., Boisvert, F.-M. and Lamond, A. I. (2010). The nucleolus under stress. *Molecular Cell* 40(2): 216-27.

Brand, A. H. and Perrimon, N. (1993). Targeted gene expression as a means of altering cell fates and generating dominant phenotypes. *Development* 118(2): 401-15.

Bras-Pereira, C., Bessa, J. and Casares, F. (2006). Odd-skipped genes specify the signaling center that triggers retinogenesis in Drosophila. *Development* 133(21): 4145-9.

Brennecke, J., Hipfner, D. R., Stark, A., Russell, R. B. and Cohen, S. M. (2003). bantam encodes a developmentally regulated microRNA that controls cell proliferation and regulates the proapoptotic gene hid in Drosophila. *Cell* 113(1): 25-36.

Britton, J. S. and Edgar, B. A. (1998). Environmental control of the cell cycle in Drosophila: nutrition activates mitotic and endoreplicative cells by distinct mechanisms. *Development* 125(11): 2149-58.

Brodsky, M. H., Nordstrom, W., Tsang, G., Kwan, E., Rubin, G. M. and Abrams, J. M. (2000). Drosophila p53 binds a damage response element at the reaper locus. *Cell* 101(1): 103-13.

Brummel, T., Abdollah, S., Haerry, T. E., Shimell, M. J., Merriam, J., Raftery, L., Wrana, J. L. and O'Connor, M. B. (1999). The Drosophila activin receptor baboon signals through dSmad2 and controls cell proliferation but not patterning during larval development. *Genes & Development* 13(1): 98-111.

Bryant, P. J. and Simpson, P. (1984). Intrinsic and extrinsic control of growth in developing organs. *Q Rev Biol* 59(4): 387-415.

Bui, T. V. and Mendell, J. T. (2010). Myc: Maestro of MicroRNAs. *Genes & Cancer* 1(6): 568-575.

Burke, R. and Basler, K. (1996). Dpp receptors are autonomously required for cell proliferation in the entire developing Drosophila wing. *Development* 122(7): 2261-9.

Capdevila, J. and Guerrero, I. (1994). Targeted expression of the signaling molecule decapentaplegic induces pattern duplications and growth alterations in Drosophila wings. *EMBO J* 13(19): 4459-68.

Chanut, F. and Heberlein, U. (1997a). Retinal morphogenesis in Drosophila: hints from an eye-specific decapentaplegic allele. *Dev Genet* 20(3): 197-207.

Chanut, F. and Heberlein, U. (1997b). Role of decapentaplegic in initiation and progression of the morphogenetic furrow in the developing Drosophila retina. *Development* 124(2): 559-67.

Chao, J.-L., Tsai, Y.-C., Chiu, S.-J. and Sun, Y. H. (2004). Localized Notch signal acts through eyg and upd to promote global growth in Drosophila eye. *Development* 131(16): 3839-47.

Chen, C., Jack, J. and Garofalo, R. S. (1996a). The Drosophila insulin receptor is required for normal growth. *Endocrinology* 137(3): 846-56.

Chen, C. M. and Struhl, G. (1999). Wingless transduction by the Frizzled and Frizzled2 proteins of Drosophila. *Development* 126(23): 5441-52.

Chen, P., Nordstrom, W., Gish, B. and Abrams, J. M. (1996b). grim, a novel cell death gene in Drosophila. *Genes & Development* 10(14): 1773-1782.

Chen, R., Amoui, M., Zhang, Z. and Mardon, G. (1997). Dachshund and eyes absent proteins form a complex and function synergistically to induce ectopic eye development in Drosophila. *Cell* 91(7): 893-903.

Cheyette, B. N., Green, P. J., Martin, K., Garren, H., Hartenstein, V. and Zipursky, S. L. (1994). The Drosophila sine oculis locus encodes a homeodomain-containing protein required for the development of the entire visual system. *Neuron* 12(5): 977-96.

Cho, K. O. and Choi, K. W. (1998). Fringe is essential for mirror symmetry and morphogenesis in the Drosophila eye. *Nature* 396(6708): 272-6.

Coller, H. A., Grandori, C., Tamayo, P., Colbert, T., Lander, E. S., Eisenman, R. N. and Golub, T. R. (2000). Expression analysis with oligonucleotide microarrays reveals that MYC regulates genes involved in growth, cell cycle, signaling, and adhesion. *Proc Natl Acad Sci USA* 97(7): 3260-5.

Couso, J. P., Bishop, S. A. and Martinez Arias, A. (1994). The wingless signalling pathway and the patterning of the wing margin in Drosophila. *Development* 120(3): 621-36.

Curtiss, J. and Mlodzik, M. (2000). Morphogenetic furrow initiation and progression during eye development in Drosophila: the roles of decapentaplegic, hedgehog and eyes absent. *Development* 127(6): 1325-36.

Dai, M.-S., Arnold, H., Sun, X.-X., Sears, R. and Lu, H. (2007a). Inhibition of c-Myc activity by ribosomal protein L11. *EMBO J* 26(14): 3332-45.

Dai, M.-S., Sears, R. and Lu, H. (2007b). Feedback regulation of c-Myc by ribosomal protein L11. *Cell Cycle* 6(22): 2735-41.

Dang, C. V., O'Donnell, K. A., Zeller, K. I., Nguyen, T., Osthus, R. C. and Li, F. (2006). The c-Myc target gene network. *Semin Cancer Biol* 16(4): 253-64.

Davis, A. C., Wims, M., Spotts, G. D., Hann, S. R. and Bradley, A. (1993). A null c-myc mutation causes lethality before 10.5 days of gestation in homozygotes and reduced fertility in heterozygous female mice. *Genes & Development* 7(4): 671-82.

Day, S. J. and Lawrence, P. A. (2000). Measuring dimensions: the regulation of size and shape. *Development* 127(14): 2977-87.

de la Cova, C., Abril, M., Bellosta, P., Gallant, P. and Johnston, L. A. (2004). Drosophila myc regulates organ size by inducing cell competition. *Cell* 117(1): 107-16.

de la Cova, C. and Johnston, L. A. (2006). Myc in model organisms: a view from the flyroom. *Seminars in Cancer Biology* 16(4): 303-12.

Deisenroth, C. and Zhang, Y. (2010). Ribosome biogenesis surveillance: probing the ribosomal protein-Mdm2-p53 pathway. *Oncogene* 29(30): 4253-4260.

Demontis, F. and Perrimon, N. (2009). Integration of Insulin receptor/Foxo signaling and dMyc activity during muscle growth regulates body size in Drosophila. *Development* 136(6): 983-93.

Derenzini, M. e. a. (2000). Nucleolar size indicates the rapidity of cell proliferation in cancer tissues. *Journal of pathology*: 1-6.

Derenzini, M. e. a. (2009). What the nucleolus says to a tumour pathologist.

Diaz-Benjumea, F. J. and Cohen, S. M. (1993). Interaction between dorsal and ventral cells in the imaginal disc directs wing development in Drosophila. *Cell* 75(4): 741-52.

Diaz-Benjumea, F. J. and Cohen, S. M. (1995). Serrate signals through Notch to establish a Wingless-dependent organizer at the dorsal/ventral compartment boundary of the Drosophila wing. *Development* 121(12): 4215-25.

Dietzl, G., Chen, D., Schnorrer, F., Su, K.-C., Barinova, Y., Fellner, M., Gasser, B., Kinsey, K., Oppel, S., Scheiblauer, S. et al. (2007). A genome-wide transgenic RNAi library for conditional gene inactivation in Drosophila. *Nature* 448(7150): 151-6.

Domínguez, M. and de Celis, J. F. (1998). A dorsal/ventral boundary established by Notch controls growth and polarity in the Drosophila eye. *Nature* 396(6708): 276-8.

Dominguez, M., Ferres-Marco, D., Gutierrez-Aviño, F. J., Speicher, S. A. and Beneyto, M. (2004). Growth and specification of the eye are controlled independently by Eyegone and Eyeless in Drosophila melanogaster. *Nat Genet* 36(1): 31-9.

Domínguez, M. and Hafen, E. (1997). Hedgehog directly controls initiation and propagation of retinal differentiation in the Drosophila eye. *Genes & Development* 11(23): 3254-64.

Donati, G., Bertoni, S., Brighenti, E., Vici, M., Trer&Eacute, D., Volarevic, S., Montanaro, L. and Derenzini, M. (2011). The balance between rRNA and ribosomal protein synthesis up- and downregulates the tumour suppressor p53 in mammalian cells. *Oncogene*: 1-15.

Dong, J., Feldmann, G., Huang, J., Wu, S., Zhang, N., Comerford, S. A., Gayyed, M. F., Anders, R. A., Maitra, A. and Pan, D. (2007). Elucidation of a universal size-control mechanism in Drosophila and mammals. *Cell* 130(6): 1120-33.

Dorstyn, L., Colussi, P. A., Quinn, L. M., Richardson, H. and Kumar, S. (1999). DRONC, an ecdysone-inducible Drosophila caspase. *Proc Natl Acad Sci USA* 96(8): 4307-12.

Draptchinskaia, N., Gustavsson, P., Andersson, B., Pettersson, M., Willig, T. N., Dianzani, I., Ball, S., Tchernia, G., Klar, J., Matsson, H. et al. (1999). The gene encoding ribosomal protein S19 is mutated in Diamond-Blackfan anaemia. *Nature genetics* 21(2): 169-75.

Edgar, B. A. (2006). How flies get their size: genetics meets physiology. *Nat Rev Genet* 7(12): 907-16.

Edgar, B. A. and Orr-Weaver, T. L. (2001). Endoreplication cell cycles: more for less. *Cell* 105(3): 297-306.

Fan, Y. and Bergmann, A. (2008). Apoptosis-induced compensatory proliferation. The Cell is dead. Long live the Cell! *Trends in Cell Biology* 18(10): 467-73.

Fan, Y., Lee, T., Xu, D., Chen, Z., Lamblin, A., Steller, H. and Bergmann, A. (2009). Dual roles of Drosophila p53 in cell death and cell differentiation. *Cell Death Differ*.

Fankhauser, G. (1945). The Effects of Changes in Chromosome Number on Amphibian Development. *The Quarterly Review of Biology* 20(1): 20-78

Fraser, A. G. and Evan, G. I. (1997). Identification of a Drosophila melanogaster ICE/CED-3-related protease, drICE. *EMBO J* 16(10): 2805-13.

Fraser, A. G., McCarthy, N. J. and Evan, G. I. (1997). drICE is an essential caspase required for apoptotic activity in Drosophila cells. *EMBO J* 16(20): 6192-9.

Gallant, P., Shiio, Y., Cheng, P. F., Parkhurst, S. M. and Eisenman, R. N. (1996). Myc and Max homologs in Drosophila. *Science* 274(5292): 1523-7.

Garcia-Bellido, A. and Merriam, J. R. (1969). Cell lineage of the imaginal discs in Drosophila gynandromorphs. *J Exp Zool* 170(1): 61-75.

Gomez-Roman, N., Grandori, C., Eisenman, R. N. and White, R. J. (2003). Direct activation of RNA polymerase III transcription by c-Myc. *Nature* 421(6920): 290-4.

Grandori, C., Gomez-Roman, N., Felton-Edkins, Z. A., Ngouenet, C., Galloway, D. A., Eisenman, R. N. and White, R. J. (2005). c-Myc binds to human ribosomal DNA and stimulates transcription of rRNA genes by RNA polymerase I. *Nat Cell Biol* 7(3): 311-318.

Greenwood, S. and Struhl, G. (1999). Progression of the morphogenetic furrow in the Drosophila eye: the roles of Hedgehog, Decapentaplegic and the Raf pathway. *Development* 126(24): 5795-808.

Grether, M. E., Abrams, J. M., Agapite, J., White, K. and Steller, H. (1995). The head involution defective gene of Drosophila melanogaster functions in programmed cell death. *Genes & Development* 9(14): 1694-1708.

Grewal, S. S. (2009). Insulin/TOR signaling in growth and homeostasis: a view from the fly world. *Int J Biochem Cell Biol* 41(5): 1006-10.

Grewal, S. S., Evans, J. R. and Edgar, B. A. (2007). Drosophila TIF-IA is required for ribosome synthesis and cell growth and is regulated by the TOR pathway. *The Journal of Cell Biology* 179(6): 1105-13.

Grewal, S. S., Li, L., Orian, A., Eisenman, R. N. and Edgar, B. A. (2005). Myc-dependent regulation of ribosomal RNA synthesis during Drosophila development. *Nat Cell Biol* 7(3): 295-302.

Guo, Q. M., Malek, R. L., Kim, S., Chiao, C., He, M., Ruffy, M., Sanka, K., Lee, N. H., Dang, C. V. and Liu, E. T. (2000). Identification of c-myc responsive genes using rat cDNA microarray. *Cancer Res* 60(21): 5922-8.

Gutierrez-Aviño, F. J., Ferres-Marco, D. and Dominguez, M. (2009). The position and function of the Notch-mediated eye growth organizer: the roles of JAK/STAT and four-jointed. *EMBO Rep* 10(9): 1051-8.

Halder, G., Callaerts, P. and Gehring, W. J. (1995). Induction of ectopic eyes by targeted expression of the eyeless gene in Drosophila. *Science* 267(5205): 1788-92.

Halder, G. and Johnson, R. L. (2011). Hippo signaling: growth control and beyond. *Development* 138(1): 9-22.

Hall, D. J., Grewal, S. S., de la Cruz, A. F. A. and Edgar, B. A. (2007). Rheb-TOR signaling promotes protein synthesis, but not glucose or amino acid import, in Drosophila. *BMC Biol* 5: 10.

Haupt, Y., Maya, R., Kazaz, A. and Oren, M. (1997). Mdm2 promotes the rapid degradation of p53. *Nature* 387(6630): 296-9.

Haynie, J. L. and Bryant, P. J. (1977). The effects of X-rays on the proliferation dynamics of cells in the imaginal wing disc of Drosophila melanogaster. *Development Genes and Evolution* 183(2): 85-100.

Heberlein, U., Singh, C. M., Luk, A. Y. and Donohoe, T. J. (1995). Growth and differentiation in the Drosophila eye coordinated by hedgehog. *Nature* 373(6516): 709-11.

Heberlein, U., Wolff, T. and Rubin, G. M. (1993). The TGF beta homolog dpp and the segment polarity gene hedgehog are required for propagation of a morphogenetic wave in the Drosophila retina. *Cell* 75(5): 913-26.

Heiss, N. S., Knight, S. W., Vulliamy, T. J., Klauck, S. M., Wiemann, S., Mason, P. J., Poustka, A. and Dokal, I. (1998). X-linked dyskeratosis congenita is caused by mutations in a highly conserved gene with putative nucleolar functions. *Nat Genet* 19(1): 32-8.

Hietakangas, V. and Cohen, S. M. (2009). Regulation of tissue growth through nutrient sensing. *Annu. Rev. Genet.* 43: 389-410.

Hölzel, M., Orban, M., Hochstatter, J., Rohrmoser, M., Harasim, T., Malamoussi, A., Kremmer, E., Längst, G. and Eick, D. (2010). Defects in 18 S or 28 S rRNA processing activate the p53 pathway. *J Biol Chem* 285(9): 6364-70.

Horsfield, J., Penton, A., Secombe, J., Hoffman, F. M. and Richardson, H. (1998). decapentaplegic is required for arrest in G1 phase during Drosophila eye development. *Development* 125(24): 5069-78.

Hufnagel, L., Teleman, A. A., Rouault, H., Cohen, S. M. and Shraiman, B. I. (2007). On the mechanism of wing size determination in fly development. *Proc Natl Acad Sci USA* 104(10): 3835-40.

Igaki, T. (2009). Correcting developmental errors by apoptosis: lessons from Drosophila JNK signaling. *Apoptosis*.

Igaki, T., Kanda, H., Yamamoto-Goto, Y., Kanuka, H., Kuranaga, E., Aigaki, T. and Miura, M. (2002). Eiger, a TNF superfamily ligand that triggers the Drosophila JNK pathway. *EMBO J* 21(12): 3009-18.

Jang, C.-C., Chao, J.-L., Jones, N., Yao, L.-C., Bessarab, D. A., Kuo, Y. M., Jun, S., Desplan, C., Beckendorf, S. K. and Sun, Y. H. (2003). Two Pax genes, eye gone and eyeless, act cooperatively in promoting Drosophila eye development. *Development* 130(13): 2939-51.

Jemc, J. and Rebay, I. (2007). Identification of transcriptional targets of the dual-function transcription factor/phosphatase eyes absent. *Dev Biol* 310(2): 416-29.

Jiang, C., Baehrecke, E. H. and Thummel, C. S. (1997). Steroid regulated programmed cell death during Drosophila metamorphosis. *Development* 124(22): 4673-83.

Jin, S., Martinek, S., Joo, W. S., Wortman, J. R., Mirkovic, N., Sali, A., Yandell, M. D., Pavletich, N. P., Young, M. W. and Levine, A. J. (2000). Identification and characterization of a p53 homologue in Drosophila melanogaster. *Proc Natl Acad Sci USA* 97(13): 7301-6.

Johnston, L. A. (2009). Competitive interactions between cells: death, growth, and geography. *Science* 324(5935): 1679-82.

Johnston, L. A., Prober, D. A., Edgar, B. A., Eisenman, R. N. and Gallant, P. (1999). Drosophila myc regulates cellular growth during development. *Cell* 98(6): 779-90.

Kaphingst, K. and Kunes, S. (1994). Pattern formation in the visual centers of the Drosophila brain: wingless acts via decapentaplegic to specify the dorsoventral axis. *Cell* 78(3): 437-448.

Kenyon, K. L., Ranade, S. S., Curtiss, J., Mlodzik, M. and Pignoni, F. (2003). Coordinating proliferation and tissue specification to promote regional identity in the Drosophila head. *Dev Cell* 5(3): 403-14.

Kohane, M. J. (1988). Stress, altered energy availability and larval fitness in Drosophila melanogaster. *Heredity* 60 (Pt 2): 273-81.

Kubbutat, M. H., Jones, S. N. and Vousden, K. H. (1997). Regulation of p53 stability by Mdm2. *Nature* 387(6630): 299-303.

Kumar, J. P. (2010). Retinal determination the beginning of eye development. *Current Topics in Developmental Biology* 93: 1-28.

Kuranaga, E., Kanuka, H., Igaki, T., Sawamoto, K., Ichijo, H., Okano, H. and Miura, M. (2002). Reaper-mediated inhibition of DIAP1-induced DTRAF1 degradation results in activation of JNK in Drosophila. *Nature cell biology* 4(9): 705-10.

Lambertsson, A. (1998). The minute genes in Drosophila and their molecular functions. *Adv Genet* 38: 69-134.

Lazaris-Karatzas, A., Montine, K. S. and Sonenberg, N. (1990). Malignant transformation by a eukaryotic initiation factor subunit that binds to mRNA 5' cap. *Nature* 345(6275): 544-7.

Lazaris-Karatzas, A., Smith, M. R., Frederickson, R. M., Jaramillo, M. L., Liu, Y. L., Kung, H. F. and Sonenberg, N. (1992). Ras mediates translation initiation factor 4E-induced malignant transformation. *Genes & Development* 6(9): 1631-1642.

Lecuit, T., Brook, W. J., Ng, M., Calleja, M., Sun, H. and Cohen, S. M. (1996). Two distinct mechanisms for long-range patterning by Decapentaplegic in the Drosophila wing. *Nature* 381(6581): 387-93.

Lee, J. D. and Treisman, J. E. (2001). The role of Wingless signaling in establishing the anteroposterior and dorsoventral axes of the eye disc. *Development* 128(9): 1519-29.

Leevers, S. J., Weinkove, D., MacDougall, L. K., Hafen, E. and Waterfield, M. D. (1996). The Drosophila phosphoinositide 3-kinase Dp110 promotes cell growth. *EMBO J* 15(23): 6584-94.

Levine, A. J. and Oren, M. (2009). The first 30 years of p53: growing ever more complex. *Nat Rev Cancer* 9(10): 749-58.

Li, L., Edgar, B. A. and Grewal, S. S. (2010). Nutritional control of gene expression in Drosophila larvae via TOR, Myc and a novel cis-regulatory element. *BMC Cell Biol* 11: 7.

Lohrum, M. A. E., Ludwig, R. L., Kubbutat, M. H. G., Hanlon, M. and Vousden, K. H. (2003). Regulation of HDM2 activity by the ribosomal protein L11. *Cancer Cell* 3(6): 577-87.

Lopes, C. S. and Casares, F. (2009). hth maintains the pool of eye progenitors and its downregulation by Dpp and Hh couples retinal fate acquisition with cell cycle exit. *Developmental Biology*.

Ma, C. and Moses, K. (1995). Wingless and patched are negative regulators of the morphogenetic furrow and can affect tissue polarity in the developing Drosophila compound eye. *Development* 121(8): 2279-89.

Maines, J. Z., Stevens, L. M., Tong, X. and Stein, D. (2004). Drosophila dMyc is required for ovary cell growth and endoreplication. *Development* 131(4): 775-86.

Mardon, G., Solomon, N. M. and Rubin, G. M. (1994). dachshund encodes a nuclear protein required for normal eye and leg development in Drosophila. *Development* 120(12): 3473-86.

Marshall, L., Kenneth, N. S. and White, R. J. (2008). Elevated tRNA(iMet) synthesis can drive cell proliferation and oncogenic transformation. *Cell* 133(1): 78-89.

Marygold, S. J., Roote, J., Reuter, G., Lambertsson, A., Ashburner, M., Millburn, G. H., Harrison, P. M., Yu, Z., Kenmochi, N., Kaufman, T. C. et al. (2007). The ribosomal protein genes and Minute loci of Drosophila melanogaster. *Genome Biol* 8(10): R216.

Masucci, J. D., Miltenberger, R. J. and Hoffmann, F. M. (1990). Pattern-specific expression of the Drosophila decapentaplegic gene in imaginal disks is regulated by 3' cis-regulatory elements. *Genes & Development* 4(11): 2011-2023.

McEwen, D. G. and Peifer, M. (2005). Puckered, a Drosophila MAPK phosphatase, ensures cell viability by antagonizing JNK-induced apoptosis. *Development* 132(17): 3935-46.

Menssen, A. and Hermeking, H. (2002). Characterization of the c-MYC-regulated transcriptome by SAGE: identification and analysis of c-MYC target genes. *Proc Natl Acad Sci USA* 99(9): 6274-9.

Metcalf, D. (1963). The autonomous behaviour of normal thymus grafts. *Aust J Exp Biol Med Sci* 41: SUPPL437-47.

Metcalf, D. (1964). Restricted growth capacity of multiple spleen grafts. *Transplantation* 2: 387-92.

Meyer, N. and Penn, L. Z. (2008). Reflecting on 25 years with MYC. *Nat Rev Cancer* 8(12): 976-90.

Montanaro, L., Treré, D. and Derenzini, M. (2008). Nucleolus, ribosomes, and cancer. *American Journal Of Pathology* 173(2): 301-10.

Moreno, E., Basler, K. and Morata, G. (2002a). Cells compete for decapentaplegic survival factor to prevent apoptosis in Drosophila wing development. *Nature* 416(6882): 755-9.

Moreno, E., Yan, M. and Basler, K. (2002b). Evolution of TNF signaling mechanisms: JNK-dependent apoptosis triggered by Eiger, the Drosophila homolog of the TNF superfamily. *Curr Biol* 12(14): 1263-8.

Moustakas, A. and Heldin, C.-H. (2009). The regulation of TGFbeta signal transduction. *Development* 136(22): 3699-714.

Narla, A. and Ebert, B. L. (2010). Ribosomopathies: human disorders of ribosome dysfunction. *Blood* 115(16): 3196-3205.

Nellen, D., Burke, R., Struhl, G. and Basler, K. (1996). Direct and long-range action of a DPP morphogen gradient. *Cell* 85(3): 357-68.

Neto-Silva, R. M., de Beco, S. and Johnston, L. A. (2010). Evidence for a Growth-Stabilizing Regulatory Feedback Mechanism between Myc and Yorkie, the Drosophila Homolog of Yap. *Dev Cell* 19(4): 507-520.

Neufeld, T. P., de la Cruz, A. F., Johnston, L. A. and Edgar, B. A. (1998). Coordination of growth and cell division in the Drosophila wing. *Cell* 93(7): 1183-93.

Ng, M., Diaz-Benjumea, F. J., Vincent, J. P., Wu, J. and Cohen, S. M. (1996). Specification of the wing by localized expression of wingless protein. *Nature* 381(6580): 316-8.

Niwa, N., Hiromi, Y. and Okabe, M. (2004). A conserved developmental program for sensory organ formation in Drosophila melanogaster. *Nat Genet* 36(3): 293-297.

O'Donnell, K. A., Wentzel, E. A., Zeller, K. I., Dang, C. V. and Mendell, J. T. (2005). c-Myc-regulated microRNAs modulate E2F1 expression. *Nature* 435(7043): 839-43.

Ohsawa, S., Sugimura, K., Takino, K., Xu, T., Miyawaki, A. and Igaki, T. (2011). Elimination of oncogenic neighbors by JNK-mediated engulfment in Drosophila. *Developmental Cell* 20(3): 315-28.

Oldham, S. and Hafen, E. (2003). Insulin/IGF and target of rapamycin signaling: a TOR de force in growth control. *Trends Cell Biol* 13(2): 79-85.

Oldham, S., Montagne, J., Radimerski, T., Thomas, G. and Hafen, E. (2000). Genetic and biochemical characterization of dTOR, the Drosophila homolog of the target of rapamycin. *Genes & Development* 14(21): 2689-94.

Ollmann, M., Young, L. M., Di Como, C. J., Karim, F., Belvin, M., Robertson, S., Whittaker, K., Demsky, M., Fisher, W. W., Buchman, A. et al. (2000). Drosophila p53 is a structural and functional homolog of the tumor suppressor p53. *Cell* 101(1): 91-101.

Orian, A., van Steensel, B., Delrow, J., Bussemaker, H. J., Li, L., Sawado, T., Williams, E., Loo, L. W. M., Cowley, S. M., Yost, C. et al. (2003). Genomic binding by the Drosophila Myc, Max, Mad/Mnt transcription factor network. *Genes & Development* 17(9): 1101-14.

Papayannopoulos, V., Tomlinson, A., Panin, V. M., Rauskolb, C. and Irvine, K. D. (1998). Dorsal-ventral signaling in the Drosophila eye. *Science* 281(5385): 2031-4.

Pardee, A. B. (1989). G1 events and regulation of cell proliferation. *Science* 246(4930): 603-8.

Parker, L., Stathakis, D. G. and Arora, K. (2004). Regulation of BMP and activin signaling in Drosophila. *Prog Mol Subcell Biol* 34: 73-101.

Peng, H., Slattery, M. and Mann, R. (2009). Transcription factor choice in the Hippo signaling pathway: homothorax and yorkie regulation of the microRNA bantam in the progenitor domain of the Drosophila eye imaginal disc. *Genes & Development*.

Pestov, D. G., Strezoska, Z. and Lau, L. F. (2001). Evidence of p53-dependent cross-talk between ribosome biogenesis and the cell cycle: effects of nucleolar protein Bop1 on G(1)/S transition. *Mol Cell Biol* 21(13): 4246-55.

Pianese, G. (1896). Beitrag Zur Histologie Und Aetiologie Des Carcinoms: Histologische Und Experimentelle Untersuchungen. *Beitr. Pathol. Anat. Allg Pathol* 142: 1-193.

Pichaud, F. and Casares, F. (2000). homothorax and iroquois-C genes are required for the establishment of territories within the developing eye disc. *Mech Dev* 96(1): 15-25.

Pierce, S. B., Yost, C., Anderson, S. A. R., Flynn, E. M., Delrow, J. and Eisenman, R. N. (2008). Drosophila growth and development in the absence of dMyc and dMnt. *Dev Biol* 315(2): 303-16.

Pierce, S. B., Yost, C., Britton, J. S., Loo, L. W. M., Flynn, E. M., Edgar, B. A. and Eisenman, R. N. (2004). dMyc is required for larval growth and endoreplication in Drosophila. *Development* 131(10): 2317-27.

Pignoni, F., Hu, B., Zavitz, K. H., Xiao, J., Garrity, P. A. and Zipursky, S. L. (1997). The eye-specification proteins So and Eya form a complex and regulate multiple steps in Drosophila eye development. *Cell* 91(7): 881-91.

Pignoni, F. and Zipursky, S. L. (1997). Induction of Drosophila eye development by decapentaplegic. *Development* 124(2): 271-8.

Quiring, R., Walldorf, U., Kloter, U. and Gehring, W. J. (1994). Homology of the eyeless gene of Drosophila to the Small eye gene in mice and Aniridia in humans. *Science* 265(5173): 785-9.

Ready, D. F., Hanson, T. E. and Benzer, S. (1976). Development of the Drosophila retina, a neurocrystalline lattice. *Dev Biol* 53(2): 217-40.

Reynolds-Kenneally, J. and Mlodzik, M. (2005). Notch signaling controls proliferation through cell-autonomous and non-autonomous mechanisms in the Drosophila eye. *Dev Biol* 285(1): 38-48.

Robertson, A. and Cohen, M. H. (1972). Control of developing fields. *Annu Rev Biophys Bioeng* 1: 409-64.

Rodriguez, A., Oliver, H., Zou, H., Chen, P., Wang, X. and Abrams, J. M. (1999). Dark is a Drosophila homologue of Apaf-1/CED-4 and functions in an evolutionarily conserved death pathway. *Nature cell biology* 1(5): 272-9.

Rogulja, D. and Irvine, K. D. (2005). Regulation of cell proliferation by a morphogen gradient. *Cell* 123(3): 449-61.

Rogulja, D., Rauskolb, C. and Irvine, K. D. (2008). Morphogen control of wing growth through the Fat signaling pathway. *Dev Cell* 15(2): 309-21.

Rubbi, C. P. and Milner, J. (2003). Disruption of the nucleolus mediates stabilization of p53 in response to DNA damage and other stresses. *EMBO J* 22(22): 6068-77.

Ruggero, D., Grisendi, S., Piazza, F., Rego, E., Mari, F., Rao, P. H., Cordon-Cardo, C. and Pandolfi, P. P. (2003). Dyskeratosis congenita and cancer in mice deficient in ribosomal RNA modification. *Science* 299(5604): 259-62.

Salzer, C. L. and Kumar, J. P. (2010). Identification of Retinal Transformation Hot Spots in Developing Drosophila Epithelia. *PLoS ONE* 5(1): e8510.

Sander, V., Eivers, E., Choi, R. H. and De Robertis, E. M. (2010). Drosophila Smad2 Opposes Mad Signaling during Wing Vein Development. *PLoS ONE* 5(4): e10383.

Santamaria, P. (1983). Analysis of haploid mosaics in Drosophila. *Dev Biol* 96(2): 285-95.

Schlosser, I., Hölzel, M., Mürnseer, M., Burtscher, H., Weidle, U. H. and Eick, D. (2003). A role for c-Myc in the regulation of ribosomal RNA processing. *Nucleic Acids Res* 31(21): 6148-56.

Schreiber-Agus, N., Stein, D., Chen, K., Goltz, J. S., Stevens, L. and DePinho, R. A. (1997). Drosophila Myc is oncogenic in mammalian cells and plays a role in the diminutive phenotype. *Proc Natl Acad Sci USA* 94(4): 1235-40.

Schwank, G. and Basler, K. (2010). Regulation of organ growth by morphogen gradients. *Cold Spring Harbor Perspectives in Biology* 2(1): a001669.

Schwank, G., Restrepo, S. and Basler, K. (2008). Growth regulation by Dpp: an essential role for Brinker and a non-essential role for graded signaling levels. *Development* 135(24): 4003-13.

Schwank, G., Tauriello, G., Yagi, R., Kranz, E., Koumoutsakos, P. and Basler, K. (2011). Antagonistic growth regulation by dpp and fat drives uniform cell proliferation. *Dev Cell* 20(1): 123-30.

Serikaku, M. A. and O'Tousa, J. E. (1994). sine oculis is a homeobox gene required for Drosophila visual system development. *Genetics* 138(4): 1137-50.

Sharma, R. P. and Chopra, V. L. (1976). Effect of the Wingless (wg1) mutation on wing and haltere development in Drosophila melanogaster. *Dev Biol* 48(2): 461-5.

Shen, W. and Mardon, G. (1997). Ectopic eye development in Drosophila induced by directed dachshund expression. *Development* 124(1): 45-52.

Shraiman, B. I. (2005). Mechanical feedback as a possible regulator of tissue growth. *Proc Natl Acad Sci USA* 102(9): 3318-23.

Silvera, D., Formenti, S. C. and Schneider, R. J. (2010). Translational control in cancer. *Nat Rev Cancer* 10(4): 254-66.

Simpson, P. (1976). Analysis of the compartments of the wing of Drosophila melanogaster mosaic for a temperature-sensitive mutation that reduces mitotic rate. *Dev Biol* 54(1): 100-15.

Simpson, P., Berreur, P. and Berreur-Bonnenfant, J. (1980). The initiation of pupariation in Drosophila: dependence on growth of the imaginal discs. *J Embryol Exp Morphol* 57: 155-65.

Singh, A., Kango-Singh, M. and Sun, Y. H. (2002). Eye suppression, a novel function of teashirt, requires Wingless signaling. *Development* 129(18): 4271-80.

Song, Z., McCall, K. and Steller, H. (1997). DCP-1, a Drosophila cell death protease essential for development. *Science* 275(5299): 536-40.

Spencer, F. A., Hoffmann, F. M. and Gelbart, W. M. (1982). Decapentaplegic: a gene complex affecting morphogenesis in Drosophila melanogaster. *Cell* 28(3): 451-61.

Steiger, D., Furrer, M., Schwinkendorf, D. and Gallant, P. (2008). Max-independent functions of Myc in Drosophila melanogaster. *Nat Genet*.

Treisman, J. E. and Rubin, G. M. (1995). wingless inhibits morphogenetic furrow movement in the Drosophila eye disc. *Development* 121(11): 3519-27.

Trumpp, A., Refaeli, Y., Oskarsson, T., Gasser, S., Murphy, M., Martin, G. R. and Bishop, J. M. (2001). c-Myc regulates mammalian body size by controlling cell number but not cell size. *Nature* 414(6865): 768-73.

Tsai, Y.-C. and Sun, Y. H. (2004). Long-range effect of upd, a ligand for Jak/STAT pathway, on cell cycle in Drosophila eye development. *genesis* 39(2): 141-53.

Twitty, V. C. and Schwind, J. L. (1931). The growth of eyes and limbs transplanted heteroplastically between two species of Amblystoma. *Journal of Experimental Zoology* 59(1): 61-86.

Tyler, D. M., Li, W., Zhuo, N., Pellock, B. and Baker, N. E. (2007). Genes affecting cell competition in Drosophila. *Genetics* 175(2): 643-57.

Verdu, J., Buratovich, M. A., Wilder, E. L. and Birnbaum, M. J. (1999). Cell-autonomous regulation of cell and organ growth in Drosophila by Akt/PKB. *Nat Cell Biol* 1(8): 500-6.

Vousden, K. H. and Lane, D. P. (2007). p53 in health and disease. *Nat Rev Mol Cell Biol* 8(4): 275-83.

Vousden, K. H. and Prives, C. (2009). Blinded by the Light: The Growing Complexity of p53. *Cell* 137(3): 413-31.

Wartlick, O., Mumcu, P., Jülicher, F. and Gonzalez-Gaitan, M. (2011a). Understanding morphogenetic growth control - lessons from flies. *Nature reviews Molecular cell biology*.

Wartlick, O., Mumcu, P., Kicheva, A., Bittig, T., Seum, C., Julicher, F. and Gonzalez-Gaitan, M. (2011b). Dynamics of Dpp Signaling and Proliferation Control. *Science* 331(6021): 1154-1159.

Weasner, B., Salzer, C. and Kumar, J. P. (2007). Sine oculis, a member of the SIX family of transcription factors, directs eye formation. *Dev Biol* 303(2): 756-71.

Weigmann, K., Cohen, S. M. and Lehner, C. F. (1997). Cell cycle progression, growth and patterning in imaginal discs despite inhibition of cell division after inactivation of Drosophila Cdc2 kinase. *Development* 124(18): 3555-63.

Weinkove, D., Neufeld, T. P., Twardzik, T., Waterfield, M. D. and Leevers, S. J. (1999). Regulation of imaginal disc cell size, cell number and organ size by Drosophila class I(A) phosphoinositide 3-kinase and its adaptor. *Curr Biol* 9(18): 1019-29.

White, K., Grether, M. E., Abrams, J. M., Young, L., Farrell, K. and Steller, H. (1994). Genetic control of programmed cell death in Drosophila. *Science* 264(5159): 677-83.

Wiersdorff, V., Lecuit, T., Cohen, S. M. and Mlodzik, M. (1996). Mad acts downstream of Dpp receptors, revealing a differential requirement for dpp signaling in initiation and propagation of morphogenesis in the Drosophila eye. *Development* 122(7): 2153-62.

Williams, J. A., Paddock, S. W., Vorwerk, K. and Carroll, S. B. (1994). Organization of wing formation and induction of a wing-patterning gene at the dorsal/ventral compartment boundary. *Nature* 368(6469): 299-305.

Wolff, T. and Ready, D. F. (1991a). The beginning of pattern formation in the Drosophila compound eye: the morphogenetic furrow and the second mitotic wave. *Development* 113(3): 841-50.

Wolff, T. and Ready, D. F. (1991b). Cell death in normal and rough eye mutants of Drosophila. *Development* 113(3): 825-39.

Xu, D., Li, Y., Arcaro, M., Lackey, M. and Bergmann, A. (2005). The CARD-carrying caspase Dronc is essential for most, but not all, developmental cell death in Drosophila. *Development* 132(9): 2125-34.

Xu, D., Wang, Y., Willecke, R., Chen, Z., Ding, T. and Bergmann, A. (2006). The effector caspases drICE and dcp-1 have partially overlapping functions in the apoptotic pathway in Drosophila. *Cell Death Differ* 13(10): 1697-706.

Xu, T. and Rubin, G. M. (1993). Analysis of genetic mosaics in developing and adult Drosophila tissues. *Development* 117(4): 1223-37.

Yoshida, S., Soustelle, L., Giangrande, A., Umetsu, D., Murakami, S., Yasugi, T., Awasaki, T., Ito, K., Sato, M. and Tabata, T. (2005). DPP signaling controls development of the lamina glia required for retinal axon targeting in the visual system of Drosophila. *Development* 132(20): 4587-98.

Yu, X., Wang, L., Acehan, D., Wang, X. and Akey, C. W. (2006). Three-dimensional structure of a double apoptosome formed by the Drosophila Apaf-1 related killer. *J Mol Biol* 355(3): 577-89.

Yuan, X., Zhou, Y., Casanova, E., Chai, M., Kiss, E., Gröne, H.-J., Schütz, G. and Grummt, I. (2005). Genetic inactivation of the transcription factor TIF-IA leads to nucleolar disruption, cell cycle arrest, and p53-mediated apoptosis. *Molecular Cell* 19(1): 77-87.

Zanet, J., Pibre, S., Jacquet, C., Ramirez, A., de Alborán, I. M. and Gandarillas, A. (2005). Endogenous Myc controls mammalian epidermal cell size, hyperproliferation, endoreplication and stem cell amplification. *J Cell Sci* 118(Pt 8): 1693-704.

Zecca, M., Basler, K. and Struhl, G. (1995). Sequential organizing activities of engrailed, hedgehog and decapentaplegic in the Drosophila wing. *Development* 121(8): 2265-78.

Zhai, W. and Comai, L. (2000). Repression of RNA polymerase I transcription by the tumor suppressor p53. *Mol Cell Biol* 20(16): 5930-8.

Zhang, H. (2000). Regulation of cellular growth by the Drosophila target of rapamycin dTOR. *Genes & Development* 14(21): 2712-2724.

Zhang, Y. and Lu, H. (2009). Signaling to p53: ribosomal proteins find their way. *Cancer Cell* 16(5): 369-77.

Zhang, Y., Wolf, G. W., Bhat, K., Jin, A., Allio, T., Burkhart, W. A. and Xiong, Y. (2003). Ribosomal protein L11 negatively regulates oncoprotein MDM2 and mediates a p53-dependent ribosomal-stress checkpoint pathway. *Mol Cell Biol* 23(23): 8902-12.

Zhu, C. C., Boone, J. Q., Jensen, P. A., Hanna, S., Podemski, L., Locke, J., Doe, C. Q. and O'connor, M. B. (2008). Drosophila Activin- and the Activin-like product Dawdle function redundantly to regulate proliferation in the larval brain. *Development* 135(3): 513-521.

Ziosi, M., Baena-López, L. A., Grifoni, D., Froldi, F., Pession, A., Garoia, F., Trotta, V., Bellosta, P., Cavicchi, S. and Pession, A. (2010). dMyc functions downstream of Yorkie to promote the supercompetitive behavior of hippo pathway mutant cells. *PLoS Genet* 6(9).

Zuzarte-Luís, V. and Hurlé, J. M. (2002). Programmed cell death in the developing limb. *Int J Dev Biol* 46(7): 871-6.

CHAPTER 2

The *Drosophila Nol12* homologue *viriato* is a dMyc target that regulates nucleolar architecture and is required for dMyc-stimulated cell growth

CONTENTS

1. ABSTRACT

The nucleolus is a subnuclear factory, the activity of which is required beyond ribosome biogenesis for the regulation of cell growth, death and proliferation. In both *Drosophila* and mammalian cells, the activity of the nucleolus is regulated by the proto-oncogene Myc. Myc induces the transcription of genes required for ribosome biogenesis and the synthesis of ribosomal RNA by Pol I, a nucleolar event that is rate limiting for cell growth. Here, we show that the fruit fly Nol12 homologue Viriato is a key determinant of nucleolar architecture and function that is required for tissue growth and cell survival during *Drosophila* development. We further show that *viriato* expression is controlled by *Drosophila* Myc, and that the ability of dMyc to stimulate nucleolar function and cellular growth depends on *viriato* expression. Therefore, *viriato* acts downstream of dMyc to ensure a coordinated nucleolar response to dMyc-induced growth and, thereby, normal organ development.

2. INTRODUCTION

Tissue and organ development require a precise coordination of cellular growth, proliferation, differentiation and apoptosis. At the core of the cell, and crucial for its growth, the nucleolus is the subnuclear compartment where ribosome biogenesis takes place (Boisvert et al., 2007). Cell mass accumulation is required for proliferation, implying that the regulation of nucleolar function plays an important role in the control of proliferation rates. Ribosome biogenesis begins in the nucleolus with the transcription of rDNA genes by Pol I into a large precursor that is subsequently chemically modified at numerous sites and endonucleolytic, exonucleolytic processed where the external and internal transcribed spacers (ETS and ITS) are removed from the precursor to release the mature 18S, 5.8S and 28S rRNAs which are assembled in 40S and 60S pre-ribosomal particles that are then exported to the cytoplasm (Long and Dawid, 1980; Tautz et al., 1988). The mechanism of ribosome maturation is not clearly understood due to its great complexity in higher eukaryotes, still is very well characterized in yeast (Venema and Tollervey, 1999), and despite considerable similarities some steps were shown to be different (Gerbi and Borovjagin, 2004). Besides its role as the ribosome factory, the

nucleolus is now also considered to be a multifunctional regulatory compartment involved in RNA processing events, sensing of cell stress, and cell cycle and apoptosis regulation (Boisvert et al., 2007).

A key step in ribosome biogenesis is pre-rRNA gene transcription by Pol I, a process that in human cells is known to be stimulated by the binding of c-MYC to rDNA promoters in the nucleolus (Arabi et al., 2005; Grandori et al., 2005). Further, *Drosophila* Myc, which is known to control the cell cycle and apoptosis, has been shown to be necessary and sufficient for the transcription of genes encoding Pol I transcription machinery factors, such as *Tif-IA* and *RpI135* (the largest Pol I subunit), genes encoding pre-rRNA processing and modifying factors, such as *Nop60B* and *Fibrillarin*, as well as a large set of ribosomal genes (Grewal et al., 2005; Pierce et al., 2008). The ability of dMyc to induce a coordinated nucleolar hypertrophy and to stimulate pre-rRNA transcription and ribosome biogenesis in general are required for dMyc-stimulated growth during *Drosophila* development (Grewal et al., 2005). Here, we identify *viriato* (*vito*) as a dMyc target gene that coordinates nucleolar and growth responses downstream of dMyc.

3. MATERIALS AND METHODS

3.1. Fly strains and genotypes

All crosses were raised at 25°C under standard conditions. The following stocks (described in FlyBase, unless stated otherwise) were used: w^{1118}, *ptc*-Gal4, hs-Gal4, Ubi-Gal4, *ey*-Gal4, GMR-Gal4, *da*-Gal4, UAS-*lacZ*, UAS-bsk^{DN}, UAS-p35, UAS-$p53^{DN(R155H)}$, GMR-$p53^{DN(R155H)}$, *y w* hs-flp^{122}; *act*>*y*+>Gal4 UAS-*GFP*, *en*-Gal4 UAS-*GFP/CyO*, *Df(3L)H99*, y^1 w^{1118};; $p53^{[5A-1-4]}$ (*p53* null allele), *rpr*-11kb-*lacZ*, (*hs*-GFP-*Nopp140True*) (Mccain et al., 2006), *y w hs-*flp^{122};; UAS-*dMyc*, dm^4/FM7(act-GFP), UAS-*dicer-2*, $vito^1$ [or $pBac(RB)CG32418^{e03237}$], RpS9-YFP/TM6c (CPTI-000493, Flannotator), RpL41-YFP/SM6a (CPTI-002881, Flannotator).

Eye-targeted RNAi knockdown of *vito* was induced by crossing *eyeless*-Gal4 with UAS-*vito*RNAi [Vienna Drosophila RNAi Center (VDRC) #34548]. A second UAS-*vito*RNAi transformant (named UAS-*vito*RNAiKK; VDRC #102513) was also tested and observed to generate a very similar eye phenotype. Thus, the stock UAS-*vito*RNAi (VDRC #34548) was used for most of the experiments.

3.2. Generation of UAS-*vito*, UAS-*vito*-GFP and UAS-Human*NOL12*-GFP transgenic strains

To obtain UAS-*vito* transgenic lines, the full-length *vito* cDNA was excised from the LD10447 clone (GenBank accession AY095185) as a *Not*I/*Xho*I fragment and subcloned into *Not*I/*Xho*I-digested pUASt.

Transgenic lines were generated by standard germline transformation methods and five independent lines were analysed. To obtain UAS-*vito*-GFP lines, the *vito* ORF was PCR amplified from the LD10447 cDNA using Pfu polymerase (Fermentas) and primers 5'-CACCATGACCAGGAAAAAGGCT-3' and 5'-GTCGGCATTCCGTTTGCG-3'. The amplified fragment was cloned into pENTR/D-TOPO (Invitrogen) according to the supplier's instructions. The ORF was cloned into the pUASt-GFP vector (pTWG; a gift of T. Murphy, The Carnegie Institution of Washington, Baltimore, MD, USA) by in vitro recombination using the Gateway LR Clonase II enzyme mix (Invitrogen).

UAS-Human*NOL12*-GFP flies were generated by in vitro recombination between the full ORF shuttle clone with Gateway entry vector pENTR223.1-*NOL12* (clone OCABo5050F031D, ImaGenes) and the destination vector pUASt-GFP (pTWG). The pUAS-*vito*-GFP and pUAS-Human*NOL12*-GFP constructs were verified by DNA sequencing. Transgenic lines were generated by standard germline transformation methods and four independent lines were analysed. The Ubi-Gal4 driver was used to drive low-level expression of Vito-GFP in salivary glands, and *ey*-Gal4 was used to drive hNOL12-GFP expression during eye development and in salivary glands. *ey*-Gal4 drives 'leaky' Gal4 expression in the salivary glands.

3.3. Mitotic recombination

Mitotic recombination was induced using the Flp/FRT method. *vito* knockdown clones, or clones overexpressing dMyc alone or together with *vito*RNAi, were induced by heat shock (1 hour at 37°C) at 48 ± 4 hours after egg laying (AEL) and dissected at 118 ± 4 hours AEL in larvae of the genotype *y w hsflp/+*; act>y+>Gal4, UAS-GFP/UAS-*vito*RNAi, *y w hsflp*/+; act>y+>Gal4, UAS-GFP/+; UAS-*dMyc*/+ and *y w hsflp*/+; act>y+>Gal4, UAS-GFP/UAS-*vito*RNAi; UAS-*dMyc*/+.

3.4 Immunostaining

Eye-antennal imaginal discs and salivary glands were prepared for immunohistochemistry using standard protocols. Primary antibodies used were: rabbit anti-cleaved Caspase-3 at 1:200 (Cell Signaling), mouse anti-Armadillo N27A1 at 1:100 [Developmental Studies Hybridoma Bank (DSHB)], mouse anti-β-galactosidase at 1:1000 (Promega, #Z3783), rat anti-Elav 7E8A10 at 1:100 (DSHB), mouse anti-Lamin ADL101 at 1:1 (DSHB), mouse anti-p53 7A4 at 1:500 (DSHB), rabbit anti-Fibrillarin at 1:250 (Abcam, #ab5821), mouse anti-RpS6 at 1:200 (Cell Signaling, #2317), rabbit polyclonal anti-RpL22 at 1:100 (a gift from Vassie Ware, Lehigh University, USA). Appropriate Alexa Fluor-conjugated secondary antibodies were from Molecular Probes. Images were obtained with the Leica SP2 confocal system and processed with Adobe Photoshop.

3.5. In situ hybridisation

A digoxigenin (DIG)-labelled *vito* antisense RNA probe was synthesized by in vitro transcription with T7 RNA polymerase and DIG-UTP after linearisation of cDNA LD10447 with *Not*I and were used for whole-

mount in situ hybridisation of fixed larvae. A sense RNA probe was used as a negative control. The DIG-labelled RNA probes were detected with an anti-DIG antibody coupled to alkaline phosphatase (Roche) using NBT/BCIP as substrate.

3.6. Scanning electron microscopy (SEM)

Female flies were transferred to 25% ethanol and incubated for 12-24 hours at room temperature. Flies were further dehydrated through an ethanol series (50%, 75%, and twice 100%; 12-24 hours each step) before being incubated twice for 30 minutes each with hexamethyldisilazane, air-dried overnight, mounted onto SEM stubs covered with carbon tape, and sputter coated with platinum. Samples were imaged using an FEI Quanta 400 microscope.

3.7. Transmission electron microscopy (TEM)

Dissected third instar salivary glands were fixed with 2.5% glutaraldehyde in 0.1 M sodium cacodylate buffer for 30 minutes and post-fixed with 4% osmium tetroxide. After washing, salivary glands were incubated with 0.5% uranyl acetate (30 minutes) and further dehydrated through a graded ethanol series (70% for 10 minutes, 90% for 10 minutes, and four changes of 100%). Salivary glands were then soaked in propylene oxide for 10 minutes and then in a mixture (1:1) of propylene oxide and Epon resin (TAAB Laboratories) for 30 minutes. This mixture was then replaced by 100% Epon resin for 24 hours. Finally, fresh Epon replaced the Epon and polymerisation took place at 60°C for 48 hours. Ultrathin sections were obtained using an ultramicrotome, collected in copper grids and then double contrasted with uranyl acetate and lead citrate. Micrographs were taken using a Zeiss EM10C electron microscope (80 kV).

3.8. Quantitative real-time PCR (qPCR)

For the experiment in which *vito*RNAi was ubiquitously induced, RNA was isolated from control (Ubi-Gal4/+) or *vito*RNAi (Ubi-Gal4/+; UAS-*vito*RNAi/+) larvae 112 hours AEL. RNA was also isolated from control (w^{1118}) and $vito^{1}$ homozygous wandering third instar larvae. Ubiquitous dMyc overexpression in wandering third instar larvae was induced by giving a heat shock (1 hour at 37°C) to hs-Gal4/UAS-*dMyc* larvae that were collected 4 hours after the heat shock. Control (hs-Gal4/+) larvae were subjected to the same treatment. For dMyc loss-of-function experiments, total RNA was isolated from either dm^{4} mutant or control larvae 24 hours AEL. Total RNA was also isolated from third instar salivary glands of the genotypes control (UAS-*lacZ*/+; *ptc*-Gal4/+), $dMyc^{OE}$ (*ptc*-Gal4/+; UAS-*dMyc*/+), $dMyc^{OE}$+*vito*RNAi (*ptc*-Gal4/UAS-*vito*RNAi; UAS-*dMyc*/+) and from eye imaginal discs of genotypes control (*ey*-Gal4/+) and *vito*RNAi (*ey*-Gal4, UAS-*vito*RNAi/+). For the analysis of ribosomal RNA transcripts using primers against the internal and external transcribed spacers, RNA was isolated from salivary glands of the genotypes control (UAS-*lacZ*/+; *ptc*-Gal4/+), >*vito*RNAi (*ptc*-Gal4/UAS-*vito*RNAi), and from eye imaginal discs of genotypes control (*ey*-Gal4/+) and *vito*RNAi (*ey*-Gal4, UAS-*vito*RNAi/+). Total RNA was isolated using TRIzol (Invitrogen) according

to the manufacturer's instructions and treated with DNase I (RNase-free; Ambion). cDNA was generated by reverse transcription with the SuperScript III First-Strand Synthesis SuperMix for qRT-PCR (Invitrogen). Quantitative real-time PCR analysis was performed in triplicate in 20 μl reactions containing iQ SYBR Green Supermix (BioRad), each gene-specific primer at 250 nM and 1 ml of cDNA template. Cycling conditions in a BioRad iQ5 instrument were 95°C for 3 minutes, followed by 40 cycles of denaturation at 95°C for 10 seconds and annealing for 30 seconds at 60 or 64°C depending on the primer set. Fold change relative to the expression of *CaMKII*, which has been used previously as a control for gene expression in dm^4 mutants and for overexpression of *dMyc* in the whole larvae (Pierce et al., 2004), was calculated using the $2^{-\Delta\Delta CT}$ method (Livak and Schmittgen, 2001). For salivary glands, data were normalised for levels of total RNA. Three to five biological replicates were analysed for each primer set. Values are presented in $\log_2$ scale or as absolute expression levels. Statistical significance was determined using the Relative Expression Software Tool [REST; http://rest.gene-quantification.info (Pfaffl et al., 2002)]. The mathematical model is based on randomisation tests, which have the advantage of making no distributional assumptions about the data.

The following primer pairs (5' to 3') were used:

CaMKII (control), TTACACCATCCCAACATAGTGC and CAAGGTCAAAAACAAGGTAGTGATAG; *Nop60B*, GAGTGGCTGACCGGTTATGT and GCTGGAGGTGCTTAACTTGC;

p53, GCGAAAAGAAACTTCCTTAGTCTTC and TTGGGGCACGTACATATTTTAAC;

Tif-IA, CAAGCCTATTTTCGAAGAACTTGT and CAAGGTGTCCGCTTCCAC;

Rpl135, CCCGGAGTTTAAGCAGATACC and CACATGTGGACCTCCCAAA;

*vito*qPCR1 (to detect *vito* transcript levels in *vito*RNAi experiments), GACCAGGAAAAAGGCTCCTAA and TTGCGCTCGTTCTTAAGGTT;

*vito*qPCR2 (to detect *vito* transcript levels in $vito^1$ homozygous larvae), AGGTGAAGATCGTGGAGCTGAC and CCTGGTCGGCTTCGTCCTC;

Fibrillarin (*Fib*), GCATCTCCGTTGAGACCAAT and GACACATGCGAGACTGTCGT;

pre-rRNA (ETS), GCTCCGCGGATAATAGGAAT and ATATTTGCCTGCCACCAAAA;

rpr, CATACCCGATCAGGCGACTC and CGGATGACATGAAGTGTACTGG;

puc, AGGCTATGGACGAGGATGGGTTTG and GGCGGCGAGGTCAATCTGGATG;

pre-rRNA (ITS1 3') TTATTGAAGGAATTGATATATGCC and ATGAGCCGAGTGATCCAC;

pre-rRNA (ITS2 5') TATGGTTGAGGGTTGTAAGACTATGC and ATGCTAGACATTTCTCAGTATTATTTGATTG and

pre-rRNA (ITS2 3') TATGTTATTATTCTTCGTTGGTTCG and TGAGTTGAGGTTGTATATAACTTTATCTTG.

3.9. Immunofluorescence detection of Vito-GFP in S2 cells

To construct the plasmid pHsp70-*vito*-GFP, the Gateway *vito* Entry clone described above for generation of Vito-GFP flies was recombined into the vector pHsp70-GFP gateway (pHWG, a gift of T. Murphy, The Carnegie Institution of Washington, Baltimore, MD, USA). Plasmid DNA was prepared and

transfected into Schneider line 2 (S2) cells. For each transient transfection 1 µg of plasmid DNA was mixed with Cellfectin® Reagent (Invitrogen). The basal activity of the Hsp70 promoter (at 25°C) was sufficient to express Vito-GFP at low-levels in S2 cells. Strong overexpression of Vito-GFP was achieved with a 30-minute heat shock (37 °C) followed by a recovery step (2 hours). Cells were harvested 48 hours post-transfection and processed for immunofluorescence as described previously (Maiato et al., 2003). The following primary antibodies were used: rabbit anti-Fibrillarin at 1:250, (Abcam #ab5821), and mouse anti-α-Tubulin at 1:8000 (Sigma-Aldrich, #B5-1-2). Appropriate Alexa Fluor-conjugated secondary antibodies were from Molecular Probes. Images were collected with an AxioImager Z1 microscope (Carl Zeiss, Germany) equipped with a Z motor, using an 100x 1.4 NA objective.

3.10. Flow cytometry

FACS analysis was carried out on dissociated wing imaginal disc cells as described previously (de la Cruz and Edgar, 2008). Approximately 60 wing discs were dissected from *vito*RNAi (*en*-Gal4, UASGFP/UAS-*vito*RNAi) wandering third instar larvae. For cell cycle analysis, GFP-positive and GFP-negative cells were sorted with a FACSAria flow cytometer (Becton Dickinson, Mountain View, CA) and fixed immediately in 70% ethanol. Prior to FACS analysis, cells were washed in PBS and incubated for 1 hour at 37°C in 10 µg/mL RNase-A and 100 µg/mL of Propidium Iodide for DNA staining. Analysis was carried out with a FACSCalibur flow cytometer (Becton Dickinson, Mountain View, CA) with excitation at 488 nm and data acquired using the CellQuest Pro software, version 4.0.2 (Becton Dickinson Mountain View, CA) included in the system.

3.11. Northern blot

Total RNA was isolated from equal numbers of similar-sized and similar-staged larvae per experimental group of the genotypes: Control (*da*-Gal4/UAS-*dicer2*), and *vito*RNAi (UAS-*vito*RNAi; *da*-Gal4/UAS-*dicer2*). Total RNA was isolated using TRIzol (Invitrogen) according to the manufacturer's instructions and treated with DNase I (RNase-free; Ambion). 5 µg of total RNA denatured samples were run for 4 hours on 1.5% agarose/formadehyde gels in MOPS buffer and UV photographed. Ribosomal RNA intensities were determined using Image J software (NIH, Bethesda, MA, USA) in order to normalize for differences in rRNA among samples. Then, RNA samples normalized for rRNA were separated in 1.5% agarose/formadehyde for 4 hours, capillary transferred to Hybond N+ membranes (GeneScreen) and UV cross-linked (Stratagene). Oligonucleotide probes were 3'-end labeled with Digoxigenin-dUTP/dATP using the enzyme terminal transferase provived in DIG Oligonucleotide Tailing Kit according to the manufacturer's instructions (Roche). The membrane was pre-hybridized for 4 hours in hybridization buffer (7% SDS, 5X SSC, 2% Blocking Reagent, 0.1% N-lauroylsarcosine, 50 mM Sodium phosphate, pH 7.0) at 42°C before an overnight hybridization under the same conditions. After stringency washes, an Alkaline Phosphatase

conjugated anti-DIG antibody at 1:10000 (Roche) was incubated with the membrane, and then followed with CDP-Star reagent (Roche) for chemiluminescent detection of the DIG-labeled oligonucleotide probes. Enzymatic reaction of CDP-Star reagent with alkaline phosphatase produces a light signal, which was detected by film.

Oligonucleotide probes, corresponding to different regions of the pre-rRNA precursor have the following sequences:

28S, 5'-GTTACAAAAGTCGTTTACAATTGATTC-3'

ITS1, 5'- GAAATTAAAAATACACCATTTTACTGGC-3'

3.12. Size and volume measurements and statistics

Eye disc areas were measured using the Straight Line tool of ImageJ 1.41o software (NIH, Bethesda, MA, USA), considering only the eye disc from the eye-antennal imaginal disc. In all the disc-proper clones assessed for clone size, nuclei were counted in the DAPI channel. Cell size estimates were obtained by dividing each clone area by the number of nuclei in the clone. For the comparison of nuclear, cytoplasmic and cell sizes in different genetic backgrounds, the radius (r) was measured using the Straight Line tool of ImageJ. Volume (V) was approximated as $V=4/3\ \pi\ r^3$. For each genotype, 62-82 nuclei were scored. GraphPad Prism 5.0 was used for statistical analysis and for generating the graphical output. Statistical significance was determined using an unpaired two-tailed Student's *t*-test, with a 95% confidence interval, after assessing the normality distribution of the data with the D'Agostino-Pearson normality test.

4. RESULTS

4.1. *vito* encodes the single *Drosophila* member of the conserved Nol12 family of nucleolar proteins and is required for tissue growth

In a search to identify genes required for tissue growth in *Drosophila*, we observed that expression of an RNAi transgene targeting the uncharacterised *CG32418* gene [which we named *viriato* (*vito*)] in the developing eye resulted in a reduced and rough eye (Fig. 2.1A). When we examined the effects of *vito*RNAi expression in the eye primordium, we observed that although posterior retinal differentiation still occurred, a very significant reduction in eye disc size was visible, particularly in the anterior proliferative region of the disc (Fig. 2.1B). This suggested that *vito* is required for growth and/or proliferation before the onset of photoreceptor differentiation. In support of this hypothesis, although widely transcribed in imaginal discs, *vito* expression is stronger in the anterior region of the eye disc (Fig. 2.2).

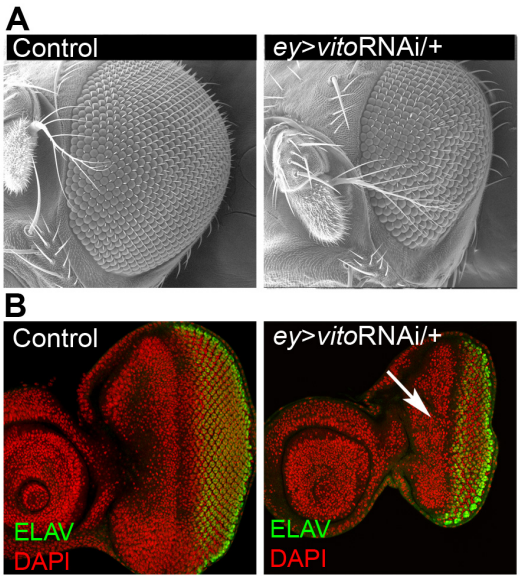

Figure 2.1 - *vito* is required for tissue growth. (A) Lateral views of control (*ey*-Gal4/+) and *vito* loss-of-function (*ey>vito*RNAi/+ is *ey*-Gal4, UAS-*vito*RNAi/+) adult *Drosophila* eyes. **(B)** Depleting *vito* in the eye causes a decrease in the size of eye primordia (arrow). Eye discs were stained with a photoreceptor-specific antibody (anti-Elav, green) and with DAPI for DNA (red).

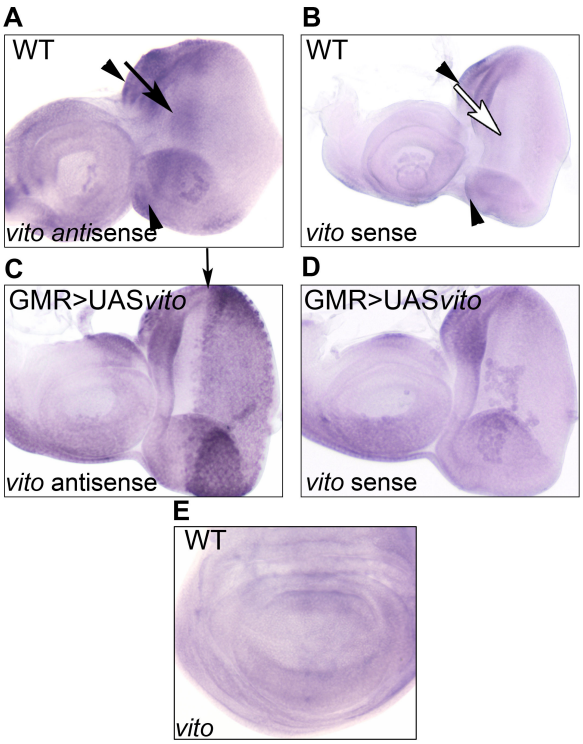

Figure 2.2 - RNA in situ hybridisation shows that *vito* is widely expressed in imaginal discs. (A) In the eye disc, expression is higher in the anterior proliferating region of the disc (arrow). The dorsal and ventral margin regions show a non-specific signal (arrowheads). **(B)** RNA in situ hybridization with a control *vito* sense probe in wild-type eye disc. The specific signal anterior to the furrow seen with the *vito* antisense probe in wild-type discs is absent here (white arrow). **(C)** *vito* mRNA is widely detected in photoreceptors after overexpression of a UAS-*vito* transgene with the GMR promoter (positive control for antisense probe). The arrow indicates the morphogenetic furrow. **(D)** Control RNA sense probe in an eye disc overexpressing *vito*. **(E)** *vito* is expressed at low levels in a wild-type wing imaginal disc.

Similar phenotypes in eye discs and adults were observed with a second RNAi line (UAS-*vito*RNAiKK) and in eye discs homozygous for the *vito*^{1} allele (*vito*^{1} results from a *PiggyBac* insertion, *PBac(RB)CG32418*^{e03237}) (Fig. 2.3A-E,H). Very significant reductions of *vito* mRNA levels were detected by qPCR in larvae expressing *vito*RNAi and in *vito*^{1} homozygous larvae (Fig. 2.3J). In addition, reduction of *vito* levels, either in *vito*^{1} homozygous larvae or induced by generalised expression of *vito*RNAi, caused a significant developmental delay and most died before pupation or even during pupal phase (Fig. 2.4A). However we could detect *vito*^{1} homozygous adult 'escapers' which displayed short and thin bristles and exhibited female sterility, and also 'escapers' of the generalised expression of *vito*RNAi showing a smaller body size in a similar manner to dMyc hypomorphic mutants (Gallant et al., 1996; Schreiber-Agus et al., 1997; Johnston et al., 1999) (Fig. 2.4B,C). *vito* might not be a formal *Minute* gene because the *vito*^{1} mutation, in heterozygosity, do not display all the common dominant Minute heterozygous mutant phenotypes (like prolonged development, low fertility, altered body size and abnormally short, thin bristles on the adult body), as we could only observe a very subtle bristle shortening and thinning. Since homozygous displays Minute-like phenotypes it is possible that *vito* knockdown could affect ribosomal function and thus growth rates. To confirm the specificity of the phenotypes observed, we attempted to rescue the effects of *vito*RNAi by co-expressing a full-length *vito* cDNA. Indeed, eye disc size, adult eye size and morphology (Fig 2.3F,I,K) were significantly rescued by supplying *vito* back.

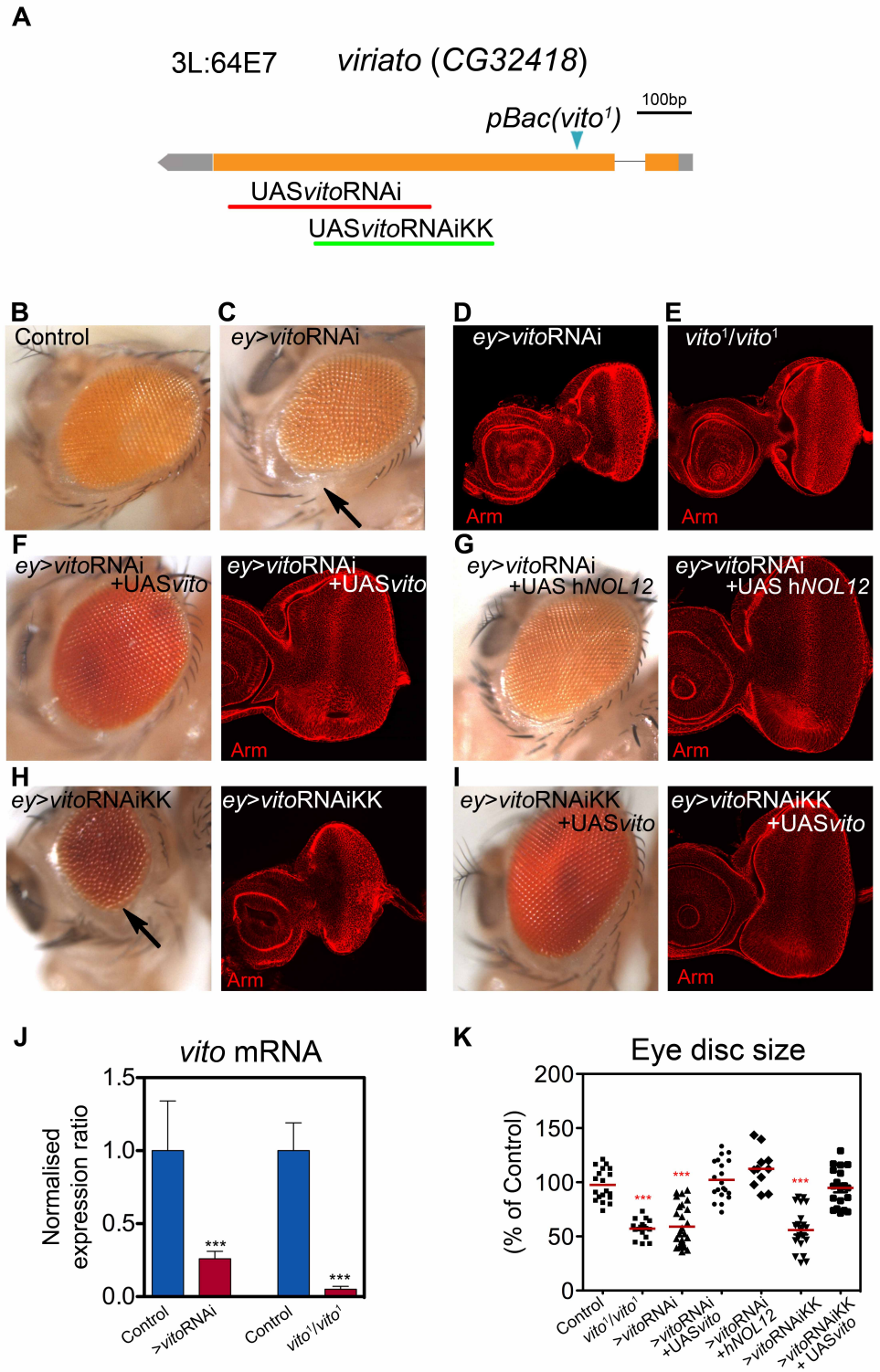

Figure 2.3 - Assessment of *vito*RNAi efficiency and specificity. (A) The *CG32418/vito* genomic region. Boxed regions represent the two *vito* exons and orange indicates the coding region. The two distinct regions targeted by the independent *vito*RNAi lines used are indicated beneath, and the position of the *PiggyBac* insertion in exon 2 of the *vito*^{1} mutant allele (*PBac(RB)CG32418*^{e03237}) is indicated above. **(B,C)** Lateral views of control (UAS-*lacZ*/+; *ey*-Gal4/+) (B) and *vito* loss-of-function (C) adult eyes. Knocking down *vito* eye expression (*ey*-Gal4, UAS-*vito*RNAi/+) causes a reduced eye phenotype (arrow). **(D,E)** Similar to *vito*RNAi-expressing discs, the size of the imaginal disc of *vito*^{1} homozygous mutants is also reduced. **(F,G)** The *vito*RNAi phenotype in the adult retina and eye imaginal disc is rescued by overexpression of a UAS-*vito* (F) or a human *NOL12* transgene (G), supporting the specificity of the *vito*RNAi. **(H,I)** A second RNAi line targeting *vito* (UAS-*vito*RNAiKK) also causes a reduction in eye size (H) and this phenotype is also rescued by overexpression of a UAS-*vito* transgene (I). Eye imaginal discs were stained for Armadillo (red). **(J)** *vito* mRNA levels were measured by qPCR using RNA isolated from control larvae or those ubiquitously expressing *vito*RNAi at 112 hours

after egg laying (AEL), and from *vito*^{1} homozygous larvae and wild-type controls. Data are presented as fold change relative to control and indicate the mean + s.d. (n=3-5). Data were normalised to the levels of *CaMKII* mRNA. (***, $P<1X10^{-4}$ relative to control). **(K)** Eye disc sizes of the indicated genotypes represented as a distribution. Dots represent individual measurements and horizontal bars show mean values (***, $P<1X10^{-4}$ relative to control). Control (UAS-*lacZ*/+; *ey*-Gal4/+); >*vito*RNAi (*ey*-Gal4, UAS-*vito*RNAi/+); >*vito*RNAi + UAS*vito* (UAS*vito*/+; *ey*-Gal4, UAS-*vito*RNAi/+); >*vito*RNAi + h*NOL12* (*ey*-Gal4, UAS-*vito*RNAi/+; UAShNOL12-GFP/+); >*vito*RNAiKK (*ey*-Gal4, UAS-*vito*RNAiKK/+); >*vito*RNAiKK + UAS*vito* (UAS*vito*/+; *ey*-Gal4, UAS-*vito*RNAiKK/+).

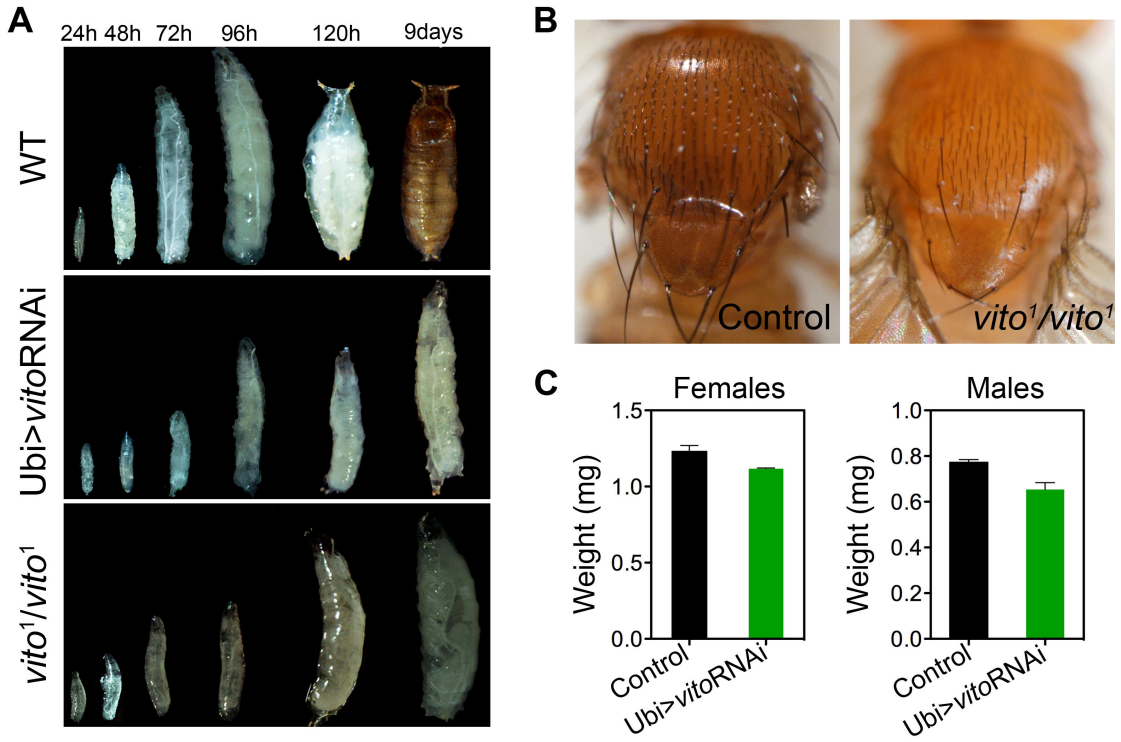

Figure 2.4 - Loss of Vito induces Minute-like phenotypes. (A) Images of wild-type, Ubi-Gal4>UAS-*vito*RNAi and *vito*^{1} homozygous mutant larvae at different stages (24 hours to 9 days) of development are shown. Both *vito* knockdown larvae and *vito*^{1} homozygous mutant larvae exhibit a growth arrest phenotype, surviving for up to 9 days as arrested L3 larvae. **(B)** *vito*^{1} homozygous adult 'escapers' have short and thin bristles in the thorax when compared to control wild-type flies. **(C)** Graphs represent the mean weight (+ s.d.) of control (Ubi-Gal4/+) and ubiquitously expressing *vito*RNAi (Ubi-Gal4/+; vitoRNAi/+) adult males and females.

Sequence comparison analysis predicts *vito* to encode a small protein with an N-terminal Nol12 domain that is conserved in the Nol12 protein family (Fig. 2.5A). The *Drosophila* genome contains only one non-redundant gene for Nol12, as do all the genomes found to encode Nol12 proteins. Therefore, we attempted to rescue the reduced growth induced by *vito*RNAi by co-expressing the single human NOL12 (hNOL12) protein. Remarkably, hNOL12 was also able to fully rescue eye disc growth, suggesting that there is an evolutionary conservation of Nol12 protein family functions in tissue growth (Fig. 2.3G,K). We concluded from these results that inducible *vito*RNAi was efficient and specific, which, together with the ease and flexibility of *vito* knockdown in

both clones and targeted tissues, led us to mainly use *vito*RNAi for the experiments described here.

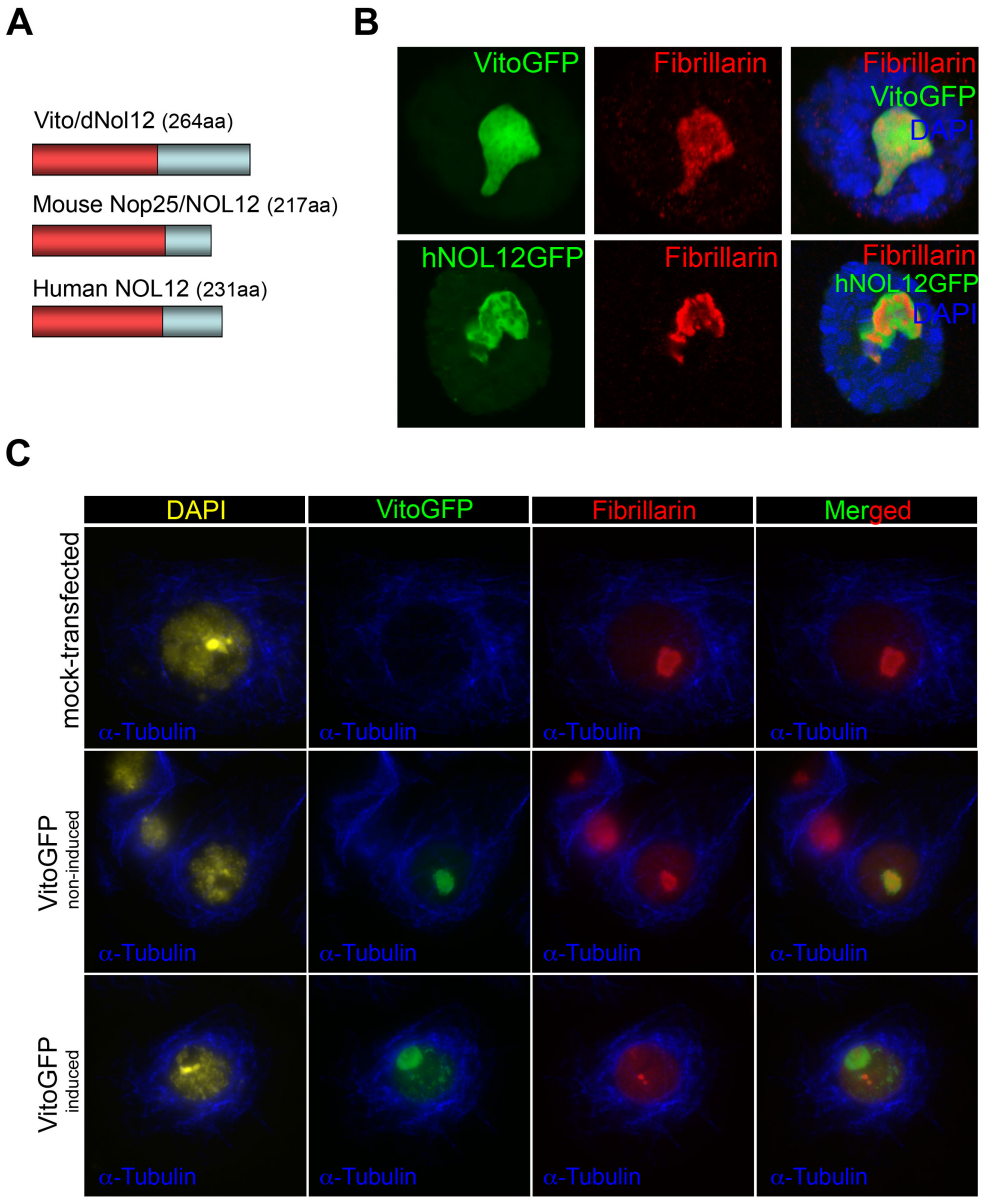

Figure 2.5 - *vito/Nol12* encodes a nucleolar protein. (A) Domain structure of Vito and human and mouse NOL12 homologues. The N-terminus of Vito is 28% identical to the N-terminus of human NOL12. **(B)** Nucleolar localisation of Vito-GFP and human NOL12-GFP in *Drosophila* larval salivary gland cells co-stained for the nucleolar protein Fibrillarin (red) and with DAPI for DNA. **(C)** *Drosophila* S2 cells mock-transfected or transfected with the plasmid pHsp70-*vito*-GFP stained with an anti-α-Tubulin antibody to detect microtubules (blue), an anti-Fibrillarin antibody to visualize the nucleoli (red) and with DAPI to counterstain DNA (yellow). The basal activity of the Hsp70 promoter was sufficient to express Vito-GFP at low levels in S2 cells (middle panel). Strong overexpression of Vito-GFP was achieved with a 30-minute heat shock followed by a 2-hour recovery step (lower panel). Acquisition settings for GFP were adjusted to similar levels owing to the strong, induced overexpression of Vito-GFP upon heat shock.

Human NOL12 has been identified in several proteomic analyses of human nucleoli (Ahmad et al., 2009). Mouse NOL12 localizes to nucleoli in COS7 cells, and

knocking down NOL12 function in this cell line results in nucleolar fragmentation (Suzuki et al., 2007). During the course of this work the budding yeast Nol12 homologue Rrp17p/Ydr412p has been implicated in nucleolar non-coding RNA processing events (Peng et al., 2003; Li et al., 2009; Oeffinger et al., 2009). Owing to the relatively low conservation of the Nol12 domain, we analyzed whether Vito localized to the nucleolus. Targeted expression of low levels of GFP-tagged Vito in *Drosophila* tissues or S2 cells showed co-localization of Vito with Fibrillarin (Fig. 2.5B,C), a nucleolar methyltransferase required for pre-rRNA modification that localizes to the fibrillar region of *Drosophila* nucleoli (Orihara-Ono et al., 2005). Consistent with its ability to functionally compensate for *vito* knockdown, hNOL12 also localized to the nucleolus when expressed in *Drosophila* larval tissues (Fig. 2.5B).

Since no in vivo functional information is thus far available for members of the Nol12 family in any metazoan, we examined the role of *vito* in tissue growth during *Drosophila* development. Using Flp/FRT-based recombination, we induced during early larval development clones of cells expressing *vito*RNAi that were analyzed later in third instar eye imaginal discs. During this period, most cells in the disc are actively proliferating. In the eye disc, *vito*RNAi-expressing clones were significantly smaller than control neutral clones, both in the peripodial epithelium and in the eye disc proper (Fig. 2.6A-C) and this was not due to a reduction in cell size (Fig. 2.6D). Similarly, cells in the posterior compartment of the wing imaginal disc expressing *vito*RNAi do not show an alteration in size or changes in cell cycle phasing in comparison to cells of the anterior compartment used as internal controls (Fig. 2.6E). Thus, the decreased clone size observed was not due to a reduction in cell size or changes in cell cycle phasing suggesting that in proliferating cells *vito* knockdown slows down proliferation while maintaining the coordination of cell growth and cell cycle.

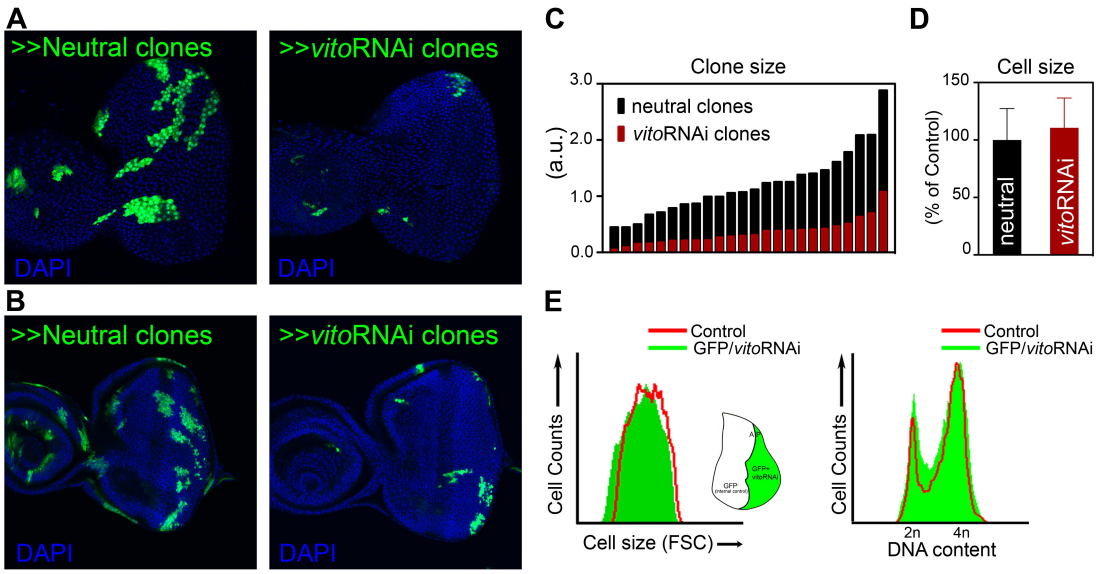

Figure 2.6 - *vito*RNAi clones have a growth disadvantage. (A,B) Neutral or *vito*RNAi clones were induced in the *Drosophila* early eye disc and analysed 72 hours later. Images show representative clones in the peripodial epithelium (A) and epithelial layers of the disc proper (B), marked positively by the presence of GFP. **(C)** Quantification of neutral and *vito*RNAi clone size in the eye disc proper represented as clonal area distributions. a.u., arbitrary units. **(D)** Mean cell size (+ s.d.) in eye disc-proper clones obtained by dividing each clonal area by the number of nuclei in the clone (n=24). **(E)** Flow cytometry analysis of cell size (left) and cell cycle profile (right) in dissociated wing imaginal disc cells expressing *vito*RNAi in the posterior compartment from the *engrailed*-Gal4 driver (*en*-Gal4, UASGFP/UAS-*vito*RNAi). Forward-scatter (FSC) and DNA content analysis of wing disc posterior compartment cells (green) expressing GFP plus *vito*RNAi. Anterior cells (non-GFP cells; red) were used as controls. No significant differences were detected in either cell size or cell cycle profile.

4.2 *vito* is required for tissue growth independently of its role in cell survival

Next, we investigated whether *vito* misregulation could also result in apoptosis, contributing to the observed defect in tissue growth. In contrast to wild-type eye discs, where apoptosis is virtually absent during larval development, *vito*RNAi eye discs exhibited a significant number of cells undergoing apoptosis, as detected by the presence of activated cleaved Caspase-3 (Fig. 2.7A,B), and this was accompanied by a substantial reduction in disc size (42%, $P<1X10^{-4}$; Fig. 2.7C). Therefore, *vito* is required for cell survival.

To determine whether the reduction in eye disc size could be explained exclusively by this increase in apoptosis, *vito*RNAi was induced in a heterozygous background for the *H99* deficiency (Fig. 2.7A), which deletes the three crucial proapoptotic genes *rpr*, *grim* and *hid* (*Wrinkled*) (White et al., 1994; Grether et al., 1995; Chen et al., 1996).

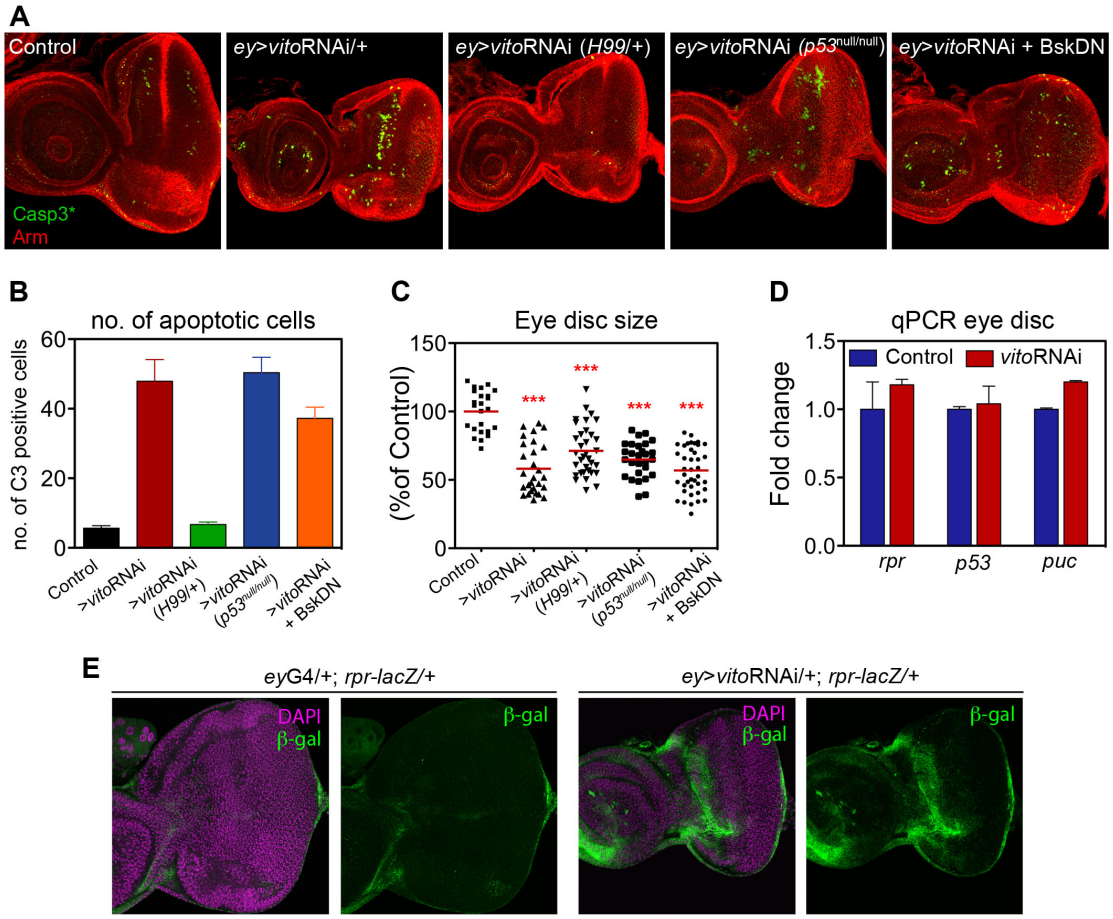

Figure 2.7 - *vito* is required for tissue growth independently of its role in cell survival. (A) Third instar *Drosophila* eye imaginal discs of the indicated genotypes stained for Armadillo (red) and cleaved Caspase-3 (green). Knocking down *vito* (*ey*>*vito*RNAi) affects the size of the eye discs and causes significant cell death. Removing one copy of each of the three pro-apoptotic genes of the Hid-Reaper-Grim complex by introducing the deficiency *H99* into the *vito*RNAi background (*ey*>*vito*RNAi/+; *H99*/+) blocks cell death in the eye imaginal disc. *vito*RNAi tissue growth and cell death phenotypes are not rescued in p53 null mutant eye discs (*ey*>*vito*RNAi/+; *p53*null). Overexpression of a dominant-negative form of JNK (Bsk^{DN}) in the *vito*RNAi background (*ey*>*vito*RNAi/+; UASBsk^{DN}) does not rescue the tissue growth phenotype. Control (UAS-*lacZ*/+; *ey*-Gal4/+); >*vito*RNAi (*ey*-Gal4, UAS-*vito*RNAi/+); >*vito*RNAi (*H99*/+) (*ey*-Gal4, UAS-*vito*RNAi/+; *Df(3L)H99*/+); >*vito*RNAi ($p53^{null/null}$) (*ey*-Gal4, UAS-*vito*RNAi/+; $p53^{[5A-1-4]}/p53^{[5A-1-4]}$); >*vito*RNAi + BskDN (*ey*-Gal4, UAS-*vito*RNAi/+; UASBsk^{DN}/+). **(B)** Quantification of cell death assessed by the number of cleaved Caspase-3 positive cells in the eye discs in A. The significant number of cells undergoing apoptosis in *vito*RNAi eye discs is abolished in a heterozygous background for the *H99* deficiency. Data are presented as the mean + s.e.m. (n=15-40). **(C)** Eye disc sizes of the indicated genotypes were measured and are represented as a distribution. Dots represent individual measurements and horizontal bars show mean values (***, $P<1X10^{-4}$ relative to control). **(D)** Transcript levels of genes involved in the apoptotic pathway were measured by qPCR using RNA isolated from either control or *vito*RNAi eye imaginal discs. Data are presented as the fold change compared with the control and represent the mean + s.d. (n=3). **(E)** The expression of *rpr* was monitored using the *rpr*-11kb-*lacZ* reporter in control and *vito*RNAi eye discs. Eye discs were stained with an anti-β-galactosidase antibody (green) and with DAPI for DNA (purple). Increased levels of *rpr* reporter activity are detected in the anterior region of *vito*RNAi eye discs.

In this genotype, in which apoptosis was almost completely suppressed (Fig. 2.7B), the average size of the eye disc was only partly rescued compared with *vito*RNAi discs (13%, P=0.0072), but was still significantly smaller than in control discs (29% reduction, $P<1X10^{-4}$) (Fig. 2.7C). Similar results were obtained when *vito*RNAi was co-induced with the baculovirus caspase inhibitor p35 (Fig. 2.8A,B). Furthermore, even though we only

detected a slight, non-statistically significant increase in *rpr* transcript levels by qPCR in whole eye-antennal *vito*RNAi discs (Fig. 2.7D), we observed a robust and localised upregulation of the *rpr*-11kb-*lacZ* transcriptional reporter (Nordstrom et al., 1996) in the anterior proliferative domain of the eye disc (Fig. 2.7E). Interestingly, most of the apoptotic death was detected in the anterior domain, where we had also detected the strongest *vito* transcription. The fact that only a fraction of cells within the eye disc upregulated *rpr* (as monitored by the *rpr*-11kb-*lacZ* reporter) might have masked the increase in *rpr* transcripts in whole discs measured by qPCR.

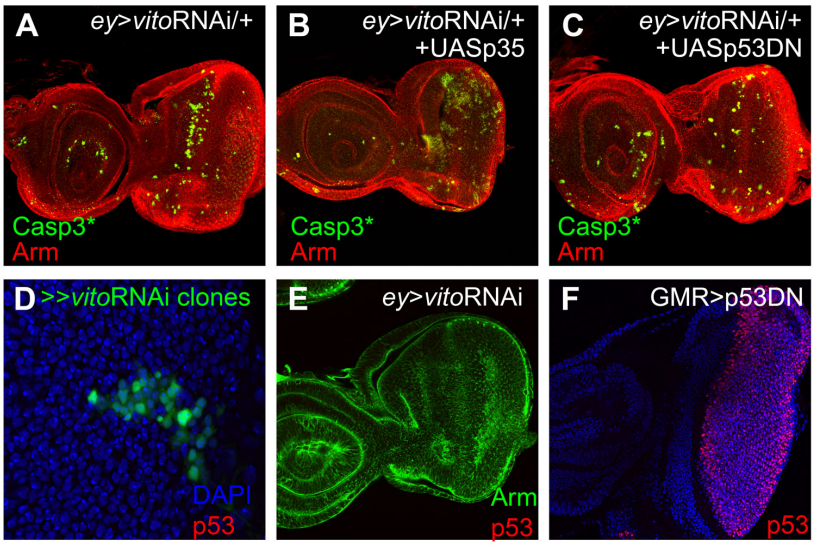

Figure 2.8 - Loss of Vito induces caspase-dependent apoptosis that is p53 independent. (A-C) Confocal images of eye imaginal discs stained for Armadillo (red) and cleaved Caspase-3 (green). (A) Knocking down *vito* (*ey*-Gal4, UAS-*vito*RNAi/+) affects the size of the eye discs and causes significant cell death. (B) Co-expression of *vito*RNAi and the caspase inhibitor p35. Caspase-3 signal is detected in a significant number of 'undead cells'; however, the apoptotic block does not rescue the small size of the disc resulting from *vito*RNAi. (C) Overexpression of a dominant-negative form of p53 in the *vito*RNAi background (*ey*Gal4,UAS-*vito*RNAi/+; UASp53^{DN}/+) does not rescue the tissue growth and cell death phenotype. **(D,E)** Vito knockdown does not lead to p53 induction. Clones expressing *vito*RNAi were induced with *act5C*>Gal4 and stained with an anti-p53 antibody (red) (D). Clones are marked positively by the presence of GFP. (E) *vito* was knocked down in the entire eye field with the *ey*-Gal4 driver (*ey*Gal4,UAS-*vito*RNAi/+) and stained with an anti-p53 antibody (red) and for Armadillo (green). (**F**) Expression of a dominant-negative form of p53 under the control of the GMR promoter (GMR>*p53*DN) was used as a positive control for the anti-p53 antibody staining (red); DNA was stained with DAPI.

Overall, these results indicate that the growth deficit induced by reducing *vito* function cannot be explained by a generalized induction of apoptosis. Since Vito is a nucleolar protein and nucleolar stress in mammalian cells leads to apoptosis mediated by p53 stabilization (Rubbi and Milner, 2003; Yuan et al., 2005), we tested whether apoptosis in *vito*RNAi eye cells was dependent on p53 function. Expression of *vito*RNAi still caused a significant level of apoptosis in a *p53* null mutant background (Fig. 2.7A,B), or when co-expressed together with a dominant-negative form of p53 (R155H) (Fig. 2.8C)

that is able to block p53 pro-apoptotic activity (Ollmann et al., 2000). The absence of p53 function did not rescue normal tissue growth in *vito*RNAi eye discs (Fig. 2.7C). In addition, we could not detect elevated p53 transcript or protein levels in *vito*RNAi eye discs (Fig. 2.7D and Fig. 2.8D-F).

In *Drosophila*, as well as in mammals, the JNK pathway has been implicated in apoptotic cell death in a variety of cellular and developmental contexts (reviewed by Igaki, 2009) and has been suggested to act both upstream (McEwen and Peifer, 2005) and downstream (Kuranaga et al., 2002) of *rpr* function. We studied the possible involvement of JNK signaling in apoptosis resulting from *vito*RNAi expression by: (1) co-expressing a dominant-negative form of JNK (BskDN) (Fig. 2.7A); and (2) analyzing *puc* transcript levels (Fig. 2.7D) and *puc-lacZ* reporter transcription (Fig. 2.9) as a read-out for JNK signaling (Martín-Blanco et al., 1998). The results of these experiments suggest that upon *vito* knockdown there is a weak activation of JNK signaling, as *puc* mRNA levels in eye discs increased by 20% (but in a non-significant manner, *P*=0.059) (Fig. 2.7D), and the co-expression of BskDN resulted in minor apoptotic rescue (Fig. 2.7A,B). We also failed to detect any upregulation of *puc-lacZ* in *vito*RNAi clones in eye discs (Fig. 2.9), suggesting that activation of JNK signaling is not the major pathway that mediates the apoptotic process resulting from *vito* knockdown.

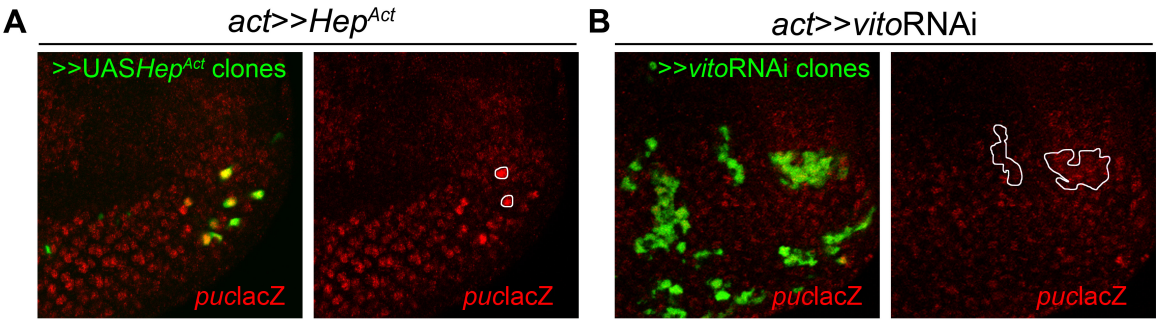

Figure 2.9 - *puc-lacZ* in *vito*RNAi clones in the eye disc. Mitotic clones were induced using the Flp/FRT method. *puc*E69 is a *puckered-lacZ* reporter used as a JNK pathway readout. **(A)** Clones overexpressing an activated form of *hemipterous* (Hep^{Act}; Hep is the *Drosophila* JNKK) were induced by heat shock (1 hour, 37°C) at 96 hours AEL in larvae of the genotype *y w hsflp/+*; *act*>y+>Gal4, UAS-GFP/ UAS-Hep^{Act}; *puc*E69/+ and analysed 24 hours later. Eye discs were stained with an anti-β-galactosidase antibody (red). **(B)** *vito* knockdown was induced in mitotic clones induced 48-72 hours AEL by heat shock (1 hour, 37°C) in larvae of the genotype *y w hsflp/+*; *act*>y+>Gal4, UAS-GFP/ UAS-*vito*RNAi; *puc*E69/+ and stained with an anti-β-galactosidase antibody (red). Whereas activation of the JNK pathway (A) led to the upregulation of *puc*E69 reporter activity, this was not the case when *vito* was knocked down (B).

Overall, these experiments show that *vito* is required for tissue growth during *Drosophila* development. This requirement can be explained only in part by the role of

vito in preventing caspase-mediated apoptosis, in which the JNK pathway itself might play a marginal role.

4.3. *vito* regulates nucleolar structure and nucleolar retention of Fibrillarin

To investigate further the mechanisms by which Vito, a nucleolar protein, might be controlling tissue growth, we analyzed the effects of reducing or increasing Vito levels on the nucleolus of salivary gland cells, which, owing to their polyploidy, have large nucleoli. As observed in the eye disc, the reduction of *vito* expression in the salivary glands also caused a substantial deficit in tissue growth (Fig. 2.10A,B). To examine nucleolar structure and activity we looked at the distribution of Fibrillarin and *Drosophila* Nopp140-True (Cui and DiMario, 2007). The human NOPP140 (NOLC1) protein is a conserved phosphoprotein that interacts with the RNA Pol I 194 kDa subunit (RPA194) and is proposed to play a role in the maintenance of nucleolar structure (Chen et al., 1999). NOPP140 is also required for the assembly or recruitment of snoRNPs to the nucleolus, where these complexes guide site-specific 2'-O-methylation and pseudouridylation of pre-rRNA (Wang et al., 2002). In *Drosophila*, as previously described (Mccain et al., 2006), a GFP-tagged Nopp140-True protein expressed from a heat-shock inducible promoter was detected uniformly in the nucleolus of salivary gland cells, where it colocalized with Fibrillarin (Fig. 2.10D). In *vito*RNAi expressing cells, Nopp140-True still localized to the nucleolus but its pattern became more dispersed and 'hollow', concentrating at the nucleolar periphery. This redistribution paralleled the redistribution of Fibrillarin, which was concentrated in the nucleolus at higher levels (Fig. 2.10E).

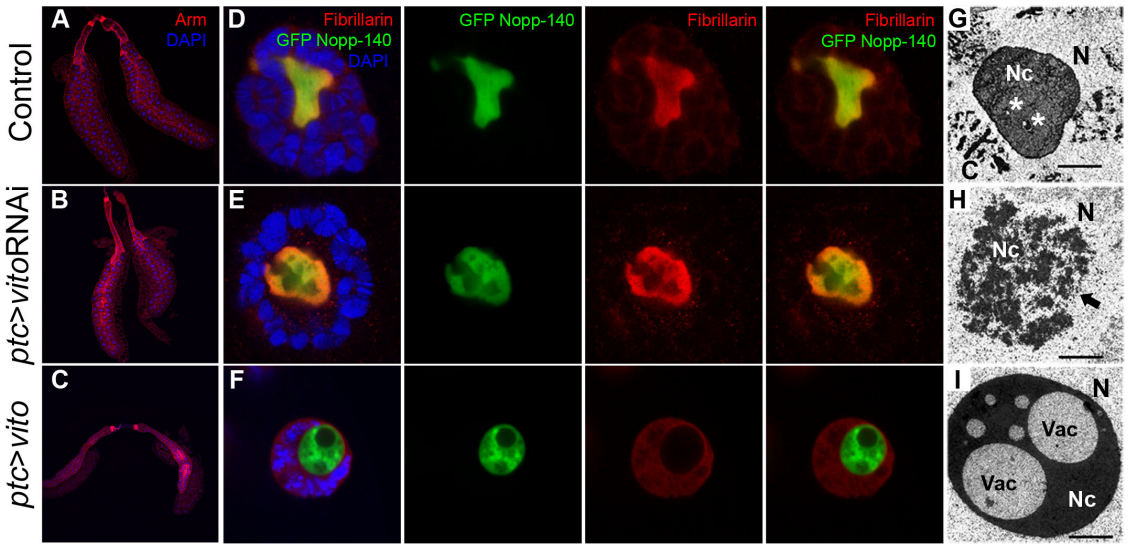

Figure 2.10 - Vito regulates nucleolar structure. (A-I) Salivary glands show a substantial reduction in overall size upon *vito* misregulation. Low magnifications of salivary glands from third instar *Drosophila* larvae expressing UAS-*lacZ* (control) (A,D,G), UAS-*vito*RNAi (B,E,H) and UAS-*vito* (C,F,I) under the control of the *ptc*-Gal4 driver. (D-F) Vito regulates nucleolar localisation of Fibrillarin. Third instar larvae heterozygous for the insertion hs-GFP-Nopp140-True were heat

shocked for 1 hour and allowed to recover for 2 hours. (D) GFP-Nopp140-True (green) and Fibrillarin (red) colocalise in the nucleolus of control salivary gland cells. (E) Fibrillarin accumulates preferentially in the nucleolar periphery of *vito*RNAi-expressing cells. (F) Vito overexpressing cells show a swollen and abnormally rounded nucleolus that loses Fibrillarin staining. (G-I) Reducing Vito levels results in nucleolar decondensation, whereas overexpressing Vito causes the opposite phenotype, with the nucleolus becoming a very dense and compact structure. (G-I) Electron micrographs of control salivary glands (G), *vito*RNAi (H) or salivary glands overexpressing Vito (I). Asterisks indicate small vacuoles and 'Vac' indicates large vacuolar-like regions. The arrow indicates granular regions. N, nucleus; Nc, nucleolus. Scale bars: 2 μm.

Similar results were obtained with *vito*^{1} mutants and rescued upon Vito and hNOL12 expression (Fig. 2.11). In *vito*-overexpressing cells (Fig. 2.10C), Nopp140-True was still recruited to the nucleolus, which became rounded and displayed large vacuoles devoid of Nopp140 signal. Interestingly, Fibrillarin was absent from Vito-overexpressing nucleoli and accumulated at low levels in the nucleoplasm (Fig. 2.10F, and see Fig. 2.5C for similar results in S2 cells).

These changes in nucleolar morphology resulting from altering Vito expression levels were confirmed by TEM (Fig. 2.10G-I). As previously noted (Orihara-Ono et al., 2005), the wild-type *Drosophila* nucleolus does not display the characteristic vertebrate tripartite organization, as only a homogeneous region with a regular surface is observed (Fig. 2.10G).

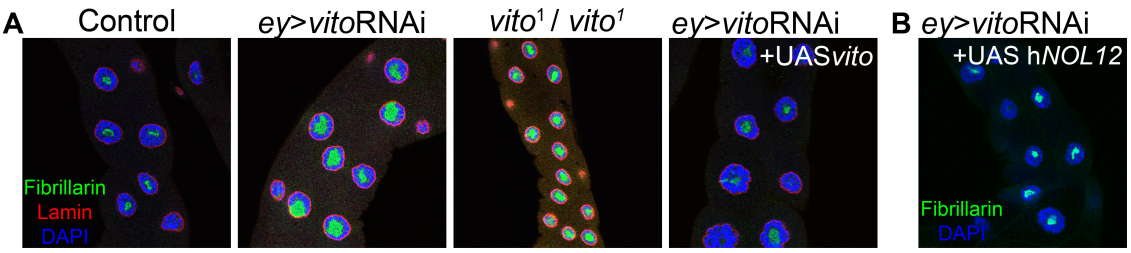

Figure 2.11 - Vito regulates nucleolar retention of Fibrillarin (**A**) Images of salivary glands of the indicated genotypes stained for the nucleolar marker Fibrillarin (green), Lamin B (red) to reveal the nuclear envelope, and counterstained with DAPI (blue). In a control situation, Fibrillarin properly localizes to the nucleolus at normal levels. Fibrillarin accumulates in the nucleolus in *vito*RNAi-expressing cells and *vito*^{1} homozygous mutant cells. In salivary gland cells overexpressing a UAS-*vito* transgene in the *vito*RNAi background, Fibrillarin nucleolar levels are reduced to wild-type levels. **(B)** Salivary gland cells expressing human *NOL12* in the *vito*RNAi background stained for Fibrillarin (green) and DAPI (blue). The co-expression of human *NOL12* significantly reverts Fibrillarin nucleolar levels back to wild-type.

Knocking down *vito* resulted in a substantial reduction in the packaging of nucleolar components, and the nucleoli exhibited a clear overall granular organization (Fig. 2.10H). By contrast, Vito overexpression induced a dramatic reorganization of the nucleolus into two distinct regions: a peripheral and highly compact region with very smooth borders that surrounded internal vacuole-like structures (Fig. 2.10I).

These results show that Vito is a major regulator of nucleolar architecture and that it regulates the recruitment of specific nucleolar components: whereas Nopp140 remains

associated to the nucleolus when Vito levels are changed, the recruitment of the snoRNP methyltransferase Fibrillarin depends critically on Vito. Interestingly, in human cells, NOPP140, but not Fibrillarin or the rRNA pseudouridylase dyskerin, can interact with ribosomal gene chromatin independently of ongoing Pol I transcription (Prieto and McStay, 2007). This suggests that Vito could act to control the recruitment or retention of a second layer of proteins, such as Fibrillarin, that require binding to nucleolar hub proteins (Emmott and Hiscox, 2009) in order to associate with the nucleolar compartment.

4.4. Vito regulates ribosomal RNA processing leading to abnormal nucleolar accumulation of large ribosomal subunit proteins

Since Vito is a nucleolar protein that regulates the nucleolar architecture and since the nucleolus is the nuclear sub-compartment where pre-rRNA transcription, modification, and processing takes place, we further studied how those events are altered when nucleolar structure is affected by Vito misregulation. In *Drosophila* as in other eukaryotes, rDNA genes are transcribed by Pol I as a single transcription unit and the mature 18S, 5.8S and 28S rRNAs are generated by extensive processing comprising endonucleolytic and exonucleolytic steps and chemical modifications. There is some flexibility in the sequence of the initial processing events, and two alternative processing pathways, A and B, have been described previously (Long and Dawid, 1980) (Fig 2.12). In *Drosophila*, the major processing pathway starts with the removal of the external transcribed spacer (ETS) with cleavage at position 1 (pathway A - see Fig. 2.12A). It is believed that when the pathway A is compromised, the pre-rRNA is first cleaved at site 3 in the internal transcribed spacer (ITS) generating intermediates d and b (Giordano et al., 1999; Fichelson et al., 2009) (Fig. 2.12A). To further investigate processing defects, we conducted a series of northern blots using oligonucleotide probes complementary to different regions of the pre-rRNA molecule in control larvae or larvae depleted of Vito by RNAi. A strong accumulation of the intermediate d (probe ITS1, Fig. 2.12B,C) points to a premature cleavage at site 3 at the ITS1 indicating the usage of the alternative pathway (pathway B). Abnormal intermediate forms with molecular weights flanked by the intermediate d (3.4kb) and 28Sb (2.1kb) are detected in *vito*RNAi (Fig. 2.12B, asterisk) and neither of these molecules corresponds to products of the previously described *Drosophila* rRNA processing pathways. The lower molecular weight band corresponds to 2.6kb, and could be a result of an ectopic cleavage of c at site 6 (28Sa (2.1kb) + e (538bp)), and the more intense higher molecular weight band could be a result of a premature

cleavage of the intermediate b at site 6. By qPCR using primers against specific regions of the ITS 1 and 2 we could detect a slight accumulation of ITS 1 containing sequences but a more pronounced accumulation of ITS 2 containing sequences (~3-fold accumulation with ITS2 5' when compared to ITS2 3') (Fig. 2.12D).

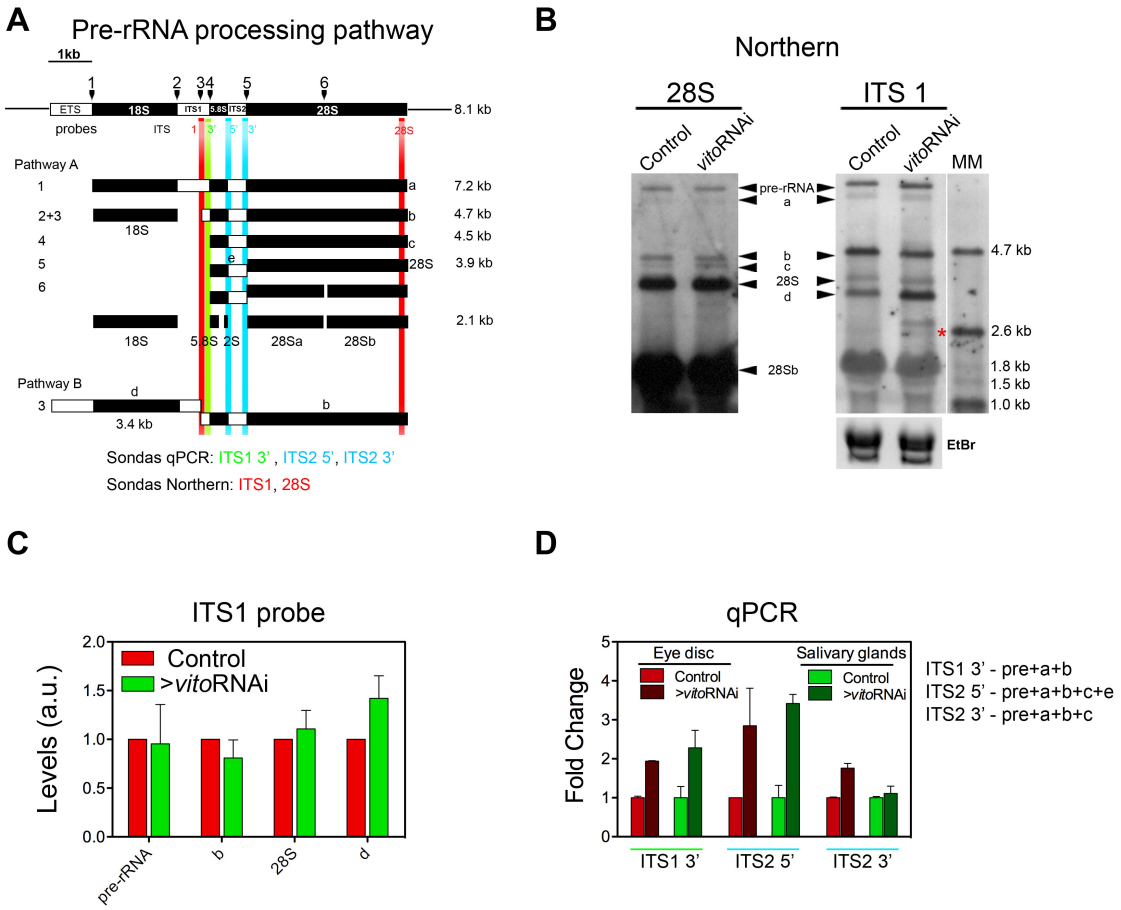

Figure 2.12 - rRNA processing is impaired after Vito depletion. **(A)** Schematic representation of the pre-rRNA processing pathways A and B (adapted from Long and Dawid, 1980). The top line shows the structure of the pre-rRNA; ETS and ITS are shown in white, the 18S, 5.8S, 2S and 28S subunits in black. Endonucleolytic cleavage sites are indicated by numbered marks (1–6). The probes used for northern blot analysis are represented as red boxes (ITS1 and 28S) and the primers used for qPCR represented as green (for ITS1 3') and blue (for ITS2) boxes. In the pathway B further processing is likely to follow the canonical pathway. **(B)** Northern blots of total RNA from control third-instar larvae *(da*G4/UAS-*dicer*2) or larvae expressing *vito*RNAi (UAS*vito*RNAi; *da*G4/UAS-*dicer*2) were hybridized with DIG-labeled oligonucleotide probes complementary to the different processing intermediates and products of the rRNA processing pathway. The blot probed with 28S was stripped and reprobed with ITS1. Loading was normalized to similar levels of mature rRNA detected by ethidium bromide (EtBr) staining (shown at the bottom). Abnormal intermediates are indicated by a red asterisk (*). MM denotes for molecular marker. **(C)** The graph shows the mean levels (+s.d.) of the different intermediates in three independent northern blots probed with the oligonucleotide ITS1. **(D)** Transcript levels of rRNA were measured by qPCR using RNA isolated from salivary glands or eye-imaginal discs of control or *vito*RNAi third instar larvae. Data are presented as fold changes compared with the control and represent the mean + s.d. (n=3-5). For eye imaginal disc: Control (UAS-*lacZ*/+; *ey*G4/+); >*vito*RNAi (*ey*G4, UAS-*vito*RNAi/+). For salivary glands: Control (UAS-*lacZ*/+; *ptc*G4/+); >*vito*RNAi (*ptc*G4/+; UAS-*vito*RNAi/+).

This result points to an accumulation of ITS2 containing sequences and could reflect an accumulation of **e** molecules because the only difference among these primer pairs is

that ITS2 5’ detects intermediate e, or 5’ extended forms of e. So far our data strongly suggest that Vito has a role in rRNA processing. During the course of this work, the budding yeast Nol12 homologue was found to be a 5’-3’ exonuclease required for efficient exonuclease digestion of the mature 5’ends of 5.8S rRNAs (Oeffinger et al., 2009), which supports our hypothesis that Vito could be required for the exonucleolytic trimming from site 3 to 4, which could explain the usage of the alternative pathway and also the abnormal cleavages of intermediates b and c at site 6.

To test whether the defects in rRNA processing could affect the export of pre-ribosomes, the localization of RpLs and RpSs was assessed in salivary glands and eye imaginal discs after Vito depletion. In control salivary gland cells RpL41 localizes to the nucleolus at low levels, whether RpL22 localizes mainly to the cytoplasm and to the nucleolus at very low levels (Fig. 2.13A,C). In Vito depleted salivary gland cells we detected an abnormal nucleolar accumulation of the large subunit ribosomal proteins RpL41 and RpL22 (Fig. 2.13A,C). Similarly RpL41 strongly accumulates in the nucleus and nucleolus of the eye imaginal disc cells particularly at the anterior region of the eye disc where most cells are actively proliferating (Fig. 2.13B). To monitor the export of the small ribosomal subunit, salivary glands of flies expressing a YFP-tagged RpS9 or staining of salivary gland cells with an anti-RpS6 antibody revealed no significant changes in the expression patterns or levels of these proteins after Vito depletion (Fig. 2.13D). Overall these results indicate that the accumulation of the large subunit proteins could be a secondary effect of the rRNA processing defects detected in the absence of Vito, or that perhaps Vito can have a role in the maturation or release of the large ribosomal subunits from the nucleolus to the nucleoplasm. Therefore, the role of Vito in rRNA processing could lead to defects in ribosome biogenesis, and be the basis for the defective growth and developmental delay observed in *vito* mutants.

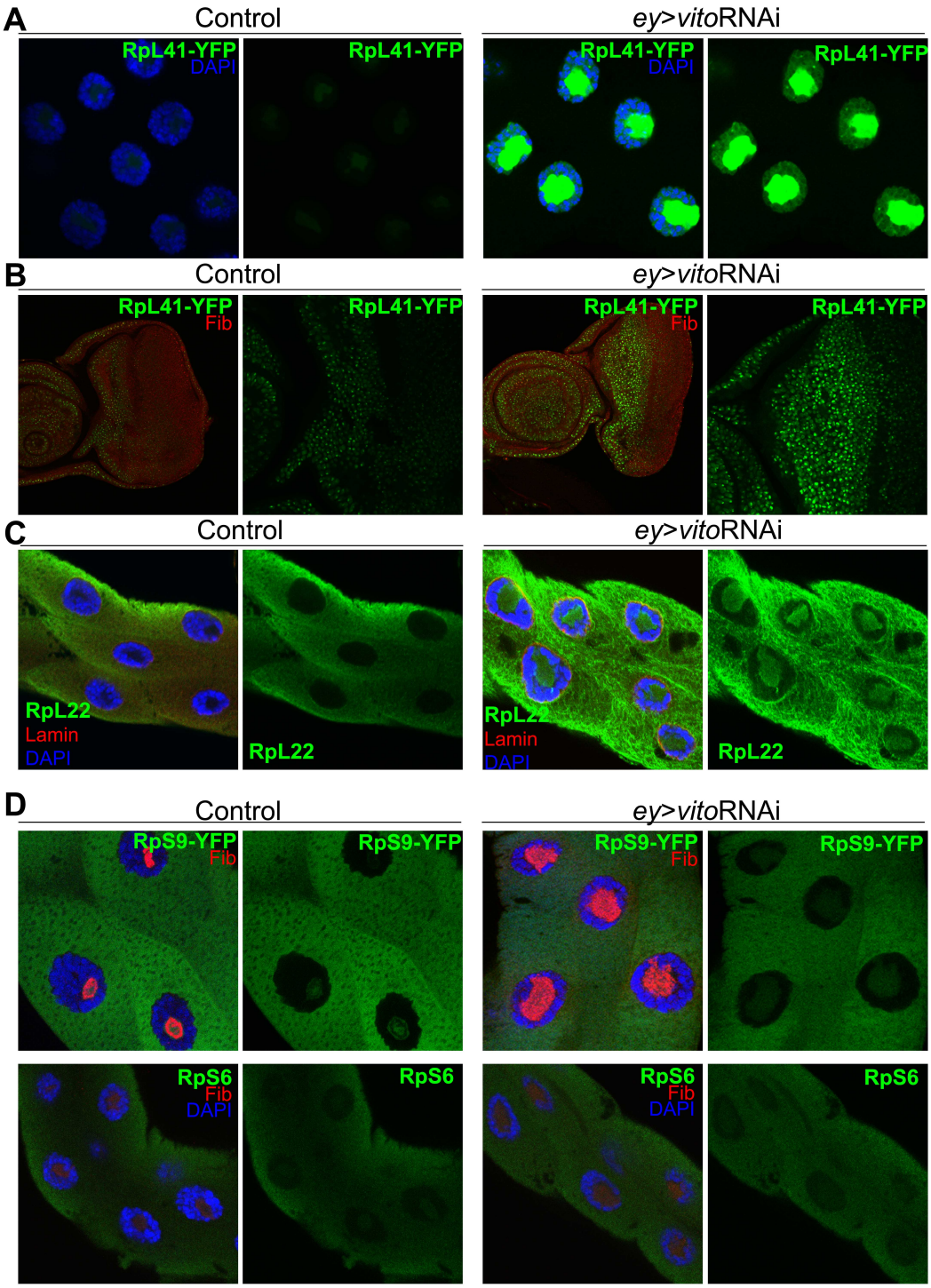

Figure 2.13 - Vito depletion results in abnormal nucleolar accumulation of large ribosomal subunit proteins. Images of salivary gland cells **(A)** and eye imaginal discs **(B)** expressing RpL41-YFP alone or together with *vito*RNAi. (A) Control salivary gland cells (*ey*-Gal4/RpL41-YFP) expressing RpL41-YFP only (green) show RpL41 localization at low levels at the nucleus and nucleolus whether depletion of Vito driven by *ey*-Gal4 'leaky' expression (*ey*-Gal4, UAS-*vito*RNAi/RpL41-YFP) leads to a strong RpL41 accumulation at the nucleus and nucleolus. (B) Eye imaginal disc cells of the above genotypes also show RpL41-YFP accumulation at the nuclear compartment and nucleolus after Vito knockdown. Note that the anterior region of the eye disc where most cells are actively proliferating are the cells in which RpL41 is mostly expressed. **(C)** Immunofluorescence staining of RpL22 in control and *vito*RNAi salivary glands of the above indicated genotypes. RpL22 is detected mainly in the cytoplasm of control cells but after Vito depletion strong nucleolar retention is observed. **(D)** In control salivary glands expressing RpS9-YFP (*ey*-Gal4/+; RpS9-YFP/+), RpS9 localizes to the cytoplasm and nucleolus and Vito knockdown has no effect on this localization pattern or levels (upper panel). Using an antibody against RpS6 we could not detect any change in the levels or localization pattern of this protein upon Vito misregulation (lower panel). Data was acquired with the same gain imaging settings for the GFP channel.

4.5. Vito levels modulate mass accumulation

We next aimed to establish correlations between the observed nucleolar alterations and tissue growth deficit caused by *vito* misregulation in salivary gland cells. Firstly, quantification of estimated salivary gland cell volumes revealed that both *vito*RNAi and Vito-overexpressing gland cells were significantly smaller than controls (51% and 77% reductions, respectively; $P<1X10^{-4}$; Fig. 2.14A). However, we noted significant differences in the impact of increasing or decreasing *vito* on cytoplasmic and nuclear sizes (Fig. 2.14B,C). The size reduction in *vito*RNAi-expressing cells was basically due to a reduction in cytoplasmic volume (55%, $P<1X10^{-4}$), as nuclear volumes were not significantly reduced (20%, $P=0.0228$). This suggests that *vito* knockdown mainly affects cytoplasmic mass accumulation, while not interfering with the endoreplication process, something that we also assessed by quantifying DAPI staining intensity (Fig. 2.15).

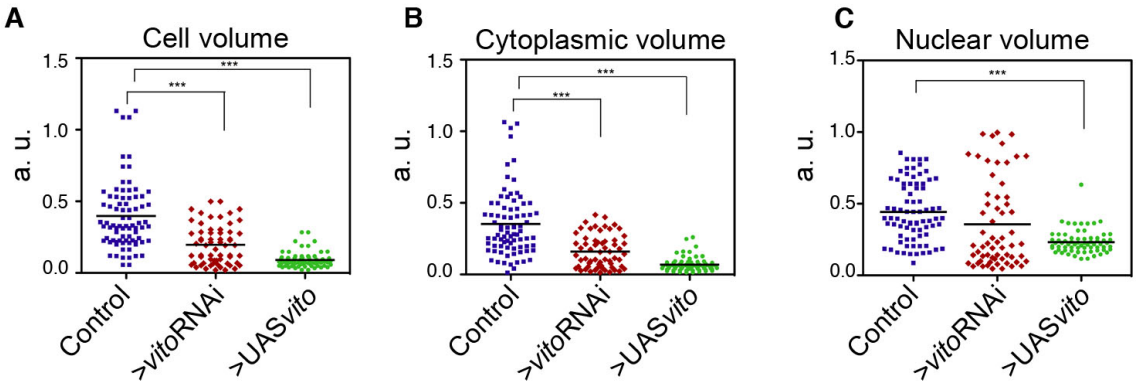

Figure 2.14 - Vito regulates mass accumulation in polyploid salivary gland cells. Scatter plots showing cellular, cytoplasmic and nuclear volumes in salivary glands from third instar Drosophila larvae expressing UAS-*lacZ* (control) **(A)**, UAS-*vito*RNAi **(B)** and UAS-*vito* **(C)** under the control of the *ptc*-Gal4 driver (n=62-80; ***, $P<1X10^{-4}$).

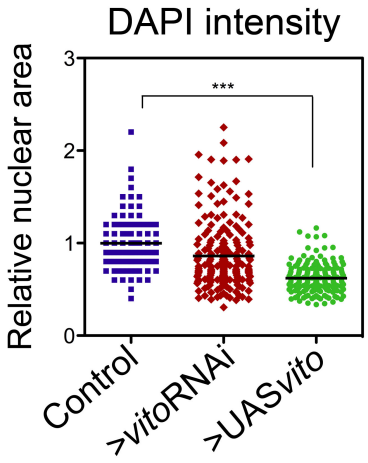

Figure 2.15 - DNA endoreduplication is not affected by Vito. Quantification of nuclear DAPI intensity as a measure of the DNA content/ploidy of cells in salivary glands of larvae expressing UAS-*lacZ* (control), UAS-*vito*RNAi and UAS-*vito* under the control of the *ptc*-Gal4 driver. Dots represent individual measurements and horizontal bars show mean values. ***, $P<1\times10^{-4}$, relative to control.

Vito overexpression caused not only a substantial reduction in cytoplasmic volume (81%, $P<1X10^{-4}$), but also a decrease in nuclear size (48%, $P<1X10^{-4}$). However, this nuclear size

reduction might be secondary to the dramatic loss of cytoplasmic mass: it is likely that the extremely aberrant nucleolar morphology compromises basic cellular processes such as protein synthesis, indirectly affecting DNA endoreplication (and hence nuclear size), as these two processes are intimately linked (reviewed by Edgar and Orr-Weaver, 2001). The overall size reduction in salivary glands is rescued by overexpressing Vito or human NOL12 (Fig. 2.16).

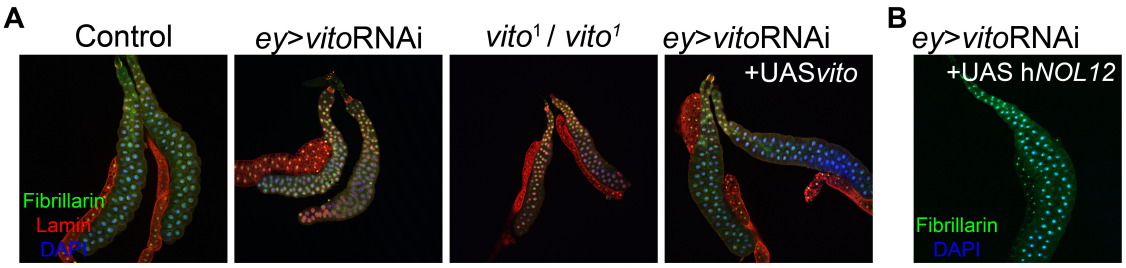

Figure 2.16 - **Nol12 protein family is evolutionary conserved in tissue growth. (A)** Images of salivary glands of the indicated genotypes stained for the nucleolar marker Fibrillarin (green), Lamin B (red) to reveal the nuclear envelope, and counterstained with DAPI (blue). Salivary glands show a strong reduction in overall size upon *vito* expression misregulation induced either by RNAi (driven by *ey*-Gal4 'leaky' expression) or in *vito*^{1} homozygous mutants. The overall size reduction in salivary glands is rescued by overexpression of UAS-*vito* in the *vito*RNAi background. **(B)** Salivary gland cells expressing human *NOL12* in the *vito*RNAi background stained for Fibrillarin (green) and DAPI (blue). The co-expression of human *NOL12* significantly reverts the small size of salivary glands.

4.6. *vito* is a dMyc target required for dMyc-stimulated growth

Our results showing that *vito* is required for the proliferation of diploid imaginal cells and for the growth of polyploid salivary gland cells led us to hypothesize that *vito* could act downstream of dMyc, a crucial regulator of *Drosophila* growth (Johnston et al., 1999) that is also known to be a major regulator of nucleolar growth (Grewal et al., 2005). Since dMyc stimulates tissue growth in part by activating the transcription of genes required for nucleolar function and ribosome biogenesis (Grewal et al., 2005; Demontis and Perrimon, 2009), we tested whether *vito* transcription was under dMyc control. Indeed, dMyc strongly regulated *vito* mRNA levels (Fig. 2.17A). When quantified by qPCR, *vito* transcript levels were reduced by 85% in larvae homozygous for the null *dMyc*^{dm4} allele, and increased 1.9-fold and 18.9-fold upon dMyc overexpression in whole larvae and in salivary glands, respectively (Fig. 2.17A).

We next assessed whether *vito*RNAi affected the transcriptional response of several known dMyc targets (Grewal et al., 2005; Pierce et al., 2008). The set of targets analyzed included genes encoding factors involved in pre-rRNA transcription (the Pol I subunit *RpI135* and the basal Pol I *Tif-IA* transcription factor), genes encoding pre-rRNA processing/modifying enzymes [the pseudouridylase *Nop60B* (the *Drosophila* homologue

of dyskerin) and *Fibrillarin*] and also primary pre-rRNA transcripts (containing the ETS region). As expected, dMyc overexpression induced strong upregulation of all these target transcripts in salivary glands. However, co-expression of *vito*RNAi did not affect their strong induction by dMyc (Fig. 2.17B). Therefore, *vito* does not appear to be required for the transcriptional induction of dMyc target genes involved in nucleolar growth and ribosome biogenesis.

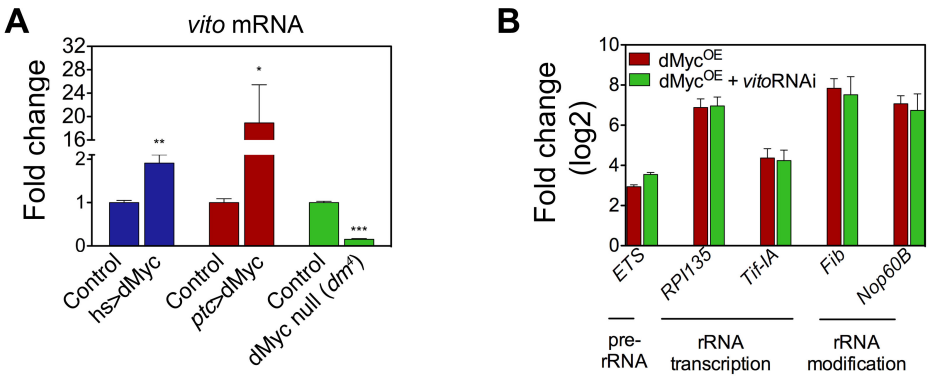

Figure 2.17 - *vito* is a dMyc transcriptional target. (A) *vito* mRNA levels were measured by qPCR upon heat shock-induced expression of dMyc in *Drosophila* third instar larvae, in salivary glands of third instar larvae overexpressing dMyc from the *ptc*-Gal4 driver, and in *dMyc* null (dm^4 allele) first instar larvae. *, P<0.01; **, P<0.001; ***, P<1X10^{-4} relative to control. **(B)** Transcript levels of genes involved in rRNA transcription and modification were measured by qPCR using RNA isolated from salivary glands of third instar larvae of the indicated genotypes. In A and B, data are presented as fold changes compared with the control and represent the mean + s.d. (n=3-5). Control (UAS-*lacZ*/+; *ptc*-Gal4/+), dMyc^{OE} (*ptc*-Gal4/+; UAS-*dMyc*/+), dMyc^{OE} + *vito*RNAi (*ptc*-Gal4/UAS-*vito*RNAi; UAS-*dMyc*/+).

To test whether *vito* function is required for dMyc-stimulated growth, we overexpressed dMyc in the diploid proliferative eye disc cells, in the presence and absence of *vito*RNAi. Whereas mitotic clones expressing dMyc were significantly larger than control clones, the co-expression of dMyc with *vito*RNAi resulted in a reduction in clone size relative to control levels (Fig. 2.18A,B). This reduction was the consequence of a partial reversion of the dMyc-induced cell size increase together with a decrease in the number of cells per clone (Fig. 2.18C,D). Similarly, in polyploid salivary gland cells, dMyc overexpression on its own dramatically increased nuclear and overall cell size (Pierce et al., 2004) (Fig. 2.19A,B). However, when *vito*RNAi was co-expressed cell growth was considerably attenuated (Fig. 2.19A,B). This resulted from significant reductions in cytoplasmic (down by 59%, P<1X10^{-4} and nuclear (down by 70%, P<1X10^{-4}) volumes when compared with dMyc overexpression (Fig. 2.19B). Therefore, genetically, *vito* lies downstream of dMyc in the control of cell growth and proliferation.

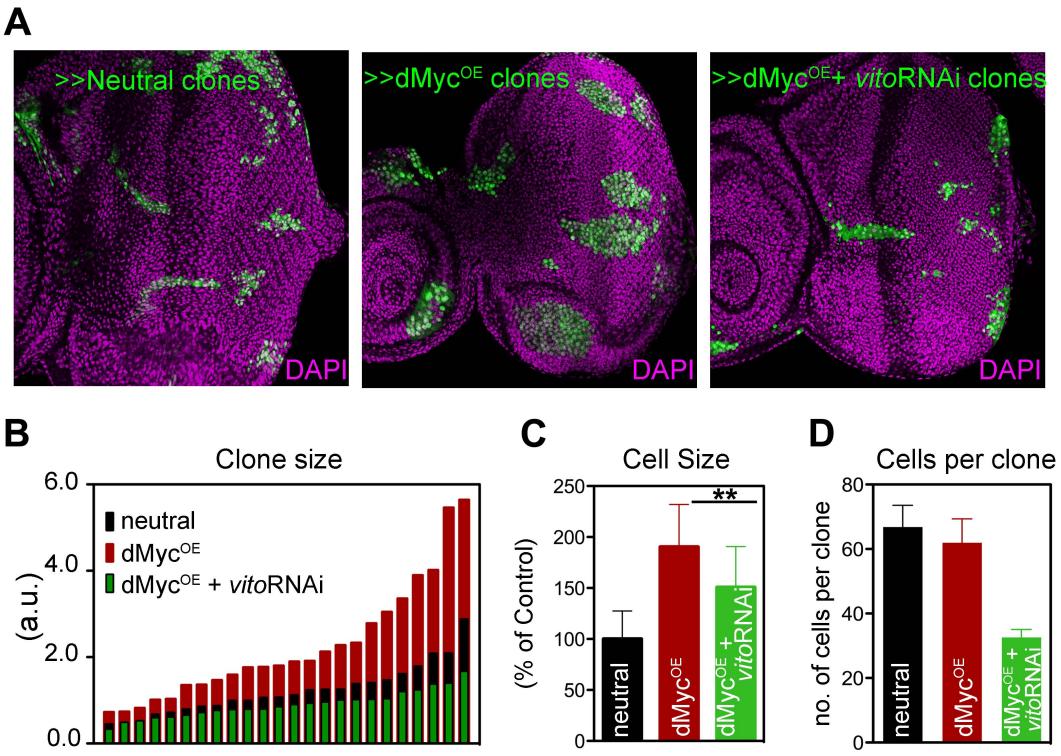

Figure 2.18 - *vito* is required for dMyc-stimulated growth. (A) dMyc-expressing clones (dMyc^{OE}) in the eye disc are larger than control clones. Co-expression with *vito*RNAi reduces dMyc-stimulated clone growth. Clones were marked positively by the presence of GFP, which were induced in the eye disc at 48 ± 4 hours AEL, and analysed at 118 ± 4 hours AEL. **(B)** Clonal size distribution of the above genotypes in the eye disc proper (n=24). **(C)** The average cell size (+ s.d.) within the clones (n=24). **, *P*=0.0012. **(D)** The number of cells of each clone was also scored and is represented as the mean + s.e.m. (n=24).

To identify the cellular function that *vito* performs during dMyc-stimulated cell growth, we examined whether Vito regulated nucleolar organization when dMyc was overexpressed. As previously described (Grewal et al., 2005), dMyc overexpression in salivary gland cells led to an enlarged nucleus and nucleolus (Fig. 2.19A). When compared with the wild-type, these nucleoli displayed slightly less compact packaging, with closely intermingled fibrillar and granular components. Crucially, when dMyc overexpression was induced together with *vito*RNAi, the nucleolus consistently displayed a segregated organization, with a peripheral granular region surrounding an internal fibrillar area (Fig. 2.19A). This nucleolar structural arrangement resembles, in part, the structure of the *vito*RNAi-only nucleolus, although in the latter case the nucleolus shows a more decondensed granular region (compare Fig. 2.19A with Fig. 2.10H). Although these experiments involve partial knockdown and not null mutations, precluding definitive statements about epistasis, overall our findings suggest that *vito* lies downstream of *dMyc* in the control of *Drosophila* nucleolar structure.

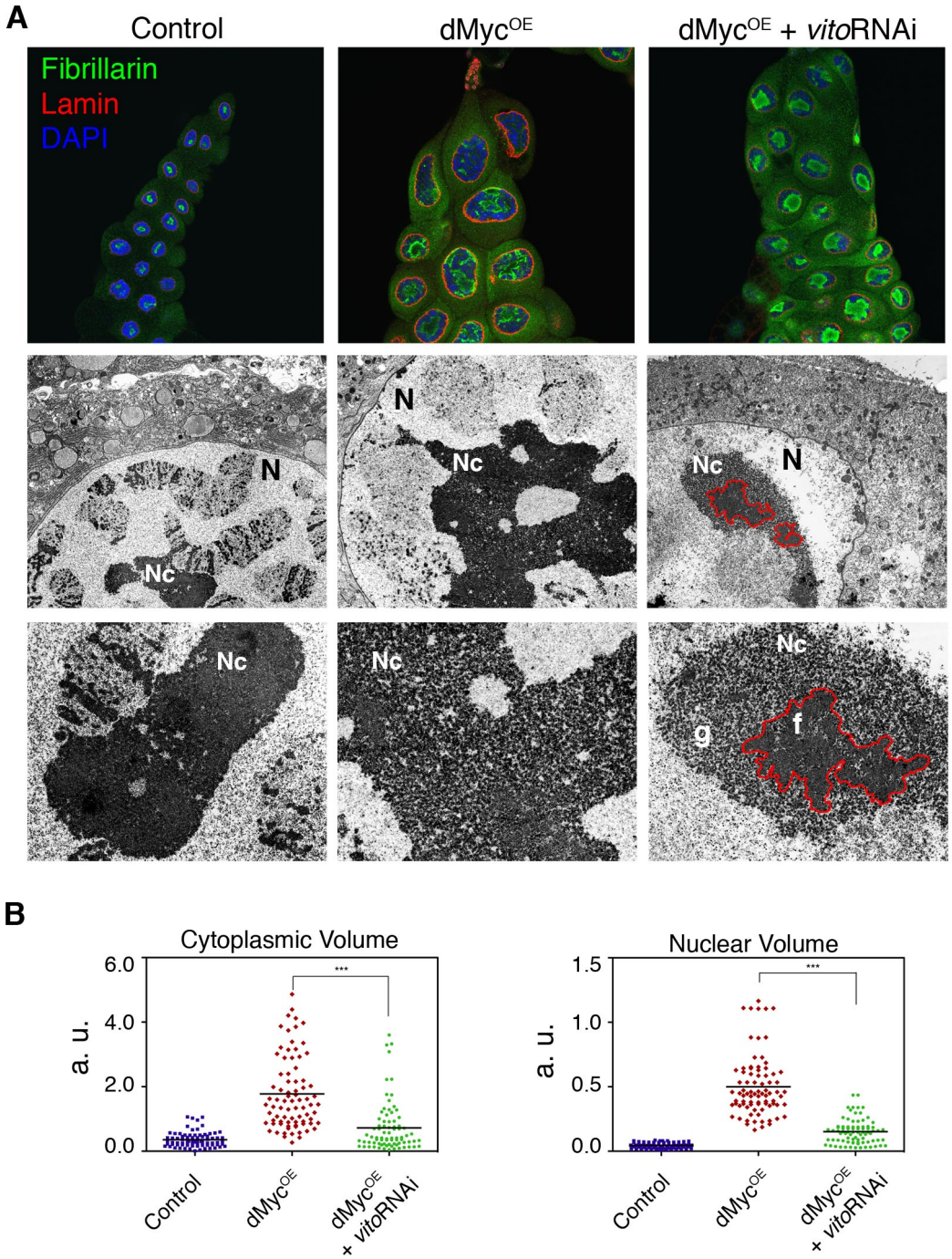

Figure 2.19 - *vito* is required for nucleolar integrity during dMyc-stimulated growth. (A) In *Drosophila* salivary gland cells, the substantial increases in cytoplasmic and nuclear volumes induced by dMyc^{OE} are significantly attenuated by *vito*RNAi co-expression. Salivary glands of the indicated genotypes were stained for the nucleolar marker Fibrillarin (green), Lamin B to reveal the nuclear envelope (red), and counterstained with DAPI (blue) (top row). Shown are transmission electron micrographs of nuclear regions of salivary gland cells (middle row) and corresponding magnifications of the nucleoli (bottom row). The red line highlights the fibrillar region that segregates from a granular component in dMyc^{OE}+*vito*RNAi nucleoli. N, nucleus; Nc, nucleolus; f, fibrillar; g, granular. **(B)** Quantification of nuclear and cytoplasmic volumes after overexpressing dMyc alone or together with UAS-*vito*RNAi (n=80-82). ***, $P<1X10^{-4}$. Control (UAS-*lacZ*/+; *ptc*-Gal4/+), dMyc^{OE} (*ptc*-Gal4/+; UAS-*dMyc*/+), dMyc^{OE} + *vito*RNAi (*ptc*-Gal4/UAS-*vito*RNAi; UAS-*dMyc*/+).

5. DISCUSSION

Our data identifies the *Nol12* homologue *vito* as an important regulator of dMyc function in the stimulation of nucleolar biogenesis and mass accumulation during *Drosophila* development. Our analysis of *vito* function during the development of *Drosophila melanogaster* is the first study of the function of a Nol12 gene in the context of a developing organism. The *Drosophila* genome contains only one non-redundant gene for Nol12, like all the genomes found to encode Nol12 proteins and we have shown that human Nol12 can rescue the knockdown of *Drosophila* Vito, which denotes not only sequence similarity but also functional homology in this family of proteins. Similarly to our rescue results, human Nol12 was also found to be able to rescue *S. cerevisae* mutants for Rrp17p/Nol12 (Oeffinger et al., 2009). Thus, an in vivo detailed analysis for this protein family is not expected to face redundancy and evolutionary divergence issues. The only characterized member, in terms of molecular function, is the budding yeast Rrp17p/Nol12. The gene encoding Rrp17p had previously been found to be required for non-coding RNA processing (including rRNA and snoRNAs) (Peng et al., 2003) and during the course of our study was found to have 5'–3' exonuclease activity essential for ribosome biogenesis (Oeffinger et al., 2009). Interestingly, we have shown that Vito plays an important role in rRNA processing, as Vito depletion impairs the normal rRNA processing pathway leading to an abnormal accumulation of intermediates and usage of the alternative processing pathway. Therefore, it is likely that the exonuclease function present in the Nol12 yeast homologue is conserved in Vito and consequently the exonuclease function would be important for exonucleolytic trimming of ITS sequences and explain the defects observed after Vito depletion. Additionally we have found that after Vito knockdown, ribosomal proteins of the large subunit ectopically accumulated in the nucleolus, which might be a reflection of the role of Vito in rRNA processing, as it was shown for other proteins involved in rRNA processing, like the nucleolar *Drosophila* Nucleostemin 1 (NS1) (Romanova et al., 2009; Rosby et al., 2009). Thus, these functional consequences of Vito misregulation could explain the defects in the development of *vito* mutants and correlate with the fact that Fibrillarin is not able to localize properly to the nucleolus when Vito is misexpressed.

We further show that dMyc controls *vito* mRNA levels to regulate nucleolar architecture and that *vito* is required for dMyc to reach its full potential as a potent cell

growth inducer. Furthermore, the knockdown of *vito* expression also correlated with an increase in p53-independent, caspase-mediated apoptotic cell death, suggesting a potential novel link between structural and functional changes in the nucleolus and activation of the pro-apoptotic *rpr*/*grim*/*hid* complex.

During development, dMyc plays a crucial role in translating intracellular and extracellular cues to regulate the pace of cell growth and proliferation. One of the main mechanisms for dMyc-stimulated growth appears to be the transcriptional control of nucleolar ribosome biogenesis genes (Grewal et al., 2005; Hulf et al., 2005; Teleman et al., 2008; Demontis and Perrimon, 2009). Cells of the salivary glands are polyploid secretory cells with very active biosynthetic pathways. In these cells, increasing or reducing Vito levels results in changes in the nucleolar localization patterns of the pre-rRNA methyltransferase Fibrillarin and in alterations in nucleolar structure. Accordingly, part of the control that dMyc exerts on the nucleolus is mediated by *vito.* Although *vito* does not appear necessary for the expression of dMyc targets implicated in ribosomal biogenesis, Vito knockdown strongly affects the process of dMyc-induced nucleolar hypertrophy, by reducing the size and altering structure of the nucleolus. In addition, several results support the hypothesis that the Myc-Nol12 regulatory relationship is evolutionarily conserved. Genome-wide chromatin immunoprecipitation analysis has shown that c-MYC binds the *NOL12* promoter in both a human transformed B-cell line (Zeller et al., 2006) and in mouse stem cells (Kim et al., 2008). We have also identified non-canonical E-box motifs (CACATG) (Zeller et al., 2006) in the putative proximal promoter regions of both *vito* and human *NOL12* (data not shown).

As previously discussed, *vito* plays a role in the proliferation and survival of diploid cells, and accordingly regulates the growth of the proliferative eye disc cells downstream of *dMyc*. *dMyc* mutants are smaller than the wild-type, and *dMyc* mutant cells grow poorly in the context of wild-type tissue (Johnston et al., 1999; Moreno and Basler, 2004; Benassayag et al., 2005; Wu and Johnston, 2010). Therefore, *vito* is a rate-limiting factor for tissue growth that links *dMyc* with nucleolar architecture. As Vito might function in the processing of rRNA or other small non-coding RNAs, a potential molecular mechanism of growth control emerges, in which Myc, by regulating the expression levels of Vito in the nucleolus might adjust cellular and tissue growth rates by indirectly controlling non-coding RNA processing events during normal development or tumor growth. The mechanisms enacting this link might prove relevant for the regulation of Myc function in tumorigenesis (Meyer and Penn, 2008).

6. REFERENCES

Ahmad, Y., Boisvert, F.-M., Gregor, P., Cobley, A. and Lamond, A. I. (2009). NOPdb: Nucleolar Proteome Database--2008 update. *Nucleic Acids Res* 37(Database issue): D181-4.

Arabi, A., Wu, S., Ridderstråle, K., Bierhoff, H., Shiue, C., Fatyol, K., Fahlén, S., Hydbring, P., Söderberg, O., Grummt, I. et al. (2005). c-Myc associates with ribosomal DNA and activates RNA polymerase I transcription. *Nat Cell Biol* 7(3): 303-310.

Benassayag, C., Montero, L., Colombié, N., Gallant, P., Cribbs, D. and Morello, D. (2005). Human c-Myc isoforms differentially regulate cell growth and apoptosis in Drosophila melanogaster. *Mol Cell Biol* 25(22): 9897-909.

Boisvert, F.-M., Van Koningsbruggen, S., Navascués, J. and Lamond, A. I. (2007). The multifunctional nucleolus. *Nat Rev Mol Cell Biol* 8(7): 574-85.

Chen, H. K., Pai, C. Y., Huang, J. Y. and Yeh, N. H. (1999). Human Nopp140, which interacts with RNA polymerase I: implications for rRNA gene transcription and nucleolar structural organization. *Mol Cell Biol* 19(12): 8536-46.

Chen, P., Nordstrom, W., Gish, B. and Abrams, J. M. (1996). grim, a novel cell death gene in Drosophila. *Genes & Development* 10(14): 1773-1782.

Cui, Z. and DiMario, P. J. (2007). RNAi knockdown of Nopp140 induces Minute-like phenotypes in Drosophila. *Mol Biol Cell* 18(6): 2179-91.

de la Cruz, A. F. A. and Edgar, B. A. (2008). Flow cytometric analysis of Drosophila cells. *Methods Mol Biol* 420: 373-89.

Demontis, F. and Perrimon, N. (2009). Integration of Insulin receptor/Foxo signaling and dMyc activity during muscle growth regulates body size in Drosophila. *Development* 136(6): 983-93.

Edgar, B. A. and Orr-Weaver, T. L. (2001). Endoreplication cell cycles: more for less. *Cell* 105(3): 297-306.

Emmott, E. and Hiscox, J. A. (2009). Nucleolar targeting: the hub of the matter. *EMBO Rep* 10(3): 231-8.

Fichelson, P., Moch, C., Ivanovitch, K., Martin, C., Sidor, C. M., Lepesant, J.-A., Bellaiche, Y. and Huynh, J.-R. (2009). Live-imaging of single stem cells within their niche reveals that a U3snoRNP component segregates asymmetrically and is required for self-renewal in Drosophila. *Nat Cell Biol* 11(6): 685-93.

Gallant, P., Shiio, Y., Cheng, P. F., Parkhurst, S. M. and Eisenman, R. N. (1996). Myc and Max homologs in Drosophila. *Science* 274(5292): 1523-7.

Gerbi, S. A. and Borovjagin, A. V. (2004). Pre-ribosomal RNA processing in multicellular organisms. in M. O. J. Olson (ed.) *In The Nucleolus*. Georgetown, Texas: Kluwer Academic/Plenum Publishers.

Giordano, E., Peluso, I., Senger, S. and Furia, M. (1999). minifly, a Drosophila gene required for ribosome biogenesis. *The Journal of Cell Biology* 144(6): 1123-33.

Grandori, C., Gomez-Roman, N., Felton-Edkins, Z. A., Ngouenet, C., Galloway, D. A., Eisenman, R. N. and White, R. J. (2005). c-Myc binds to human ribosomal DNA and stimulates transcription of rRNA genes by RNA polymerase I. *Nat Cell Biol* 7(3): 311-318.

Grether, M. E., Abrams, J. M., Agapite, J., White, K. and Steller, H. (1995). The head involution defective gene of Drosophila melanogaster functions in programmed cell death. *Genes & Development* 9(14): 1694-1708.

Grewal, S. S., Li, L., Orian, A., Eisenman, R. N. and Edgar, B. A. (2005). Myc-dependent regulation of ribosomal RNA synthesis during Drosophila development. *Nat Cell Biol* 7(3): 295-302.

Hulf, T., Bellosta, P., Furrer, M., Steiger, D., Svensson, D., Barbour, A. and Gallant, P. (2005). Whole-genome analysis reveals a strong positional bias of conserved dMyc-dependent E-boxes. *Mol Cell Biol* 25(9): 3401-10.

Igaki, T. (2009). Correcting developmental errors by apoptosis: lessons from Drosophila JNK signaling. *Apoptosis*.

Johnston, L. A., Prober, D. A., Edgar, B. A., Eisenman, R. N. and Gallant, P. (1999). Drosophila myc regulates cellular growth during development. *Cell* 98(6): 779-90.

Kim, J., Chu, J., Shen, X., Wang, J. and Orkin, S. H. (2008). An extended transcriptional network for pluripotency of embryonic stem cells. *Cell* 132(6): 1049-61.

Kuranaga, E., Kanuka, H., Igaki, T., Sawamoto, K., Ichijo, H., Okano, H. and Miura, M. (2002). Reaper-mediated inhibition of DIAP1-induced DTRAF1 degradation results in activation of JNK in Drosophila. *Nature cell biology* 4(9): 705-10.

Li, Z., Lee, I., Moradi, E., Hung, N.-J., Johnson, A. W. and Marcotte, E. M. (2009). Rational extension of the ribosome biogenesis pathway using network-guided genetics. *PLoS Biol* 7(10): e1000213.

Livak, K. J. and Schmittgen, T. D. (2001). Analysis of relative gene expression data using real-time quantitative PCR and the 2(-Delta Delta C(T)) Method. *Methods* 25(4): 402-8.

Long, E. O. and Dawid, I. B. (1980). Alternative pathways in the processing of ribosomal RNA precursor in Drosophila melanogaster. *J Mol Biol* 138(4): 873-8.

Maiato, H., Sunkel, C. E. and Earnshaw, W. C. (2003). Dissecting mitosis by RNAi in Drosophila tissue culture cells. *Biol Proced Online* 5: 153-161.

Martín-Blanco, E., Gampel, A., Ring, J., Virdee, K., Kirov, N., Tolkovsky, A. M. and Martinez-Arias, A. (1998). puckered encodes a phosphatase that mediates a feedback loop regulating JNK activity during dorsal closure in Drosophila. *Genes & Development* 12(4): 557-70.

Mccain, J., Danzy, L., Hamdi, A., Dellafosse, O. k. and Dimario, P. (2006). Tracking nucleolar dynamics with GFP-Nopp140 during Drosophila oogenesis and embryogenesis. *Cell Tissue Res* 323(1): 105-15.

McEwen, D. G. and Peifer, M. (2005). Puckered, a Drosophila MAPK phosphatase, ensures cell viability by antagonizing JNK-induced apoptosis. *Development* 132(17): 3935-46.

Meyer, N. and Penn, L. Z. (2008). Reflecting on 25 years with MYC. *Nat Rev Cancer* 8(12): 976-90.

Moreno, E. and Basler, K. (2004). dMyc transforms cells into super-competitors. *Cell* 117(1): 117-29.

Nordstrom, W., Chen, P., Steller, H. and Abrams, J. M. (1996). Activation of the reaper gene during ectopic cell killing in Drosophila. *Developmental Biology* 180(1): 213-26.

Oeffinger, M., Zenklusen, D., Ferguson, A., Wei, K. E., El Hage, A., Tollervey, D., Chait, B. T., Singer, R. H. and Rout, M. P. (2009). Rrp17p Is a Eukaryotic Exonuclease Required for 5' End Processing of Pre-60S Ribosomal RNA. *Molecular Cell* 36(5): 768-781.

Ollmann, M., Young, L. M., Di Como, C. J., Karim, F., Belvin, M., Robertson, S., Whittaker, K., Demsky, M., Fisher, W. W., Buchman, A. et al. (2000). Drosophila p53 is a structural and functional homolog of the tumor suppressor p53. *Cell* 101(1): 91-101.

Orihara-Ono, M., Suzuki, E., Saito, M., Yoda, Y., Aigaki, T. and Hama, C. (2005). The slender lobes gene, identified by retarded mushroom body development, is required for proper nucleolar organization in Drosophila. *Dev Biol* 281(1): 121-33.

Peng, W. T., Robinson, M. D., Mnaimneh, S., Krogan, N. J., Cagney, G., Morris, Q., Davierwala, A. P., Grigull, J., Yang, X., Zhang, W. et al. (2003). A panoramic view of yeast noncoding RNA processing. *Cell* 113(7): 919-33.

Pfaffl, M. W., Horgan, G. W. and Dempfle, L. (2002). Relative expression software tool (REST) for group-wise comparison and statistical analysis of relative expression results in real-time PCR. *Nucleic Acids Res* 30(9): e36.

Pierce, S. B., Yost, C., Anderson, S. A. R., Flynn, E. M., Delrow, J. and Eisenman, R. N. (2008). Drosophila growth and development in the absence of dMyc and dMnt. *Dev Biol* 315(2): 303-16.

Pierce, S. B., Yost, C., Britton, J. S., Loo, L. W. M., Flynn, E. M., Edgar, B. A. and Eisenman, R. N. (2004). dMyc is required for larval growth and endoreplication in Drosophila. *Development* 131(10): 2317-27.

Prieto, J.-L. and McStay, B. (2007). Recruitment of factors linking transcription and processing of pre-rRNA to NOR chromatin is UBF-dependent and occurs independent of transcription in human cells. *Genes & Development* 21(16): 2041-54.

Romanova, L., Grand, A., Zhang, L., Rayner, S., Katoku-Kikyo, N., Kellner, S. and Kikyo, N. (2009). Critical role of nucleostemin in pre-rRNA processing. *J Biol Chem* 284(8): 4968-77.

Rosby, R., Cui, Z., Rogers, E., deLivron, M. A., Robinson, V. L. and DiMario, P. J. (2009). Knockdown of the Drosophila GTPase nucleostemin 1 impairs large ribosomal subunit biogenesis, cell growth, and midgut precursor cell maintenance. *Mol Biol Cell* 20(20): 4424-34.

Rubbi, C. P. and Milner, J. (2003). Disruption of the nucleolus mediates stabilization of p53 in response to DNA damage and other stresses. *EMBO J* 22(22): 6068-77.

Schreiber-Agus, N., Stein, D., Chen, K., Goltz, J. S., Stevens, L. and DePinho, R. A. (1997). Drosophila Myc is oncogenic in mammalian cells and plays a role in the diminutive phenotype. *Proc Natl Acad Sci USA* 94(4): 1235-40.

Suzuki, S., Fujiwara, T. and Kanno, M. (2007). Nucleolar protein Nop25 is involved in nucleolar architecture. *Biochemical and Biophysical Research Communications* 358(4): 1114-9.

Tautz, D., Hancock, J. M., Webb, D. A., Tautz, C. and Dover, G. A. (1988). Complete sequences of the rRNA genes of Drosophila melanogaster. *Mol Biol Evol* 5(4): 366-76.

Teleman, A. A., Hietakangas, V., Sayadian, A. C. and Cohen, S. M. (2008). Nutritional control of protein biosynthetic capacity by insulin via Myc in Drosophila. *Cell Metab* 7(1): 21-32.

Venema, J. and Tollervey, D. (1999). Ribosome synthesis in Saccharomyces cerevisiae. *Annu Rev Genet* 33: 261-311.

Wang, C., Query, C. C. and Meier, U. T. (2002). Immunopurified small nucleolar ribonucleoprotein particles pseudouridylate rRNA independently of their association with phosphorylated Nopp140. *Mol Cell Biol* 22(24): 8457-66.

White, K., Grether, M. E., Abrams, J. M., Young, L., Farrell, K. and Steller, H. (1994). Genetic control of programmed cell death in Drosophila. *Science* 264(5159): 677-83.

Wu, D. C. and Johnston, L. A. (2010). Control of wing size and proportions by Drosophila myc. *Genetics* 184(1): 199-211.

Yuan, X., Zhou, Y., Casanova, E., Chai, M., Kiss, E., Gröne, H.-J., Schütz, G. and Grummt, I. (2005). Genetic inactivation of the transcription factor TIF-IA leads to nucleolar disruption, cell cycle arrest, and p53-mediated apoptosis. *Molecular Cell* 19(1): 77-87.

Zeller, K. I., Zhao, X., Lee, C. W. H., Chiu, K. P., Yao, F., Yustein, J. T., Ooi, H. S., Orlov, Y. L., Shahab, A., Yong, H. C. et al. (2006). Global mapping of c-Myc binding sites and target gene networks in human B cells. *Proc Natl Acad Sci USA* 103(47): 17834-9.

CHAPTER 3

A targeted RNAi screen identifies a genetic interaction between TGF-β signaling pathway and the nucleolar regulator Viriato during eye development

CONTENTS

1. ABSTRACT

The correct patterning of body structures, like the fly eye or any other organ, is regulated by signaling pathways that orchestrate the timing and spatial organization of cellular proliferation and differentiation. In *Drosophila,* the TGF-β family of cytokines signaling pathway plays multiple essential roles during development. During eye development Dpp, a member of the BMP2/4 class of the TGF-β family of cytokines, plays a dual role: earlier in development it promotes growth (mass accumulation) and cell survival, but in later stages it switches its function to induce a developmentally regulated cell cycle arrest in the G1 phase of the cell cycle, and neuronal photoreceptor differentiation. In Chapter 2 of this thesis we described the identification of *Drosophila* Vito as a nucleolar protein that is required for proper tissue growth in the developing *Drosophila* eye. In the present Chapter we performed a targeted in vivo double RNAi screen to identify genes and pathways working with Vito during eye development. We have identified a strong genetic interaction between *vito* and members of the Dpp signaling pathway (including the TGF-β receptor type I and II, *tkv* and *put* and the co-Smad *med*). We demonstrate that Vito acts downstream of Dpp, collaborating in the promotion of eye disc growth and regulation of photoreceptor differentiation. Moreover, the Vito/Dpp interaction appears to be particularly strong in the context of eye development, as it is not detected in the wing. We propose that when Dpp signaling is compromised, Vito is important for the regulation of Dpp activity in the eye imaginal disc and maintenance of a uniform Dpp signaling in the furrow.

2. INTRODUCTION

Tissue-specific integration of growth and patterning signals must occur to control the basic events necessary for cell and organ growth, but how they are controlled and coordinated is still poorly understood. In recent years, genetic studies in *Drosophila* allowed the identification of several key signaling pathways regulating cell and tissue growth. The progressive nature of *Drosophila* eye patterning makes it a very good model to study how cellular growth, proliferation, and apoptosis events shape and control the achievement of size and patterning (reviewed in Amore and Casares, 2010).

In the previous Chapter, we have identified a previously uncharacterised nucleolar protein, *Drosophila* Vito, as crucial for the regulation of nucleolar architecture, cell proliferation, and cell survival during *Drosophila* development. *vito* is a novel transcriptional target of *Drosophila* Myc, and acts downstream of the dMyc ensuring a

coordinated nucleolar response to dMyc-induced growth, thereby allowing normal organ development. Consistent with its higher expression anteriorly in the eye imaginal disc, Vito was shown to be required for growth and proliferation before the onset of photoreceptor differentiation. In this Chapter we performed an eye-targeted double RNAi screen with the goal to search for Vito partners during the process of eye development.

Genome-wide RNAi screens have been important to study novel gene functions in specific contexts (Mohr et al., 2010). However it is now important to start to uncover the relationships between genes and pathways to provide insights into the global structure of biological networks. Large-scale systematic genetic interactions have been widely used in yeast and are now starting to be used in higher organisms, as *Drosophila* and mammalians, but mainly in cell culture systems (Bakal et al., 2008). In this Chapter we performed a targeted screen that although not done in a global scale, to our knowledge is the first in vivo double RNAi screen to study synthetic genetic interactions during *Drosophila* development. Moreover, although quantifying genetic interactions have been a challenge, here we took advantage of the recently used multiplicative model to quantitatively score our genetic interactions using a phenotype rather than the fitness of a cell (Baryshnikova et al., 2010; Horn et al., 2011).

Different genetic relationships are uncovered by the detection of aggravating synthetic interactions. A pair of genes could act in parallel pathways converging on the same biological process ('between-pathway' interaction), or can either act at the same level or different levels of the pathway ('within pathway' interaction). Ultimately, it is also possible that each gene may act in unrelated processes revealing an indirect interaction, even tough the breakdown of the system occurs when both genes are compromised (Costanzo et al., 2011).

Our eye-targeted double RNAi screen looking for Vito partners during eye development identified a strong genetic interaction between Vito and members of the Dpp signaling pathway (including TGF-β receptor type I and II, *tkv* and *put* and the co-Smad *med*). We demonstrate that when Dpp signaling is compromised, Vito cooperates with Dpp in the regulation of growth during early eye development and later on in the process of retina differentiation. Moreover, *vito* seems to promote uniform Dpp signaling in the morphogenetic furrow and be required to regulate Dpp activity in the eye imaginal disc. Furthermore, and surprisingly, we show that Dpp type II receptor Put regulates nucleolar structure and functions by an unknown mechanism. Therefore if any integration

with the signaling pathways also described to control growth occur at the level of ribosome biosynthesis remains to be explored.

3. MATERIALS AND METHODS

3.1. Fly strains and genotypes

All crosses were raised at 25°C under standard conditions. The following stocks (described in FlyBase, unless stated otherwise) were used: *dpp*-Gal4, *MS1096*-Gal4, *en*-Gal4, UASGFP/CyO, *sal*^{EPv}-Gal4, *ey*-Gal4, *y w* hs-*flp*^{122}; *act*>*y*+>Gal4 UAS-*GFP*, UAS-*lacZ*, UAS-*dpp*^{D}/TM6B, UAS-*tkv*^{QD}/TM6B, UAS-*vito*, UAS-*vito*-GFP, *dpp3.0-lacZ*, UAS-*dmyc*RNAi (Vienna Drosophila RNAi Center (VDRC) #2947), Tkv-YFP (CPTI-002487; Flannotator). Eye-targeted RNAi knockdown of *vito* was induced by crossing *eyeless*-Gal4 with UAS-*vito*RNAi (VDRC #34548). A second UAS-*vito*RNAi transformant (named UAS-*vito*RNAiKK, VDRC #102513) observed to generate a very similar eye phenotype was also used throughout experiments.

3.2. Double-RNAi screen and genetic interaction scores

All 209 UAS-RNAi lines used in our screen (supplementary table 1) were obtained from VDRC, NIG-Fly stock center (http:/www.shigen.nig.ac.jp/fly/nigfly/index.jsp) and Transgenic RNAi Project (TRiP) at Harvard Medical School. Eye-targeted RNAi knockdown was induced by crossing males from the RNAi stocks carrying an inducible UAS-RNAi construct to virgins of the *eyeless*-Gal4 driver line or *ey*-Gal4, UAS-*vito*RNAiKK. All crosses were done at 25°C. The flies were examined under a stereomicroscope (Stemi 2000, Zeiss) equipped with a digital camera (Nikon Digital Sight DS-2Mv), and several representative pictures for each transgenic line were taken, if alterations in eye size were detected. In a primary analysis eye phenotypes with *ey*-Gal4 driver were qualitatively classified as positive (if an eye size reduction was observed), negative (if no phenotype in the eye was observed) or lethal. For the crosses with *ey*-Gal4, UAS-*vito*RNAiKK, genetic interactions were identified by comparing the phenotype of the single RNAis to that of the combined double RNAis. Interactions were classified as small (+) if the phenotype observed was slightly more severe than the independent single RNAi phenotypes, medium (++) if there was a significant reduction in the eye size and strong (+++) if the eye was absent. The medium and strong interactions detected in the screen were further analyzed and quantified by measuring the size of the adult retinas in single RNAis and the observed adult size retina obtained in the double RNAi using the Straight-line tool of ImageJ 1.41o software (NIH, Bethesda, MA, USA). Genetic interactions scores (π) were calculated based on the differences between the adult retina size observed in the double RNAi and the estimation of the expected double RNAi adult retina size, which was calculated based on a widely accepted model that assumes that the effects of mutations in independent genes combine in a multiplicative manner (Dixon et al., 2009; Baryshnikova et al., 2010). Consequently, the expected adult retina size in the double RNAi is the result of the product between the two individual adult retina size values for the single RNAis. In our screen,

deviations between the expected and the experimentally observed double RNAi phenotype revealed only negative genetic interactions (aggravating).

3.3. Interaction Map

Vito interaction map was done using Cytoscape 2.7 (http://www.cytoscape.org/) and interaction data generated using the DroID-Plugin for Cytoscape (Murali et al., 2011), which provides access to the *Drosophila* Interactions Database (DroID) from within the Cytoscape environment.

3.4. Mitotic recombination

Mitotic recombination was induced using the Flp/FRT method. Clones overexpressing Tkv^{QD} alone or together with *vito*RNAi, were induced by heat-shock (30 minutes at 37°C) at 72 hours AEL in larvae of the genotype: Tkv^{QD}: *y w hsflp/+*; *act*>y+>Gal4, UAS-GFP/+; UAS-tkv^{QD}/+, Tkv^{QD}+ *vito*RNAi: *y w hsflp*/+; *act*>y+>Gal4, UAS-GFP/UAS-*vito*RNAi; UAS-tkv^{QD}/+ and control: *y w hsflp*/+; *act*>y+>Gal4, UAS-GFP/UAS-*lacZ. vito* knockdown clones were induced by heat shock (1 hour at 37°C) at 72 hours AEL in larvae of the genotype: *y w hsflp/+*; *act*>y+>Gal4, UAS-GFP/+; UAS-*vito*RNAi.

3.5 Immunostaining

Eye-antennal imaginal discs and salivary glands were prepared for immunohistochemistry using standard protocols. Primary antibodies used were: rabbit anti-cleaved Caspase-3 at 1:200 (Cell Signaling), mouse anti-Armadillo N27A1 at 1:100 (Developmental Studies Hybridoma Bank, DSHB), rabbit anti-β-galactosidase at 1:1000 (Cappel), rat anti-Elav 7E8A10 at 1:100 (DSHB), rabbit anti-Fibrillarin at 1:250 (Abcam, #ab5821), rabbit polyclonal anti-RpL22 at 1:100 (gift from Vassie Ware, Lehigh University, USA), rabbit anti-p-Mad at 1:100 (gift from Ginés Morata), mouse anti-Cyclin B F2F4 at 1:100 (DSHB), guinea-pig anti-Hth at 1:3000 (Casares and Mann, 1998), mouse anti-Eya (10H6) at 1:400 (DHSB), guinea-pig anti-Otd at 1:750 (Ranade et al., 2008). Appropriate Alexa-Fluor conjugated secondary antibodies were from Molecular Probes. Images were obtained with the Leica SP2 confocal system and processed with Adobe Photoshop.

3.6. Transmission electron microscopy (TEM)

Dissected third instar salivary glands were fixed with 2.5% glutaraldehyde in 0.1 M sodium cacodylate buffer for 30 minutes and post-fixed with 4% osmium tetroxide. After washing, salivary glands were incubated with 0.5% uranyl acetate (30 minutes) and further dehydrated through a graded ethanol series (70% for 10 minutes, 90% for 10 minutes, and four changes of 100%). Salivary glands were then soaked in propylene oxide for 10 minutes and then in a mixture (1:1) of propylene oxide and Epon resin (TAAB Laboratories) for 30 minutes. This mixture was then replaced by 100% Epon resin for 24 hours. Finally, fresh Epon replaced the Epon and polymerisation took place at 60°C for 48 hours. Ultrathin sections

were obtained using an ultramicrotome, collected in copper grids and then double contrasted with uranyl acetate and lead citrate. Micrographs were taken using a Zeiss EM10C electron microscope (80 kV).

3.7. 3D histograms

Tkv-YFP 3D histograms were done using the SurfacePlot_3D plugin for the ImageJ 1.41o software (NIH, Bethesda, MA, USA) (http://rsb.info.nih.gov/ij/plugins/surface-plot-3d.html). This plugin creates interactive surface plots where the luminance of each pixel in the image is interpreted as the height for the plot.

3.8. Size and intensity measurements and statistics

Eye disc areas were measured using the Straight-line tool of ImageJ 1.41o software (NIH, Bethesda, MA, USA), considering only the eye disc from the eye-antennal imaginal disc from at least 20 discs for each genotype. Tkv-YFP intensities in the eye imaginal discs were measured in the anterior region of the eye disc, next to the MF, and in the differentiating photoreceptors by using the elliptical tool of ImageJ 1.41o software. GraphPad Prism 5.0 was used for statistical analysis and generating the graphical output. Statistical significance was determined using an unpaired, two-tailed Student's *t*-test, with a 95% confidence interval, after assessing the normality distribution of the data with D'Agostino-Pearson normality test.

4. RESULTS

4.1. Eye-targeted double RNAi screen to identify Vito interactors during eye development

In order to identify genes that cooperate with *vito* during eye development we performed a targeted in vivo functional double RNAi screen in the eye of *Drosophila*, which has been widely used in genetic screens because is not required for viability, is very sensitive to manipulations and phenotypes are easy to score. Since the release of the first *Drosophila* genome-wide UAS-RNAi transgenic library in 2007 (Dietzl et al., 2007), in vivo genome-wide RNAi screens, targeting a specific gene in a specific manner are starting to be commonly used, presenting a real breakthrough over the classic genetic screens done through random generation of mutations. The identification of novel gene functions is now facilitated with RNAi screens, as the hypomorphic conditions and control of the place and time of expression allowed to overcome the lethality of most essential genes. Additionally, and very importantly it is also possible to combine multiple UAS-RNAis to study synthetic interactions. Although very promising, RNAi screens also offer some

disadvantages such as the variability of knockdowns, and the potential off-target effects that can, however, be overcome by the usage of two independent double-stranded RNAs to each target and implementation of secondary screens in order to validate the targets.

In a genome-wide analysis to identify direct targets of the key regulator of *Drosophila* eye development, the retinal determination protein Ey, Ostrin and co-workers identified by microarray analysis 188 *ey*-induced, eye-enriched and atonal-independent genes (Ostrin et al., 2006). We took advantage of this group of 188 potential *ey*-target genes to design a targeted double RNAi genetic screen to identify synthetic genetic interactions with Vito during eye development (see materials and methods for details) (Fig. 3.1A). In a first step, we tested 148 UAS-RNAi lines targeting 148 genes out of a total of 188 *ey*-induced genes. The 148 genes tested were associated with a variety of functional categories including genes characterized as being involved in eye development, genes related to cell cycle, transcription and translation, but for the majority (36%) the function and/or biological process has not been characterized yet (Fig. 3.1B). Using Gene Ontology (GO) annotations referring to biological processes in order to identify common and enriched properties in this gene list, we found a particular enrichment in genes related to eye-antennal disc development, eye development, and neuron differentiation (Fig. 3.1C).

Since *vito* is expressed in a dynamic pattern in the eye disc, with high expression in the anterior region dropping to very low levels in the region posterior to the morphogenetic furrow where differentiation occurs, we decided to further include in the screen genes belonging to signaling pathways important for growth and patterning during eye development, such as TGF-β, Hh, and Wg signaling pathway components (Fig. 3.1A, Supplementary Table 1).

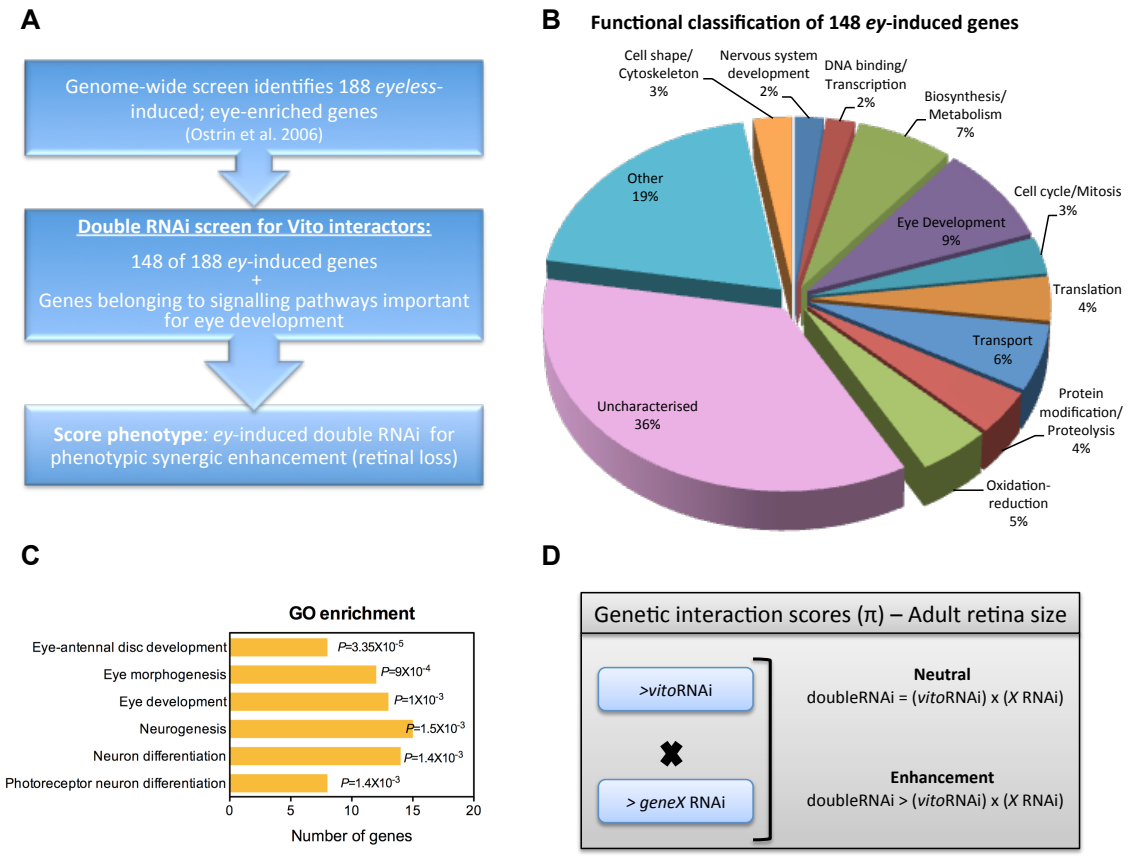

Figure 3.1 – Methodology to identify Vito genetic interactions by double RNAi screen. (A) Targeted double RNAi screen design to identify Vito genetic interactions. **(B)** A pie diagram showing the functional classification of the 148 RNAi lines tested out of the 188 *ey*-induced genes identified by Ostrin et al. 2006, according to GO, assisted by manual data mining of references in Flybase. A total of 36% of the genes have an unknown function and/or biological process. **(C)** Chart of enriched GO annotations from the list of 148 *ey*-induced genes tested when compared with the *Drosophila* genome. Each category listed is significantly enriched (with *P*-value <0.01 as shown), and the number of genes belonging to the annotation is shown. GO enrichment analysis was performed using the web-based tool WebGestalt (http://bioinfo.vanderbilt.edu/webgestalt) (Zhang et al., 2005). **(D)** Schematic overview of the calculation of the genetic interactions scores (π). Genetic interaction scores represented as (π), were calculated based on the difference between the expected double RNAi retina size, calculated by the product of the individual RNAi retina sizes, and the measured double RNAi retina size. When the retina size of the double RNAi was equal to the predicted by a multiplicative model no interaction is detected, however if the retina loss is greater than expected by the multiplicative model, an enhancement is revealed, which indicates a genetic interaction.

Initially genes were individually knocked down by RNAi in the eye using the *ey*-Gal4 driver and the resulting eye phenotypes were examined. After the initial individual RNAi screen with *ey*-Gal4, only 15 gene knockdowns of the 148 *ey*-induced genes presented visible eye phenotype (retina loss), among them some genes already known to be required for proper eye development as for example the RD genes *eya*, *so* and *ey* (see Supplementary Table 1).

To test for Vito genetic interactions we crossed flies expressing an RNAi targeting *vito* (*ey*-Gal4, UAS-*vito*RNAiKK) to flies carrying a UAS-RNAi targeting the gene of interest. A genetic interaction can be defined by how the phenotype of an organism lacking both genes deviates from the expected combination of the individual genetic phenotypes

(Mani et al., 2008; Phillips, 2008). Therefore, genetic interactions were identified by comparing the phenotype of experimental double RNAi with the expected phenotype of double RNAis based on individual single RNAis, being the adult retina size the scored phenotype. To score the expected double RNAi phenotypes we used the widely accepted model, which assumes that the expected double mutant phenotype can be the result of the multiplicative combination of the single mutant phenotypes (Baryshnikova et al., 2010; Costanzo et al., 2011). This assumption has been widely used in a variety of screens performed in yeast, focusing on fitness phenotypes, although more recently it was implemented in higher organisms and tested using phenotypes rather than fitness (Jonikas et al., 2009; Horn et al., 2011). To determine Vito genetic interactions in a first approach the adult retina size of the single RNAis was compared, by eye inspection, to that of the combined double RNAis, and interactions were classified as small (+), medium (++), or strong (+++) depending on the differences observed (see Supplementary Table 1). Subsequently, for the medium and strong interactions detected in the screen, genetic interactions scores (π) were then calculated based on the differences between the expected and the observed double RNAi adult retina sizes (Fig 3.1D).

From the 169 RNAi lines targeting 162 genes that were tested, we obtained a narrowed list of 12 interactions, all of them displaying aggravating or synergistic interactions, i.e. exhibiting a more severe eye phenotype than expected by the combination of the single RNAi phenotypes (Table 3.1). Among the list of the *ey*-target genes strong interactions were detected with the RD genes *ey*, *eya* and *so*. Overall, the strongest interaction observed was with the Dpp signaling pathway, as a very strong synergistic effect upon RNAi interfering with both *vito* and components of the Dpp signal transduction pathway was observed (Table 3.1, Fig. 3.2A,B).

Table 3.1 – List of Vito genetic interactions. This table shows information about the genes identified in the screen as Vito interactors, as well as quantifications of retina sizes of the individual RNAis, expected phenotypes based on the multiplicative model, and the measured retina sizes in the double RNAis. Genetic interaction scores (π) were calculated as described in materials and methods. * Expected retina sizes were calculated based on the value for *vito*RNAi retina size of 0.70. n.d. not determined.

		FBgn	Transformant ID	Gene ID	Symbol	Gene name	Function	Single RNAi (retina size)	Double RNAi *vito*RNAi X singleRNAi (expected retina size)*	Double RNAi (observed retina size)	Interaction score (π)
eyeless-induced, eye-enriched genes	TGF-β signaling pathway	FBgn0032420	GD 44880	CG6583	CG6583		Unknown	1.00	0.70	0.54	0.16
		FBgn0000463	GD 3720	CG3619	Dl	Delta	Notch binding	1.00	0.70	0.32	0.38
		FBgn0250876	GD 9428	CG5661	Sema-5c	Semaphorin-5c	Receptor activity	1.00	0.70	0.41	0.29
		FBgn0000635	GD 8392	CG3665	Fas2	Fasciclin 2	Protein binding	1.00	0.70	0.42	0.28
		FBgn0005558	KK 106628	CG1464	ey	eyeless	DNA binding/transcriptional regulator	0.67	0.47	0.00	0.47
		FBgn0000320	GD 43911	CG9554	eya	eyes absent	Protein tyrosine phosphatase activity	0.44	0.31	0.00	0.31
		FBgn0003460	KK 104386	CG11121	so	sine oculis	DNA binding	0.50	0.35	0.00	0.35
	Dpp pathway	FBgn0003716	GD 3059 (line1)	CG14026	tkv	thickveins	Transforming growth factor beta receptor activity, type I	0.74	0.52	0.00	0.52
		FBgn0003716	GD 862 (line 2)	CG14026	tkv	thickveins	Transforming growth factor beta receptor activity, type I	1.00	0.70	0.36	0.34
		FBgn0003169	GD 849 (line 1)	CG7904	put	punt	Transforming growth factor beta receptor activity, type II	0.95	0.67	0.44	0.23
		FBgn0003169	GD 37279 (line 2)	CG7904	put	punt	Transforming growth factor beta receptor activity, type II	0.00	0.00	Synthetic lethal	n.d.
		FBgn0011655	GD 19688 (line 1)	CG1775	Med	Medea	Sequence-specific DNA binding	0.95	0.67	0.00	0.67
		FBgn0011655	GD 19689 (line 2)	CG1775	Med	Medea	Sequence-specific DNA binding	0.92	0.64	0.00	0.64
	Act-β	FBgn0011300	TRIP 25933	CG8224	babo	baboon	Activin receptor activity, type I	1.00	0.70	0.51	0.19
		FBgn0025800	TRIP 26756	CG2262	Smox	Smad on X	Sequence-specific DNA binding	1.00	0.70	0.51	0.19

Furthermore, the interactions detected support the potential of our screen to determine Vito interactors during eye development, considering what has been shown in terms of the function and expression patterns for the positive genes. Fasciclin 2 (Fas2) was recently found to be expressed in a dynamic pattern during eye imaginal disc development, and to act in the inhibition of epidermal growth factor receptor (EGFR) signaling in the developing eye (Mao and Freeman, 2009); Delta is the Notch ligand, being important to establish dorsal and ventral compartments and regulate growth in the developing eye (reviewed in Kumar, 2011); and Sema-5c, although not apparently related to eye development, was shown to regulate Dpp signaling in a *Drosophila* tumor metastasis model (*l(2)gl*) being required for the activation of the Dpp pathway in *l(2)gl* tumors (Woodhouse et al., 2003). Interestingly, Vito/TGF-β signaling pathway interaction appears not to be restricted to the Dpp branch. A significant interaction was also detected with members of the Activin pathway such as the type I receptor Babo, which was shown to influence growth and proliferation in the developing eye, and the R-Smad Smox that is highly expressed anteriorly in the eye imaginal disc (Brummel et al., 1999) (Table 3.1, Fig. 3.2A,B).

To overcome false positives and off-target effects, we tested, for all the positive interactions, at least a second RNAi line, and we have also tested the interactions with a second UAS-*vito*RNAi transformant obtaining similar results (data not shown).

In order to have an insight about the interactions already described among these genes we built a network using an open source bioinformatics software platform, named Cytoscape, for visualizing molecular interaction networks and integrate these networks with annotations, gene expression profiles and other data (http://www.cytoscape.org). Using the DroID-Plugin for Cytoscape (Murali et al., 2011), which includes gene-gene and protein-protein interactions, we created a network only representing direct interactions between the *vito* interactors hereby identified (Fig. 3.2C). An examination of the GO terms of the *vito* interactor genes revealed a significant enrichment for genes involved in nervous system development (11 out of 12 genes) and eye development (8 out of 12 genes). Significantly, all interactor genes except *CG6583* are annotated as being involved in nervous system development, and eight of them together with *vito* are involved in eye development and/or eye-antennal disc development (Fig. 3.2C). Therefore it is very likely that Vito, besides being required for disc growth in the anterior proliferating region, might be involved in processes related to nervous system development in the eye, as neuronal photoreceptor differentiation.

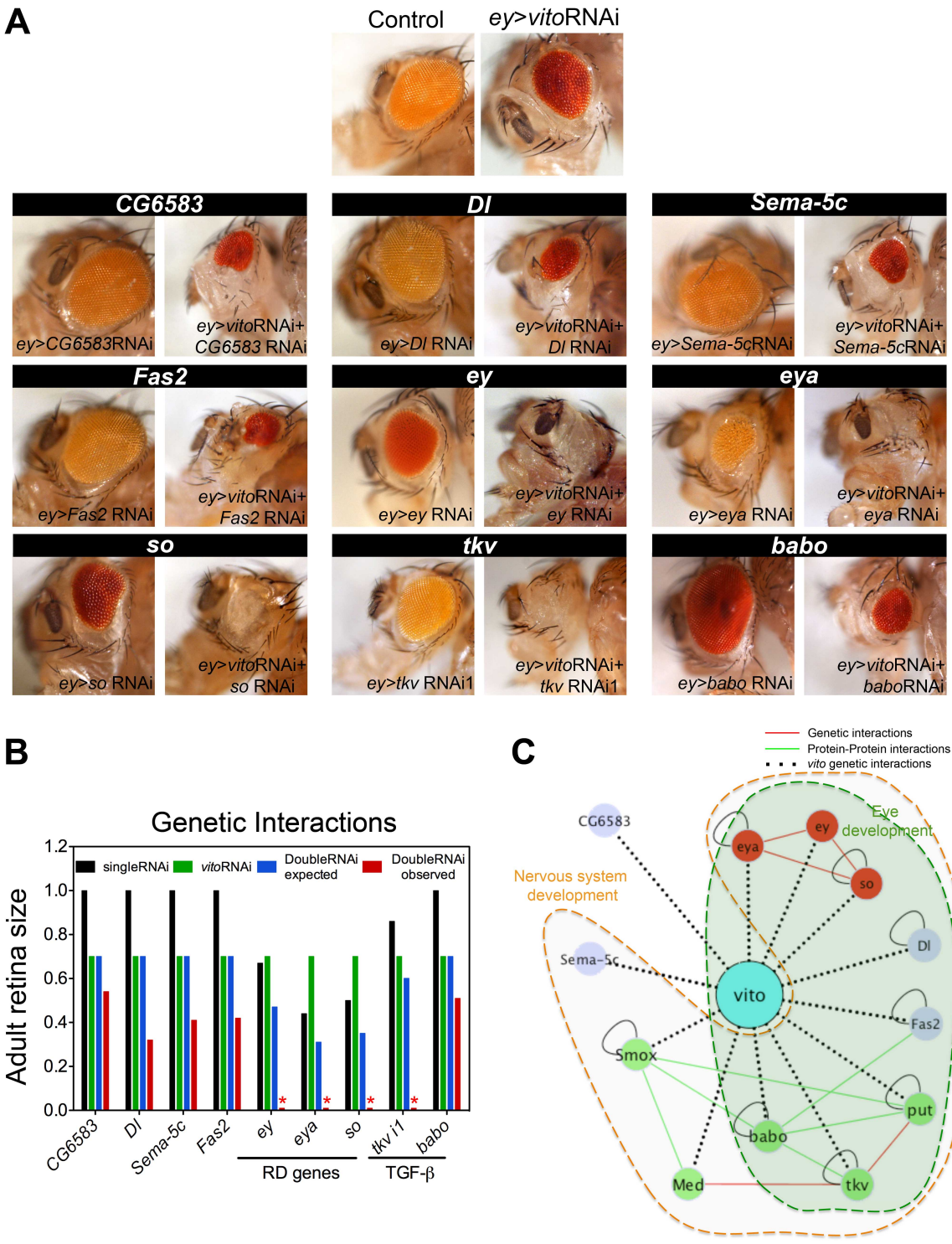

Figure 3.2 – Analysis of the Vito genetic interactions. (A) Adult eye phenotypes of the individual and double RNAis for each of the interactions identified in the screen**.** For Dpp and Activin signaling pathways only an example is shown. **(B)** Graphical representation of how genetic interactions were inferred from the adult retina sizes. Retina loss was quantified by measuring the retina size using the Image J software. When the eye is similar to a wild-type, and no retina loss is visible, the adult retina size has the value 1.0. Taking *CG6583* as an example, the expected phenotype of the double RNAi based on the multiplicative model is 0.7 (1.0X0.7). Deviations from the expected value indicate synthetic genetic interactions. The graph also shows that the strongest Vito interactions are revealed with the RD genes and the Dpp signaling pathway. Asterisks indicate absent eyes. **(C)** Represented is a network of interactions between all the Vito interactor genes and Vito itself gathered from DroID and displayed here as an interaction network using Cytoscape. Proteins are indicated by circular nodes and interactions by lines or edges. In red, Retinal determination proteins, in green, proteins belonging to the TGF-β signaling pathway, and in light blue the remaining Vito interactors. Dashed line

clouds represent GO enrichment of the Vito interactor genes and Vito itself compared to the entire *Drosophila* genome. Eleven genes show GO term enrichment in nervous system development (P=2.97X10^{-11}) (orange) and GO enrichment in eye development (P=1.45X10^{-7}) and/or eye-antennal disc development (P=2.75X10^{-8}) is shown in green for nine genes. GO enrichment analysis was performed using the web-based tool WebGestalt (http://bioinfo.vanderbilt.edu/webgestalt) (Zhang et al., 2005).

Since we found a very strong interaction between Vito and the Dpp pathway, we wanted to address whether our screen could reveal any potential genetic interactions between the Dpp pathway components and the remaining Vito interactors, i.e. transitive genetic interactions (Friedman and Perrimon, 2006). For that we crossed all the RNAis of the Vito interactors with the RNAi for the Dpp pathway members, *tkv* and *med*. The single transitive genetic interaction we detected was between *med* and the retinal determination gene *ey* (Fig. 3.3A,B and not shown), which was previously shown to function synergistically with Dpp to promote eye development (Chen et al., 1999; Curtiss and Mlodzik, 2000; Kango-Singh et al., 2003).

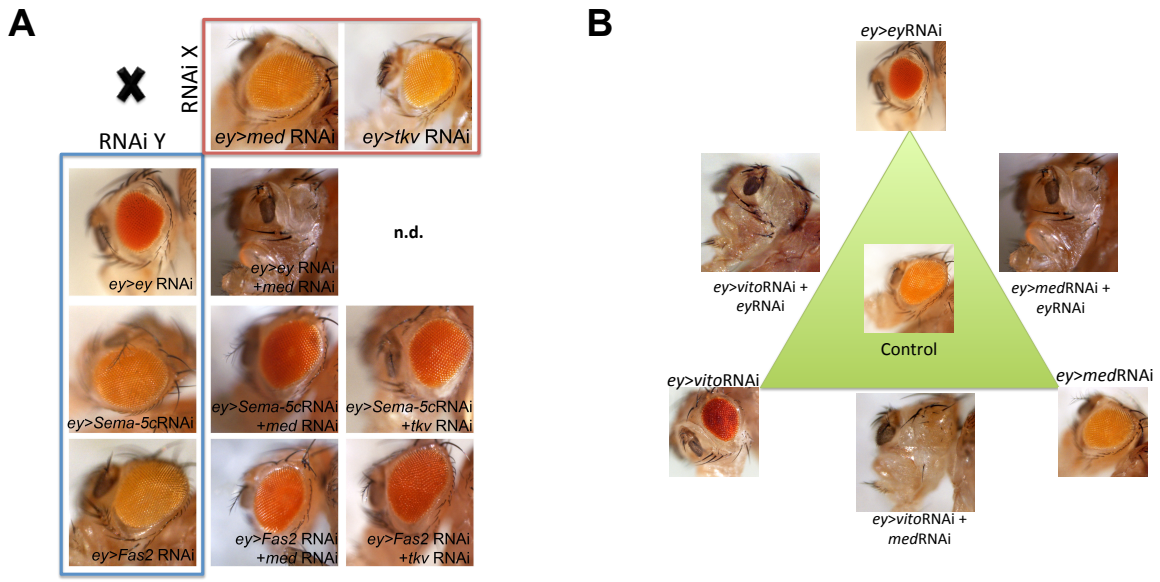

Figure 3.3 – Transitive genetic interactions between the Dpp pathway and Vito interactors. (A) Lateral views of the adult retinas expressing the RNAi for the Dpp pathway type I receptor *tkv* or the co-Smad *med* alone or in combination with the RNAis for some of the Vito interactors, shown as examples to illustrate the detection of transitive genetic interactions. Besides interaction with *ey*, no further interactions were detected with these Dpp signaling pathway components. n.d. not determined. **(B)** Schematic diagram representing the results of the genetic interactions between *vito*, *med* and *ey*. Single RNAi adult eye phenotypes are represented at the vertices and the double RNAis at the edges.

Therefore, and taking into consideration all the data so far, our approach to identify Vito interactors proved to be very efficient due to the small and specific number of interactions detected.

In Chapter 2 of this thesis we have shown that Vito is a transcriptional target of *Drosophila* Myc acting downstream of dMyc in the control of cell growth. Interestingly, it

was previously shown that expression of a constitutively active form of the type I Dpp receptor Tkv increases dMyc protein levels in the wing, whereas loss of Tkv causes a reduction in dMyc levels, suggesting that dMyc can function downstream of Dpp as a growth effector (Prober and Edgar, 2002). Therefore, we wanted to determine if Vito/Dpp interaction could stem from Dpp regulation of Myc protein levels. For that we analyzed the effects on eye development upon co-depletion of the *dmyc* and *med*. Although a double RNAi targeting dMyc and Med reveals a synthetic interaction, a stronger interaction is observed after co-depleting *vito* and *med*, as both retinas were absent in 100% of the flies (Fig. 3.4), in contrast to 50% of the flies with absent retinas observed in *dmyc*RNAi+*med*RNAi (Fig. 3.4). Since depletion of dMyc, on its own, induces a reduction in the size of the eye similar to what is observed for *vito*RNAi retinas, overall these results point to a specific and direct interaction of *vito* with Dpp signaling pathway that is not simply an indirect effect from the previously described Myc-Vito interaction.

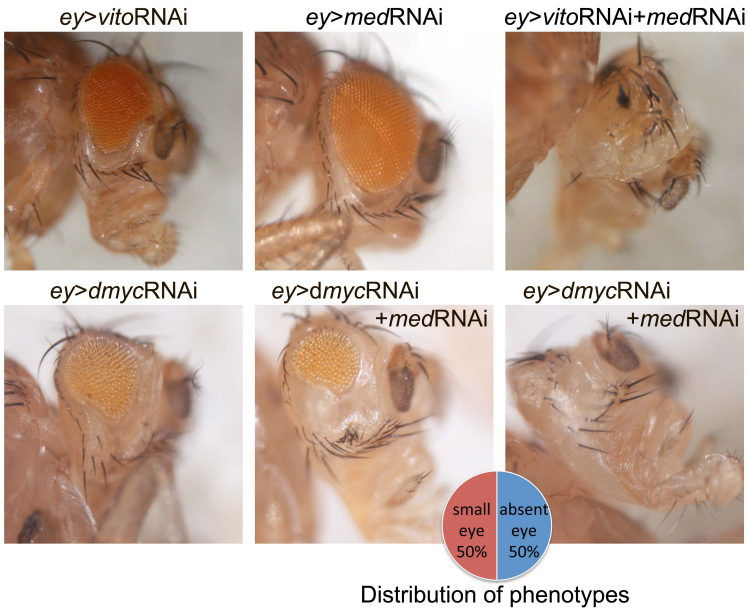

Figure 3.4 – Vito interaction with Dpp signaling is not simply due to the requirement of *vito* for dMyc function outputs. Depletion of *vito* together with *med* (*ey*-Gal4, UAS-*vito*RNAi/UAS-*med*RNAi1) induces loss of both retinas in 100% of the flies, whereas co-depletion of *dmyc* and *med* (*ey*-Gal4, UAS-*dmyc*RNAi/*med*RNAi) leads to a small eye phenotype in 50% of the flies, with the remaining 50% having absent eyes. *ey>vito*RNAi: (*ey*-Gal4, UAS-*vito*RNAi/+); *ey>med*RNAi: (*ey*-Gal4/UAS-*med*RNAi1;+); *ey>dmyc*RNAi: (*ey*-Gal4, UAS-*dmyc*RNAi;+).

4.2. *vito* genetically interacts with Dpp signaling pathway during eye development

Our screen looking for Vito interactors during eye development identified a strong genetic interaction with the Dpp branch of the TGF-β signaling pathway. To investigate further this genetic interaction we examined, in more detail, the highly dynamic process of eye development. For that, we depleted Vito together with different components of

the Dpp signaling pathway in the eye primordia and examined not only the adult eye but also the eye imaginal disc growth. As previously shown in Chapter 2 of this thesis (Marinho et al., 2011), *vito*RNAi expression in the eye primordium resulted in a very significant reduction in eye disc size, as well as a reduced and rough adult eye (Fig. 3.5A).

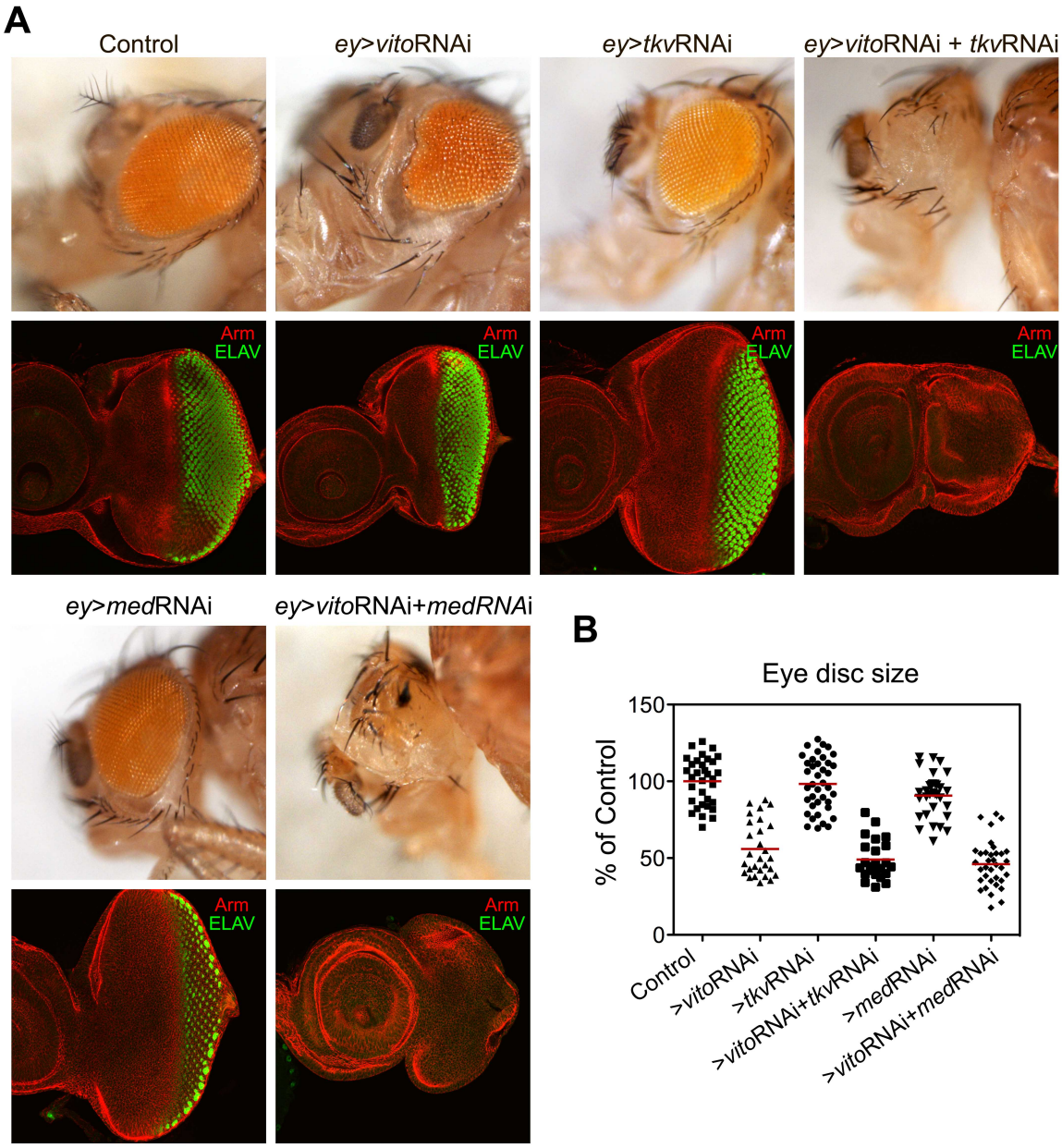

Figure 3.5 – *vito* genetically interacts with Dpp pathway. (A) Lateral views of adult eyes and the corresponding eye imaginal discs of the indicated genotypes stained for Armadillo (red) and a photoreceptor-specific antibody (anti-Elav, green). Knocking down *vito* (*ey*-Gal4, UAS-*vito*RNAi/+) causes a reduced eye phenotype and affects the size of the imaginal disc when compared to control. Removing *tkv* function by RNAi (*ey*-Gal4/UAS-*tkv*RNAi1;+) or *med* (*ey*-Gal4/UAS-*med*RNAi1;+) causes a reduction in adult eye size and the imaginal disc shows a delay in retinal differentiation at the lateral margins. Retinal differentiation is absent in discs or retinas co-expressing an RNAi against *tkv* and *vito* (*ey*-Gal4, UAS-*vito*RNAi/UAS-*tkv*RNAi1), or *med* and *vito* (*ey*-Gal4, UAS-*vito*RNAi/UAS-*med*RNAi1). **(B)** Eye disc sizes of the indicated genotypes were measured and represented as a distribution. Dots represent individual measurements and horizontal bars show mean values.

Reducing Dpp signaling by using RNAi for the type I receptor *tkv* or *med* resulted in a very small reduction in adult eye size (Fig. 3.5A,B). In the eye imaginal discs of these genotypes a slight delay in the progression of differentiation at the disc margins was observed, although retinal differentiation still occurred, which is characteristic of a partial loss-of-function of Dpp signaling (Chanut and Heberlein, 1997b) and is consistent with the hypomorphic conditions of the RNAi (Fig. 3.5A). Interestingly, the differentiation defects in the eye disc caused by RNAi against *tkv* or *med* are strongly enhanced by *vito*RNAi, as the double RNAi eye discs totally lack differentiation and are reduced in size (Fig. 3.5A,B). However, the reductions in eye disc sizes, seen after co-expression of *vito*RNAi and *tkv* or *med* RNAi, are not statistically different from the reductions seen for *vito*RNAi only expressing discs (44% reduction for *vito*RNAi against 52% or 53% reduction for co-expression of *vito*RNAi with *tkv*RNAi or *med*RNAi, respectively), suggesting that in these experimental conditions the lack of differentiation was not simply due to a strong reduction in tissue growth (Fig. 3.5A,B). Furthermore, the antennal disc sizes remain unaltered excluding a systemic effect of the RNAi and supporting the specificity of the interaction towards the eye disc (Fig. 3.5A).

Next, taking advantage of two independent RNAi lines targeting the type II receptor *put*, we were able to clarify the role of Vito in Dpp signaling during eye disc growth and patterning. Flies expressing a weak RNAi against *put* (*put*RNAi1; Table 3.1) do not show any visible defects in adult eyes and eye discs (Fig. 3.6A). Consistent with the results observed for *tkv* and *med*, eye discs depleted of Vito and Put show a clear delay in MF progression resembling the phenotype of a weak *dpp* loss-of-function allele (Fig. 3.6A) (Chanut and Heberlein, 1997a). Interestingly, a strong downregulation of Dpp signaling achieved using a strong RNAi line against *put* (*put*RNAi2), produces eye discs completely lacking retinal differentiation (Fig. 3.6B).

These experiments point to a role of Vito in controlling Dpp signaling during eye disc patterning, where Vito could be cooperating with Dpp in the process of retinal differentiation, since depleting *vito* and Dpp signaling using a weak RNAi line against a component of the pathway (as *tkv*, *med or put*), is similar, in terms of phenotype, to a strong downregulation of Dpp signaling (as seen using a strong RNAi against *put*). Furthermore, Vito also appears to be involved in the role of Dpp in growth stimulation during early stages of eye disc development. This is revealed by Vito depletion in eye discs that already lack differentiation by loss of Dpp signaling (*put*RNAi2), where a strong tissue growth deficit is visible in the eye disc (Fig. 3.6B). Overall these results strongly support a dual role of Vito during eye development: early in development Vito is required for tissue

growth, and also collaborates with Dpp in the promotion of growth; in later stages of eye disc development cooperates with the Dpp signaling to regulate retinal differentiation.

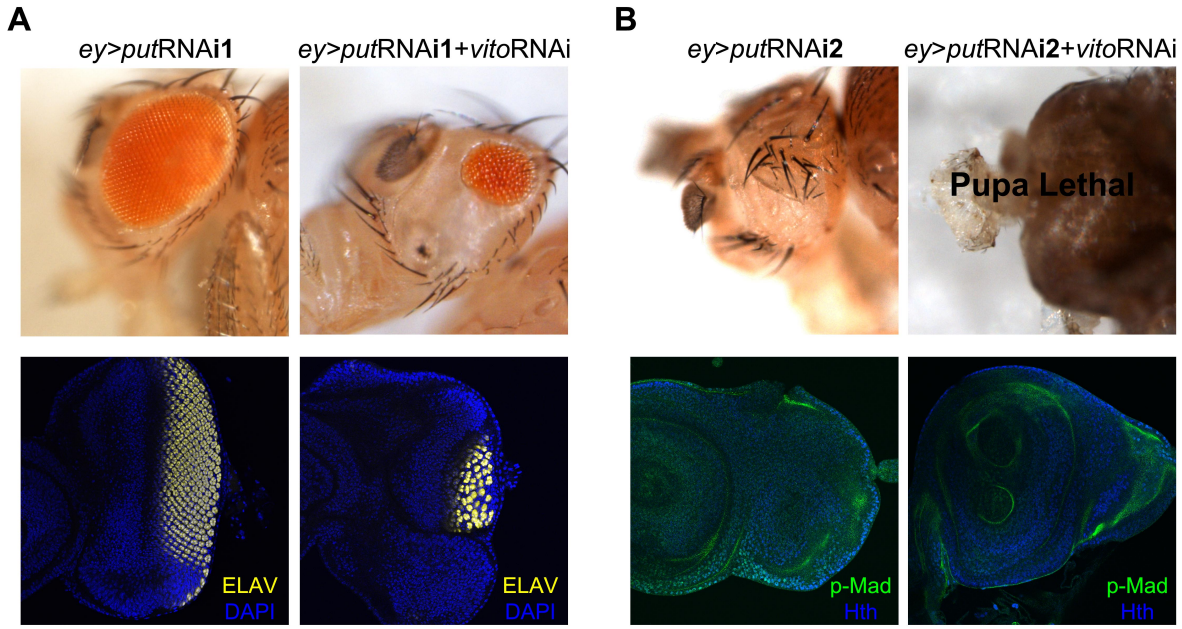

Figure 3.6 – Vito is required for eye disc growth and patterning when Dpp signaling is compromised. (A) Lateral views of adult eyes and the corresponding eye imaginal discs of the indicated genotypes stained with a photoreceptor-specific antibody (anti-Elav, yellow) and DAPI (blue). Downregulation of Dpp signaling using a weak RNAi line against *put* (*put*RNAi1: (*ey*-Gal4/UAS-*put*RNAi1)) does not apparently produce any visible phenotype in adult eyes and eye discs. Co-expression of RNAis against *put* and *vito* (*ey*-Gal4, UAS-*vito*RNAi/UAS-*put*RNAi1) induces a reduction in adult eye size reflecting the delay in retinal differentiation observed in the eye discs. **(B)** Lateral views of adult eyes and the corresponding eye imaginal discs of the indicated genotypes stained with an anti-p-Mad antibody (green) and for Hth (blue). A strong downregulation of Dpp signaling using *put*RNAi2 (*ey*-Gal4/UAS-*put*RNAi2) induces lack of differentiation. Co-expression of Vito in these flies (*ey*-Gal4, UAS-*vito*RNAi/UAS-*put*RNAi2) leads to synthetic lethality, with the flies reaching the pupal phase without head formation. A strong tissue growth deficit can be observed in the corresponding eye discs.

Vito was shown to be required for cell survival particularly in the anterior region of the eye disc, next to the MF (Marinho et al., 2011). Therefore, Vito's requirement for cell survival could be related to a deficient ability to transduce or respond to Dpp signaling. We next investigated whether the absence of retinal differentiation, seen in *vito* and *tkv* double RNAi could be explained by a generalized induction of apoptosis. As previously shown in Chapter 2 of this thesis, *vito*RNAi eye discs presented a significant number of cells undergoing apoptosis, as detected by the presence of activated cleaved Caspase-3 (Fig. 3.7A,B) (Marinho et al., 2011). After knocking-down *tkv*, apoptosis is also detected, particularly in the anterior domain close to the discs margin (Fig. 3.7A,B). However, when *vito*RNAi is co-expressed with *tkv*RNAi the number of cells undergoing apoptosis is not statistically different from those seen in *vito*RNAi eye discs (Fig. 3.7A,B), and we could not detect cells undergoing apoptosis in the posterior margin of the eye disc, where retinal differentiation begins (Fig. 3.7A). Therefore the absence of retinal differentiation is not

explained by an increase in apoptosis.

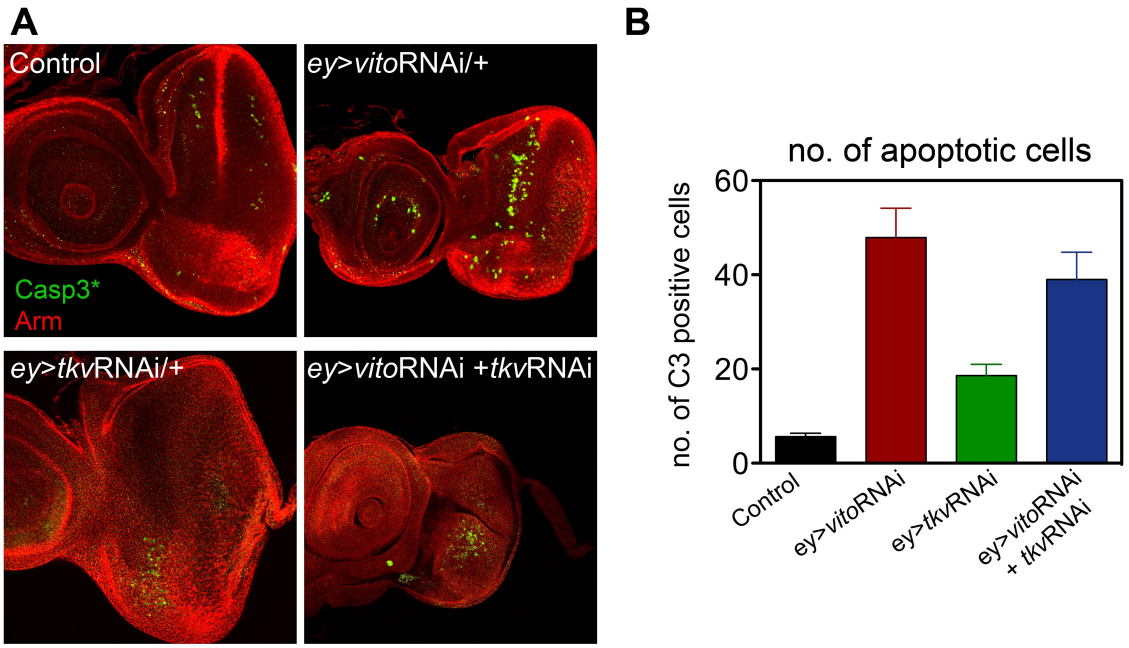

Figure 3.7 – Induction of apoptosis does not explain *vito*/Dpp genetic interaction. (A) Third instar *Drosophila* eye imaginal discs of the indicated genotypes stained for Armadillo (red) and cleaved Caspase-3 (green). Depleting *vito* (*ey*-Gal4, UAS-*vito*RNAi/+) causes significant cell death in the anterior domain of the eye disc. Reduced Dpp signaling by expression of *tkv*RNAi (*ey*-Gal4/UAS-*tkv*RNAi1;+) also caused cell death anteriorly in the eye disc. In discs co-expressing *tkv*RNAi and *vito*RNAi (*ey*-Gal4, UAS-*vito*RNAi/UAS-*tkv*RNAi1) no significant differences in the number of apoptotic cells are seen comparing to *vito*RNAi. **(B)** Quantification of cell death assessed by the number of cleaved Caspase-3 positive cells in the eye discs in A. Data are presented as the mean + s.e.m (n=19-24).

4.3. Tissue specificity of the interaction between *vito* and Dpp signaling

In the eye disc *vito* is expressed in a dynamic pattern, with high expression in the anterior region, however *vito* transcripts are also detected in the wing and other imaginal discs albeit at low levels and without a specific pattern of expression. We therefore tested whether *vito*/Dpp interaction was eye-specific. For that we used several wing-specific drivers such as the wing pouch drivers *MS1096*-Gal4 and sal^{EPv}-Gal4 (central domain of the wing pouch) (Cruz et al., 2009), the posterior compartment driver *engrailed* (*en*-Gal4) and *dpp*-Gal4 driver (expressed in the anterior compartment at the level of the boundary between the AP compartments), to downregulate both *vito* and *tkv* and scanned for growth and patterning defects.

Downregulation of Dpp signaling in the wing with *tkv*RNAi leads to wing size reductions and/or patterning defects depending on the driver used (Fig. 3.8). Interestingly, in all the cases knocking down both *vito* and *tkv* did not produce a modification of the *tkv*RNAi phenotype, unless when *en*-Gal4 driver was used, which caused lethality (Fig. 3.8C). The *en*-Gal4 driver expression is not exclusive to the wing posterior compartment, and is also expressed early in the embryo. We also tested the

interaction using *med*RNAi and *sal*^{EPv}-Gal4 driver and observed similar results (Fig. 3.8D).

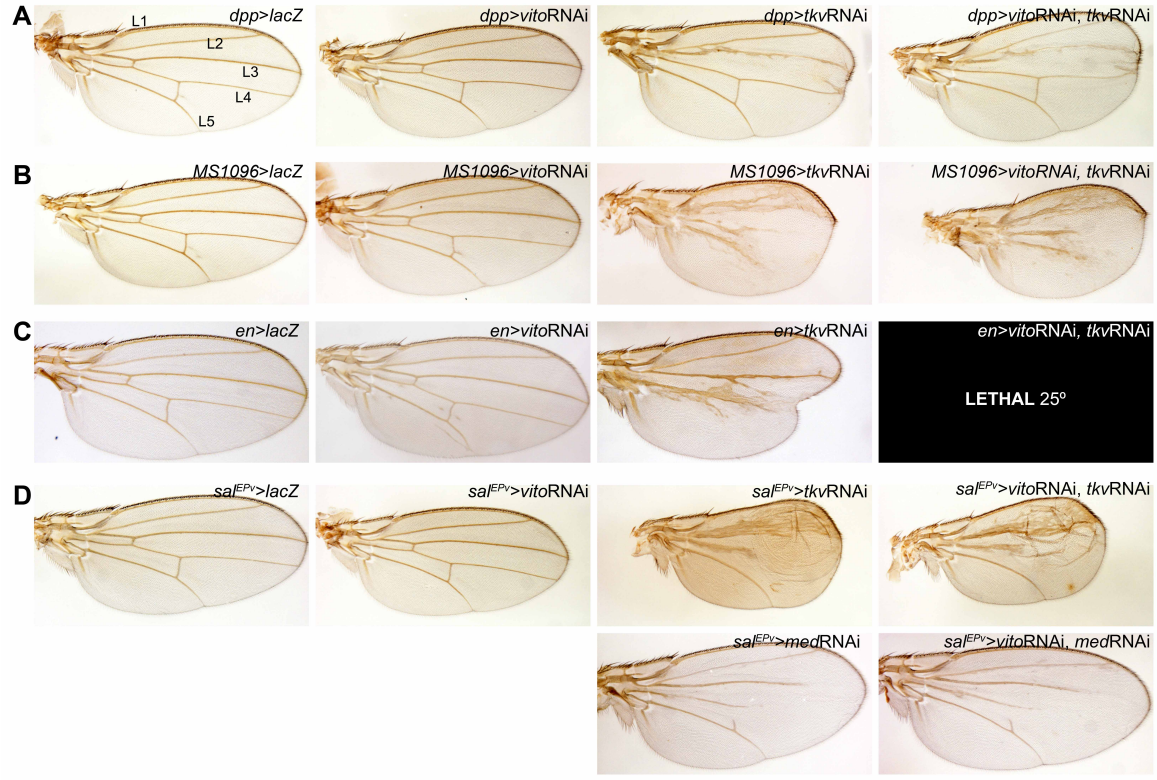

Figure 3.8 – *vito*/Dpp strong genetic interaction in the eye is not detected in the wing. Adult wings of controls, *vito*RNAi, or RNAi towards *tkv* and *med* alone or together with *vito* under the control of different wing drivers. **(A)** *dpp*-Gal4 driving of *tkv*RNAi causes vein defects in longitudinal vein 3 (L3), phenotype that is not affected by co-depletion of *vito.* **(B)** *MS1096*-Gal4 driving *tkv*RNAi results in small wings almost lacking veins. *vito*, *tkv* double RNAi wings show identical phenotypes to *tkv* depletion alone. **(C)** Depleting *tkv* by RNAi in the wing posterior compartment using *en*-Gal4 driver resulted in a small and unpatterned posterior compartment. Double RNAi for *vito* and *tkv* caused lethality. **(D)** *sal*^{EPv}-Gal4 driving depletion of *tkv* by RNAi results in small wings with patterning defects that are not altered after co-depletion of Vito. *med*RNAi causes marked reduction of veins in the distal part of the wing. Simultaneous depletion of Med and Vito affects vein formation in a similar way as knockdown of Med alone.

On the basis of these results we can conclude that *vito*/Dpp interaction is strong in the eye and not detected in the wing, as lethality with *en*-Gal4 driver could indicate a possible interaction in other tissues.

4.4. *vito* is a positive regulator of the Dpp signaling pathway

Until now we have shown that when Dpp signaling is compromised Vito cooperates with Dpp in eye disc growth and patterning, as growth and/or differentiation defects caused by RNAi towards Dpp signaling pathway components are strongly enhanced by *vito*RNAi. Next we decided to address whether *vito* could modulate phenotypes resulting from Dpp overexpression in the eye. When overexpressing *dpp* under *ey*-Gal4 driver, 100% of the flies did not survive until adulthood, dying as pupae (Fig 3.9A). Consistent with the role of Dpp in MF initiation and progression, we observed in the eye primordia

that the ommatidial array prolonged into regions of the disc that normally give rise to head cuticle, forming clusters covering the entire disc (Fig. 3.9B). Interestingly, we found that depletion of Vito is able to rescue excessive activation of Dpp by reverting lethality in 30% of the flies (Fig. 3.9C).

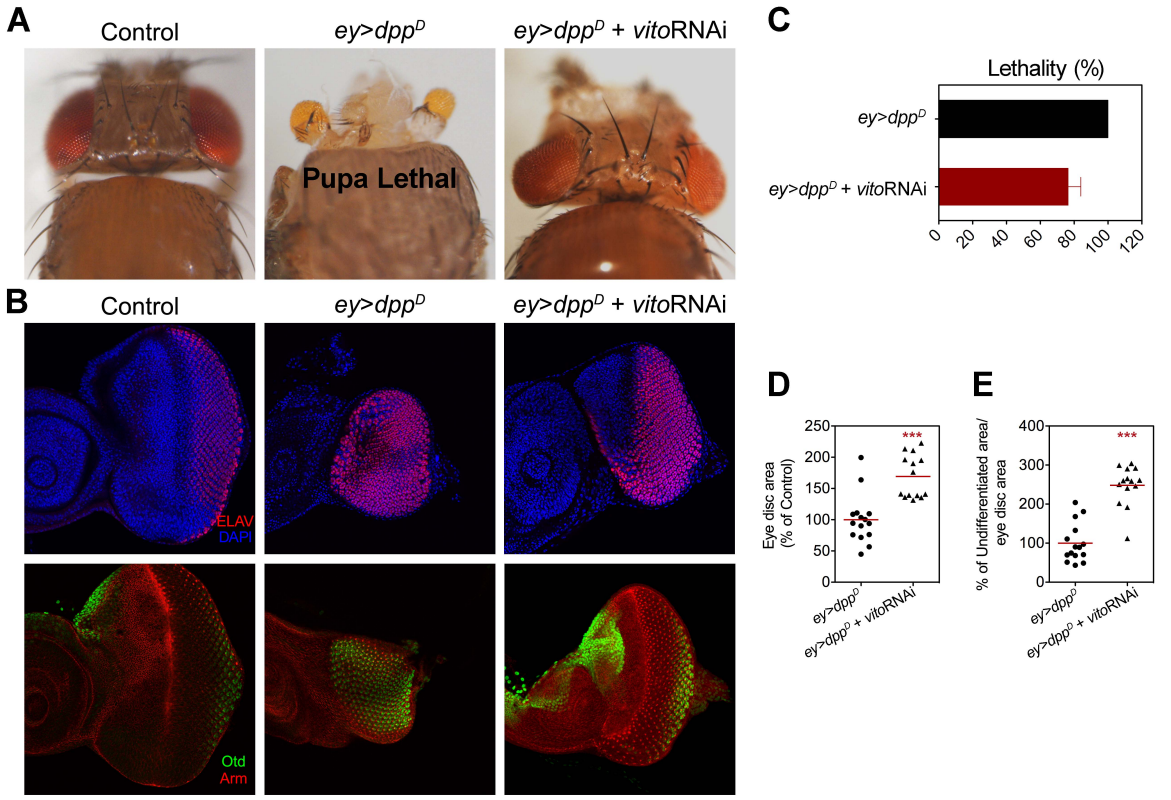

Figure 3.9 – Vito depletion rescues lethality induced by Dpp overexpression. (A) Dorsal views of control (*ey*-Gal4/+; UAS-*lacZ*/+), overexpression of Dpp (*ey*-Gal4/+; UAS-dpp^D/+) and UASdpp^D+*vito*RNAi (*ey*-Gal4, UAS-*vito*RNAi; UAS-dpp^D/+) heads. **(B)** Eye discs of the above genotypes were stained with a photoreceptor-specific antibody (anti-Elav, red) and DAPI (blue) (top row), or stained with an anti-Otd antibody (green) and Armadillo (red) (bottom row). **(C)** Percentage of lethality (animals surviving to adult stage) after Dpp overexpression or overexpression of Dpp and Vito depletion. **(D)** Eye disc areas of the indicated genotypes were measured and represented as a distribution. Dots represent individual measurements and horizontal bars show mean values (n=15). (***, $P<1x10^{-4}$ relative to overexpression of Dpp alone). **(E)** The percentage of undifferentiated area in the eyes discs was measured and normalized for the corresponding total disc areas. Dots represent individual measurements and horizontal bars show mean values (n=15). (***, $P<1x10^{-4}$ relative to overexpression of Dpp alone).

To understand in more detail what was the cause for the rescue of lethality we analyzed the eye primordia and noticed eye discs with larger areas (1.7 times bigger) in comparison to Dpp overexpressing discs (Fig. 3.9B,D) that in contrast to the latter, were not completely differentiated in the eye part of the imaginal disc. Importantly, when the area that remained undifferentiated in the eye discs was quantified, a 2.5 times increase in the percentage of undifferentiated area was observed after depleting Vito in Dpp overexpressing discs (Fig. 3.9E) indicating that Vito/Dpp interaction is not due to a simply role of Vito in promoting tissue growth.

Because of the disc morphology in UAS*dpp* and UAS*dpp*+*vito*RNAi it was difficult to determine whether the increase in eye disc area and undifferentiated area corresponded to a ventral or dorsal domain of the disc. Consequently we decided to use a Wg target, Orthodenticle (Otd) that in control discs is expressed in an anterior dorsal patch, a region of the head primordia and in the developing ommatidia (Fig. 3.9B). We observed that Otd dorsal expression in UASdpp^{D}+*vito*RNAi discs was normal and similar to control discs, indicating that indeed the undifferentiated domain corresponded to the dorsal domain of the eye disc (Fig. 3.9B). Overall these results suggest that Vito modulates the cellular response downstream of Dpp.

Similarly to what we showed in loss-of-function experiments, Vito's capacity to modulate Dpp overexpression is specific to the eye, since in the wing we could not detected any effect after depleting Vito in Dpp overexpressing wings (Fig. 3.10).

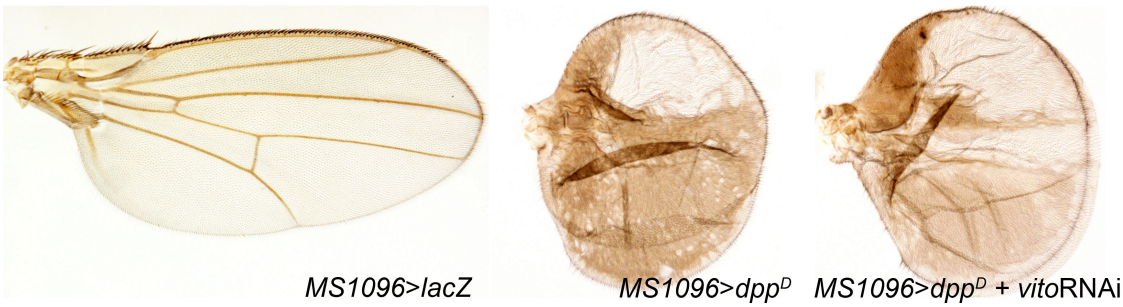

Figure 3.10 – Vito modulation of Dpp overexpression is eye-specific. Adult wings of control (*MS1096*; UAS-*lacZ*/+), Dpp overexpressing (*MS1096*;;UAS-dpp^{D}/+), and UAS*dpp* + *vito*RNAi (*MS1096*;UAS-*vito*RNAi/+;UAS-dpp^{D}/+) flies. Overexpressing Dpp in the wing leads to an overproduction of vein tissue, resulting in wings of reduced size. A similar phenotype is observed after Vito depletion in Dpp overexpressing wings.

Next, to test whether Vito could augment Dpp signaling we overexpressed, using the *ey*-Gal4 driver, low levels of Vito with a UAS-*vito* transgene, which does not cause an eye phenotype, in a background RNAi for the Dpp signaling (*put*RNAi2). 77% of the flies expressing a strong RNAi for *put* eclode without both retinas, 23% exhibit only one retina and we could not observe flies presenting both retinas (Fig. 3.11A,B). In contrast, 65% of the flies depleted of *put* and overexpressing Vito show both retinas, despite their small size (Fig. 3.11A,B). We also observed the presence of differentiated photoreceptors in the eye discs of these flies (Fig. 3.11A).

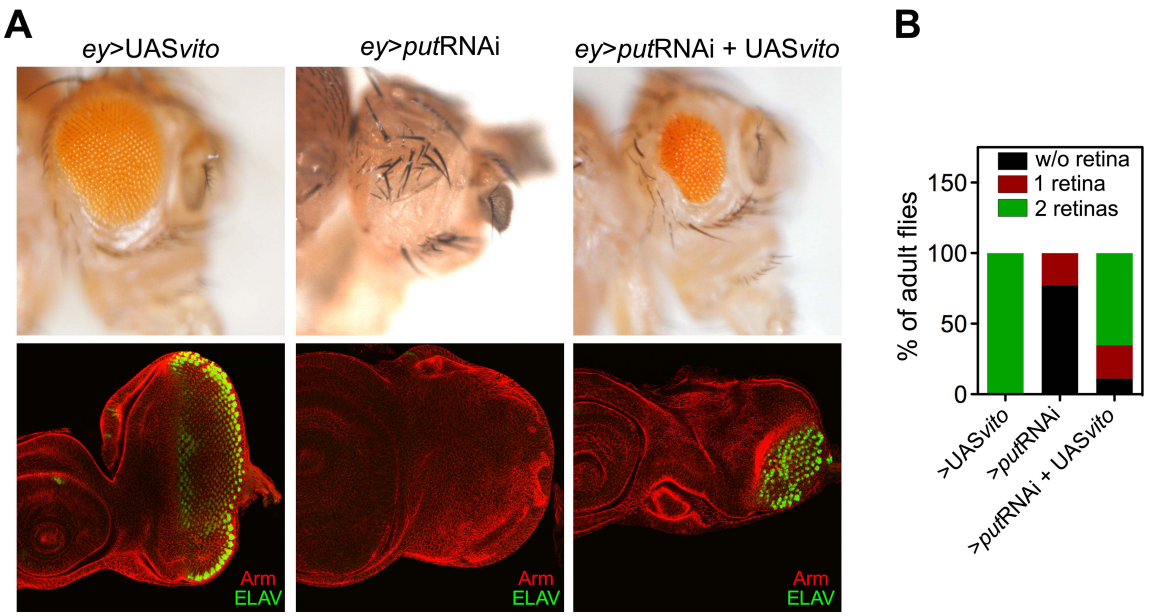

Figure 3.11 – Overexpression of Vito restores retina differentiation in *put* loss-of-function flies. (A) Lateral views of adult eyes and the corresponding eye imaginal discs of the indicated genotypes stained for Armadillo (red) and Elav (green). Flies overexpressing Vito exhibit no eye phenotype. Loss of *put* flies lack differentiation that is almost completely suppressed by overexpressing Vito. **(B)** Percentage of adult flies presenting 2 retinas, 1 retina or without (w/o) retinas (n=57-81). >UAS*vito* (*ey*-Gal4/+; UAS-*vito*/+); >*put*RNAi (*ey*-Gal4/*put*RNAi2); >*put*RNAi + UAS*vito* (*ey*-Gal4/*put*RNAi2; UAS-*vito/+*).

These series of results are consistent with the idea that Vito could positively regulate Dpp signaling: depletion of Vito partially reverts Dpp overexpression; the phenotype of depleting Vito in a Dpp weak RNAi background resembles a strong RNAi for a Dpp pathway component; and overexpression of Vito can have the opposite role and partially compensate for a reduction in the activity of Dpp signaling.

4.5. *vito* is not required in the eye disc for the activation of all Dpp targets

To determine the epistatic position of Vito within the Dpp pathway, we co-expressed *vito*RNAi with a constitutively active form of the Tkv receptor (Tkv^{QD}) (Nellen et al., 1996). Mitotic clones expressing Tkv^{QD} are able to activate expression of the RD gene *eya*, and repress transcription of the homeodomain factor Hth in the anterior region of the eye disc (Bessa et al., 2002; Bessa and Casares, 2005) (Fig. 3.12A). We found that clone size for cells expressing Tkv^{QD} together with *vito*RNAi is reduced towards wild-type size while maintaining characteristic regulation of *eya* and *hth* (Fig. 3.12A,C). Additionally, in this experiment Vito depletion did not interfere with the ability of Tkv^{QD}-expressing clones to induce early G1 arrest (Fig. 3.12B).

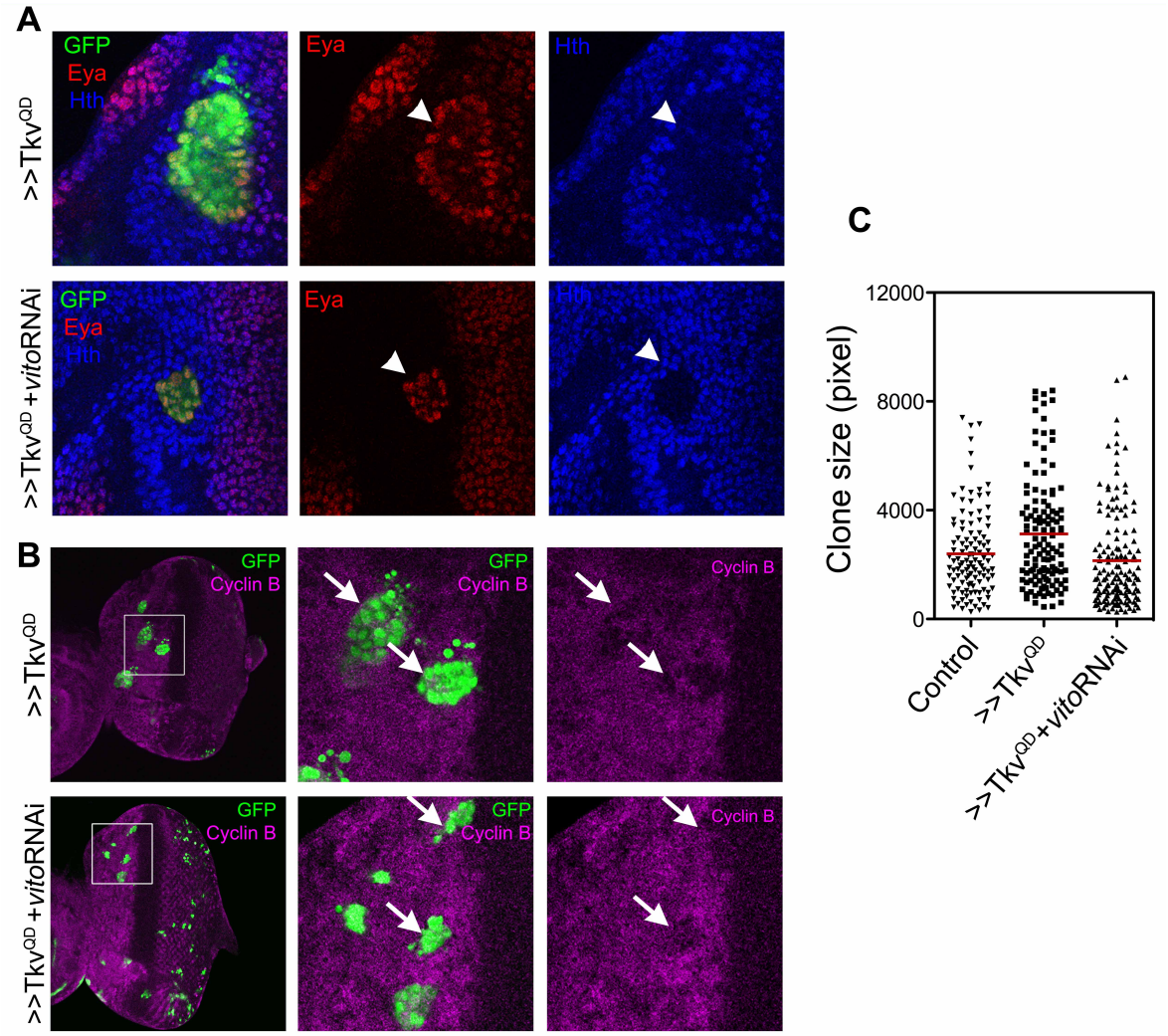

Figure 3.12 – Loss of Vito reduces Tkv^{QD} clone size to control levels while maintaining characteristic regulation of Eya, Hth and G1 arrest. (A,B) Tkv^{QD} and Tkv^{QD} + *vito*RNAi expressing clones were induced in the early eye disc and analyzed 48 hours later. Images show representative clones marked positively by the presence of GFP. Clones in anterior regions of the disc co-expressing Tkv^{QD} + *vito*RNAi, as Tkv^{QD}-expressing clones, derepress Eya (red) and lose Hth expression (blue) (A). Arrowheads point to clones. (B) Anti-Cyclin B antibody (violet), which was used as a marker for cell cycle, show that cells in Tkv^{QD}-expressing clones that lie near the MF, accelerate G1 arrest. Co-expression of *vito*RNAi does not change this early arrest. Arrows point to clones. **(C)** The size of the clones anterior to the MF were measured and represented as a distribution. Dots represent individual measurements, and horizontal bars show mean values (n=114-149).

The fact that we could not detect modulation of the examined Dpp targets could be related to the conditions of this experiment, since the time of clonal induction must be precise in order to get overgrowth in Tkv^{QD}-expressing clones without excessive apoptosis. Consequently, the time frame since the RNAi induction until the analysis of the discs might not be sufficient to observe effects at the protein level.

Therefore, although not regulating the examined Dpp targets in the eye disc, Vito contribution could be restricted to the activation of unknown Dpp targets involved in cell growth and proliferation acting in a downstream branch of Tkv.

4.6. *vito* regulates uniform Dpp signaling in the morphogenetic furrow

To gain insight into the mechanism by which Vito was modulating Dpp signaling pathway, we investigated if knocking-down Vito changed the levels and localization pattern of the pathway's transcriptional effector phosphorylated Mad (p-Mad). Vito depletion in mitotic clones induced in the early eye disc failed to affect p-Mad levels (Fig. 3.13A). However, when *vito*RNAi was induced in the entire eye imaginal disc with the *ey*-Gal4 driver, an abnormal p-Mad pattern of expression was detected (Fig. 3.13B,C). Even though differentiation occurs in *vito*RNAi eye discs, MF progression is irregular, and an abnormal p-Mad pattern near the furrow is observed, together with a broader activation of p-Mad anteriorly in the disc (Fig. 3.13C-C''). A uniform MF propagation and ommatidial differentiation requires a re-initiation of the MF along the margins, being *dpp* expressed at the lateral margin until the MF has passed in wild-type discs (Wiersdorff et al., 1996; Chanut and Heberlein, 1997b; Pignoni and Zipursky, 1997). Curiously, we observed that at the lateral margins of *vito*RNAi eye discs p-Mad was significantly reduced, suggesting that Vito could be required for the activation of Dpp signaling at the disc margins (Fig. 3.13C').

Furthermore, when examining p-Mad patterns of expression in discs expressing double RNAi for *vito* and *tkv* or *med*, we found a complete absence of p-Mad staining in the double RNAi eye discs, which is similar to what is observed with a strong RNAi for Dpp signaling (*put*RNAi2) (Fig. 3.13D), suggesting once again a role of Vito in positively regulating Dpp signaling.

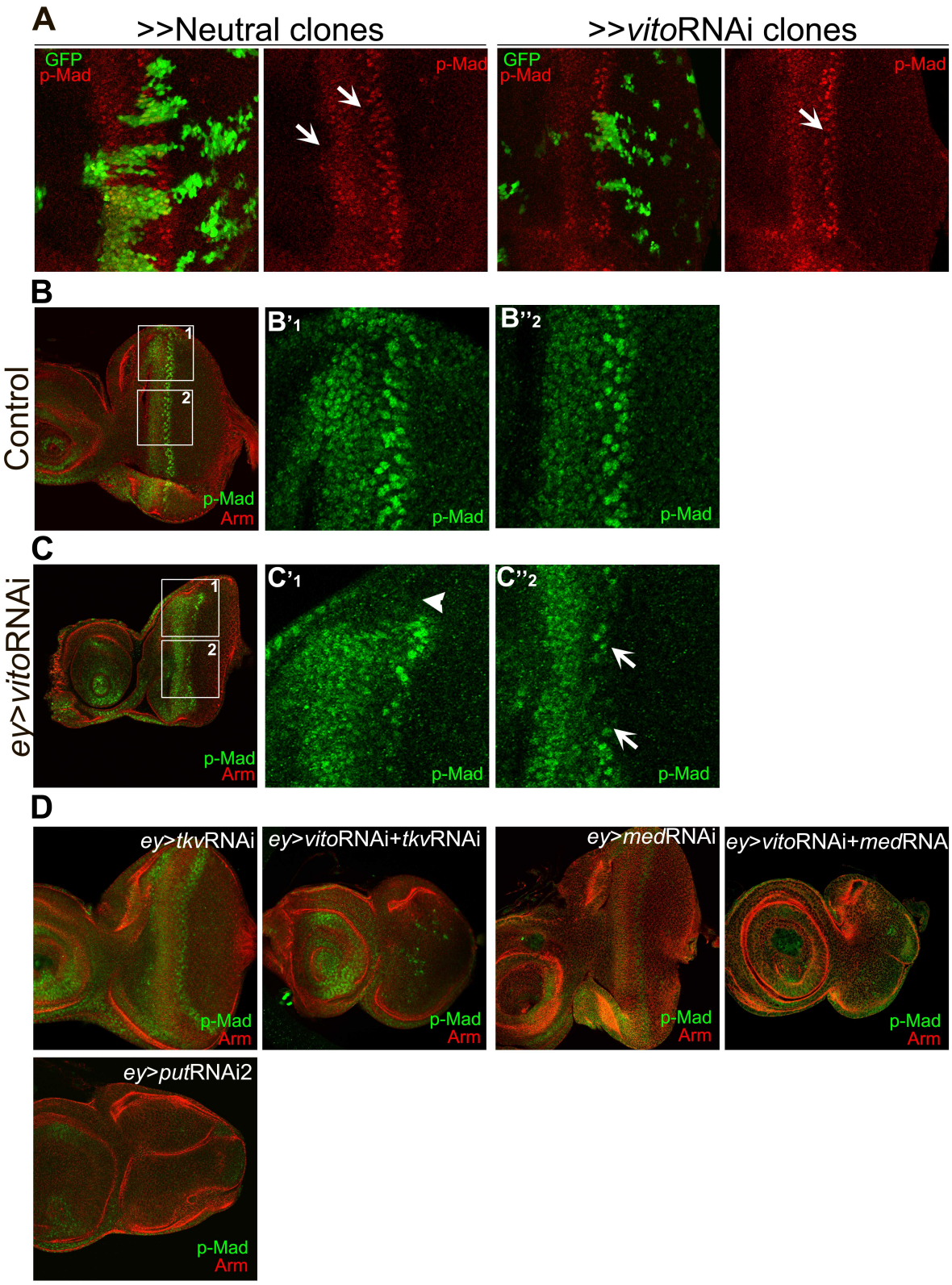

Figure 3.13 – Vito regulates uniform Dpp signaling in the furrow. (A) Neutral and *vito* loss-of-function clones were induced in the early eye disc and analyzed 48 hours later. Images show representative clones marked positively by the presence of GFP, and stained with an anti-p-Mad antibody (red). Notice that the intensity of p-Mad signal does not change in *vito*RNAi clones (arrows). **(B,C)** Control (*ey*-Gal4/UAS-*lacZ*) and *vito*RNAi (*ey*-Gal4, UAS-*vito*RNAi/+) eye imaginal discs were stained for Armadillo (red) and p-Mad (green). (B-B'') In control discs two stripes of p-Mad signal are detected in the MF. Magnifications of the lateral margin (B') and a more central region (B'') of the control disc showing p-Mad pattern of expression. (C-C'') Knocking down Vito expands the domain of p-Mad activation. Magnifications show the absence of p-Mad signal at the lateral margins (C', arrowheads) and the irregular p-Mad

activation in the stripe closer to the MF (C'', arrows). **(D)** Eye discs of the indicated genotypes were stained for Armadillo (red) and p-Mad (green). Removing *tkv* function by RNAi (*ey*-Gal4/UAS-*tkv*RNAi1;+) or *med* (*ey*-Gal4/UAS-*med*RNAi1;+) delays furrow progression at the lateral margins resulting in an efficient p-Mad activation at the discs margin. Eye discs co-expressing an RNAi against *tkv* and *vito* (*ey*-Gal4, UAS-*vito*RNAi/UAS-*tkv*RNAi1), or *med* and *vito* (*ey*-Gal4, UAS-*vito*RNAi/UAS-*med*RNAi1) do not show p-Mad characteristic stripe activation similarly to a strong downregulation of Dpp signal using *put*RNAi2 (*ey*-Gal4, UAS-*put*RNAi2).

Next we decided to monitor *dpp* expression in *vito*RNAi eye discs. For that we used a *dpp-lacZ* reporter that accurately reflects the expression pattern of the endogenous *dpp* gene (Blackman et al., 1991). Before furrow initiation *dpp-lacZ* is expressed along the posterior and lateral margins (Fig. 3.14A). After initiation, *dpp* expression progresses with the furrow and its expression is shut down anteriorly (Fig. 3.14A). In *vito*RNAi discs of similar age, we clearly observed that already early in development *dpp* expands at the lateral margins and consequently all the program leading to furrow initiation could already be compromised (Fig. 3.14B). Once differentiation starts, although *dpp* expression still progresses with furrow movement, as seen for control discs, the domains of expression are larger, particularly at the disc margins. Similarly in the furrow there is an extended domain of *dpp* expression (Fig. 3.14B).

dpp is required to maintain its own expression, and together with other components of the pathway is involved in an autoregulatory loop downregulating its own expression along the disc margins with the progression of retinal differentiation (Chanut and Heberlein, 1997b). The genetic interactions data from this study, the absence of *dpp* downregulation at the anterior lateral domains in *vito*RNAi eye discs, and the decrease in p-Mad laterally suggest that Vito affects activation of Dpp signaling, by a still unknown mechanism.

In order to clarify this mechanism we assessed the levels and expression pattern of the Dpp type I receptor Tkv by using a YFP exon trap insertion that reflects Tkv endogenous expression (Yuva-Aydemir et al., 2011). In control discs, Tkv strongest expression is detected in differentiated photoreceptors and in the anterior region of the eye disc. In Vito depleted eye discs, although Tkv expression patterns are not altered, its levels are reduced in the MF and adjacent regions (Fig 3.14C,D). By quantifying Tkv levels in the posterior differentiated and anterior regions of the eye disc, we observed that the knockdown of Vito only affects anterior levels of Tkv right behind the furrow (Fig. 3.14D). Tkv is crucial for Dpp signaling and Dpp diffusion (Burke and Basler, 1996; Lecuit and Cohen, 1998) so the observed alterations suggest that modulation of Tkv levels by Vito could be one of the mechanisms supporting the positive input of Vito for Dpp signaling activity.

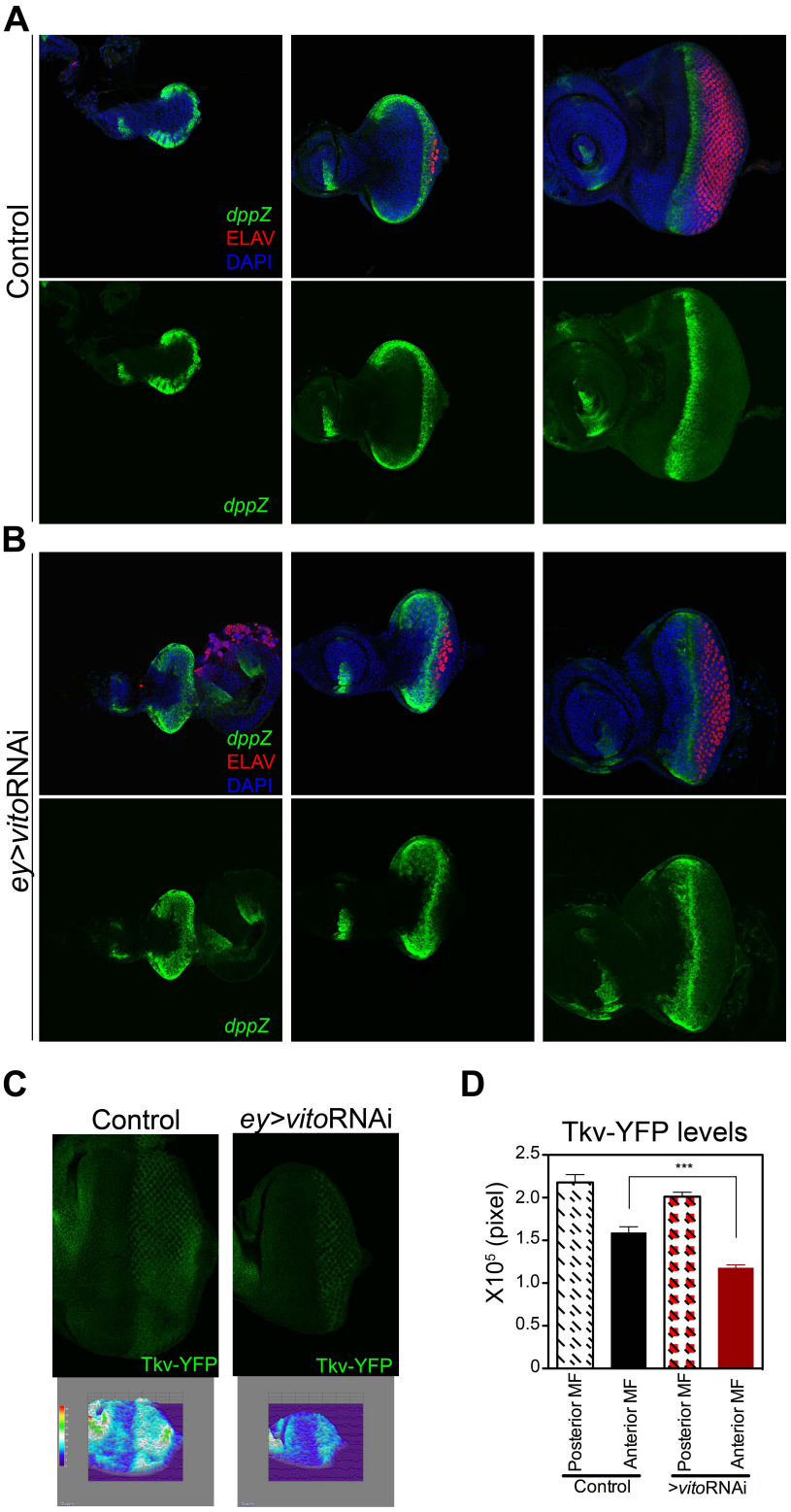

Figure 3.14 – Vito regulates Dpp signaling by affecting Tkv levels. (A,B) Control (*ey*-Gal4/+; *dpp3.0-LacZ*/+) and *vito* loss of function (*ey*-Gal4, UAS-*vito*RNAi/+; *dpp3.0-lacZ*/+) eye imaginal discs carrying a *dpp-lacZ* reporter construct were stained for β-galactosidase activity (green) to visualize *dpp* expression, for the neuronal specific marker Elav (red) to monitor ommatidial differentiation and DAPI (blue). (A) In control discs, before the beginning of differentiation *dpp* is expressed all around the posterior and lateral margins. After initiation expression becomes restricted to the MF. (B) In *vito*RNAi eye discs, early in development *dpp* expression is already spread along the posterior and lateral margins. After MF initiation, *dpp* expression follows furrow progression, however at the lateral margins its expression continues very broad and spread and not confined to the furrow. **(C)** Eye imaginal discs expressing Tkv-YFP alone or together with *vito*RNAi. Control imaginal discs (*ey*-Gal4/Tkv-YFP) show Tkv-YFP expression at high levels in photoreceptors, being downregulated in the MF and ahead, whether depletion of Vito (*ey*-Gal4, UAS-*vito*RNAi/Tkv-YFP) induces a strong

downregulation in the MF region and more anteriorly. The images were submitted to image analysis by the Interactive 3D Surface Plot, a plug-in for ImageJ software. The 3D surface translates the luminance of the images in the figures above as height for the plot. **(D)** Quantification of Tkv-YFP levels in posterior and anterior regions adjacent to the MF in control and *vito*RNAi eye discs (n=16-18). ***$P<1X10^{-4}$.

4.7 Does Dpp regulate cell growth by dynamic regulation of nucleolar function?

As feedback loops are a frequent control mechanism for the activity of signaling pathways, we assessed whether the Dpp pathway regulated Vito expression or localization. For that we studied if the stability or the nucleolar localization of Vito-GFP was regulated by Dpp pathway. We assessed Vito nucleolar localization in salivary gland cells, because owing to their polyploidy, these cells have large nucleoli. We did not observe any changes in Vito nucleolar localization or levels after Tkv depletion (Fig 3.15A-B).

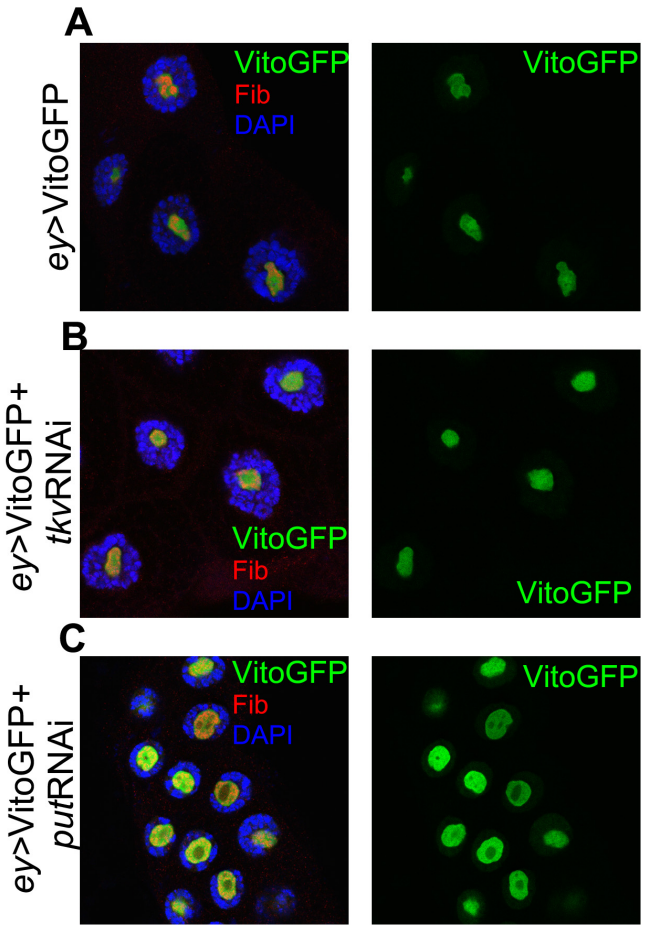

Figure 3.15 – Vito nucleolar localization is not affected by Dpp signaling. A UAS-*vito*GFP transgene was overexpressed in salivary glands with or without RNAi for the Dpp receptors Tkv and Put, using the "leaky" expression of the *ey*-Gal4 driver in salivary glands. **(A)** Overexpressed Vito-GFP (*ey*-Gal4/+;UAS-*vito*GFP/+) localizes to the nucleolus. **(B)** When *tkv*RNAi is co-expressed (*ey*-Gal4,UAS-*tkv*RNAi;UAS-*vito*GFP/+) Vito-GFP levels and nucleolar localization remains unaltered. **(C)** The nucleolar localization of Vito-GFP is not altered upon *put*RNAi expression (*ey*-Gal4/UAS-*put*RNAi2;UAS-*vito*GFP/+), however Vito-GFP becomes spread at the nucleolus and the nucleolar structure is altered.

However, when we looked with more detail to the nucleolus of the salivary gland cells after Put depletion we made an extremely surprising observation: TGF-β signaling pathway seems to regulate the nucleolar structure. VitoGFP in *put*RNAi salivary gland cells becomes more dispersed accompanying the enlargement of the nucleolar structure (Fig. 3.15C), therefore we decided to study this nucleolar effect in more detail.

After a strong reduction in the TGF-β signaling in salivary glands by using a strong RNAi for *put* (*put*RNAi2), we investigated the localization patterns and expression levels for both the nucleolar methyltransferase Fibrillarin and the large subunit ribosomal protein RpL22. In these salivary gland cells, an abnormal ectopic nucleolar accumulation of RpL22 and Fibrillarin is detected, with the presence of small dark vacuoles at the nucleolus (Fig 3.16A). These nucleolar changes were inspected in more detail by TEM. *put*RNAi salivary gland nucleolus appears larger than controls, with internal vacuolar structures although different from the nucleolar changes resulting from Vito misregulation (Fig. 3.16B) (Marinho et al., 2011). Furthermore, we found accumulation of what appears to be pre-ribosomes at the nucleus of *put*RNAi salivary gland cells (Fig. 3.16B, see insets).

Even though these results are preliminary and need further enlightenment they raise a lot of questions: Does Dpp/TGF-β regulate nucleolar function in a dynamic manner during developmental processes? Is Dpp regulation of growth related to the control of nucleolar activity, ribosome production, or general protein synthesis? Overall, the results presented in this Chapter support that Vito's requirement for some outcomes of the Dpp signaling pathway could involve the regulation of nucleolar architecture and function.

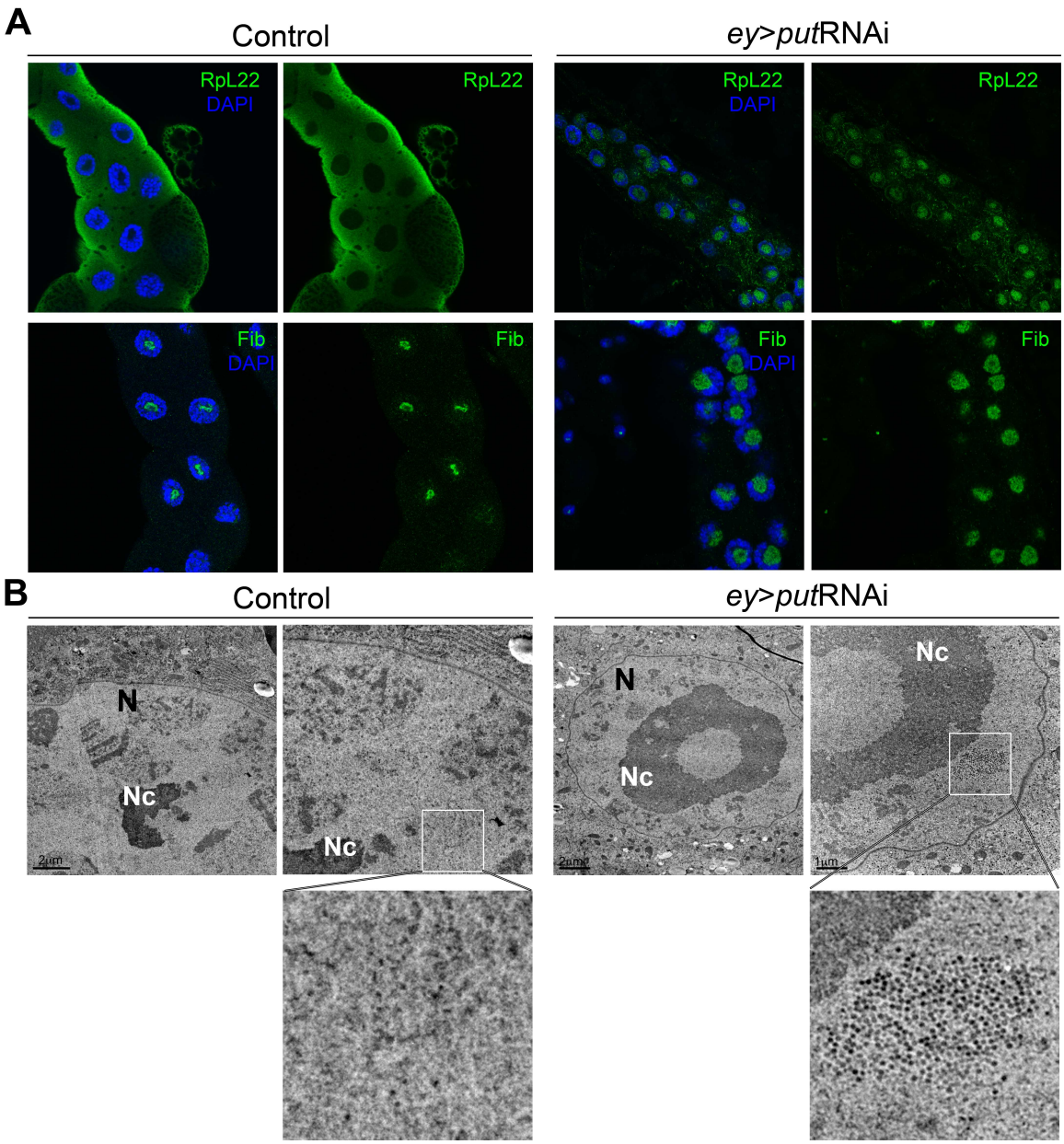

Figure 3.16 – Dpp signaling regulates nucleolar structure and its depletion results in abnormal accumulation of nucleolar proteins. (A) Images of control (*ey*-Gal4/UAS-*lacZ*) and *put*RNAi (*ey*-Gal4/*put*RNAi2) salivary glands stained for the ribosomal protein RpL22 (top row) and Fibrillarin (bottom row). RpL22, which is mainly detected in the cytoplasm of control cells, becomes accumulated at the nucleolus after Put depletion. Similarly, Fibrillarin accumulates strongly at the nucleolus in *put*RNAi cells. **(B)** Transmission electron micrographs of nuclear regions of the salivary gland cells and the corresponding magnifications are shown. Insets show magnifications of the nucleoplasm where pre-ribosomes accumulate in *put*RNAi cells in contrast to controls. N, nucleus; Nc, nucleolus.

5. DISCUSSION

In this work we show the first in vivo double RNAi screen to study synthetic genetic interactions during *Drosophila* development, providing evidence that targeted screens for the analysis of genetic interactions can be done in vivo, and are capable of detecting weak and strong interactions.

The first step of our screen for *vito* interactors allowed us to identify 15 genes

knockdowns, among the 148 *ey*-targets tested, in which the single RNAi caused a visible eye phenotype with the *ey*-Gal4 driver. It would be interesting to validate whether these genes are direct *ey*-targets, and consequently what is their role in eye development, as among them are several genes with unknown functions. Our in vivo double RNAi screen to identify genes and pathways working with the nucleolar regulator Vito during eye development culminated with the identification of 12 interactor genes. As 11 out of the 12 Vito interactor genes found in the screen were involved in nervous system development it is likely that *vito* despite being required for tissue growth during early eye development, might regulate differentiation events in the eye. Accordingly, we have identified a genetic interaction of *vito* with the TGF-β signaling pathway, particularly strong with the Dpp signaling pathway receptors *tkv* and *put* and the Co-Smad *med*. Interactions with genes belonging to other signaling pathways, such as Hh and Wg, were not identified, revealing the specificity of Vito/Dpp signaling interaction.

We demonstrate that Vito acts downstream of Dpp, having a dual role during eye development when Dpp signaling is compromised: Vito cooperates with Dpp in growth stimulation during early stages of eye disc development and also in latter stages during the process of eye disc patterning. Vito/Dpp interaction does not seem to be based on Vito's requirement for survival in the developing eye, as no increase in the number of apoptotic cells was detected when Vito was depleted together with the Dpp receptor *tkv*.

Our data is consistent with a role of Vito in positively regulating Dpp signaling as depletion of Vito partially reverts Dpp overexpression, the phenotype of depleting Vito in a Dpp weak RNAi background resembles a strong RNAi for a Dpp pathway component, and overexpression of Vito can have the opposite role and partially compensate for a reduction in Dpp activity. As the clone size for cells simultaneously expressing a constitutively active form of the Dpp type I receptor Tkv and *vito*RNAi is reduced towards wild-type size while maintaining the regulation of the Dpp eye targets *eya* and *hth*, it is possible that Vito is acting in a branch downstream of *tkv* contributing to the activation by Dpp of unknown targets involved in cell growth and proliferation.

Moreover, *vito*RNAi eye discs show a delay in MF progression and an irregular activation of p-Mad within the furrow. Consistent with these results is the fact that early in development we can already detect a spread activation of Dpp in eye discs, which can affect MF initiation and consequently progression. We also show that, in Vito depleted eye discs, low levels of Tkv are detected in the MF and adjacent regions. Whether Vito regulates Dpp expression directly, or by regulation of Tkv levels remains unanswered, however it is clear that Vito is required for a controlled Dpp signaling thereby allow

normal organ development. Interestingly, Vito/Dpp interaction appears restricted to the eye, as Vito does not modulate the wing growth and patterning defects induced by Dpp loss-of-function.

Finally and surprisingly we show that Dpp type II receptor Put regulates the nucleolar structure and function. Put is the shared type II receptor for both branches of TGF-β signaling pathway: Activin and Dpp. The recent demonstration that the novel role for dSmad2 on wing disc growth requires Mad might indicate that both branches of the TGF-β signaling pathway could cooperate and be dependent on one another (Sander et al., 2010). Consequently, it would be important to determine the exact contribution of each branch for regulation of nucleolar functions, as both branches were shown to regulate growth (Spencer et al., 1982; Zecca et al., 1995; Lecuit et al., 1996; Nellen et al., 1996; Brummel et al., 1999).

In conclusion, although our genetic data do not reveal the molecular mechanism for Vito/Dpp interaction, it suggests a potential molecular mechanism of growth control in which Vito can regulate Dpp signaling by controlling nucleolar RNA processing events during development.

6. REFERENCES

Amore, G. and Casares, F. (2010). Size matters: the contribution of cell proliferation to the progression of the specification Drosophila eye gene regulatory network. *Developmental Biology* 344(2): 569-77.

Bakal, C., Linding, R., Llense, F., Heffern, E., Martin-Blanco, E., Pawson, T. and Perrimon, N. (2008). Phosphorylation networks regulating JNK activity in diverse genetic backgrounds. *Science* 322(5900): 453-6.

Baryshnikova, A., Costanzo, M., Kim, Y., Ding, H., Koh, J., Toufighi, K., Youn, J.-Y., Ou, J., San Luis, B.-J., Bandyopadhyay, S. et al. (2010). Quantitative analysis of fitness and genetic interactions in yeast on a genome scale. *Nat Meth* 7(12): 1017-1024.

Bessa, J. and Casares, F. (2005). Restricted teashirt expression confers eye-specific responsiveness to Dpp and Wg signals during eye specification in Drosophila. *Development* 132(22): 5011-20.

Bessa, J., Gebelein, B., Pichaud, F., Casares, F. and Mann, R. S. (2002). Combinatorial control of Drosophila eye development by eyeless, homothorax, and teashirt. *Genes & Development* 16(18): 2415-27.

Blackman, R. K., Sanicola, M., Raftery, L. A., Gillevet, T. and Gelbart, W. M. (1991). An extensive 3' cis-regulatory region directs the imaginal disk expression of decapentaplegic, a member of the TGF-beta family in Drosophila. *Development* 111(3): 657-66.

Brummel, T., Abdollah, S., Haerry, T. E., Shimell, M. J., Merriam, J., Raftery, L., Wrana, J. L. and O'Connor, M. B. (1999). The Drosophila activin receptor baboon signals through dSmad2 and controls cell proliferation but not patterning during larval development. *Genes & Development* 13(1): 98-111.

Burke, R. and Basler, K. (1996). Dpp receptors are autonomously required for cell proliferation in the entire developing Drosophila wing. *Development* 122(7): 2261-9.

Casares, F. and Mann, R. S. (1998). Control of antennal versus leg development in Drosophila. *Nature* 392(6677): 723-6.

Chanut, F. and Heberlein, U. (1997a). Retinal morphogenesis in Drosophila: hints from an eye-specific decapentaplegic allele. *Dev Genet* 20(3): 197-207.

Chanut, F. and Heberlein, U. (1997b). Role of decapentaplegic in initiation and progression of the morphogenetic furrow in the developing Drosophila retina. *Development* 124(2): 559-67.

Chen, R., Halder, G., Zhang, Z. and Mardon, G. (1999). Signaling by the TGF-beta homolog decapentaplegic functions reiteratively within the network of genes controlling retinal cell fate determination in Drosophila. *Development* 126(5): 935-43.

Costanzo, M., Baryshnikova, A., Myers, C. L., Andrews, B. and Boone, C. (2011). Charting the genetic interaction map of a cell. *Current Opinion in Biotechnology* 22(1): 66-74.

Cruz, C., Glavic, A., Casado, M. and De Celis, J. F. (2009). A Gain-of-Function Screen Identifying Genes Required for Growth and Pattern Formation of the Drosophila melanogaster Wing. *Genetics* 183(3): 1005-1026.

Curtiss, J. and Mlodzik, M. (2000). Morphogenetic furrow initiation and progression during eye development in Drosophila: the roles of decapentaplegic, hedgehog and eyes absent. *Development* 127(6): 1325-36.

Dietzl, G., Chen, D., Schnorrer, F., Su, K.-C., Barinova, Y., Fellner, M., Gasser, B., Kinsey, K., Oppel, S., Scheiblauer, S. et al. (2007). A genome-wide transgenic RNAi library for conditional gene inactivation in Drosophila. *Nature* 448(7150): 151-6.

Dixon, S. J., Costanzo, M., Baryshnikova, A., Andrews, B. and Boone, C. (2009). Systematic Mapping of Genetic Interaction Networks. *Annu. Rev. Genet.* 43(1): 601-625.

Friedman, A. and Perrimon, N. (2006). High-throughput approaches to dissecting MAPK signaling pathways. *Methods* 40(3): 262-71.

Horn, T., Sandmann, T., Fischer, B., Axelsson, E., Huber, W. and Boutros, M. (2011). Mapping of signaling networks through synthetic genetic interaction analysis by RNAi. *Nat Meth* 8(4): 341-6.

Jonikas, M. C., Collins, S. R., Denic, V., Oh, E., Quan, E. M., Schmid, V., Weibezahn, J., Schwappach, B., Walter, P., Weissman, J. S. et al. (2009). Comprehensive characterization of genes required for protein folding in the endoplasmic reticulum. *Science* 323(5922): 1693-7.

Kango-Singh, M., Singh, A. and Henry Sun, Y. (2003). Eyeless collaborates with Hedgehog and Decapentaplegic signaling in Drosophila eye induction. *Developmental Biology* 256(1): 49-60.

Kumar, J. P. (2011). My what big eyes you have: How the Drosophila retina grows. *Devel Neurobio*: n/a-n/a.

Lecuit, T., Brook, W. J., Ng, M., Calleja, M., Sun, H. and Cohen, S. M. (1996). Two distinct mechanisms for long-range patterning by Decapentaplegic in the Drosophila wing. *Nature* 381(6581): 387-93.

Lecuit, T. and Cohen, S. M. (1998). Dpp receptor levels contribute to shaping the Dpp morphogen gradient in the Drosophila wing imaginal disc. *Development* 125(24): 4901-7.

Mani, R., St Onge, R. P., Hartman, J. L., Giaever, G. and Roth, F. P. (2008). Defining genetic interaction. *Proc Natl Acad Sci USA* 105(9): 3461-6.

Mao, Y. and Freeman, M. (2009). Fasciclin 2, the Drosophila orthologue of neural cell-adhesion molecule, inhibits EGF receptor signalling. *Development* 136(3): 473-481.

Marinho, J., Casares, F. and Pereira, P. S. (2011). The Drosophila Nol12 homologue viriato is a dMyc target that regulates nucleolar architecture and is required for dMyc-stimulated cell growth. *Development* 138(2): 349-357.

Mohr, S., Bakal, C. and Perrimon, N. (2010). Genomic Screening with RNAi: Results and Challenges. *Annu. Rev. Biochem.* 79(1): 37-64.

Murali, T., Pacifico, S., Yu, J., Guest, S., Roberts, G. G. and Finley, R. L. (2011). DroID 2011: a comprehensive, integrated resource for protein, transcription factor, RNA and gene interactions for Drosophila. *Nucleic Acids Research* 39(Database issue): D736-43.

Nellen, D., Burke, R., Struhl, G. and Basler, K. (1996). Direct and long-range action of a DPP morphogen gradient. *Cell* 85(3): 357-68.

Ostrin, E. J., Li, Y., Hoffman, K., Liu, J., Wang, K., Zhang, L., Mardon, G. and Chen, R. (2006). Genome-wide identification of direct targets of the Drosophila retinal determination protein Eyeless. *Genome Research* 16(4): 466-76.

Phillips, P. C. (2008). Epistasis — the essential role of gene interactions in the structure and evolution of genetic systems. *Nat Rev Genet* 9(11): 855-867.

Pignoni, F. and Zipursky, S. L. (1997). Induction of Drosophila eye development by decapentaplegic. *Development* 124(2): 271-8.

Prober, D. A. and Edgar, B. A. (2002). Interactions between Ras1, dMyc, and dPI3K signaling in the developing Drosophila wing. *Genes & Development* 16(17): 2286-99.

Ranade, S. S., Yang-Zhou, D., Kong, S. W., McDonald, E. C., Cook, T. A. and Pignoni, F. (2008). Analysis of the Otd-dependent transcriptome supports the evolutionary conservation of CRX/OTX/OTD functions in flies and vertebrates. *Dev Biol* 315(2): 521-34.

Sander, V., Eivers, E., Choi, R. H. and De Robertis, E. M. (2010). Drosophila Smad2 Opposes Mad Signaling during Wing Vein Development. *PLoS ONE* 5(4): e10383.

Spencer, F. A., Hoffmann, F. M. and Gelbart, W. M. (1982). Decapentaplegic: a gene complex affecting morphogenesis in Drosophila melanogaster. *Cell* 28(3): 451-61.

Wiersdorff, V., Lecuit, T., Cohen, S. M. and Mlodzik, M. (1996). Mad acts downstream of Dpp receptors, revealing a differential requirement for dpp signaling in initiation and propagation of morphogenesis in the Drosophila eye. *Development* 122(7): 2153-62.

Woodhouse, E. C., Fisher, A., Bandle, R. W., Bryant-Greenwood, B., Charboneau, L., Petricoin, E. F. and Liotta, L. A. (2003). Drosophila screening model for metastasis: Semaphorin 5c is required for l(2)gl cancer phenotype. *Proc Natl Acad Sci USA* 100(20): 11463-8.

Yuva-Aydemir, Y., Bauke, A.-C. and Klambt, C. (2011). Spinster Controls Dpp Signaling during Glial Migration in the Drosophila Eye. *Journal of Neuroscience* 31(19): 7005-7015.

Zecca, M., Basler, K. and Struhl, G. (1995). Sequential organizing activities of engrailed, hedgehog and decapentaplegic in the Drosophila wing. *Development* 121(8): 2265-78.

Zhang, B., Kirov, S. and Snoddy, J. (2005). WebGestalt: an integrated system for exploring gene sets in various biological contexts. *Nucleic Acids Research* 33(Web Server issue): W741-8.

CHAPTER 4

GENERAL DISCUSSION

CONTENTS

The main focus of this thesis was the identification and characterization of the function of a novel gene, the *Drosophila vito*, which was identified for the first time in an ongoing screen to search for novel gene functions required for proper tissue growth in the eye of *Drosophila*.

1. Vito's role in the nucleolus: structural and functional consequences of Vito misregulation

The results of this thesis show that the sole *Drosophila* member of the Nol12 family of proteins Vito is a nucleolar protein required for tissue growth. In fact we show that the human Nol12 can rescue the knockdown of *Drosophila* Vito, which denotes not only sequence similarity but also functional homology in this family of proteins. We further show that Vito regulates the nucleolar architecture and that altering Vito levels results in changes in the nucleolar localization patterns of the pre-rRNA methyltransferase Fibrillarin.

To date the only characterized Nol12 protein, in terms of molecular function, is the budding yeast Rrp17p/Nol12. The gene encoding Rrp17p had previously been found to be required for non-coding RNA processing (including rRNA and snoRNAs) (Peng et al., 2003) and during the course of this work was found to have 5'-3' exonuclease activity essential for ribosome biogenesis (Oeffinger et al., 2009). Similarly to our rescue results, the human Nol12 was also found to be able to rescue *S. cerevisae* mutants for Rrp17p/Nol12 (Oeffinger et al., 2009).

rRNA processing, a process essential for the biogenesis of ribosomes, follows a series of processing and modifying events that ensures the proper maturation of the ribosomes. There is some flexibility in the initial order of the processing events to generate the 18S rRNA, which reflects in the existence of two processing pathways. In one pathway, cleavage occurs first at site 1 in the ETS region to generate 18S rRNA, whether alternatively the first cleavage can occur within the ITS1 region (Fig. 4.1). The two processing pathways may vary among cell types, or can even exist within the same cell type (Winicov, 1976; Bowman et al., 1981; Hadjiolova et al., 1993), and the pathway choice seems to be influenced by U3 snoRNA (Borovjagin and Gerbi, 1999). In *Drosophila* the rRNA processing pathway has not been extensively characterized as in other species,

particularly in yeast (Venema and Tollervey, 1999; Gerbi and Borovjagin, 2004). There are two main differences between *Drosophila* and yeast rRNA processing cleavages: first, whether endonucleolytic cleavage occurs at site 3 and subsequent trimming by a 5'-exonuclease is required in *Drosophila* is unclear, moreover, whether there is a potential cleavage site within the ITS2 in *Drosophila* is also obscure (Fig. 4.1).

Our analysis of Vito's role in rRNA processing has revealed that upon Vito knockdown in developing tissues there is accumulation of atypical pre-RNA intermediates suggesting a role of Vito in rRNA processing. The budding yeast Nol12 homologue is required for efficient 5'-3' exonuclease digestion of the mature 5'ends of 5.8S and 25S rRNAs acting in conjunction with the already known 5'-3' exonucleases Rat1 and Xrn1 (Oeffinger et al., 2009).

The fact that in Vito mutants the alternative processing pathway is preferred and abnormal cleavages of intermediates b and c at site 6 are seen, support the hypothesis that Vito could be required for the exonucleolytic trimming from site 3 to 4 (Fig. 4.1).

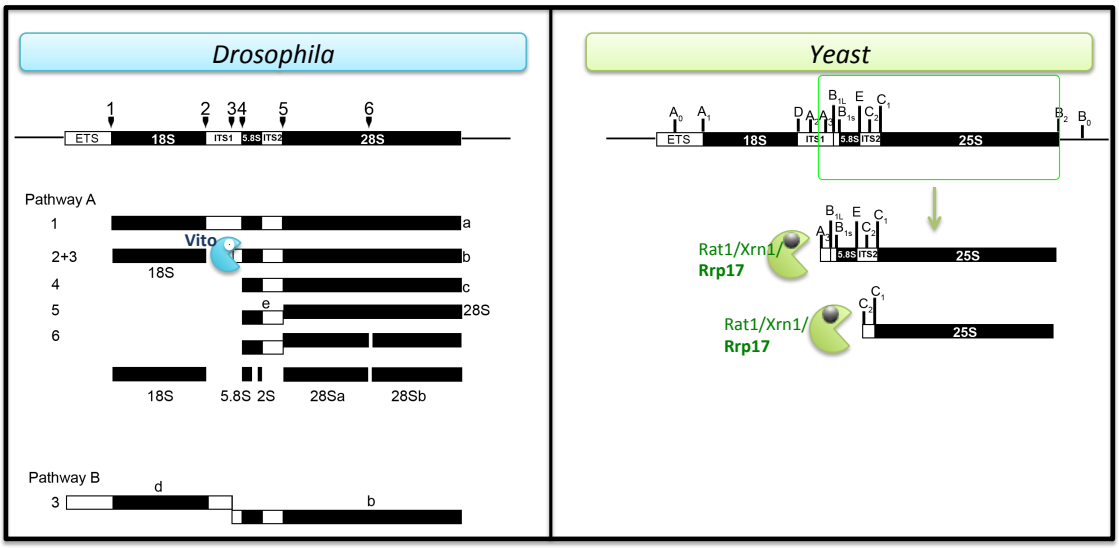

Figure 4.1 – A model for the function of Vito in rRNA processing. Pre-rRNA processing scheme in *Drosophila* (A) and yeast (B). **(A)** Schematic representation of the *Drosophila* pre-rRNA processing pathways A and B (adapted from(Long and Dawid, 1980). The top line shows the pre-rRNA; ETS and ITS are shown in white, the 18S, 5.8S, 2S and 28S subunits in black. Endonucleolytic cleavage sites are indicated by numbers (1–6). We propose a model in which after an endonucleolytic cleavage at site 3, Vito is required for the exonucleolytic trimming of the b fragment. **(B)** Pre-rRNA processing scheme in yeast. The top line shows the structure of the pre-rRNA; ETS and ITS are shown in white, the 18S, 5.8S and 25S subunits in black. The locations of processing sites on the 35S pre-rRNA are indicated. The 5' region of 5.8S and 25S fragments are exonucleolytically trimmed by the Rat1, Xrn1 and the Vito homologue Rrp17 5'–3' exonucleases. The pacmac represents the exonuclease function.

In addition to Vito, other genes were shown to be important for growth and were implicated in the regulation of rRNA processing events. Loss-of-function mutations in the

Drosophila pseudouridine synthase *Nop60B*/*minifly*, important to properly modify the rRNA, cause a strong body size reduction and affects organ size as it decreases both the size and number of cells in the wing imaginal disc (Giordano et al., 1999; Tortoriello et al., 2010). Additionally, Nop60 might also be involved in the regulation of developmental processes by the modulation of the Notch signaling pathway (Tortoriello et al., 2010). Moreover, conditional deletion of the mouse *dyskerin* gene, the mammalian homologue of the *Drosophila* Nop60B, blocks rRNA processing halting ribosome biogenesis and induces a reduction in cell proliferation in mouse hepatocytes (Ge et al., 2010). Another nucleolar protein, Nucleostemin (NS), was shown to be involved in the regulation of cell proliferation, inducing cell cycle arrest via the p53 pathway when misexpressed (Ma and Pederson, 2007). In addition, NS was also implicated in the maintenance of a correct nucleolar architecture and in the processing of pre-rRNA particularly affecting large ribosomal subunit biogenesis both in *Drosophila* and mammalian cells (Romanova et al., 2009a; Romanova et al., 2009b; Rosby et al., 2009). *Drosophila* has four members of the NS family, and NS2 that has nucleolar localization was recently demonstrated to be essential for early eye development and cell survival (Matsuo et al., 2010).

Our results also show an abnormal nucleolar accumulation of large ribosomal subunit proteins in cells depleted of Vito. Therefore, the role of Vito in rRNA processing could lead to defects in ribosome biogenesis, and be the basis for the defective growth and developmental delay observed in *vito* mutants. The ribosomal protein accumulation could be a consequence of the defects in the rRNA processing or might reflect problems with maturation or release of the ribosomal subunits from the nucleolus to the nucleoplasm, and perhaps in the eventual transport of these subunits from the nucleus to the cytoplasm. Resembling what is observed for Vito, depletion of the nucleolar *Drosophila* NS1 was shown to induce nucleolar accumulation of large ribosomal subunit proteins, which may also be a reflection of the role of the mammalian NS in the rRNA processing (Romanova et al., 2009a; Rosby et al., 2009).

The nucleolar retention of RpLs observed in our results could have further consequences in the nucleolar stress response. Nucleolar structural and functional changes have been linked directly to p53 activation in mammalian cells (reviewed in(Boulon et al., 2010). In this thesis we have shown that *vito* is required for cell survival and that apoptosis in *vito*RNAi eye discs was dependent on caspases, and on the function

of three crucial pro-apoptotic genes (*rpr*, *grim*, and *hid*). However, apoptosis in *vito*RNAi eye discs was observed to be p53-independent. Consequently, we postulated that a caspase-dependent but p53-independent apoptotic process could provide a potential novel link between structural and functional changes in the nucleolus and activation of the pro-apoptotic *rpr*/*grim*/*hid* complex. In addition, we can also suggest that as RpLs are trapped in the nucleolus in Vito depleted cells, the mechanism of MDM2 inhibition by ribosome-free forms of ribosomal proteins in the nucleoplasm would be ceased due to the lack of free ribosomal proteins at the nucleoplasm, explaining the absence of p53 activation in Vito depleted cells. Although MDM2 is not conserved in *Drosophila*, recently another E3 ubiquitin ligase targeting p53, TRIM24/Bonus, has been shown to be necessary to prevent p53-mediated apoptosis in *Drosophila* (Allton et al., 2009). Alternatively, p53 might not be important for the nucleolar stress response in *Drosophila*.

In addition, as reducing or increasing Vito levels induces changes in the localization pattern of some nucleolar proteins, we can speculate that Vito could act in the recruitment of second layer proteins in the nucleolus that require binding to nucleolar hub proteins in order to associate with the nucleolar compartment (Emmott and Hiscox, 2009). Therefore, a disassembly of the nucleolus induced by loss of Vito could be the cause for the induction of apoptosis.

Despite the fact that *vito* loss-of-function apoptosis was dependent on caspases, we were not able to address the upstream activating signal triggering apoptosis. Our results show that the absence of p53 function partially rescued eye disc size reduction induced by Vito depletion, and also show a minor apoptotic rescue after co-expression of a dominant negative form of JNK in Vito depleted eye discs. Therefore, an hypothesis is that both JNK and p53 might act in conjunction to induce apoptosis in Vito loss-of-function.

JNK and p53 were recently shown to act downstream of the initiator caspase Dronc (Shlevkov and Morata, 2011). This study further shows that JNK and p53 can activate each other, and that both are able to induce *rpr* and *hid*, being the latter capable of reciprocally induce JNK and p53 expression, in that way establishing a loop that amplifies the initial apoptotic stimuli (Shlevkov and Morata, 2011). Therefore we cannot rule out that apoptosis in *vito* loss-of-function could be dependent on an initial upstream

JNK and p53 signal, that is further amplified downstream and that's why independent knockdown of both pathways did not explain *vito* apoptotic phenotype.

In addition to Vito, other nucleolar proteins were shown to have roles beyond ribosome biogenesis, regulating developmental processes. The nucleolar phosphoprotein Nopp140 was shown to cause developmental wing defects such as missed wing margins and blister formation (Cui and DiMario, 2007), and the pseudouridine synthase NS affects wing morphogenesis in a similar way to the Notch signaling pathway (Tortoriello et al., 2010). Moreover, a new role for ribosomes in tissue patterning was recently unveiled. The ribosomal protein L38 was shown to regulate the translation of Hox mRNAs, inducing tissue-specific patterning defects without changing global protein synthesis when mutated in mice (Kondrashov et al., 2011). In addition, they show that RpL38 is not ubiquitously expressed and is particularly enriched in the developing tissues of the mice suggesting that ribosomal proteins play a critical role during embryonic development (Kondrashov et al., 2011).

Exonucleases are required for the processing of other non-coding RNAs besides rRNA, as showed for the yeast Rrp17p/Nol12 (Peng et al., 2003). snoRNA maturation involves the combined action of endo- and exonucleases (Filipowicz and Pogacić, 2002). snoRNAs guide rRNA modifications and can be required for rRNA cleavage itself: for instance rRNA cleavage at site 3 was shown to be dependent on several snoRNAs as U3, E3 and U8 snoRNAs (Peculis and Steitz, 1993; Mishra and Eliceiri, 1997; Borovjagin and Gerbi, 1999), therefore, although less likely, the defects in the pre-rRNA processing pathway seen after Vito misregulation cloud also be indirectly related to a deficient processing of snoRNAs. Additionally, the finding that several miRNAs localize to the nucleolus, either in their mature form, or in their precursor forms suggests a possible role of the nucleolus in their processing (Ritland Politz et al., 2009). Consequently a role of Vito in the biogenesis of regulatory non-coding RNAs, as snoRNAs or even miRNAs with nucleolar location is also likely. The potential role of Nol12 family members in miRNA biogenesis has not been addressed yet. Enlightenment of Vito's role in ribosome biogenesis could provide useful insight about this poorly characterized pathway in higher eukaryotes and Vito's role in the processing of miRNAs might clarify if any nucleolar role in pri-miRNA processing or modification is possible.

2. Vito's requirement for dMyc-stimulated growth

Our data identifies *vito* as an important regulator of dMyc function in the stimulation of nucleolar biogenesis and mass accumulation during *Drosophila* development. We show that *vito* is a novel transcriptional target of dMyc, and that *vito* is strongly required for the maintenance of a normal nucleolar structure during the process of nucleolar enlargement resulting from dMyc overexpression. Importantly, *vito* is functionally required for dMyc to reach its full potential as a potent cell growth inducer. Therefore, *vito* is a rate limiting factor for tissue growth that links dMyc with nucleolar architecture.

The nucleolus has been shown to be a key nuclear compartment mediating Myc functions in normal cells, as well as in cells overexpressing this transcription factor. dMyc was shown to be necessary and sufficient to induce a large number of Pol II-dependent ribosomal genes and pre-rRNA processing and modifying enzymes, and also to stimulate Pol III transcription (Grewal et al., 2005; Grewal et al., 2007; Pierce et al., 2008; Steiger et al., 2008; Li et al., 2010). Interestingly, the ability of dMyc to induce a coordinated nucleolar hypertrophy and to stimulate pre-rRNA transcription and ribosome biogenesis in general was found to be required for dMyc-stimulated growth (Grewal et al., 2005).

The fact that *vito* does not appear essential for the expression of dMyc targets implicated in ribosomal biogenesis suggests that part of the control that dMyc exerts on the nucleolus is mediated independently of its regulation of *vito* expression. In addition, several results support the hypothesis that the Myc-Nol12 regulatory relationship is evolutionarily conserved. Genome-wide chromatin immunoprecipitation analysis has shown that c-MYC binds the *NOL12* promoter in both a human transformed B-cell line (Zeller et al., 2006) and in mouse stem cells (Kim et al., 2008). We have also identified non-canonical E-box motifs (CACATG) (Zeller et al., 2006) in the putative proximal promoter regions of both *vito* and human *NOL12* (our analysis).

In addition to its role as a potent growth inducer in normal cells, Myc is also one of the most frequently activated oncogenes and is estimated to be involved in 20% of all human cancers (Dang et al., 2006). Ectopic expression of c-MYC in murine liver was found to induce cell and nucleolar enlargement by altering the expression of genes that increase protein synthesis in the absence of cell proliferation (Kim et al., 2000).

The hypothesis that a larger nucleoli, characteristic of transformed cells, could just reflect the higher proliferation rates of these cells has been discarded in the recent years since some data has been suggested an active role of ribosome biogenesis in tumorigenesis (Montanaro et al., 2008). Interestingly, recently the oncogenic activity of Myc in driving lymphomagenesis in the Eμ-Myc transgenic mice model was found to be suppressed if protein synthesis is restored down to normal levels by haploinsufficiency for the ribosomal protein RpL24 or RpL38, linking the capacity of Myc to induce tumorigenesis to its ability to regulate ribosome biogenesis (Barna et al., 2008).

As Vito might function in the processing of rRNA or other small non-coding RNAs, a potential molecular mechanism of growth control emerges, in which Myc, by regulating the expression levels of Vito in the nucleolus might adjust cellular and tissue growth rates by indirectly controlling non-coding RNA processing events during normal development or tumor growth. The mechanisms enacting this link might prove relevant for the regulation of Myc function in tumorigenesis (Meyer and Penn, 2008).

2.1 Myc-Nol12 protein family: implications in tumorigenesis

More than a century ago an hypertrophic and irregularly shaped nucleoli was noticed as characteristic of highly transformed cells (Pianese, 1896). Since then the evaluation of nucleolar size provides a diagnostic tool to determine the clinical outcome for cancer malignancy: the larger the nucleolar size, the poorer the tumor prognosis (Derenzini, 2000; Derenzini, 2009).

Prostate cancer cells are characterized by an increased nucleolar function like alterations in nucleolar size and/or architecture that were recently correlated with elevated rRNA levels (Uemura et al., 2011). Additionally, Myc overexpression in the mouse prostate induces Prostatic Intraepithelial Neoplasia (PIN), which is characterized by the enlargement of the nucleus, nucleolus and changes in chromatin structure (Iwata et al., 2010). Interestingly, Iwata's *et al*. study shows that accumulation of Myc protein is sufficient to transform prostate luminal epithelial cells into PIN cells, providing evidence that nucleolar alterations can be the consequence of neoplastic transformation, and placing this subnuclear compartment with a key role in cancer (Iwata et al., 2010).

Recently an anticancer drug targeting the nucleolar activity, more precisely an inhibitor of rRNA biogenesis, reached clinical trials (Drygin et al., 2009). CX-

3543/Quarfloxin is currently under evaluation against carcinoid/neuroendocrine tumours in a phase II clinical trial (Cylene Pharmaceuticals). This small molecule fluoroquinolone derivative targets and disrupts nucleolin/rDNA G-quadruplex complexes: four-stranded DNA structures consisting of two or more G-tetrads (a G-tetrad is made up of four hydrogen-bonded guanines in a planar arrangement) (Drygin et al., 2009). Curiously, these G-quadruplexes can also be formed in a particular guanine-rich region of the *c-myc* promoter called the nuclease hypersensitive element, which accounts for 90% of the total *c-myc* transcription (Davis et al., 1989). Therefore a potential novel therapy for tumors where *c-myc* is amplified emerges (reviewed in(Brooks and Hurley, 2010; Lin et al., 2010). It was shown that the disruption of G-quadruplexes by Quarfloxin results in a redistribution of the nucleolin into the nucleoplasm (Drygin et al., 2009), where it binds to the Myc G-quadruplexes reducing *c-myc* mRNA (González et al., 2009).

As our data shows that *vito* is a dMyc transcriptional target, and due to the conservation shown for the Nol12 protein family in terms of molecular functions, we hypothesize that Vito/Nol12 could be important downstream of Myc in the control of the nucleolar enlargement in the process of tumorigenesis. Therefore it would be important to determine whether Nol12 levels change in Myc-induced tumors.

The role of the nucleolar protein Vito in the regulation of the nucleolar structure and functions, together with the increasing role of the nucleolus in tumorigenesis prompted us to investigate whether Vito/Nol12 could have a broader function and be linked to cancer. Consequently, we took advantage of a cancer microarray database and web-based data-mining platform, Oncomine, to determine whether the human Nol12 expression was altered in tumor tissues (http://www.oncomine.org). Oncomine provides information about differentially expressed mRNAs in normal *versus* cancer tissues making available all public cancer microarrays in just one platform. By analyzing the human Nol12 gene information in Oncomine we got interesting results: Nol12 is downregulated in Head-neck squamous cell carcinoma in two independent studies, and upregulated in Superficial Bladder Cancer (Fig. 4.2). Additionally, a preliminary analysis done by our group detected relatively lower Nol12 protein levels in three human gastric cancer cell lines: NCI-N87, GP202 and IPA220 (unpublished data).

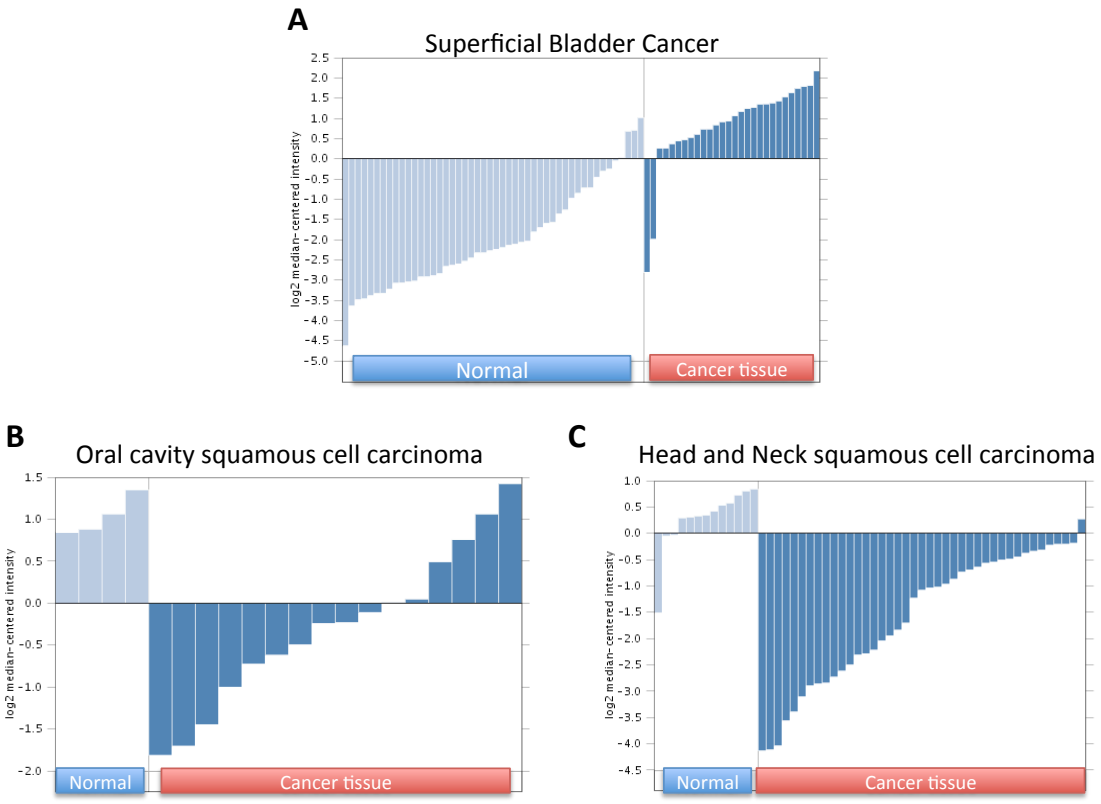

Figure 4.2 – Differential expression of the human Nol12 mRNA between normal *versus* tumor tissues. Using the Oncomine database (www.oncomine.org), we found deregulation of Nol12 mRNA expression in different tumors. Each bar represents one sample tissue. **(A)** Nol12 mRNA expression in 48 normal samples was compared to 28 Superficial Bladder Cancer tissues and found upregulated (fold change= 7.099 *P* value=7.8X10^{-16}). **(B,C)** In contrast, Nol12 was downregulated in two independent studies of Head and Neck carcinomas. (B) 4 normal sample tissues were compared to 16 oral cavity squamous cell carcinomas and Nol12 was downregulated (fold change=-2.496 *P* value=4.28X10^{-5}). (C) 13 normal samples were compared to 41 samples from Head and Neck squamous cell carcinoma and Nol12 was found downregulated (fold change=-3.663 *P* value=2.7X10^{-9}).

Therefore, in the future, it would be interesting to determine if these cell lines and tissues with deregulated Nol12 levels show nucleolar alterations, and determine whether this correlates with alterations in Myc expression.

3. Vito, TGF-β signaling pathway and the nucleolus: are they partners?

In this thesis we performed, to our knowledge, the first in vivo double RNAi screen to study synthetic genetic interactions during *Drosophila* development. Taking advantage of Ostrin's list of 188 potential *ey*-targets we were able to identify, not only Vito partners during eye development, but also to determine new downstream targets of the transcriptional factor *ey*. Future studies could contribute to a better understanding of the molecular, cellular and developmental mechanisms regulated by *ey* to establish a normal

eye and functionally characterize some of these genes with unknown functions in the context of a multicellular organism development.

Our search for Vito interactors culminated with the identification of a particularly strong interaction between Vito and the TGF-β signaling pathway. We have already demonstrated that *vito* was required for tissue growth particularly during early stages of eye disc development. However, with this screen, we were able to show that besides cooperating with Dpp signaling in the promotion of early eye disc growth, a novel role of Vito in the regulation of photoreceptor differentiation together with Dpp signaling pathway was unveiled. Further characterization revealed that *vito* acts downstream of Dpp and its receptor *tkv*, positively regulating Dpp signaling activation by an yet unknown mechanism.

dpp is required to maintain its own expression along the eye disc margins with the progression of retinal differentiation (Chanut and Heberlein, 1997b) and was shown to negatively regulate *tkv* expression (Lecuit and Cohen, 1998). We observe that loss of Vito affects Dpp signaling activation, and is accompanied by an increase in *dpp* transcription and downregulation of Tkv levels anteriorly to the MF in the eye disc. At the moment it is difficult to determine whether *vito* regulates Tkv levels and by doing so affects Dpp signal activation, or if the results observed are a consequence of a role of *vito* in the regulation of Dpp signal activation in a downstream branch of Tkv by an unknown mechanism.

Of particular importance for our study would be to analyze whether the regulation of the Dpp signaling by Vito is extensive to the Activin branch of the TGF-β signaling pathway. In higher eukaryotes the TGF-β signaling pathway in addition to TGF-βs, includes the BMPs, growth and differentiation factors (GDFs), Activins and nodal. TGF-β/activin pathways signal via Smad2 and Smad3, and BMP/GDF pathways via Smad1, Smad5 and Smad8. Recently, several studies demonstrated that in a diversity of cellular contexts TGF-β signaling could also activate Smad1 and Smad5, showing that switches of Smad proteins among branches of the pathway can happen (reviewed in(Moustakas and Heldin, 2009). The fact that specific cellular and developmental contexts might need the inter-regulation between branches of the TGF-β signaling pathway was recently shown during *Drosophila* wing patterning, where dSmad2 opposes Dpp/Mad signaling (Sander et al., 2010). Therefore, as we showed a significant genetic interaction between Vito and members of the Activin pathway Babo and Smad2, and because both members were

shown to influence growth and proliferation in the developing eye and to be highly expressed anteriorly in the eye imaginal disc (Brummel et al., 1999), it would be crucial to determine whether Vito might also regulate Activin signaling, or if any cooperation between Dpp and Activin exists during eye development.

Besides the traditional role as the ribosome factory, the nucleolus is now also considered to be a multi-functional regulatory compartment involved in RNA processing events, sensing of cell stress, and cell cycle and apoptosis regulation that possibly result from the multifunctionality of the nucleolar proteins (Boisvert et al., 2007).

The surprising involvement of TGF-β signaling with the nucleolus is a real breakthrough and can unveil a novel function for the pathway, or increase the non-traditional functions of this subnuclear compartment. Our study shows that knocking down the TGF-β type II receptor Put induces profound changes in the structure of the nucleolus and the nucleolar retention of ribosomal proteins. However these observations are preliminary and further studies are needed. Firstly, the nucleolar results were obtained using an RNAi against the type II receptor Put, which is shared by both branches of the TGF-β signaling pathway, Dpp and Activin, therefore it is important to determine whether the regulation of the nucleolus is exclusive for one or common for both branches of the pathway. Secondly, as we strongly expect that nucleolar structure alterations will correlate with functional consequences it would be important to characterize the molecular alterations induced by deregulation of TGF-β signaling in the processes that take place in the nucleolus, like the biogenesis of small non-coding RNAs. Accordingly, it was recently shown in human cells that upon TGF-β or BMP4 stimulation, the R-Smads Smad1 and Smad5 relocalize from the cytoplasm to the nucleus, where they bind to the pri-microRNAs enhancing its processing to mature miRNAs (Davis et al., 2008; Davis et al., 2011).

We have previously shown in this thesis that Vito regulates the processing of rRNAs in the nucleolus, and we consider that it might be involved in the regulation of other non-coding RNAs. The role of miRNAs in controlling target gene expression at the post-transcriptional level contributes to animal developmental complexity; as for example the miRNA bantam that similarly to *vito* controls growth and apoptosis in a patterned manner during eye disc development (Brennecke et al., 2003; Peng et al., 2009). We can

speculate that *vito* might cooperate with TGF-β in the processing of non-coding RNAs, as miRNAs, important to regulate growth and survival.

Looking to our screen results, a curious observation was that among the Vito interactors, 6 out of 12 proteins localize to the cytoplasmic membrane. Thus, one can ask how a nucleolar localized protein as Vito acts to regulate membrane events. Interesting but poorly explored is the involvement of the nucleolus in the signal recognition particle (SRP) assembly, as SRP RNA was found to traffic into the nucleolus transiently (Jacobson and Pederson, 1998; Pederson, 1998; Politz et al., 2000; Sommerville et al., 2005). The SRP is a ribonucleoprotein that arrests the translational elongation of nascent secretory and membrane proteins controlling the translation and intracellular sorting of membrane and secreted proteins. As SRP components traffic through the nucleolus, we can hypothesize that upon RNAi for Vito nucleolar disassemble might compromise the secretory pathway and therefore directly affect membrane proteins, or that Vito could be directly involved on SRP assembly in the nucleolus.

3.1 Vito/Nol12 and TGF-β: broader implications

TGF-β is known to induce fibrotic diseases and desmoplasia, characterized by the formation of excess connective tissue in an organ or tissue in a reparative process after an injury (reviewed in(Leask and Abraham, 2004). The desmoplastic reaction is characteristic of several human tumors, moreover little is known about the mechanisms that induce these diseases and no effective treatment exists (Löhr et al., 2001). The understanding of the normal tissue repair, where TGF-β plays a role, could provide insight on the mechanism of fibrotic diseases. Additionally, the expression of TGF-β1 was demonstrated to be able to induce carcinoma-associated fibroblasts (that promote tumor progression of pre-neoplastic epithelial cells) from normal human fibroblasts (San Francisco et al., 2004). Although it is clear the role of TGF-β signaling pathway in the promotion of growth in *Drosophila*, in vertebrates TGF-β inhibits epithelial cell proliferation while it promotes proliferation of fibroblasts in wound healing processes, where it produces extracellular matrix and induces a fibrotic response by a poorly understand mechanism (Leask and Abraham, 2004). Recently, the discovery that TGF-β activates TOR complexes in fibroblasts opened a new prospect for fibrotic diseases, as several clinically approved drugs targeting TOR complexes are already available (Rahimi et

al., 2009). TOR signaling is an essential regulator of cell and tissue growth that adjust protein biosynthesis by regulating several components of the translation initiation and elongation pathway, as well as ribosome biogenesis, in particular Pol I-dependent rRNA synthesis (reviewed in(Hietakangas and Cohen, 2009).

The results of this thesis provide evidence that Vito cooperates with TGF-β in growth control. Although we could not provide the molecular mechanism by which Vito and TFG-β interact, we can speculate that TGF-β control of fibroblast proliferation in desmoplasmic reactions could be mediated by Vito/Nol12, as we already discussed the deregulation of Vito mRNA levels in several human tumors. Therefore, it would be interesting to test whether TGF-β regulation of fibroblast proliferation is achieved by indirectly controlling protein synthesis and ribosome biogenesis via TOR, and if Vito/Nol12 might also play a role downstream of TGF-β.

In summary this thesis advanced our understanding on the regulation of cell and tissue growth in the context of animal development, particularly in the knowledge of how a novel nucleolar protein, Vito, functions to regulate growth and survival in a context-dependent fashion during *Drosophila* development. The fact that the processes we studied in the thesis are general during organ development, and taking into consideration the sequence conservation in the Vito/Nol12 protein family members from insects to mammals, we expect our results to be of general relevance, and hope that future work contribute to a better understanding of Vito functions during normal animal development and tumor formation.

4. References

Allton, K., Jain, A. K., Herz, H.-M., Tsai, W.-W., Jung, S. Y., Qin, J., Bergmann, A., Johnson, R. L. and Barton, M. C. (2009). Trim24 targets endogenous p53 for degradation. *Proc Natl Acad Sci USA* 106(28): 11612-6.

Barna, M., Pusic, A., Zollo, O., Costa, M., Kondrashov, N., Rego, E., Rao, P. H. and Ruggero, D. (2008). Suppression of Myc oncogenic activity by ribosomal protein haploinsufficiency. *Nature* 456(7224): 971-5.

Boisvert, F.-M., Van Koningsbruggen, S., Navascués, J. and Lamond, A. I. (2007). The multifunctional nucleolus. *Nat Rev Mol Cell Biol* 8(7): 574-85.

Borovjagin, A. V. and Gerbi, S. A. (1999). U3 small nucleolar RNA is essential for cleavage at sites 1, 2 and 3 in pre-rRNA and determines which rRNA processing pathway is taken in Xenopus oocytes. *J Mol Biol* 286(5): 1347-63.

Boulon, S., Westman, B. J., Hutten, S., Boisvert, F.-M. and Lamond, A. I. (2010). The nucleolus under stress. *Molecular Cell* 40(2): 216-27.

Bowman, L. H., Rabin, B. and Schlessinger, D. (1981). Multiple ribosomal RNA cleavage pathways in mammalian cells. *Nucleic Acids Res* 9(19): 4951-66.

Brennecke, J., Hipfner, D. R., Stark, A., Russell, R. B. and Cohen, S. M. (2003). bantam encodes a developmentally regulated microRNA that controls cell proliferation and regulates the proapoptotic gene hid in Drosophila. *Cell* 113(1): 25-36.

Brooks, T. A. and Hurley, L. H. (2010). Targeting MYC Expression through G-Quadruplexes. *Genes & Cancer* 1(6): 641-649.

Brummel, T., Abdollah, S., Haerry, T. E., Shimell, M. J., Merriam, J., Raftery, L., Wrana, J. L. and O'Connor, M. B. (1999). The Drosophila activin receptor baboon signals through dSmad2 and controls cell proliferation but not patterning during larval development. *Genes & Development* 13(1): 98-111.

Cui, Z. and DiMario, P. J. (2007). RNAi knockdown of Nopp140 induces Minute-like phenotypes in Drosophila. *Mol Biol Cell* 18(6): 2179-91.

Dang, C. V., O'Donnell, K. A., Zeller, K. I., Nguyen, T., Osthus, R. C. and Li, F. (2006). The c-Myc target gene network. *Semin Cancer Biol* 16(4): 253-64.

Davis, B. N., Hilyard, A. C., Lagna, G. and Hata, A. (2008). SMAD proteins control DROSHA-mediated microRNA maturation. *Nature* 454(7200): 56-61.

Davis, B. N., Hilyard, A. C., Nguyen, P. H., Lagna, G. and Hata, A. (2011). Smad Proteins Bind a Conserved RNA Sequence to Promote MicroRNA Maturation by Drosha. *Molecular Cell* 39(3): 373-384.

Davis, T. L., Firulli, A. B. and Kinniburgh, A. J. (1989). Ribonucleoprotein and protein factors bind to an H-DNA-forming c-myc DNA element: possible regulators of the c-myc gene. *Proc Natl Acad Sci USA* 86(24): 9682-6.

Derenzini, M. e. a. (2000). Nucleolar size indicates the rapidity of cell proliferation in cancer tissues. *Journal of pathology*: 1-6.

Derenzini, M. e. a. (2009). What the nucleolus says to a tumour pathologist.

Drygin, D., Siddiqui-Jain, A., O'Brien, S., Schwaebe, M., Lin, A., Bliesath, J., Ho, C. B., Proffitt, C., Trent, K., Whitten, J. P. et al. (2009). Anticancer activity of CX-3543: a direct inhibitor of rRNA biogenesis. *Cancer Research* 69(19): 7653-61.

Emmott, E. and Hiscox, J. A. (2009). Nucleolar targeting: the hub of the matter. *EMBO Rep* 10(3): 231-8.

Filipowicz, W. and Pogacić, V. (2002). Biogenesis of small nucleolar ribonucleoproteins. *Current Opinion in Cell Biology* 14(3): 319-27.

Ge, J., Rudnick, D. A., He, J., Crimmins, D. L., Ladenson, J. H., Bessler, M. and Mason, P. J. (2010). Dyskerin ablation in mouse liver inhibits rRNA processing and cell division. *Molecular and Cellular Biology* 30(2): 413-22.

Gerbi, S. A. and Borovjagin, A. V. (2004). Pre-ribosomal RNA processing in multicellular organisms. in M. O. J. Olson (ed.) *The Nucleolus*: Kluwer Academic/Plenum Publishers.

Giordano, E., Peluso, I., Senger, S. and Furia, M. (1999). minifly, a Drosophila gene required for ribosome biogenesis. *The Journal of Cell Biology* 144(6): 1123-33.

González, V., Guo, K., Hurley, L. and Sun, D. (2009). Identification and characterization of nucleolin as a c-myc G-quadruplex-binding protein. *J Biol Chem* 284(35): 23622-35.

Grewal, S. S., Evans, J. R. and Edgar, B. A. (2007). Drosophila TIF-IA is required for ribosome synthesis and cell growth and is regulated by the TOR pathway. *The Journal of Cell Biology* 179(6): 1105-13.

Grewal, S. S., Li, L., Orian, A., Eisenman, R. N. and Edgar, B. A. (2005). Myc-dependent regulation of ribosomal RNA synthesis during Drosophila development. *Nat Cell Biol* 7(3): 295-302.

Hadjiolova, K. V., Nicoloso, M., Mazan, S., Hadjiolov, A. A. and Bachellerie, J. P. (1993). Alternative pre-rRNA processing pathways in human cells and their alteration by cycloheximide inhibition of protein synthesis. *Eur J Biochem* 212(1): 211-5.

Hietakangas, V. and Cohen, S. M. (2009). Regulation of tissue growth through nutrient sensing. *Annu. Rev. Genet.* 43: 389-410.

Iwata, T., Schultz, D., Hicks, J., Hubbard, G. K., Mutton, L. N., Lotan, T. L., Bethel, C., Lotz, M. T., Yegnasubramanian, S., Nelson, W. G. et al. (2010). MYC overexpression induces prostatic intraepithelial neoplasia and loss of Nkx3.1 in mouse luminal epithelial cells. *PLoS ONE* 5(2): e9427.

Jacobson, M. R. and Pederson, T. (1998). Localization of signal recognition particle RNA in the nucleolus of mammalian cells. *Proc Natl Acad Sci USA* 95(14): 7981-6.

Kim, J., Chu, J., Shen, X., Wang, J. and Orkin, S. H. (2008). An extended transcriptional network for pluripotency of embryonic stem cells. *Cell* 132(6): 1049-61.

Kim, S., Li, Q., Dang, C. V. and Lee, L. A. (2000). Induction of ribosomal genes and hepatocyte hypertrophy by adenovirus-mediated expression of c-Myc in vivo. *Proc Natl Acad Sci USA* 97(21): 11198-202.

Kondrashov, N., Pusic, A., Stumpf, C. R., Shimizu, K., Hsieh, Andrew C., Xue, S., Ishijima, J., Shiroishi, T. and Barna, M. (2011). Ribosome-Mediated Specificity in Hox mRNA Translation and Vertebrate Tissue Patterning. *Cell* 145(3): 383-397.

Leask, A. and Abraham, D. J. (2004). TGF-beta signaling and the fibrotic response. *FASEB J* 18(7): 816-27.

Li, L., Edgar, B. A. and Grewal, S. S. (2010). Nutritional control of gene expression in Drosophila larvae via TOR, Myc and a novel cis-regulatory element. *BMC Cell Biol* 11: 7.

Lin, C.-P., Liu, C.-R., Lee, C.-N., Chan, T.-S. and Liu, H. E. (2010). Targeting c-Myc as a novel approach for hepatocellular carcinoma. *World J Hepatol* 2(1): 16-20.

Löhr, M., Schmidt, C., Ringel, J., Kluth, M., Müller, P., Nizze, H. and Jesnowski, R. (2001). Transforming growth factor-beta1 induces desmoplasia in an experimental model of human pancreatic carcinoma. *Cancer Research* 61(2): 550-5.

Long, E. O. and Dawid, I. B. (1980). Alternative pathways in the processing of ribosomal RNA precursor in Drosophila melanogaster. *J Mol Biol* 138(4): 873-8.

Ma, H. and Pederson, T. (2007). Depletion of the nucleolar protein nucleostemin causes G1 cell cycle arrest via the p53 pathway. *Mol Biol Cell* 18(7): 2630-5.

Matsuo, E., Kanno, S., Matsumoto, S. and Tsuneizumi, K. (2010). Drosophila Nucleostemin 2 Proved Essential for Early Eye Development and Cell Survival. *Biosci. Biotechnol. Biochem.* 74(10): 2120-2123.

Meyer, N. and Penn, L. Z. (2008). Reflecting on 25 years with MYC. *Nat Rev Cancer* 8(12): 976-90.

Mishra, R. K. and Eliceiri, G. L. (1997). Three small nucleolar RNAs that are involved in ribosomal RNA precursor processing. *Proc Natl Acad Sci USA* 94(10): 4972-7.

Montanaro, L., Treré, D. and Derenzini, M. (2008). Nucleolus, ribosomes, and cancer. *American Journal Of Pathology* 173(2): 301-10.

Moustakas, A. and Heldin, C.-H. (2009). The regulation of TGFbeta signal transduction. *Development* 136(22): 3699-714.

Oeffinger, M., Zenklusen, D., Ferguson, A., Wei, K. E., El Hage, A., Tollervey, D., Chait, B. T., Singer, R. H. and Rout, M. P. (2009). Rrp17p Is a Eukaryotic Exonuclease Required for 5' End Processing of Pre-60S Ribosomal RNA. *Molecular Cell* 36(5): 768-781.

Peculis, B. A. and Steitz, J. A. (1993). Disruption of U8 nucleolar snRNA inhibits 5.8S and 28S rRNA processing in the Xenopus oocyte. *Cell* 73(6): 1233-1245.

Pederson, T. (1998). The plurifunctional nucleolus. *Nucleic Acids Res* 26(17): 3871-6.

Peng, H., Slattery, M. and Mann, R. (2009). Transcription factor choice in the Hippo signaling pathway: homothorax and yorkie regulation of the microRNA bantam in the progenitor domain of the Drosophila eye imaginal disc. *Genes & Development*.

Peng, W. T., Robinson, M. D., Mnaimneh, S., Krogan, N. J., Cagney, G., Morris, Q., Davierwala, A. P., Grigull, J., Yang, X., Zhang, W. et al. (2003). A panoramic view of yeast noncoding RNA processing. *Cell* 113(7): 919-33.

Pianese, G. (1896). Beitrag Zur Histologie Und Aetiologie Des Carcinoms: Histologische Und Experimentelle Untersuchungen. *Beitr. Pathol. Anat. Allg Pathol* 142: 1-193.

Pierce, S. B., Yost, C., Anderson, S. A. R., Flynn, E. M., Delrow, J. and Eisenman, R. N. (2008). Drosophila growth and development in the absence of dMyc and dMnt. *Dev Biol* 315(2): 303-16.

Politz, J. C., Yarovoi, S., Kilroy, S. M., Gowda, K., Zwieb, C. and Pederson, T. (2000). Signal recognition particle components in the nucleolus. *Proc Natl Acad Sci USA* 97(1): 55-60.

Rahimi, R. A., Andrianifahanana, M., Wilkes, M. C., Edens, M., Kottom, T. J., Blenis, J. and Leof, E. B. (2009). Distinct Roles for Mammalian Target of Rapamycin Complexes in the Fibroblast Response to Transforming Growth Factor- *Cancer Research* 69(1): 84-93.

Ritland Politz, J. C., Hogan, E. M. and Pederson, T. (2009). MicroRNAs with a nucleolar location. *RNA* 15(9): 1705-1715.

Romanova, L., Grand, A., Zhang, L., Rayner, S., Katoku-Kikyo, N., Kellner, S. and Kikyo, N. (2009a). Critical role of nucleostemin in pre-rRNA processing. *J Biol Chem* 284(8): 4968-77.

Romanova, L., Kellner, S., Katoku-Kikyo, N. and Kikyo, N. (2009b). Novel role of nucleostemin in the maintenance of nucleolar architecture and integrity of small nucleolar ribonucleoproteins and the telomerase complex. *Journal of Biological Chemistry* 284(39): 26685-94.

Rosby, R., Cui, Z., Rogers, E., deLivron, M. A., Robinson, V. L. and DiMario, P. J. (2009). Knockdown of the Drosophila GTPase nucleostemin 1 impairs large ribosomal subunit biogenesis, cell growth, and midgut precursor cell maintenance. *Mol Biol Cell* 20(20): 4424-34.

San Francisco, I. F., Dewolf, W. C., Peehl, D. M. and Olumi, A. F. (2004). Expression of transforming growth factor-beta 1 and growth in soft agar differentiate prostate carcinoma-associated fibroblasts from normal prostate fibroblasts. *Int J Cancer* 112(2): 213-8.

Sander, V., Eivers, E., Choi, R. H. and De Robertis, E. M. (2010). Drosophila Smad2 Opposes Mad Signaling during Wing Vein Development. *PLoS ONE* 5(4): e10383.

Shlevkov, E. and Morata, G. (2011). A dp53/JNK-dependant feedback amplification loop is essential for the apoptotic response to stress in Drosophila. *Cell Death and Differentiation*.

Sommerville, J., Brumwell, C. L., Politz, J. C. R. and Pederson, T. (2005). Signal recognition particle assembly in relation to the function of amplified nucleoli of Xenopus oocytes. *J Cell Sci* 118(Pt 6): 1299-307.

Steiger, D., Furrer, M., Schwinkendorf, D. and Gallant, P. (2008). Max-independent functions of Myc in Drosophila melanogaster. *Nat Genet*.

Tortoriello, G., De Celis, J. F. and Furia, M. (2010). Linking pseudouridine synthases to growth, development and cell competition. *FEBS Journal* 277(15): 3249-3263.

Uemura, M., Zheng, Q., Koh, C. M., Nelson, W. G., Yegnasubramanian, S. and De Marzo, A. M. (2011). Overexpression of ribosomal RNA in prostate cancer is common but not linked to rDNA promoter hypomethylation. *Oncogene*.

Venema, J. and Tollervey, D. (1999). Ribosome synthesis in Saccharomyces cerevisiae. *Annu Rev Genet* 33: 261-311.

Winicov, I. (1976). Alternate temporal order in ribosomal RNA maturation. *J Mol Biol* 100(2): 141-55.

Zeller, K. I., Zhao, X., Lee, C. W. H., Chiu, K. P., Yao, F., Yustein, J. T., Ooi, H. S., Orlov, Y. L., Shahab, A., Yong, H. C. et al. (2006). Global mapping of c-Myc binding sites and target gene networks in human B cells. *Proc Natl Acad Sci USA* 103(47): 17834-9.

APPENDIXES

APPENDIX 1 - SUPPLEMENTARY TABLE 1

Supplementary Table 1 - List of the 188 *eyeless*-induced, eye-enriched, atonal independent genes identified by Ostrin and co-workers and the genes belonging to the signaling pathways tested in the targeted in vivo double RNAi screen to identify genes and pathways working with Vito during eye development.

	FBgn	Transformant ID	Gene ID	Symbol	Gene name	Single RNAi (*ey*-Gal4)	Double RNAi (*ey* Gal4, *vito*RNAi)
188 *eyeless*-induced, eye-enriched, atonal independent genes	FBgn0000180	GD 8892	CG4722	bib	big brain		N
	FBgn0001311	GD 42610	CG2666	kkv	krotzkopf verkehrt		N
	FBgn0003016	GD 3010	CG3479	osp	outspread		N
	FBgn0003187	GD 27623	CG6433	qua	quail		N
	FBgn0003285	GD 951	CG4125	rst	roughest		N
	FBgn0003326	GD 44527	CG17579	sca	scabrous		N
	FBgn0003353	GD 3606	CG3182	sei	seizure		N
	FBgn0005630	GD 12573	CG12052	lola	longitudinals lacking		N
	FBgn0010014	GD 21611	CG4209	CanB	Calcineurin B		N
	FBgn0010433	GD 48675	CG7508	ato	atonal		N
	FBgn0012051	GD 35261	CG7563	CalpA	Calpain-A		N
	FBgn0014029	GD 26413	CG4173	Sep2	Septin-2		N
	FBgn0014073	GD 27087	CG7525	Tie	Tie-like receptor tyrosine kinase		N
	FBgn0014135	GD 5730	CG4608	bnl	branchless		N
	FBgn0014342	GD 37563	CG10390	mia	meiosis I arrest		N
	FBgn0015221	GD 14491	CG1469	Fer2LCH	Ferritin 2 light chain homologue		N
	FBgn0017566	GD 52047	CG2286	ND75	NADH:ubiquinone reductase 75kD subunit precursor		N
	FBgn0017590	GD 39515	CG6669	klg	klingon		N
	FBgn0019650	GD 15919	CG11186	toy	twin of eyeless		N
	FBgn0020269	GD 15194	CG10145	mspo	M-spondin		N
	FBgn0020304	GD 43763	CG3365	drongo	drongo		N
	FBgn0020639	GD 23530	CG10533	Lcp65Af	Lcp65Af		N
	FBgn0022702	GD 7609	CG2054	Cht2	Chitinase 2		N
	FBgn0023516	GD 42332	CG14815	CG14815			N
	FBgn0024836	GD 1665	CG11895	stan	starry night		N
	FBgn0026592	GD 7477	CG1079	Fie	Fire exit		N
	FBgn0027280	GD 30843	CG2206	l(1)G0193	lethal (1) G0193		N
	FBgn0027538	GD 4867	CG8536	beta4GalNAcTA	beta4GalNAcTA		N
	FBgn0027575	GD 1784	CG6706	GABA-B-R2	metabotropic GABA-B receptor subtype 2		N
	FBgn0027600	GD 7652	CG4778	obst-B	obstructor-B		N
	FBgn0027780	GD 43571	CG13401	U26	U26		N
	FBgn0028523	GD 12413	CG5888	CG5888			N
	FBgn0028527	GD 7705	CG18507	CG18507			N
	FBgn0028572	GD 17349	CG14039	qtc	quick-to-court		N
	FBgn0028662	GD 33343	CG7007	VhaPPA1-1	Vacuolar H[+] ATPase subunit PPA1-1		N
	FBgn0029761	GD 28155	CG10706	SK	small conductance calcium-activated potassium channel		N
	FBgn0030171	GD 46285	CG43374	Cht6	Cht6		N
	FBgn0030342	GD 16025	CG10347	CG10347			N
	FBgn0030452	GD 11078	CG4330	CG4330			N
	FBgn0030528	GD 37911	CG11095	CG11095			N
	FBgn0030640	GD 46349	CG6294	CG6294			N
	FBgn0030648	GD 34159	CG6340	CG6340			N
	FBgn0030716	GD 29066	CG9170	CG9170			N
	FBgn0030723	GD 45821	CG14948	dpr18	dpr18		N
	FBgn0031037	GD 44831	CG14207	CG14207			N
	FBgn0031309	GD 12559	CG5041	Tfb4	Tfb4		N
	FBgn0031360	GD 3449	CG31937	CG31937			N
	FBgn0031609	GD 40877	CG15443	CG15443			N
	FBgn0031610	GD 39986	CG15436	CG15436			N
	FBgn0031815	GD 51450	CG9526	frj	farjavit		N
	FBgn0032022	GD 7642	CG14275	CG14275			N
	FBgn0032192	GD 15543	CG5731	CG5731			N
	FBgn0032225	GD 8262	CG5022	CG5022			N
	FBgn0032405	GD 38306	CG14946	CG14946			N
	FBgn0032846	GD 44327	CG6412	CG6412			N
	FBgn0032685	GD 12352	CG10211	CG10211			N
	FBgn0032899	GD 8609	CG9338	CG9338			N
	FBgn0032946	GD 44486	CG8663	nrv3	nervana 3		N
	FBgn0033134	GD 11331	CG12840	Tsp42El	Tetraspanin 42El		N
	FBgn0033183	GD 12681	CG1620	CG1620			N
	FBgn0033205	GD 8729	CG2064	CG2064			N
	FBgn0033225	GD 26129	CG1550	CG1550			N
	FBgn0033226	GD 41405	CG1882	CG1882			N
	FBgn0033358	GD 23270	CG8216	CG8216			N
	FBgn0033382	GD 13314	CG8058	Hydr1	alpha/beta hydrolase 1		N
	FBgn0033495	GD 31689	CG12214	CG12214			N
	FBgn0033529	GD 32404	CG17765	CG17765			N
	FBgn0033631	GD 37794	CG9027	CG9027			N
	FBgn0033872	GD 13319	CG6329	CG6329			N
	FBgn0033876	GD 8784	CG10808	synaptogyrin	synaptogyrin		N
	FBgn0033886	GD 23874	CG13349	CG13349			N
	FBgn0034312	GD 31379	CG10916	CG10916			N
	FBgn0034350	GD 40318	CG5189	CG5189			N
	FBgn0034452	GD 38462	CG11237	Oseg6	Oseg6		N
	FBgn0034978	GD 34578	CG3257	CG3257			N
	FBgn0035157	GD 32078	CG13894	CG13894			N
	FBgn0035160	GD 39733	CG13897	CG13897			N
	FBgn0035237	GD 32082	CG13917	CG13917			N
	FBgn0035287	GD 3373	CG13937	CG13937			N
	FBgn0035542	GD 41186	CG11347	DOR			N
	FBgn0035636	GD 31258	CG10546	Cralbp	Cellular retinaldehyde binding protein		N
	FBgn0035983	GD 9026	CG4080	CG4080			N
	FBgn0036545	GD 44441	CG17035	GXIVsPLA2	GXIVsPLA2		N
	FBgn0036595	GD 41496	CG13046	CG13046			N
	FBgn0036805	GD 21788	CG4108	Chmp1	Chmp1		N
	FBgn0036986	GD 5387	CG5282	CG5282			N
	FBgn0037028	GD 6977	CG3618	CG3618			N
	FBgn0037297	GD 18161	CG1116	CG1116			N
	FBgn0037551	GD 26085	CG7891	Gie	novel GTPase indispensable for equal segregation of chromosomes		N
	FBgn0037653	GD 38623	CG11982	CG11982			N
	FBgn0037722	GD 15723	CG8319	CG8319			N
	FBgn0037796	GD 9066	CG12814	CG12814			N
	FBgn0037847	GD 26000	CG6584	SelR	SelR		N
	FBgn0037930	GD 12828	CG14715	CG14715			N
	FBgn0038504	GD 27410	CG5407	Sur-8	Sur-8		N
	FBgn0038682	GD 33358	CG5835	CG5835			N
	FBgn0038984	GD 40935	CG5315	CG5315			N
	FBgn0039065	GD 26539	CG4449	CG4449			N
	FBgn0039249	GD 18170	CG11168	CG11168			N
	FBgn0039430	GD 35010	CG5455	CG5455			N
	FBgn0039665	GD 1337	CG2310	CG2310			N
	FBgn0039702	GD 43415	CG18112	Vps16B	Vacuolar protein sorting 16B		N
	FBgn0039908	GD 45121	CG11533	Asator	Asator		N
	FBgn0040752	GD 21216	CG30483	Prosap	Prosap		N
	FBgn0041707	GD 30816	CG1168	7B2	7B2		N
	FBgn0042138	GD 33414	CG18815	CG18815			N
	FBgn0051038	GD 25656	CG31038	CG31038			N
	FBgn0051072	GD 1252	CG31072	Lerp	lysosomal enzyme receptor protein		N
	FBgn0051712	GD 21401	CG31712	CG31712			N
	FBgn0051997	GD 12928	CG31997	CG31997			N
	FBgn0259736	GD 22197	CG42390	CG42390			N
	FBgn0260634	GD 18031	CG10192	eIF4G2	eukaryotic translation initiation factor 4G2		N
	FBgn0261258	GD 31067	CG6014	rgn	regeneration		N
	FBgn0261451	GD 24549	CG33950	trol	terribly reduced optic lobes		N
	FBgn0261556	GD 46771	CG42674	CG42674			N
	FBgn0039737	GD 21577	CG7920	CG7920			N
	FBgn0038271	GD 40466	CG3731	CG3731			N
	FBgn0035765	GD 49933	CG8600	CG8600			N
	FBgn0034009	GD 24221	CG8155	CG8155			N
	FBgn0086356	GD 17145	CG13345	tum	tumbleweed		N
	FBgn0250874	GD 5586	CG2713	ttm50	tiny tim 50		N
	FBgn0029818	GD 7086	CG3033	CG3033			N
	FBgn0029664	GD 39765	CG10802	CG10802			N

Eye phenotypes with *ey*-Gal4 driver:	
	Positive
	Negative
	Lethal
n.t.	not tested

Vito interactions	
N	Negative interaction
+	Small interaction
++	Medium interaction
+++	Strong interaction
n.t.	not determined

Supplementary Table 1 (Continued)

	FBgn	Transformant ID	Gene ID	Symbol	Gene name	Single RNAi (*ey*-Gal4)	Double RNAi (*ey* Gal4, *vito*RNAi)
188 eyeless-induced, eye-enriched, atonal independent genes	FBgn0029523	GD 39348	CR18275	CR18275			N
	FBgn0017551	GD 35489	CG10800	Rca1	Regulator of cyclin A1		N
	FBgn0002921	GD 12330	CG5670	Atpalpha	Na pump alpha subunit		N
	FBgn0003996	GD 30033	CG2759	w	white		N
	FBgn0025463	GD 12675	CG4303	Bap60	Brahma associated protein 60kD	Lethal	Lethal
	FBgn0001942	GD 42202	CG9075	eIF-4a	Eukaryotic initiation factor 4a	Lethal	Lethal
	FBgn0033902	8309-R1 NIG-fly	CG8309	Tango7	Transport and Golgi organization 7	Lethal	Lethal
	FBgn0014026	GD 43760	CG3314	RpL7A	Ribosomal protein L7A	Lethal	Lethal
	FBgn0005558	KK 106628	CG1464	ey	eyeless		+++
	FBgn0003460	KK 104386	CG11121	so	sine oculis		+++
	FBgn0000320	GD 43911	CG9554	eya	eyes absent		+++
	FBgn0030085	GD 41828	CG6999	CG6999			+
	FBgn0027791	GD 41361	CG14789	O-fut2	O-fucosyltransferase 2		+
	FBgn0261111	GD 38249	CG8616	BHD	Birt-Hogg-Dube homolog		+
	FBgn0086254	GD 27551	CG6084	CG6084			+
	FBgn0027525	GD 33649	CG7686	CG7686			+
	FBgn0036196	GD 16255	CG11658	CG11658			+
	FBgn0005677	GD 2942	CG4952	dac	dachshund		+
	FBgn0025692	GD 4671	CG3814	CG3814			+
	FBgn0023526	GD 20924	CG2865	CG2865			+
	FBgn0000451	GD 14003	CG6611	ect	ectodermal		+
	FBgn0259876	GD 9428	CG5681	Sema-5c	Semaphorin-5c		++
	FBgn0032420	GD 44880	CG6583	CG6583			++
	FBgn0000463	GD 3720	CG3619	Dl	Delta		++
	FBgn0000635	GD 8392	CG3665	Fas2	Fasciclin 2		++
	FBgn0037696	GD 24011	CG9362	CG9362			n.t.
	FBgn0030151	GD 17235	CG1354	CG1354			n.t.
	FBgn0031530	GD 26163	CG3254	pgant2	polypeptide GalNAc transferase 2		n.t.
	FBgn0030816	GD 45188	CG16700	CG16700			n.t.
	FBgn0038424	GD 32951	CG17565	CG17565			n.t.
	FBgn0029648	GD 51663	CG3603	CG3603			n.t.
	FBgn0038679	GD 21025	CG6040	CG6040			n.t.
	FBgn0261551	GD 34509	CG42669	CG42669			n.t.
	FBgn0037126	GD 41248	CG14567	CG14567			n.t.
	FBgn0043550	CG37440	CG32136	Tsp68C	Tetraspanin 68C		n.t.
	FBgn0051641		CG31641	stai	stathmin	n.t.	n.t.
	FBgn0046874		CG33720	Pif1B	PFTAIRE-interacting factor 1B	n.t.	n.t.
	FBgn0030793		CG9125	CG9125		n.t.	n.t.
	FBgn0028473		CG8801	CG8801		n.t.	n.t.
	FBgn0039507		CG3361	mrt	martik	n.t.	n.t.
	FBgn0032681		CG10283	CG10283		n.t.	n.t.
	FBgn0034094		CG3666	Tsf3	Transferrin 3	n.t.	n.t.
	FBgn0052521		CG32521	CG32521		n.t.	n.t.
	FBgn0259985		CG8889	CG8889		n.t.	n.t.
	FBgn0263038		CG43333	CG43333		n.t.	n.t.
	FBgn0028990		CG11331	Spn27A	Serpin 27A	n.t.	n.t.
	FBgn0029997		CG2258	CG2258		n.t.	n.t.
	FBgn0025360		CG18455	Optix	Optix	n.t.	n.t.
	FBgn0025608		CG10372	Faf	Fas-associated factor	n.t.	n.t.
	FBgn0026077		CG10287	Gasp	Gasp	n.t.	n.t.
	FBgn0011653		CG15002	mas	masquerade	n.t.	n.t.
	FBgn0052645		CG32645	CG32645		n.t.	n.t.
	FBgn0261015		CG42599	Pif1A	PFTAIRE-interacting factor 1A	n.t.	n.t.
	FBgn0039883		CG1976	RhoGAP100F	RhoGAP100F	n.t.	n.t.
	FBgn0086758		CG31666	chinmo	Chronologically inappropriate morphogenesis	n.t.	n.t.
	FBgn0046875		CG31558	Obp83g	Odorant-binding protein 83g	n.t.	n.t.
	FBgn0263077		CG43340	CG43340		n.t.	n.t.
	FBgn0015589		CG1451	Apc	APC-like	n.t.	n.t.
	FBgn0037525		CG17816	CG17816		n.t.	n.t.
	FBgn0035347		CG33232	CG33232		n.t.	n.t.
	FBgn0003890		CG4869	betaTub97EF	beta-Tubulin at 97EF	n.t.	n.t.
	FBgn0037921		CG6808	CG6808		n.t.	n.t.
	FBgn0001098		CG5320	Gdh	Glutamate dehydrogenase	n.t.	n.t.
	FBgn0004856		CG8264	Bx42	Bx42	n.t.	n.t.
	FBgn0005586		CG7576	Rab3	Rab-protein 3	n.t.	n.t.
TGF-β signaling pathway – Dpp pathway	FBgn0003716	GD 3059	CG14026	tkv	thickveins		+++
	FBgn0003716	GD 862	CG14026	tkv	thickveins		++
	FBgn0003169	GD 849	CG7904	put	punt		++
	FBgn0003169	GD 37279	CG7904	put	punt		Synthetic lethal
	FBgn0011655	GD 19688	CG1775	Med	Medea		+++
	FBgn0011655	GD 19689	CG1775	Med	Medea		+++
	FBgn0011648	TRIP 31315	CG12399	Mad	Mothers against dpp	Lethal	Lethal
	FBgn0003317	GD 42457	CG1891	sax	saxophone		N
	FBgn0003317	GD 46350	CG1891	sax	saxophone		N
	FBgn0003317	GD 46356	CG1891	sax	saxophone		N
	FBgn0020493	GD 42840	CG5201	Dad	Daughters against dpp		N
TGF-β signaling pathway – Act-β	FBgn0011300	TRIP 25933	CG8224	babo	baboon		++
	FBgn0025800	TRIP 26756	CG2262	Smox	Smad on X		++
Wg pathway	FBgn0001085	GD 43075	CG17697	fz	frizzled		N
	FBgn0001085	GD 43077	CG17697	fz	frizzled		N
	FBgn0004009	GD 13351	CG4889	wg	wingless		N
	FBgn0004009	GD 13352	CG4889	wg	wingless		N
	FBgn0026597	GD 7748	CG7926	Axn	Axin		n.t.
	FBgn0031902	GD 27610	CG4969	Wnt6	Wnt6		N
Hedgehog	FBgn0004644	GD 1402	CG4637	hh	hedgehog		N
	FBgn0003444	GD 9542	CG11561	smo	smoothened		N